



National Library  
of Canada

Bibliothèque nationale  
du Canada

Canadian Theses Service

Service des thèses canadiennes

Ottawa, Canada  
K1A 0N4

## NOTICE

The quality of this microform is heavily dependent upon the quality of the original thesis submitted for microfilming. Every effort has been made to ensure the highest quality of reproduction possible.

If pages are missing, contact the university which granted the degree.

Some pages may have indistinct print especially if the original pages were typed with a poor typewriter ribbon or if the university sent us an inferior photocopy.

Reproduction in full or in part of this microform is governed by the Canadian Copyright Act, R.S.C. 1970, c. C-30, and subsequent amendments.

## AVIS

La qualité de cette microforme dépend grandement de la qualité de la thèse soumise au microfilmage. Nous avons tout fait pour assurer une qualité supérieure de reproduction.

S'il manque des pages, veuillez communiquer avec l'université qui a conféré le grade.

La qualité d'impression de certaines pages peut laisser à désirer, surtout si les pages originales ont été dactylographiées à l'aide d'un ruban usé ou si l'université nous a fait parvenir une photocopie de qualité inférieure.

La reproduction, même partielle, de cette microforme est soumise à la Loi canadienne sur le droit d'auteur, SRC 1970, c. C-30, et ses amendements subséquents.

***INTERRELATIONSHIPS OF ENDOTHELIAL AND SMOOTH MUSCLE  
CELLS TO ELASTIC LAMINAE IN THE MOUSE AORTIC WALL DURING  
DEVELOPMENT: AN ULTRASTRUCTURAL, IMMUNOHISTOCHEMICAL  
AND RADIOAUTOGRAPHIC STUDY***

*Elaine C. Davis  
Department of Anatomy  
McGill University, Montreal  
February, 1992*

*A Thesis submitted to the Faculty of Graduate Studies and Research  
in partial fulfillment of the requirements for the degree of  
Doctor of Philosophy*

©Elaine C. Davis 1992



National Library  
of Canada

Bibliothèque nationale  
du Canada

Canadian Theses Service Service des thèses canadiennes

Ottawa, Canada  
K1A 0N4

The author has granted an irrevocable non-exclusive licence allowing the National Library of Canada to reproduce, loan, distribute or sell copies of his/her thesis by any means and in any form or format, making this thesis available to interested persons.

The author retains ownership of the copyright in his/her thesis. Neither the thesis nor substantial extracts from it may be printed or otherwise reproduced without his/her permission.

L'auteur a accordé une licence irrévocable et non exclusive permettant à la Bibliothèque nationale du Canada de reproduire, prêter, distribuer ou vendre des copies de sa thèse de quelque manière et sous quelque forme que ce soit pour mettre des exemplaires de cette thèse à la disposition des personnes intéressées.

L'auteur conserve la propriété du droit d'auteur qui protège sa thèse. Ni la thèse ni des extraits substantiels de celle-ci ne doivent être imprimés ou autrement reproduits sans son autorisation.

ISBN 0-315-74947-4

Canada

## ABSTRACT

The association of endothelial and smooth muscle cells to elastic laminae in the developing mouse aortic wall was investigated by electron microscopy and immunohistochemistry. Early in development, bundles of contractile filaments traverse the long axis of the cell obliquely to anchor in membrane-associated dense plaques on either side. From these sites, microfibrils extend in the same direction to link the cell to the adjacent elastic laminae. The microfibrils become infiltrated with elastin to form elastin extensions, which together with the intracellular contractile filaments bundles, forms a "contractile-elastic unit". The ordered arrangement of contractile-elastic units revealed in the adult vessel provides a mechanism for the transmission of tension throughout the vessel wall. During development, endothelial cells are similarly connected to the subjacent elastic lamina by filamentous structures. These "endothelial cell connecting filaments" show morphological feature similar to microfibrils. Immunolocalization of fibrillin, a constituent protein of microfibrils, to the connecting filaments provides further evidence for their microfibrillar nature. These results suggest that microfibrils may play an important role in cell anchorage and the maintenance of tissue integrity. A longterm radioautographic study was performed to provide quantitative data concerning the stability of aortic elastin. Results from this study demonstrate the remarkable longevity of elastin in the aortic wall and suggest that, like elastin, cell to elastic lamina connections remain stable throughout development and exist as functional structures in the adult vessel.

## RÉSUMÉ

L'association de membranes élastiques avec les cellules musculaires lisses ainsi qu'avec l'endothélium de la paroi aortique chez la souris en développement a été examinée en microscopie électronique et à l'aide de l'immunohistochimie. Au début du développement, il apparaît dans la cellule des faisceaux obliques de filaments contractiles qui se terminent à sa surface; au même endroit mais à l'extérieur de la cellule, des microfibrilles s'insèrent à la surface cellulaire et, de là, vont rejoindre une membrane élastique. Au cours de la croissance les microfibrilles s'infiltrèrent peu-à-peu d'élastine pour former des faisceaux élastiques extra-cellulaires. Conjointement avec les faisceaux contractiles intracellulaires, ils forment l'unité structurale de base, une unité à la fois contractile et élastique. L'organisation de ces unités dans le vaisseau adulte fournit un mécanisme par lequel la tension se transmet d'un côté à l'autre de la paroi vasculaire. Comme les cellules musculaires lisses, les cellules endothéliales acquièrent au cours du développement des faisceaux de filament contractiles qui s'insèrent à la surface où, de l'autre côté, se retrouvent des filaments connecteurs; ceux-ci présentent des caractères morphologiques semblables à ceux des microfibrilles et vont, comme elles, rejoindre une membrane élastique. La localisation immunologique de la fibrilline, une protéine constituante des microfibrilles, le long des filaments connecteurs fournit une preuve de plus de leur nature microfibrillaire. Ces résultats suggèrent que les microfibrilles jouent un rôle important dans l'"ancrage" des cellules et le maintien de l'intégrité du tissu. Finalement, une étude radioautographique de longue durée a démontré que l'élastine est d'une stabilité

remarquable dans la paroi aortique. Il est probable que, non seulement l'élastine, mais aussi les connections entre cellule et membrane élastique persistent en tant qu'unité fonctionnelle dans le vaisseau adulte.

*to my family*

## ACKNOWLEDGEMENTS

The work for this thesis was carried out in the Department of Anatomy under the chairmanship of Dr. D.G. Osmond and the supervision of Dr. C.P. Leblond. I am grateful to Dr. Leblond for giving me the opportunity to study under his supervision and for his support and patience.

I would like to acknowledge the following people for their technical assistance:

Ms. Sonia Bujold - electron microscopy sectioning

Ms. Matilda Cheung - electron microscopy sectioning

Dr. Mohammed El-Alfy - radioautography and LM photography

Mr. Fernando Evaristo - radioautography

Mr. Tony Graham - LM photography

Mr. Charles Hodge - photography of thesis plates

Ms. Jeannie Mui - electron microscopy sectioning

Ms. Margo Oeltzschner - artwork

I would like to thank Dr. B. Lowell Langille for critically reading Chapter two of this thesis and Dr. Norman Nadler for his assistance with statistical analyses and for critically reading Chapter five of this thesis.

I would also like to thank Ms. Audrey Innes and Ms. Karen Halse for their secretarial assistance during the course of my degree. In addition, I am grateful to



Dr. Yves Clermont, Dr. Eugene Daniels, Dr. Louis Hermo, and Dr. Mike Lalli for many stimulating and encouraging discussions.

Many thanks must also go to my family for their never ending support and understanding.

My deepest thanks, however, goes to the graduate students of this department; for without their constant reassurance and encouragement, I don't think I would have made it. Special thanks to Carol, Rick and Thomas.

The work of this thesis was carried out with support of grants to Dr. C.P. Leblond from the Medical Research Council of Canada and the National Institutes of Health of the USA (DEO-5690).

## **PREFACE**

All planning of experiments, conduct of experimental procedures, electron microscopy photography and data analysis presented in this thesis was carried out by the candidate, Elaine C. Davis. Technical assistance for animal perfusions was provided by Carol S. Heck and Thomas B. Shima. The French abstract was translated by Dr. C.P. Leblond.

# TABLE OF CONTENTS

	<i>page</i>
Abstract	ii
Résumé	iii
Dedication	v
Acknowledgements	vi
Preface	viii
Table of Contents	ix
List of Plates	xv
List of Tables and Graphs	xx
<b>CHAPTER 1: LITERATURE REVIEW</b>	<b>1</b>
<b>1.1 INTRODUCTION - BACKGROUND ON ELASTIC TISSUES</b>	<b>2</b>
<b>1.2 ELASTIC FIBER COMPOSITION</b>	<b>5</b>
1.2.1 Elastin	5
1.2.1.1 Elastin composition	5
1.2.1.2 Ultrastructural organization of elastin	7
1.2.2 Microfibrils	11
1.2.2.1 Microfibril distribution	11
1.2.2.2 Microfibril ultrastructure	13
1.2.2.3 Microfibril composition	17
1.2.2.4 Microfibril-associated proteins	25
<b>1.3 ELASTIC FIBER FORMATION</b>	<b>31</b>
1.3.1 Synthesis and secretion of tropoelastin	31
1.3.2 Deposition of elastin - elastic fiber assembly	34
1.3.2.1 Stages of elastin deposition	34
1.3.2.2 Role of microfibrils	36
1.3.2.3 Role of the elastin-producing cell	38

1.3.3	Lysyl oxidase	39
1.4	ELASTIN RECEPTORS	43
1.4.1	The 67 kDa elastin-binding protein	43
1.4.1.1	Structural features	43
1.4.1.2	Functions	45
1.4.2	Other elastin-binding proteins	48
1.5	ELASTIN KINETICS	51
1.6	THESIS OBJECTIVES	54
1.6.1	Hypothesis	54
1.6.2	Plan of the thesis	54
<b>CHAPTER 2: ULTRASTRUCTURAL FEATURES OF THE DEVELOPING MOUSE AORTIC MEDIA: SMOOTH MUSCLE CELL - ELASTIC LAMINA ASSOCIATION</b>		<b>57</b>
2.1	INTRODUCTION	58
2.2	MATERIALS AND METHODS	61
2.2.1	Tissue Dissection	61
2.2.2	Preparation of Epon embedded tissue	61
2.3	RESULTS	65
2.3.1	Developing mouse aortic wall - 5-day post-natal age	65
2.3.1.1	General histological features	65
2.3.1.2	Smooth muscle cell ultrastructure	67

2.3.1.3	Intercellular features	69
2.3.1.4	Smooth muscle cell - elastic lamina association	71
2.3.2	Developmental changes in the smooth muscle cell - elastic lamina association	72
2.3.2.1	Fetal aorta - 15-days gestation	72
2.3.2.2	Post-natal aorta - 1-day	73
2.3.2.3	Post-natal aorta - 21-days	74
2.3.2.4	Adult aorta - 3 months	75
2.4	DISCUSSION	102
2.4.1	Smooth muscle cell morphology	102
2.4.2	Development of smooth muscle cell to elastic lamina connections	104
2.4.3	Aortic media organization in the adult vessel	107
	<b>CHAPTER 3: ULTRASTRUCTURAL FEATURES OF THE DEVELOPING AORTIC INTIMA: ENDOTHELIAL CELL - ELASTIC LAMINA ASSOCIATION</b>	111
3.1	INTRODUCTION	112
3.2	MATERIALS AND METHODS	115
3.3	RESULTS	116
3.3.1	Developing mouse aortic intima - 5-day post-natal age	116
3.3.1.1	General histological features	116
3.3.1.2	Endothelial cell ultrastructure	116
3.3.1.3	Endothelial cell - elastic lamina association	120
3.3.2	Developmental changes in the endothelial cell - elastic lamina association	122
3.3.2.1	Fetal aorta - 15-days gestation	122
3.3.2.2	Post-natal aorta - 1-day	124

3.3.2.3	Post-natal aorta - 10-days	124
3.3.2.4	Adult aorta - 3 months	125
3.4	DISCUSSION	141
3.4.1	Endothelial cell morphology	141
3.4.2	Endothelial cell to elastic lamina connections	143
<b>CHAPTER 4: IMMUNOLocalIZATION OF MICROFIBRIL AND MICROFIBRIL-ASSOCIATED PROTEINS ON ENDOTHELIAL CELL CONNECTING FILAMENTS</b>		149
4.1	INTRODUCTION	150
4.2	MATERIALS AND METHODS	154
4.2.1	Preparation of Lowicryl embedded tissue	154
4.2.2	Antibodies	156
4.2.3	Immunolabeling	158
4.3	RESULTS	159
4.3.1	Technical details	159
4.3.1.1	Appearance of Lowicryl embedded tissue	159
4.3.1.2	Effects of fixation on immunolabeling	160
4.3.1.3	Effects of reductive guanidine-hydrochloride on immunolabeling	160
4.3.1.4	Immunolabeling control	161
4.3.2	Immunolabeling of the developing aortic intima - 5-day old post-natal age	161
4.3.2.1	Fibrillin	161
4.3.2.2	Microfibril-associated glycoprotein (MAGP)	162
4.3.2.3	Fibronectin	163
4.3.2.4	Heparan sulfate proteoglycan (HSPG)	163
4.3.2.5	Amyloid P component (AP)	164

4.3.3 Immunolabeling of the fetal aortic intima - 15-days gestational age	164
4.3.3.1 Fibrillin	164
4.3.3.2 Microfibril-associated glycoprotein (MAGP)	165
4.3.3.3 Fibronectin	165
4.3.3.4 Heparan sulfate proteoglycan (HSPG)	165
4.3.3.5 Amyloid P component (AP)	166
4.3.4 Immunolabeling summary	166
 4.4 DISCUSSION	 180
 <b>CHAPTER 5: RADIOAUTOGRAPHIC STUDY OF ELASTIN STABILITY AND ELASTIC LAMINA GROWTH IN THE MOUSE AORTA</b>	 187
 5.1 INTRODUCTION	 188
 5.2 MATERIALS AND METHODS	 191
5.2.1 Experimental design	191
5.2.2 Preparation and administration of radiolabel	192
5.2.3 Preparation of tissue for radioautography	192
5.2.4 Light microscope radioautography	193
5.2.5 Electron microscope radioautography	194
5.2.6 Quantitation and statistics	196
 5.3 RESULTS	 198
5.3.1 Elastin stability	198
5.3.1.1 Light microscope radioautography	198
5.3.1.2 Electron microscope radioautography, quantitation and statistical analysis	200

5.3.2 Elastic lamina growth	203
5.3.2.1 Light microscope radioautography	203
5.3.2.2 Electron microscope radioautography	204
5.4 DISCUSSION	223
<b>CHAPTER 6: SUMMARY</b>	230
6.1 GENERAL DISCUSSION	231
6.2 CONTRIBUTIONS TO ORIGINAL KNOWLEDGE	236
<b>REFERENCES</b>	238



## LIST OF PLATES

<i>figure</i>		<i>page</i>
2-1	Cross-section of a 5-day old mouse aortic wall	77
2-2	Longitudinal section of a 5-day old mouse aortic wall	78
2-3	Cross-section of a 5-day aortic wall - developmental features	79
2-4	Cross-section of a 5-day aortic wall - elastic lamina features	80
2-5	Cross-section of a 5-day aortic adventitia	81
2-6	Cross-sections of a 5-day aortic smooth muscle cell surfaces - basement membrane features	82
2-7	Longitudinal section of a 5-day aortic smooth muscle cell - cell organelles	83
2-8	Cross-sections of 5-day aortic smooth muscle cells - Golgi regions	84
2-9	Smooth muscle cells in a 5-day aortic media - exocytosis of dense core vesicles	85
2-10	Smooth muscle cells in a 5-day aortic media - large dense core vesicles	86
2-11	Smooth muscle cells in a 5-day aortic media - possible fusion of small and large dense core vesicles	86
2-12	Longitudinal section of a 5-day aortic smooth muscle cell - oblique contractile filament bundles	87
2-13	(a) Longitudinal section and (b) cross-section of a membrane-associated dense plaque in 5-day aortic smooth muscle cells	87
2-14	(a) Cross-section and (b) longitudinal section of the intercellular region of a 5-day aortic media - elastic lamina features	88
2-15	Longitudinal section of a 5-day aortic media - collagen features	89

2-16	(a) Cross-section and (b) longitudinal section of a 5-day aortic media - elastin-associated microfibril orientation	90
2-17	Intercellular matrix in a 5-day aortic media	90
2-18	(a) Cross-section and (b) longitudinal section of a 5-day aortic media - smooth muscle cell-elastic lamina association	91
2-19	Cross-section of a 15-day gestational aortic wall	92
2-20	Cross-section of a 15-day gestational aortic media - smooth muscle cell-elastic lamina association	93
2-21	Cross-section of a 1-day aortic wall	94
2-22	Cross-section of a 1-day aortic media - smooth muscle cell-elastic lamina association	95
2-23	(a-c) Cross-section of a 21-day aortic media - smooth muscle cell-elastic lamina association	96
2-24	Cross-section of an adult aortic wall - light microscope	97
2-25	Cross-section of an adult aortic wall - electron microscope	98
2-26	Longitudinal section of an adult aortic wall - light microscope	99
2-27	Longitudinal section of an adult aortic wall - electron microscope	100
2-28	Schematic models of aortic media architecture in (a) cross-section and (b) longitudinal section	101
3-1	(a) Cross-section and (b) longitudinal section of a 5-day aortic intima	126
3-2	Cross-section of a 5-day aortic intima - endothelial cell division	127
3-3	Longitudinal section of a 5-day aortic intima - endothelial cell-smooth muscle cell contact	128
3-4	Cross-section of a 5-day aortic intima - developmental features	128
3-5	Endothelial cell Golgi region in a 5-day aortic intima	129

3-6	Endothelial cell Golgi region in a 5-day aortic intima	130
3-7	Small dense core vesicle in an endothelial cell from a 5-day aortic intima	130
3-8	Large dense core vesicle in an endothelial cell from a 5-day aortic intima	130
3-9	(a,b) Weibel-Palade bodies in an endothelial cell from a 5-day aortic intima	131
3-10	Longitudinal section of a Weibel-Palade body in an endothelial cell from a 5-day aortic intima	131
3-11	Cross-sections of Weibel-Palade bodies in an endothelial cell from a 5-day aortic intima	131
3-12	Mixed vesicle in an endothelial cell from a 5-day aortic intima	131
3-13	(a) Longitudinal section and (b,c) cross-sections of endothelial cell stress fibers in a 5-day aortic intima	132
3-14	(a) Longitudinal section of a 5-day aortic intima (b) Longitudinal section of endothelial cell connecting filaments	133
3-15	(a) Cross-section of a 5-day aortic intima (b) Cross-section of endothelial cell connecting filaments	134
3-16	High magnification of cross-sectioned endothelial cell connecting filaments in a 5-day aortic intima	135
3-17	High magnification of longitudinally sectioned endothelial cell connecting filaments in a 5-day aortic intima	136
3-18	High magnification of individual endothelial cell connecting filaments in (a,b) cross-sections and (c) longitudinal section from a 5-day aortic media	137
3-19	(a) Cross-section and (b) oblique section of endothelial cell connecting filaments in a 15-day gestational aortic intima	138
3-20	(a,b) Cross-sections of endothelial cell connecting filaments in a 1-day aortic intima	139

3-21	Cross-section of the subendothelial matrix in a 10-day aortic intima	140
3-22	Cross-section of the subendothelial matrix in an adult aortic intima	140
4-1	Cross-section of a 5-day aortic intima - Lowicryl section	168
4-2	Endothelial cell connecting filaments in a 5-day aortic intima - control section	169
4-3	Endothelial cell connecting filaments in a 5-day aortic intima - fibrillin immunolocalization	170
4-4	(a,b) Endothelial cell connecting filaments in a 5-day aortic intima - fibrillin immunolocalization	171
4-5	(a,b) Endothelial cell connecting filaments in a 5-day aortic intima - MAGP immunolocalization	172
4-6	(a,b) Endothelial cell connecting filaments in a 5-day aortic intima - fibronectin immunolocalization	173
4-7	(a,b) Endothelial cell connecting filaments in a 5-day aortic intima - heparan sulfate proteoglycan immunolocalization	174
4-8	(a,b) Endothelial cell connecting filaments in a 15-day gestation aortic intima - fibrillin immunolocalization	175
4-9	(a,b) Endothelial cell connecting filaments in a 15-day gestation aortic intima - MAGP immunolocalization	176
4-10	(a,b) Endothelial cell connecting filaments in a 15-day gestation aortic intima - fibronectin immunolocalization	177
4-11	(a,b) Endothelial cell connecting filaments in a 15-day gestation aortic intima - heparan sulfate proteoglycan immunolocalization	178
5-2	Light microscope radioautographs - fate of radiolabel in the aortic wall over time	207
5-3	Light microscope radioautographs - incorporation of radiolabel in the aorta at different ages	208

5-4	Electron microscope radioautograph of the aortic wall from an animal injected at 3 days and killed at 4 days of age	209
5-5	Electron microscope radioautograph of the aortic wall from an animal injected at 3 days and killed at 28 days of age	210
5-6	Electron microscope radioautograph of the aortic wall from an animal injected at 3 days and killed at 4 days of age - tracing of elastin	211
5-11	Light microscope radioautographs of cross-sectioned aortic walls from animals injected at (a) 3 days, (b) 14 days and (c) 21 days and killed at 4 months of age	216
5-12	Light microscope radioautographs of longitudinally sectioned aortic walls from animals injected at (a) 3 days, (b) 14 days and (c) 21 days and killed at 4 months of age	217
5-13	(a,b) Electron microscope radioautographs of the aortic media from an animal injected at 3 days and killed at 4 days of age - fine grain	218
5-14	Electron microscope radioautograph of the aortic media from an animal injected at 3 days and killed at 4 days of age - fine grain	219
5-15	(a,b) Electron microscope radioautographs of the aortic media from an animal injected at 3 days and killed at 118 days of age - fine grain	220
5-16	(a,b) Electron microscope radioautographs of the aortic media from an animal injected at 14 days and killed at 15 days of age - fine grain	221
5-17	(a,b) Electron microscope radioautographs of the aortic media from an animal injected at 14 days and killed at 118 days of age - fine grain	222

## LIST OF TABLES AND GRAPHS

<i>figure</i>		<i>page</i>
4-12	Summary of immunolabeling results for microfibril and microfibril-associated proteins on elastin-associated microfibrils and endothelial cell connecting filaments	179
5-1	Radioautographic study experimental groups	206
5-7	Graphic representation of radioautographic quantitative data of silver grains per area of elastin, cell and extracellular matrix	212
5-8	Silver grain density with respect to animal age for elastin, cell and extracellular matrix	213
5-9	(a) Elastin per silver grain - 4d to 21d range (b) Regression line of the plot in figure 5-9a	214
5-10	(a) Silver grains per area of elastin - 28d to 118d range (b) Regression line of the plot in figure 5-10a	215

*CHAPTER ONE*

*LITERATURE REVIEW*

## 1.1 INTRODUCTION - BACKGROUND ON ELASTIC TISSUE

Elastic fibers are components of virtually all mammalian connective tissues. Elastin, the major protein component of elastic fibers, has unique elastomeric properties which provide the reversible deformability that is critical to extracellular matrices, such as those of arterial vessels, lungs and skin. Without such a property, the structural integrity and function of these tissues would be greatly impaired.

The distribution and organization of elastic fibers in various tissues and organs can be demonstrated at the light microscope level by characteristic staining reactions which date back to the turn of the century. Unna-Tanzaer's orcein (Unna, 1891), Weigert's resorcin-fuchsin (Weigert, 1898), Verhoeff's iron hematoxylin (Verhoeff, 1908) and Gomori's aldehyde fuchsin (Gomori, 1950) are four of the commonly used stains for histological examination of elastic tissues. By light microscopy, a number of elastic fiber configurations have been observed; of these, three morphologically distinct forms have been identified. In ligamentum nuchae, interwoven rope-like fibers are observed which branch and rejoin in a three-dimensional network (Ayer, 1964; Wirtschafter et al., 1967). Elastic fibers of the lung appear similarly arranged; however, without the longitudinal orientation of ligament fibers (Carton et al., 1960). In the aorta, elastin takes on a different form; that of concentric sheets or lamellae (Ayer, 1964). A combination of these two forms is seen in the skin; flattened bands of elastin in the dermis and fine filamentous networks in the papillary layer. A third form of elastin is apparent in elastic cartilage

where large anastomosing fibers form a three-dimensional honeycomb pattern (Sheldon and Robinson, 1958).

Elastic fibers have been shown by electron microscopy to consist of two morphologically distinct components: an amorphous core of insoluble elastin and a peripheral mantle of 10 - 12 nm microfibrils (Low, 1961; Greenlee et al., 1966; Ross and Bornstein, 1969). Fullmer and Lillie (1958) described morphologically similar microfibrils in a number of tissues which appeared independent of elastin. These microfibrils showed resistance to acid hydrolysis and were thus named oxytalan fibers, meaning acid enduring. Gawlik (1965) described another component of connective tissue intermediate to oxytalan fibers and elastic fibers, termed elaunin fibers. Elaunin fibers consist of amorphous elastin deposits intermingled with microfibrils. Cotta-Pereira and colleagues (1976) described an "elastic system" in human skin which consists of an interconnected progression of fibers, oxytalan to elaunin to elastic, involved in anchorage of the epidermis to the dermis. The oxytalan fibers are most superficial and form a close association with the basement membrane of the epidermal cells. These fibers were suggested to have remained in a more primitive stage of development than the elaunin and elastic fibers found deeper in the dermis (Cotta-Pereira et al., 1976, 1977). Studies of elastogenesis in aortae of human fetuses and newborns, demonstrated that aortic fibers initially have staining properties of oxytalan fibers and during development, progressively acquire staining characteristics of elaunin and finally elastic fibers (Gawlik, 1965). Additional studies of elastic fiber formation, both *in vivo* (Fahrenbach et al., 1966; Albert, 1972) and *in vitro* (Ross, 1971; Mecham et al., 1981), corroborate these findings, in that, microfibrils initially deposited

in the extracellular matrix, become subsequently infiltrated with elastin deposits which ultimately merge to form mature elastic fibers.

## 1.2 ELASTIC FIBER COMPOSITION

### 1.2.1 ELASTIN

#### *1.2.1.1 Elastin composition*

Elastin is the most insoluble protein in the body and is extremely resilient to the standard denaturation and degradation techniques usually employed to isolate proteins. For this reason it has been one of the more difficult proteins to study; however, its stability in harsh isolation procedures has been utilized as a basis for successful methods of elastin purification. One of the original methods used to purify elastin was an extraction procedure using aortic tissue that included 0.1 N sodium hydroxide at 95°C for 45 minutes (Lansing et al., 1951). Purified elastin was also prepared by repeatedly autoclaving ligamentum nuchae tissue for 1 hour periods until protein no longer appeared in the supernatant (Partridge et al., 1955). Other purification methods based on treatment with proteases, chaotropic and reducing agents (Ross and Bornstein, 1969) or cyanogen bromide followed by extraction of nonelastin peptides (Rasmussen et al., 1975) have also been utilized. Although these methods are relatively successful, the hot alkali and autoclaving techniques first employed to purify elastin have provided some of the best samples of elastin for the establishment of its nature and composition.

Elastin is extremely hydrophobic due to a high content of nonpolar amino acids such as glycine, alanine, valine and proline. Valine and proline account for approximately

14% and 12% of the amino acids, respectively; while, one-third of the residues are glycine and almost one-quarter are alanine (data in Rucker and Tinker, 1977). The polar amino acids aspartate, glutamate, lysine and arginine comprise only 5% of the residues of the insoluble elastic fiber (Sandberg et al., 1981). Unique to elastin is the predominance of nonpolar amino acids; thus, the amino acid composition of the protein has been a useful guide for its identification (Sandberg et al., 1981).

More than 99% of the total amount of elastin present in normal arterial tissue is in a mature form; a highly cross-linked insoluble network (Rucker and Tinker, 1977). As mentioned above, mature insoluble elastin has very few lysine residues; only 3-8 residues per thousand. The soluble elastin precursor, however, contains over 40 lysine residues per thousand total residues. The difference in lysine content is due to the conversion of lysine residues into the cross-links desmosine and isodesmosine; a process mediated by the copper-dependant enzyme, lysyl oxidase (Kagan and Trackman, 1991; see section 1.3.3). Since cross-linking the soluble form of elastin renders the protein insoluble, large quantities of native soluble elastin are only able to be obtained from tissues in which cross-linking does not occur or has been blocked (Rucker and Tinker, 1977).

Soluble elastin was first isolated by Smith and colleagues (1968) from aortae of copper-deficient pigs. As expected, the protein showed a higher content of lysine as compared to insoluble elastin and contained no desmosines (Sandberg et al., 1969; Smith et al., 1972). Using the nomenclature used for collagen at the time, the protein was named tropoelastin.

Elastin mRNA is translated on membrane-bound polysomes as a polypeptide of

approximately 70,000 daltons (Saunders and Grant, 1984; Prosser and Mecham, 1988). Examination of the cell-free translation product of elastin mRNA showed the polypeptide to contain a signal sequence of 24-26 residues (Karr and Foster, 1981; Davidson et al., 1982). During translocation, the signal sequence of this "pretropoelastin" molecule is cleaved and the completed tropoelastin polypeptide chain enters the endoplasmic reticulum (Saunders and Grant, 1984). Some hydroxylation of proline residues occurs by the membrane-bound endoplasmic reticulum enzyme, proline hydroxylase (Davidson and Giro, 1986); however, in contrast to collagen, hydroxyproline appears unnecessary for tropoelastin secretion or stability (Rosenbloom and Cywinski, 1976; Uitto et al., 1976). It has been suggested that hydroxylation of tropoelastin may even occur by accident in cells that are simultaneously synthesizing elastin and collagen (Rosenbloom, 1982). Besides hydroxylation of proline residues, tropoelastin appears to undergo little other post-translational modifications, with no hydroxylation of lysine and no glycosylation (Mecham and Heuser, 1991).

#### *1.2.1.2 Ultrastructural organization of elastin*

The elastomeric properties of elastin suggest that individual tropoelastin molecules should be disordered and randomly linked to behave thermodynamically as a rubber-like material (Hoeve and Flory, 1974). Increasing evidence, however, based on protein structure, electron microscopy, freeze-fracture and freeze-etch techniques, suggests that some degree of three-dimensional organization of elastin may exist.

One of the first proposals for an ordered substructure of elastin was predicted from

gel filtration studies using columns packed with purified elastin (Partridge, 1967). Based on the ability of sugars to penetrate the gel and on electron microscope studies, elastin was suggested to consist of 4 - 5 nm globular elements with 3 nm interstices. The hydrophobic residues of the molecule were assumed to be sequestered within the globule, while the cross-links protruded from the globule surface. By expanding on this model, Weis-Fogh and Anderson (1970) proposed a two-phased "liquid drop" model in which spherical monomers were cross-linked into a three-dimensional network within an aqueous environment. Deformation of the network would expose the hydrophobic residues to the aqueous environment and result in strong protein-water interactions as predicted by the thermodynamic properties of elastin.

Based on amino acid sequence data, it has been suggested that elastin must contain some ordered substructure to allow lysine residues to be correctly oriented for cross-linking. In addition, the potential for an ordered substructure in non-cross-linked regions exists due to an abundance of repetitive sequences (Rucker and Tinker, 1977). These assumptions, together with other sequence data and physical measurements, lead to the prediction of two further models for elastin organization: one, termed the "oiled-coil" model by Gray and colleagues (1973); and the other, a "fibrillar" model based on the work of Urry and colleagues (1974). In the "oiled-coil" model, the regions that contain the cross-links are separated from each other by broad coils that consist of hydrophilic residues on the outside and hydrophobic residues facing the center. During distension, the coil would open to expose the hydrophobic residues to the polar environment resulting in a thermodynamically unstable configuration; thus the molecule would tend to recoil to its

original state (Gray et al., 1973). The major difference between the "oiled-coil" model and the "fibrillar" model is the orientation of the hydrophobic residues and important conformational aspects of glycine residues. In the "fibrillar" model (Urry et al., 1974), glycine residues, which can form near right-angle turns in the polypeptide backbone, alternate with  $\alpha$ -helical regions containing cross-links to form sequential  $\beta$ -spirals. Unlike the "oiled-coil" model, the hydrophobic residues constitute the sides of the spiral and by hydrophobic interactions, individual chains may be aligned before they are enzymatically cross-linked.

Electron microscope observations of elastin in vivo and tropoelastin coacervates in vitro have provided additional evidence in support of a fibrillar substructure of elastin. In studies of early elastogenesis in fetal calf ligamentum nuchae, Fahrenbach and colleagues (1966) noted that mature elastin appeared to consist of a branching "tangle" of 3 nm wide filaments. Similar filaments were observed in preparations of alkali purified, sonicated elastin from ligamentum nuchae negatively stained with uranyl acetate (Gotte et al., 1974). Such preparations showed filaments 3 - 4 nm in diameter, arranged approximately parallel to the long axis of the elastic fiber, with a regular periodicity of about 4 nm along their length. Consistent with these observations, Serafini-Fracassini and colleagues (1976) identified "beaded" filaments, with a 4 nm periodicity, in negatively stained preparations of isolated insoluble elastin. The filaments were found to form lateral arrays with a center-to-center spacing of approximately 5 nm. The presence of 5 nm wide filaments aligned in parallel arrays has also been described in coacervates of both  $\alpha$ -elastin, a cross-linked protein fragment product of chemical degradation (Cox et al.,

1973), and tropoelastin, the non-cross-linked precursor of elastin (Cox et al., 1974; Volpin and Pasquali-Ronchetti, 1977; Bressan et al., 1983). In addition, tropoelastin coacervates incubated at 40°C for over 10 hours form a precipitate that, when observed by electron microscopy, consists of 0.5 - 2.0  $\mu\text{m}$  branching fibers identical to those of elastic tissue (Bressan et al., 1986). The observation of aligned filaments in tropoelastin coacervates provides evidence that the tropoelastin molecule possesses the ability to form an ordered structure prior to cross-linking. From these observations, a model has been proposed for the assembly of tropoelastin molecules into elastin fibers that involves an initial end-to-end alignment of the molecules, followed by a side-to-side association through hydrophobic forces, and finally intrafilamentous and interfilamentous cross-link formation (Bressan et al., 1986).

The fibrillar nature of elastic fibers has also been revealed by freeze-fracture, although the filaments are slightly larger than those observed by routine electron microscopy (Pasquali-Ronchetti et al., 1979; Morocutti et al., 1988; Pasquali-Ronchetti and Fornieri, 1984). Recently, quick freeze, deep etch electron microscopy has been used to provide a more detailed view of elastic fiber substructure (Mecham and Heuser, 1991). Without the need of fixation, dehydration or staining, this technique provides an accurate three-dimensional surface view of macromolecular structures (Heuser, 1981; Mecham and Heuser, 1990). In an unstretched elastic fiber teased from adult bovine ligamentum nuchae, randomly arranged filaments with an average diameter of 7 nm were observed. The filaments appeared so tightly packed that little or no etching occurred during sample preparation. In areas of the elastic fiber subjected to stretch, the filaments appeared to be

linearly oriented (Mecham and Heuser, 1991). Purified tropoelastin monomers visualized by freeze-etching followed by rotary shadowing revealed individual globules of similar diameter as the filaments observed in the mature fiber (Mecham and Heuser, 1991). These results suggest that the filaments observed by quick freeze, deep etch techniques are a three-dimensional assembly of tropoelastin molecules.

The ultrastructural organization of elastin suggested from the numerous studies of protein structure, chemical and physical studies, electron microscope observations of purified elastin and freeze-fracture/freezing-etch preparations, not only provide information concerning the properties of elastin, but in addition, may be important in the understanding of elastic fiber assembly.

## 1.2.2 MICROFIBRILS

### *1.2.2.1 Microfibril distribution*

Early studies of aortic ultrastructure revealed the presence of small filaments at the surface of developing elastic laminae (Karrer, 1960, 1961). Similar fine extracellular filaments became so routinely observed in a variety of tissues that they were assigned a specific name, collectively termed "microfibrils" (Low, 1961, 1962). Although the distribution of microfibrils appeared wide spread, they were found in greatest concentration around small elastic fibers (Low, 1961, 1962). Microfibrils were established as distinct components of elastic fibers based on characteristic staining properties that

were different than those of elastin (Greenlee et al., 1966) and on their separation from elastic fibers and partial characterization (Ross and Bornstein, 1969). Studies on elastic fiber formation showed that microfibrils appear first in the extracellular matrix prior to the deposition of elastin (Fahrenbach et al., 1966; Greenlee et al., 1966), thus suggesting an involvement in elastogenesis (Cleary et al., 1981).

Microfibrils that appear morphologically similar to those of elastic fibers have been observed in a number of different tissues that are subjected to mechanical stress. In the skin (Kobayasi, 1968, 1977; Cotta-Pereira et al., 1976), gingiva (Chavrier et al., 1988) and epiglottis (Böck, 1983), bundles of microfibrils devoid of elastin appear to anchor the epithelial cells to the underlying connective tissue. These microfibrils, termed oxytalan fibers (Fullmer and Lillie, 1958), are continuous with those of elaunin fibers, microfibrils partially infiltrated with elastin (Gawlik, 1965), which are in turn continuous with completely infiltrated elastic fibers. The oxytalan, elaunin and elastic fibers have been termed "elastic system fibers" (Cotta-Pereira et al., 1977).

In addition to anchoring epidermal cells, elastic system fibers have also been shown to form "elastic tendons" which attach hair follicles to arrector pili muscles (Rodrigo et al., 1975). Oxytalan fibers can also occur alone, such as in the periodontal ligament (Carmichael and Fullmer, 1966), or with elaunin fibers in the absence of elastic fibers, such as in hyaline and fibrous cartilage (Cotta-Pereira et al., 1984).

Microfibrils have also been observed in the subendothelial matrix of lymphatic capillaries (Leak and Burke, 1968; Gerli et al., 1990), bone marrow sinusoids (Campbell, 1987) and the aorta (Gerrity and Cliff, 1972) where they appear to anchor the endothelial

cells to elastic fibers or elastic laminae. Similar microfibrils, although apparently larger in diameter, have been described in the mesangial matrix of the glomerulus (Mundel et al., 1988) and in the ciliary zonule of the eye (Raviola, 1971; Steeten and Licari, 1983; Inoue and Leblond, 1986).

The mechanisms which controls the extent of elastin infiltration of microfibril bundles remains to be established. It has been suggested that the structural differences may reflect the degree of stress imposed upon the tissue and the degree of elasticity required of the anchoring system (Caldini et al., 1990). Clearly, the distribution of microfibrils and their association with elastic elements indicates that the role of microfibrils extends past that of mere templates for elastin deposition during elastic fiber formation.

#### *1.2.2.2 Microfibril ultrastructure*

The microfibrils observed by Low (1961, 1962) ranged in diameter from 4 - 12 nm; with an average diameter of approximately 8 nm. In addition to the wide range in diameter, these microfibrils also showed a considerable variation in morphological features, including beaded appearances, branching, electron-lucent centers and irregular variations in widths. It was later determined that the smallest "microfibrils", those with a diameter of less than 5 nm, were related to a number of specific extracellular matrix components, such as fibronectin (Chen et al., 1978) and type VI collagen (von der Mark et al., 1984).

Microfibrils associated with elastic fibers have been described as being approximately 10 nm in diameter with an electron lucent core of about 4 nm (Fahrenbach

et al., 1966; Greenlee et al., 1966). In cross-section, 3 - 5 densely staining spots were noted in the electron dense peripheral rim of the microfibril (Cleary et al., 1981). These spots were thought to represent densely staining filaments arranged in a spiral manner around the microfibril core. Further cross-sectional details of microfibrils have come from ultrastructural studies of ciliary zonular fibrils. Raviola (1971) described the zonular fibrils to consist of densely packed subunits surrounding a electron lucent center which occasionally appeared to contain of a centrally located dot. In high magnification, the zonular fibrils were shown to be pentagonal in shape with radiating spike-like projections; and the centrally located dot or "spherule", was shown to be a 1 - 2 nm bead-like structure (Inoue and Leblond, 1986).

In longitudinal section, some periodicity along the length of microfibrils has usually been noted. Haust (1965) described a 7 - 14 nm periodicity which appeared as a "chain-like aggregate of tiny vesicles". Other investigators have reported a "beaded appearance" (Low, 1961; Greenlee et al., 1966), "cross-striations" (Raviola, 1971; Inoue and Leblond, 1986) or "alternating light and dark staining bands" (Cleary et al., 1981). Raviola (1971) observed that the cross-striations appeared faint when the microfibrils were loosely aggregated; however, when the microfibrils were tightly grouped, a 49 nm periodicity was evident along their length. This transverse banding pattern often appeared to extend across the entire width of the microfibril bundle. Consistent with this observation, Streeten and Licari (1983) showed a 12 - 14 nm periodicity along the length of single microfibrils, whereas a 40 - 45 nm periodicity was discernible when the microfibril were in bundles. Inoue and Leblond (1986) have suggested that the banding

pattern observed in longitudinal section actually represents a "surface band" that wraps around the microfibril at an interval of approximately 10 nm. In longitudinal sections closer to the center of the microfibril, individual subunits juxtaposed with a center-to-center distance of 4 nm were revealed (Inoue and Leblond, 1986).

Recently, the technique of rotary shadowing with platinum has provided new insights into the structure of microfibrils. Wright and Mayne (1988) noted the presence of beaded fibrils in rotary shadowed preparations of fresh chicken vitreous humor. The beads were approximately 22 nm in diameter with an axial periodicity of 50 nm. In preparations of vitreous humor that were not fresh, the beaded fibril appeared to be partially dissociated; the beads were often closer together and several fine filaments could be seen to extend from the surface of the beads and from one bead to the next (Wright and Mayne, 1988). On occasion, beads could be seen alone, as monomers, or in small groups, as dimers or trimers. Extending from the surface of these beads, at least 8 filaments were seen in a crab-like arrangement. The length of the filaments suggests that there must be considerable overlap in the assembled fibril (Wright and Mayne, 1988). The only previous report of such beaded fibrils was in chromium shadowed preparations of bovine vitreous humor where beaded fibrils with a bead diameter of 15 - 20 nm and an axial periodicity of 50 - 85 nm were observed (Matoltsy et al., 1951).

Wright and Mayne (1988) suggested that the beaded fibrils were derived from zonular fibrils. By electron microscopic observations, zonular fibrils were shown to have a similar axial periodicity of 49 nm, but a smaller diameter of 11 - 12 nm (Raviola, 1971). Since rotary shadowing results in markedly wider structures (Vaughan et al., 1988;

Keene et al., 1991), the diameter of the fibril could not be accurately compared. An additional feature of zonular fibrils, however, is the appearance of an electron lucent core when observed in cross-section (Raviola, 1971). Wright and Mayne (1988) suggested that this might arise if the section passed through the interconnecting filamentous regions.

The association of the beaded fibrils observed in vitreous humor with zonular fibrils was verified by rotary shadowing zonular fibrils dissected from bovine eyes (Ren et al., 1991). The rotary shadowed zonular fibrils showed extensive arrays of beaded fibrils with a bead diameter of approximately 23 nm and an axial periodicity of 40 nm. The shorter periodicity was suggested to be due to the retraction of the zonular fibrils during dissection from the eye since the axial periodicity could be increased by stretching the fibrils during preparation (Ren et al., 1991). Fixed zonular fibrils appeared slightly different than the unfixed fibrils; the interconnecting filamentous area was denser and individual filaments were not easily discerned. In addition, two cross-bands were observed in this region which may be important structural components involved in the filament organization (Wright and Mayne, 1988; Ren et al., 1991).

Beaded fibrils have also been shown to be present in rotary shadowed preparations of microfibrils isolated from skin fibroblast cultures (Fleischmajer et al., 1991a) and collagen isolated from chicken tendon (Fleischmajer et al., 1991b). Electron microscope observations of the chicken tendon showed the presence of bundles of microfibrils among the collagen fibrils which in longitudinal section reveal periodic "spherules" along their length (Fleischmajer et al., 1991b). Additional evidence that the beaded fibrils are microfibrils has come from the use of an antibody specific for a component of

microfibrils, fibrillin (Sakai et al., 1986; see section 1.2.2.3). Extracts from human amnion, shown to contain beaded fibrils in both rotary shadowed and negatively stained preparations, incubated with anti-fibrillin antibody demonstrated that the beaded fibrils contained fibrillin (Keene et al., 1991).

In tissues routinely prepared for conventional thin section electron microscopy, the beaded nature of microfibrils is usually not apparent. However, if tissues are manually stretched and the tension is maintained during fixation, dehydration and embedding, beaded microfibrils can be seen that were never observed in unstretched tissue (Keene et al., 1991). In addition, beaded filaments seen in tissue homogenates can be "converted" to microfibrils by routine preparation for electron microscopy (Keene et al., 1991). Furthermore, it has been demonstrated that by changing the conditions of tissue preparation, such as using potassium permanganate as a fixative or using reduced osmium as an en bloc stain, beaded microfibrils are apparent (F.L. Chan, unpublished). These results suggest that routine tissue processing for conventional electron microscopy may cause microfibrils to compact and artifactually produce a microfibril that is relatively homogeneous in appearance when the actual structure is beaded in nature.

### ***1.2.2.3 Microfibril composition***

The composition of microfibrils has proven difficult to determine due to their insolubility and their association with other extracellular matrix components. Ross and Bornstein (1969) demonstrated that microfibrils could be separated from elastic fibers of fetal bovine ligamentum nuchae using the chaotropic agent, guanidine-hydrochloride, in

the presence of dithiothreitol to reduce disulfide bonds. Following extraction, electron microscope analysis showed that the microfibrils had apparently been removed from the periphery of elastic fibers. Since the extracted material contained carbohydrate and it was concluded that microfibrils are glycoprotein in nature (Ross and Bornstein, 1969); this has only more recently been confirmed (Fanning and Cleary, 1985).

Kewley and colleagues (1977a) used a similar extraction procedure and prepared an antiserum against the "microfibrillar extract". Immunofluorescence studies demonstrated that the antiserum had an affinity not only for elastin-associated microfibrils but also for a wide variety of basement membranes (Kewley et al., 1977b). The antiserum was subsequently used to immunoprecipitate two glycoproteins from the medium of ligamentum nuchae fibroblast cultures (Sear et al., 1978, 1981). The proteins were designated MFP I, a 150 kDa collagenous glycoprotein, and MFP II, a 300 kDa non-collagenous glycoprotein. Both glycoproteins were claimed to be constituents of microfibrils, although the relationship of the glycoproteins to elastin-associated microfibrils was never established with monospecific antibodies. In addition, it was shown that the technique used to obtain the "microfibrillar extract" yields a heterogenous preparation (Gibson and Cleary, 1982; Prosser et al., 1984).

Gibson and Cleary (1982) also isolated a glycoprotein from reductive guanidine-hydrochloride extracts of elastin-rich tissue. Similar to MFP I, the glycoprotein had a molecular weight of approximately 140 kDa and because of its collagen-like features it was named CL glycoprotein. Immunolocalization of CL glycoprotein demonstrated a pattern of distribution similar to that of interstitial collagens. No avidity of the anti-CL

glycoprotein for elastic tissue elements was observed (Gibson and Cleary, 1983). Based on these observations, it was concluded that CL glycoprotein was unlikely to be a constituent of elastin-associated microfibrils. It was later shown that CL glycoprotein was the undegraded tissue form of type VI collagen (Gibson and Cleary, 1985), which has been shown to be unrelated to elastic fibers (von der Mark et al., 1984). Similarly, a relationship between MFP I and type VI collagen was acknowledged (Knight et al., 1984); however it was suggested that a second immunologically distinct species, with a molecular weight of 150 kDa, may have been present in the reductive guanidine-hydrochloride extracts (Ayad et al., 1985). The relationship of this second species or MFP II to elastin-associated microfibrils has yet to be determined.

Several other investigators have also claimed the production of antisera that reacts with microfibrils. Streeten and colleagues (1981) first used isolated ciliary zonular fibrils and later (Streeten and Licari, 1983) used the "microfibrillar extract" of Kewley and coworkers (1977a) to raise an antisera that reacted with elastin-associated microfibrils and microfibrils devoid of elastin. Schwartz and colleagues (1985) used "insoluble microfibril proteins" isolated from calf aortic smooth muscle cell cultures to produce an antiserum apparently specific for microfibrils after the antibody was absorbed with fibronectin. A monoclonal antibody raised against human "subepidermal basement membrane zone substances" was also shown to react with elastin-associated microfibrils (Kambe and Hashimoto, 1987). In all these studies, however, the specificity of the antisera for a structural component of microfibrils rather than an associated protein has not adequately been established.

Two of the best characterized glycoproteins that appear to be constituents of microfibrils are a) a 350 kDa glycoprotein named fibrillin (Sakai et al., 1986) and b) a 31 kDa glycoprotein termed microfibril-associated glycoprotein (MAGP) (Gibson et al., 1986).

a) Fibrillin: Fibrillin was isolated from medium of human skin fibroblast cell cultures (Sakai et al., 1986). Immunofluorescence localization of fibrillin with a specific monoclonal antibody demonstrated its widespread distribution in the extracellular matrix of skin, lung, kidney, blood vessels, tendon, muscle, cornea and ciliary zonular fibrils. Immunogold electron microscopic localization show fibrillin to be specific to microfibrils (Sakai et al., 1986). The molecular structure of fibrillin was investigated by the isolation and characterization of 3 pepsin-resistant fibrillin fragments, designated PF1, PF2 and PF3 (Maddox et al., 1989). PF1 has an apparent molecular weight of 94 kDa and is a uniform thin rod when observed by rotary shadowing. PF2, with a molecular weight of approximately 68 kDa, is also a rod shaped molecule, although slightly shorter than PF1. PF3 appears to consist of at least 6 and possibly 10 disulfide bonded, cross-linked molecules with molecular weights ranging from 30 - 50 kDa. Rotary shadowing of PF3 revealed a crab-like structure composed of up to 8 flexible filaments extending from a central dense region. Two or more PF3 units were also observed in an aggregated form (Maddox et al., 1989). The appearance of PF3 is very similar to that of the beaded fibrils observed in rotary shadowed preparations of ciliary zonular fibrils (Wright and Mayne, 1988; Ren et al., 1991) and human amnion extracts (Keene et al., 1991). Antibodies to PF3 showed a periodic distribution on the beads of the beaded fibrils; thus, it was

suggested that microfibrils may consist of globular domains attached by a number of filamentous molecules (Keene et al., 1991). Antibodies were also raised against PF1 and PF2. Both of these antibodies specifically labeled microfibrils and showed no cross-reactivity; thus PF1 and PF2 appear to be from different regions of the intact fibrillin molecule (Maddox et al., 1989). Fibrillin molecules have been purified from human skin fibroblast and ligament cell cultures (Sakai et al., 1991). Rotary shadowing revealed fibrillin to be an extended, flexible molecule, approximately 148 nm in length. These results suggest that fibrillin may form at least the filamentous links in the linear beaded structures identified as microfibrils with the possibility that additional molecules besides fibrillin may be constituents of the final structure.

Recently, fibrillin has been linked to Marfan syndrome, one of the most common connective tissue disorders, following cloning and mapping of the fibrillin gene to chromosome 15 (Dietz et al., 1991; Lee et al., 1991). A second fibrillin gene, linked to congenital contractural arachnodactyly, was also isolated and mapped to chromosome 5 (Lee et al., 1991). The genomic heterogeneity of fibrillin thus suggests that microfibrils may consist of a family of morphologically and immunologically similar filaments rather than a single entity.

b) MAGP: Gibson and colleagues (1986) isolated MAGP from reductive guanidine-hydrochloride extracts of fetal bovine ligamentum nuchae. MAGP contains two structurally distinct regions: an amino-terminal, rich in glutamine, proline and acidic amino acids; and a carboxyl-terminal, containing all 13 of the cysteine residues and most of the basic amino acids (Gibson et al., 1991). Immunofluorescence localization of MAGP

with affinity purified antibodies, showed the distribution of the glycoprotein to correspond to that of elastin-associated microfibrils and oxytalan fibers of skin, periodontal ligament and ciliary zonular fibrils (Gibson and Cleary, 1987). The specificity of the anti-MAGP antibody for microfibrils in a wide range of tissues was further demonstrated by immunogold labeling at the electron microscope level (Kumaratilake et al., 1989). Using a more specific procedure for solubilization of elastin-associated microfibrils, Gibson and colleagues (1989) obtained a ligamentum nuchae extract that contained only five major proteins of molecular weights 340, 78, 70, 31 and 25 kDa. The 340 kDa protein has been identified as fibrillin (M.A. Gibson, personal communication) and the 31 kDa protein had been previously identified as MAGP (Gibson et al., 1986). The 78 kDa protein (MP78) was demonstrated by immunogold electron microscopy with an affinity purified antibody to bind specifically to elastin-associated microfibrils (Gibson et al., 1989). Similarly, the 25 kDa protein (MP25) also appears to be a microfibrillar component, while the origin of the 70 kDa protein has yet to be determined (Gibson et al., 1991). Results from immunoblotting experiments and cyanogen bromide peptide mapping suggest that MAGP and MP78 are immunologically related to fibrillin but not to each other, and that MAGP and fibrillin are structurally related (Gibson et al., 1989). Using cDNA cloning, MAGP was determined to be a distinct glycoprotein and not derived from fibrillin (Gibson et al., 1991). Although the relationship of MAGP and fibrillin remains to be established, the possibility exists that part of the fibrillin molecule may be an aggregate of covalently linked MAGP.

In addition to fibrillin and MAGP, other components of reductive guanidine-

hydrochloride extracts have been isolated from elastin-rich tissues and used to produce antisera that label elastin-associated microfibrils. These components include 32 kDa and 250 kDa proteins isolated from bovine zonular fibrils (Streeten and Gibson, 1988), a 70 kDa protein also isolated from bovine zonular fibrils (Mecham et al., 1988) and a 35 kDa protein isolated from bovine ligamentum nuchae that shows amine oxidase activity and aggregates to form 11 nm fibrils (Serafini-Fracassini et al., 1981; Jaques and Serafini-Fracassini, 1986). The relationship of these proteins to fibrillin and MAGP remains to be determined.

Recently, the 450 kDa adhesive glycoprotein thrombospondin has been implicated as a constituent of microfibrils (Arbeille et al., 1991). Immunofluorescence localization of an antiserum against thrombospondin isolated from human platelets showed a positive reaction associated with glandular epithelia and the dermal-epidermal junction of skin. In addition, a positive reaction was observed around small blood vessels, however confined to the intimal region of larger vessels (Wight et al., 1985). Fauvel-Lafeve and colleagues (1988) identified a 128 kDa glycoprotein (GP 128) in reductive guanidine-hydrochloride extracts from human umbilical arteries that showed antigenic homology with thrombospondin. Electron microscope immunogold localization of both GP 128 and thrombospondin showed diffuse labeling, claimed to be associated with microfibrils, in the subendothelial matrix of the aorta and subepidermal matrix in the skin (Arbeille et al., 1991). Based on the localization of thrombospondin in the dermal-epidermal junction where fibrillin positive microfibrils are known to be located (Dahlbäck et al., 1990), and on the appearance of thrombospondin early in fetal development (O'Shea and Dixit, 1988)

unlike some microfibril-associated proteins (Khan and Walker, 1984; Dahlbäck et al., 1989), it was concluded that thrombospondin must be considered as a constituent of microfibrils (Arbeille et al., 1991). However, immunogold localization of GP 128 and thrombospondin did not appear to label elastin-associated microfibrils and preferentially labeled interconnecting regions of fine "microfibrils" (8 nm diameter) in the subendothelial matrix in the aorta (Arbeille et al., 1991). In addition, the immunofluorescence localization of thrombospondin at the dermal-epidermal junction appeared closely associated with the basal surface of the epidermal cells with no fluorescence apparent in the dermal connective tissue (Wight et al., 1985). In contrast, immunofluorescence localization of fibrillin in the dermal-epidermal region has shown an extensive network of fibers throughout the dermis and fine fibrils radiating from the dermis to the dermal-epidermal junction (Dahlbäck et al., 1990). Furthermore, although thrombospondin was shown by immunofluorescence to be present in fetal tissues (O'Shea and Dixit, 1988), no specific association of thrombospondin to microfibrils was demonstrated. These facts suggest that further investigation is needed to determine the relationship of thrombospondin to microfibrils. In any event, microfibrils associated with elastin in arterial elastic laminae have been shown to be thrombogenic (Birembaut et al., 1982; Fauvel et al., 1983; Fauvel-Lafeve et al., 1988), and since microfibril-induced platelet aggregation can be inhibited by both anti-GP 128 and anti-thrombospondin (Fauvel-Lafeve et al., 1988), it appears that thrombospondin may be an important microfibril-associated protein, particularly in the aortic intima.

#### *1.2.2.4 Microfibril-associated proteins*

Microfibrils appear to be associated with a number of different proteins. These proteins have often caused difficulty in attempts to establish the true constituents of microfibrils. Proteins identified as microfibril-associated proteins include a) fibronectin, b) amyloid P component, c) vitronectin and d) lysyl oxidase.

a) Fibronectin: Fibronectin has been immunolocalized to elastin-associated microfibrils in the aorta (Kraus, 1983; Goldfischer et al., 1985) and skin (Fleischmajer and Timpl, 1984) and to microfibrils of the ciliary zonule which are devoid of elastin (Goldfischer et al., 1985; Inoue et al., 1989). In reductive guanidine-hydrochloride extracts from ciliary zonular fibrils, fibronectin was found to be present along with the "microfibrillar proteins" suggesting that fibronectin was tightly associated to the microfibrils (Streeten and Gibson, 1988). Similarly, antiserum raised against "insoluble microfibrillar proteins" isolated from calf aortic smooth muscle cell cultures showed reactivity to microfibrils as well as to fibronectin (Schwartz et al., 1985). When this antiserum was absorbed with fibronectin, it reacted positively with microfibrils in young cultures; however, as the cells reached confluency the microfibrils no longer reacted with the absorbed antiserum. In contrast, fibronectin showed a reaction that became more intense with growth of the culture. These results suggested that microfibrils initially deposited in the extracellular matrix become increasingly coated with fibronectin (Schwartz et al., 1985). This was further demonstrated by ability of the absorbed antiserum to react positively with the microfibrils of a confluent culture following the dissociation of fibronectin from the microfibril surface by treatment of the cultures with

urea (Schwartz et al., 1985). Since fibronectin is known to have binding sites for cell surfaces, collagen and proteoglycans (Hynes, 1985; Yamada et al., 1985), its role on the surface of microfibrils is likely as an adhesive protein to aid in the association of microfibrils to cells and other extracellular matrix components.

b) Amyloid P component: Breathnach and colleagues (1981) demonstrated by immunolocalization that serum amyloid P component, which is apparently identical to tissue amyloid P component (Skinner et al., 1980; Baltz et al., 1986), was located on elastin-associated microfibrils in human skin and blood vessels. Similarly, amyloid P component was localized on microfibrils of the ciliary zonule by immunoperoxidase and immunogold labeling (Inoue et al., 1986a). Amyloid P component isolated from Engelbreth-Holm-Swarm tumor and negatively stained showed 8.5 nm pentagonal units with a central lumen (Inoue et al., 1986b). These units were often observed "stacked" in rod-like structures with a center-to-center distance of 4 nm. Based on the immunolocalization of amyloid P component to microfibrils in mature mice and on the remarkable ultrastructural similarities between microfibrils and isolated amyloid P component, Inoue and colleagues (1986a) proposed that amyloid P component constitutes the central core of ciliary zonular microfibrils. However, Khan and Walker (1984) demonstrated that amyloid P component did not appear to be associated with any structural component, including microfibrils, in normal human skin until after 2 years of age. Similarly, amyloid P component was not detected on microfibrils in neo-natal human skin or on microfibrils in bovine fetal tissues (Gibson and Cleary, 1987). In addition, studies using 2 year old human aorta showed amyloid P component to be localized mainly to the

intima and adventitia, whereas MAGP co-distributed with elastic fibers throughout the vessel wall (Gibson et al., 1986). From these results, it appears that amyloid P component is a microfibril-associated protein and not likely a major core constituent.

Breathnach and colleagues (1989) demonstrated the ability to extract amyloid P component from normal adult human dermis using chaotropic agents alone, whereas MAGP was only extractable using both chaotropic and reducing agents. These results suggests that the majority of amyloid P component is non-covalently bound to the microfibril. Recently, immunofluorescence localization of fibrillin and amyloid P component in the subepidermal region of normal adult skin showed both proteins to be distributed in microfibril bundles in the dermis, whereas only fibrillin was found to be present in the microfibrillar bundles near the dermal-epidermal junction (Dahlbäck et al., 1990).

Minute 3 nm particles have been observed in association with microfibrils in the foot pad and in the posterior chamber of the eye in mouse (Inoue, 1991). These particles, termed "pentosomes", are usually aligned in rows at intervals of 10 nm and are often interconnected by a fine filament. The pentosomes were shown to stain positively for the presence of amyloid P component by an immunoperoxidase technique (Inoue, 1991). In addition, negatively stained preparations of purified amyloid P component showed the pentagonal unit of amyloid P component to consist of 5 subunits identical in structure to pentosomes; thus the pentosomes observed in connective tissue were proposed to be subunits of amyloid P component. Treatment of adult mouse eyes with heparitinase, nitrous acid or magnesium chloride caused a disruption to the linear structure of the

ciliary zonule microfibrils and an increase in associated pentosomes (Inoue et al., 1991). These results, together with the observation of pentosomes associated with microfibrils in normal connective tissue, have suggested that amyloid P component is associated with microfibrils and may be important for their structural integrity (Inoue, 1991; Inoue et al., 1991). Furthermore, amyloid P component may play an important role in the organization of microfibrils by its ability to bind fibronectin (de Beer et al., 1981; Rostagno et al., 1986; Inoue et al., 1989) and in the overall maintenance of extracellular matrix architecture through calcium-dependent binding to glycosaminoglycans (Hamazaki, 1987).

c) Vitronectin: Vitronectin has been demonstrated immunohistochemically to co-localize with elastic fibers in normal human skin and kidney (Dahlbäck et al., 1986, 1987). Immunogold localization at the electron microscope level showed the presence of vitronectin closely associated to elastin-associated microfibrils (Dahlbäck et al., 1989). However, vitronectin immunolabeling could not be detected in human skin from subjects younger than six years of age suggesting that, like amyloid P component, vitronectin is deposited on microfibrils in an age-dependant manner (Dahlbäck et al., 1989). Vitronectin was also shown to co-localize with amyloid P component on dermal elastin-associated microfibrils, whereas microfibril bundles immediately subjacent to the epidermis showed only presence of fibrillin (Dahlbäck et al., 1990). These results provide evidence that vitronectin is an adsorbed protein and not a constituent of microfibrils. Since vitronectin is an adhesive glycoprotein, it has been suggested that elastin-associated vitronectin may be important for cell migration or anchorage (Dahlbäck et al., 1990).

d) Lysyl oxidase: Lysyl oxidase is a catalytic enzyme necessary for the formation

of cross-linkages that stabilize both elastin and collagen fibers (Kagan and Trackman, 1991; see section 1.3.3). Ultrastructural immunolocalization of lysyl oxidase in aortic connective tissue demonstrated the presence of the enzyme at the interface between the amorphous elastin and the peripheral microfibrils of elastic fibers; however, microfibrils bundles distant from elastin did not react with the anti-lysyl oxidase antibody (Kagan et al., 1986). In contrast to these results, Baccarani-Contri and colleagues (1989), showed no specific localization of lysyl oxidase antibodies to elastin-associated microfibrils in human placenta, skin and aorta. When lysyl oxidase antibodies were associated with elastic fiber, the localization was mostly over the amorphous elastin. Since immunolocalization was scarce in tissues of young subjects and practically absent in adult tissues, it was suggested that their may be an age-related expression of the enzyme or that the epitope may become masked with development (Baccarani-Contri et al., 1989). The apparent association of lysyl oxidase with elastin-associated microfibrils suggests that the enzyme may function at such sites to cross-link newly synthesis tropoelastin to the developing elastic fiber (Kagan and Trackman, 1991). Further experimentation, however, is needed to better establish the distribution of lysyl oxidase and its association with elastic fiber microfibrils.

Recently, a new 36 kDa microfibril-associated protein (36 kDa MAP) has been isolated and characterised from porcine aorta (Kobayashi et al., 1989). Both light and electron microscope immunolocalization of 36 kDa MAP showed the distribution of the glycoprotein to be restricted to microfibrils in the aortic adventitia; with no localization in skin, liver, placenta and esophagus (Kobayashi et al., 1989). The reason for 36 kDa

MAP to be specifically localized to aortic adventitial microfibrils is unknown. In a similar manner, thrombospondin has been shown to be preferentially located at the dermal-epidermal junction of skin and in the subendothelial matrix of the aorta (Wight et al., 1985).

The selective distribution of microfibril-associated proteins to microfibrils suggests that some constituent(s) of microfibrils may differ in different regions; however, the widespread distribution of fibrillin (Sakai et al., 1986) and MAGP (Gibson et al., 1986) suggests that at least some constituents may be ubiquitous. Whether microfibrils constitute a family of structures or whether they are a single entity remains to be established. Future research concerning microfibrils will not only allow identification of their constituent proteins, but will aid in the understanding of the role of microfibrils in elastogenesis and cell anchorage, and provide valuable information concerning the association of microfibrils with connective tissue diseases, such as scleroderma (Fleischmajer et al., 1991c) and Marfan syndrome (Dietz et al., 1991; Lee et al., 1991).

## 1.3 ELASTIC FIBER FORMATION

### 1.3.1 SYNTHESIS AND SECRETION OF TROPOELASTIN

The appearance of elastin occurs early in embryonic life as elastic tissues, such as the aorta, lungs and skin, develop in preparation for post-natal demands. In the aorta, early growth of the vessel wall commences with the formation of several mesenchymal cell layers closely apposed to the endothelium (Nakamura, 1988). As these mesenchymal cells begin to differentiate to form myoblasts and fibroblasts, an active secretory apparatus becomes evident. The specific cell types involved in this early elastogenesis remained controversial for some time (Serafini-Fracassini, 1984). Multiple cell types were suggested to be responsible for elastin synthesis in the aorta (Takagi, 1969; Thyberg et al., 1979); however, other investigators believed only smooth muscle cells to be involved (Kadar et al., 1971). More recently, evidence supporting a multiple cell type involvement in elastin synthesis has come from studies that demonstrate intracellular labeling for elastin precursor molecules in endothelial cells, smooth muscle cells and fibroblasts (Damiano et al., 1984; Daga-Gordini et al., 1987). The endothelial cell cytoplasm was found to react positively for the presence of elastin precursor molecules even prior to that of myoblasts and before the appearance of extracellular elastin deposits (Daga-Gordini et al., 1987).

The formation of elastin involves the synthesis and secretion of tropoelastin; a

soluble precursor molecule that becomes tightly cross-linked in the extracellular space to form insoluble elastin fibers. Early radioautographic investigations of the secretory pathway of elastin demonstrated that the rough endoplasmic reticulum and Golgi apparatus were involved in the synthesis of tropoelastin (Ross and Klebanoff, 1971; Gerrity et al., 1975). In an attempt to further explore the synthesis and secretion of elastin, Thyberg and colleagues (1979) used electron microscopy and cytochemical methods to investigate the production of elastin by endothelial cells, smooth muscle cells and fibroblasts in the aortic wall of young mice. These investigators found small vesicles with electron dense cores in the vicinity of the Golgi apparatus and cell periphery in all three cell types. The amorphous material of the dense core had staining properties identical to that of elastin and similar material was observed within the cisternae of rough endoplasmic reticulum and Golgi saccules. The presence of tropoelastin in the rough endoplasmic reticulum, Golgi apparatus and vesicles containing electron dense material was confirmed by immunolocalization studies of tropoelastin in cells of the embryonic chick aorta (Damiano et al., 1984; Daga-Gordini et al., 1987). Additional support for a Golgi-dependant pathway comes from studies showing that monensin, a cationophore that inhibits the transfer of secretory proteins from the cis to trans elements of the Golgi apparatus (Ledger and Tanzer, 1984), causes tropoelastin secretion to be suppressed in rat smooth muscle cells (Frisch et al., 1985) and embryonic chick aortic cells (Saunders and Grant, 1985). These results demonstrate that tropoelastin appears to follow the classical pathway for protein synthesis and secretion.

Large vesicles observed most frequently near the cell periphery have also shown

a positive immunoreaction for tropoelastin (Damiano et al., 1984). The label is primarily associated with electron dense material contained within the vesicles which are especially prevalent during maximal elastin deposition (Daga-Gordini et al., 1987). Although the functional implications of such vesicles are unresolved, their morphology and their close association with smaller vesicles is suggestive of a specific involvement in the storage and secretion of tropoelastin (Thyberg et al., 1979; Damiano et al., 1984; Daga-Gordini et al., 1987). Two pathways for the secretion of tropoelastin may thus exist; one involving a direct migration of small vesicles newly emerged from the Golgi apparatus to the plasma membrane, and the other involving a shuttle of small vesicles to larger vesicles for storage near the cell periphery prior to secretion (Damiano et al., 1984). The movement of tropoelastin containing vesicles does not appear to involve the use of microtubules as it has been demonstrated that agents such as colchicine, which depolymerize microtubules, do not disrupt or inhibit tropoelastin secretion (Saunders and Grant, 1985).

Secretory vesicles containing tropoelastin presumably release their contents into the extracellular space by exocytosis. Both small and large vesicles, showing positive immunoreactions for tropoelastin, have been observed closely apposed to the cell membrane where they appear to fuse to discharge their contents (Damiano et al., 1984). Vesicles in the process of exocytosis, however, are rarely observed by electron microscopy. A similar lack of exocytic profiles has been reported in fibroblasts actively involved in collagen synthesis and has been attributed to the rapidity of the exocytic process (Marchi and Leblond, 1983). In contrast, exocytosis is clearly observed in both odontoblasts (Weinstock and Leblond, 1974) and osteoblasts (Weinstock, 1975) and

appears associated with an abundance of coated pits and vesicles at the cell surface. A similar accumulation of coated pits and vesicles has been noted in fibroblasts actively producing tropoelastin in the ligamentum nuchae (Fahrenbach et al., 1966). Although the possibility existed that the coated vesicles were involved in the secretion of tropoelastin, the membrane flow concept of Palay (1963) suggested that coated vesicles may represent membrane circulating between the cell surface and internal membrane systems and thus some question as to the directionality of the process was raised. Recently, immunolabeling evidence has demonstrated that coated pits and vesicles of embryonic chick aortic cells only weakly label for tropoelastin thus suggesting that these organelles are not directly involved in the secretion of the elastin precursor molecule (Daga-Gordini et al., 1987). The coated pits and vesicles may therefore be remnants of the exocytic process and may exist to function in instantaneous membrane retrieval possibly associated with the maintenance of membrane integrity.

### **1.3.2 DEPOSITION OF ELASTIN - ELASTIC FIBER ASSEMBLY**

#### ***1.3.2.1 Stages of elastin deposition***

Pre-natal elastogenesis in the rat aorta has been divided into four distinct "phases" based on morphological observations (Nakamura, 1988). Similar "stages" of elastogenesis have been defined in the chick aorta combining morphological data with immunocytochemical labeling of tropoelastin (Daga-Gordini et al., 1987). The ability to

detect intracellular tropoelastin immunocytochemically has allowed earlier events of elastogenesis to be perceived and thus, combined with morphological evidence, has provided a more complete sequence of this process.

The four stages outlined by Daga-Gordini and colleagues (1987) are: a pre-elastin stage, an initiation stage, the appearance of elastin and the maturation of elastic fibers. In the pre-elastin stage, the aorta is comprised of a continuous endothelium with several subjacent layers of mesenchymal cells. The extracellular matrix is scant and consists of few 10 - 12 nm microfibrils and smaller 6 - 8 nm filaments of irregular diameter and orientation. At this stage, there is no reactivity for tropoelastin except for a faint reaction in the endothelial cell cytoplasm. In the stage of initiation, mesenchymal cells increase in number around the endothelial cell layer. Some discontinuous basement membrane becomes apparent as the cells commence differentiation. A positive reaction for tropoelastin is localized to bundles of microfibrils; however, no visible elastin can be discerned at this stage. During the stage of the appearance of elastin, amorphous elastin deposits of variable diameter are observed among the bundles of microfibrils and filamentous material. Extracellular matrix components, such as collagen and proteoglycans, are also rapidly accumulating at this time (El-Magharaby and Gardner, 1972; Davidson et al., 1986). Immunolabeling of tropoelastin is localized to the elastin deposits and to microfibril bundles not yet in association with elastin. In the final stage of development, the elastin deposits expand by direct apposition of tropoelastin and subsequently fuse to form mature fibers.

### *1.3.2.2 Role of microfibrils*

The association of microfibrils with the biogenesis of elastic fibers is accepted, although the precise nature of the ultrastructural and functional interrelationship between the two components remains uncertain. In the developing elastic fiber, 10 - 12 nm microfibrils are abundant at the periphery of the amorphous elastin and to a lesser extent within its substance. As the fiber matures, however, the relative proportion of microfibrils to elastin decreases; the adult fiber being only sparsely surrounded by a microfibrillar mantle (Prosser and Mecham, 1988).

The presence of microfibrils precedes that of elastin in the extracellular space during early embryonic development of elastic fibers (Fahrenbach et al., 1966; Greenlee et al., 1966; Ross and Bornstein, 1969; Cleary et al., 1981; Daga-Gordini et al., 1987). The microfibrils are observed throughout the intercellular space and are often organized into small bundles. Prior to the deposition of visible elastin in this area, anti-tropoelastin antibodies positively label the microfibrils (Daga-Gordini et al., 1987). Although this does not prove direct binding of tropoelastin molecules to microfibrils, it does suggest that microfibrils may have a central role in elastic fiber formation and organization. Later in development, characteristic amorphous elastin deposits appear in association with the microfibrils. These deposits label heavily for the presence of tropoelastin, however, the peripheral mantle of microfibrils is only slightly immunoreactive (Daga-Gordini et al., 1987). Stronger labeling of microfibrils persists, though, in regions where elastin deposits are still not yet morphologically evident. These findings have been interpreted to suggest that microfibrils may be involved in the initial organization and priming of elastin



deposition, which then may proceed in a more independent manner (Daga-Gordini et al., 1987). Although this is a prepossessing hypothesis, the supporting evidence is largely circumstantial.

Recently, another constituent of the extracellular matrix has been implicated in elastogenesis. A non-microfibrillar, basement membrane-like material has been observed in association with initial elastin deposition in the subendothelial space and surrounding smooth muscle cells (Lethias et al., 1988). This material is especially prevalent in various pathological conditions (Suzuki et al., 1980; Nikai et al., 1983). In the rat aorta, arterial grafts show elastin aggregates within basement membrane-like material that is apparently devoid of surrounding microfibrils (Lethias et al., 1988). Such observations suggest that a non-microfibrillar component of the extracellular matrix may be involved in early elastogenesis and that at least elastin deposition can occur independently of microfibrils.

The physical association of microfibrils and elastin is not well understood. During early embryonic elastogenesis, microfibrils and elastin deposits have been observed in close association with fine filamentous material of approximately 6 - 8 nm in diameter (Daga-Gordini et al., 1987). The possibility exists that such material may be partially responsible for the interaction between microfibrils and other extracellular matrix components. Recently, more definitive results concerning a microfibril-elastin association have come from work on a 67 kDa cell surface elastin-binding protein (Hinek et al., 1988; Mecham et al., 1989a; see section 1.4.1). As will be discussed in more detail below, this protein binds to both elastin (Wrenn et al., 1988) and galactoside sugars (Hinek et al., 1988). The bifunctional nature of the 67 kDa elastin-binding protein,

therefore, may be critical in the microfibril-elastin association, in that, it has a binding site(s) for elastin and may also bind with the highly glycosylated microfibrils (Prosser and Mecham, 1988).

In addition to other extracellular matrix components and the 67 kDa elastin-binding protein, the tropoelastin molecule may in itself directly interact with the microfibrils. A newly described carboxyl-terminal region of tropoelastin has recently been implicated as having a role in complexing the molecule with microfibrils (Wrenn et al., 1987).

#### *1.3.2.3 Role of the elastin-producing cell*

The functional relationship between the developing elastic fiber and elastin producing cells has been a matter of speculation. Electron microscopic observations have shown newly forming elastic fibers within folds or crevices of the plasma membrane of elastin synthesizing cells (Greenlee et al., 1966; Greenlee and Ross, 1967; Takagi and Kawase, 1967; Vaccaro and Brody, 1978). These observations lead to the suggestion that elastogenesis requires intimate contact between the plasma membrane of the elastogenic cell and the surface of the developing elastic fiber (Jacques and Serafini-Fracassini, 1985). Possibly, the cell can control the orientation of the fiber by secreting elastin and/or microfibrillar proteins over a specific cell surface area (Rosenbloom, 1987). This hypothesis is supported by the demonstration that newly synthesized elastin appears unevenly distributed on the surface of the elastic fibers; often forming continuous strips of variable width arranged in a helical pattern around the fiber (Jacques and Serafini-Fracassini, 1985). Since this observation is not consistent with a non-controlled, passive

process of elastic fiber formation, a special dynamic relationship between the elastin producing cells and the elastic fiber has been insinuated.

### 1.3.3 LYSYL OXIDASE

A high degree of cross-linking of individual tropoelastin molecules is crucial for the stabilization of the fibrous structure of elastin and to provide functional anchoring points vital to elastic properties. Upon reaching the developing elastic fiber, tropoelastin molecules are cross-linked; a process mediated by a copper-dependant metallo-enzyme, peptidyl lysine oxidase (lysyl oxidase). This enzyme deaminates selective lysine residues in the tropoelastin molecule to form allysine, which in turn reacts with a similar product on an adjacent molecule to form an allysine aldol cross-link. Two adjacent cross-links can then be oxidised without further enzymatic involvement to form the stable pyridinium rings of the desmosine and isodesmosine linkages characteristic of mature elastic fibers (Serafini-Fracassini, 1984; Gosline and Rosenbloom, 1984). These final cross-linking steps are likely a result of a series of spontaneous condensation reactions (Paz et al., 1982; Eyre et al., 1984). In addition to tropoelastin, lysyl oxidase is also responsible for similar enzymatic reactions in the initiation of collagen cross-linking (Siegel and Fu, 1976).

Highly purified lysyl oxidase, with a molecular weight of 30 - 32 kDa, has been isolated from bovine aorta and lung (Kagan et al., 1979, Cronlund and Kagan, 1986),

human placenta (Kuivaniemi et al., 1984) and rat lung (Almassian et al., 1990). Until recently, little has been known about the biosynthetic and intracellular processing events leading to the production of this enzyme. Sequence analysis of lysyl oxidase cDNA clones combined with immunoprecipitation and cell-free translation studies has now provided some information concerning the amino acid sequence and intracellular processing of lysyl oxidase (Trackman et al., 1990). Specifically, a putative 46 kDa lysyl oxidase precursor polypeptide has been identified that contains the sequence of the mature 32 kDa active enzyme (Trackman et al., 1990).

Tropoelastin secreted into the extracellular space is highly hydrophobic. The hydrophobic nature of this polypeptide is thought to be responsible, at least in part, for the self-aggregation tendencies of isolated tropoelastin observed *in vitro* under physiological conditions. Spontaneously formed aggregates often take the form of filamentous bundles with a substructure similar to that of natural elastic fibers (Volpin and Pasquali-Ronchetti, 1977; Bressan et al., 1983). *In vivo*, such a self-aggregation property would lead to the formation of random elastin deposits rather than organized elastic fibers. Newly secreted tropoelastin must, therefore, be prevented from interacting upon release from the cell until adjoined to the maturing elastic fiber by lysyl oxidase. Using lysyl oxidase inhibitors, the developing edges of the elastic fibers were found to be associated with glycosaminoglycan aggregates of abnormal number and size (Fornieri et al., 1987). Since the deamination actions of lysyl oxidase were inhibited, the highly negatively charged glycosaminoglycans appeared to remain bound to the positively charged amino groups of the tropoelastin molecules. Thus, the interaction of matrix glycosaminoglycans

with newly secreted tropoelastin molecules may prevent spontaneous elastin aggregation until the surface of the developing elastic fiber is reached and deamination by lysyl oxidase can occur.

Relatively few studies have provided information concerning the ultrastructural localization of lysyl oxidase. Siegel and colleagues (1978) demonstrated the presence of lysyl oxidase in the collagenous septae of fibrotic rat liver and in chick tendons using indirect immunofluorescence with antibodies to lysyl oxidase purified from chicken cartilage. In newborn rat and calf aortae, electron microscope immunolocalization of lysyl oxidase, using polyclonal antibodies raised in chicken against bovine aortic lysyl oxidase, showed the enzyme to be present at the surface of elastic fibers in association with microfibrils (Kagan et al., 1986). Microfibrils that were not in association with elastin did not label positively for the presence of lysyl oxidase, nor did collagen fibers in the same tissue. The same antibodies, however, did show a positive immunoreaction to collagen fibers reconstituted in vitro (Kagan et al., 1986). In direct contradiction to these results, Baccarani-Contri and coworkers (1989), using polyclonal antibodies to human placental lysyl oxidase, showed no specific immunolocalization of lysyl oxidase on or adjacent to elastin-associated microfibrils in human skin or aorta, while the immunoreaction on collagen fibers in both tissues was positive. A number of reasons for the discrepancy have been postulated, including the possibility that lysyl oxidase isolated from bovine aorta (Kagan et al., 1986) may be antigenically different than that isolated from human placenta (Kuivaniemi et al., 1984) with respect to elastin and collagen specificity (Baccarani-Contri et al., 1989). Recently, lysyl oxidase has been shown to be present in a number of

fibroblastic and non-fibroblast cells using immunofluorescence with a monoclonal antibody to lysyl oxidase purified from human umbilical cord (Wakasaki and Ooshima, 1990). A strong filamentous immunoreaction was also shown in cultured cells, suggestive of an association of lysyl oxidase with cytoskeletal proteins (Wakasaki and Ooshima, 1990). Clearly, considerable information concerning both the intracellular and extracellular distribution of lysyl oxidase remains to be established.

## 1.4 ELASTIN RECEPTORS

### 1.4.1 THE 67 kDa ELASTIN-BINDING PROTEIN

#### *1.4.1.1 Structural features*

The existence of a functional elastin receptor was suggested by early studies that showed that both interstitial and inflammatory cells could detect and move towards tropoelastin and elastin-derived peptides in chemotaxis assays (Senior et al., 1982, 1984). The chemotactic activity of elastin was found to be associated, at least in part, with the sequence Val-Gly-Val-Ala-Pro-Gly (VGVAPG) (Senior et al., 1984); a hydrophobic hexapeptide that repeats several times in one tryptic fragment of porcine tropoelastin (Sandberg et al., 1981). Direct evidence for an elastin-binding protein on the surface of elastin-producing cells that displays characteristics of a true receptor has come from tropoelastin binding studies with ligamentum nuchae fibroblasts (Wrenn et al., 1988). Results from these studies showed a time-dependent, saturable and reversible binding of tropoelastin to protease-sensitive sites on fibroblasts that occurs with a high affinity ( $K_d = 8 \text{ nM}$ ) comparable to receptor binding of other matrix proteins.

Detergent extracts of ligamentum nuchae fibroblast plasma membrane produce four polypeptides of molecular masses 67, 61, 55, and 43 kDa that bind to an elastin-affinity column (Wrenn et al., 1988). The 67 kDa protein displays properties of a peripheral membrane protein associated with the cell surface (Hinek et al., 1988). The 61 kDa and

55 kDa proteins have properties of integral membrane proteins and require detergent for extraction from cells. Extracellular iodination indicates that part of these proteins is exposed on the external cell surface, however, it is not known if one or both proteins span the membrane and are exposed to the cytoplasm (Mecham et al., 1989a). The 43 kDa protein has been identified as actin (Mecham et al., 1989a).

The 67 kDa protein was found to be the true elastin-binding protein. The 67 kDa protein can bind elastin in the absence of the 61 kDa and 55 kDa proteins, however, the 61 kDa and 55 kDa proteins can not bind elastin in the absence of the 67 kDa protein (Mecham et al., 1989a). Since the binding of the 61 kDa and 55 kDa proteins to elastin can be restored in the presence of the 67 kDa protein, the 67 kDa elastin-binding protein is thought to associate with the 61 kDa and 55 kDa proteins to form an elastin receptor complex (Mecham et al., 1989a).

In addition to cell-binding and elastin-binding sites, the 67 kDa protein is a galactoside-binding protein, suggesting it has lectin-like properties (Hinek et al., 1988; Mecham et al., 1989a,b). The 67 kDa protein can be eluted from an elastin column with lactose (Hinek et al., 1988; Mecham et al., 1989b) and dissociates from the surface of cultured elastin-producing cells by the addition of lactose or galactose to the media (Hinek et al., 1988). Thus, both the affinity of the 67 kDa protein for elastin and for the cell surface appears regulated to some extent by the occupancy of the carbohydrate binding site.

Recently, a high degree of similarity was found between the 67 kDa elastin-binding protein and a 67 kDa laminin-binding protein found on the surface of tumor cells that

synthesize laminin but not elastin (Mecham et al., 1989b). A 67 kDa collagen type IV-binding protein in neutrophils has also been identified (Senoir et al., 1989). All three proteins bind both laminin and elastin. Current research involves further characterization of the 67 kDa proteins to determine if the 67 kDa proteins are a family of receptors or a single receptor with multiple ligand-binding properties.

#### *1.4.1.2 Functions*

The definitive function(s) for the elastin receptor complex has yet to be established. The term "receptor" implies a functional involvement of signal transduction (Mecham et al., 1989a). The chemotactic response (Senior et al., 1984) and an alteration of ion fluxes (Jacob et al., 1987; Varga et al., 1988) seen in elastin-binding cells exposed to elastin peptides provides evidence that elastin binding indeed functions to initiate some biological response within the cell.

The elastin receptor complex also appears to play a significant role in elastic fiber formation; both intracellularly, in the secretory pathway and extracellularly, in elastic fiber assembly. Within the cell, the 67 kDa elastin-binding protein has been shown to colocalize with tropoelastin, suggesting that newly formed tropoelastin in the secretory pathway is bound intracellularly to the 67 kDa protein (Hinek and Mecham, 1990). The colocalization of these two proteins, together with the fact that elastic fiber assembly appears to be a non-random event at the cell surface (Jaques and Serafini-Fracassini, 1985; Mecham et al., 1989a), suggests that the 67 kDa protein may be involved in trafficking the tropoelastin molecules to the proper location on the cell surface (Mecham

and Heuser, 1991). Since tropoelastin is not glycosylated (Hinek et al., 1988), and thus does not have the ability to utilize sugar residues for intracellular segregation and sorting, this hypothesis provides a credible solution to the intracellular transport of tropoelastin.

The intracellular colocalization of the 67 kDa protein with tropoelastin may also serve to prevent tropoelastin molecules from forming aggregates within the cell (Mecham and Heuser, 1991). As previously discussed, tropoelastin is extremely hydrophobic and has a tendency to self-associate forming a coacervate under physiological conditions (Cox et al., 1974; Bressan et al., 1983, 1986). Although the property of coacervation may be important in the appropriate location of the extracellular space, it would cause severe problems within the secretory pathway of the cell.

In addition to functions within the cell, the 67 kDa protein has been demonstrated to play an important role in the extracellular assembly of elastic fibers. Immunolocalization of the 67 kDa protein has shown it to be present over the surface of cultured elastin-producing cells (Mecham et al., 1988; Hinek and Mecham, 1990). Electron microscope examination of chondrocyte cultures after the addition of lactose to the culture medium showed numerous small elastin deposits that were irregularly distributed and did not coalesce to form typical large elastic fibers (Hinek et al., 1988). Lactose binds to the 67 kDa protein at the galactoside sugar binding site and causes the 67 kDa protein to be released from the cell surface. Immunofluorescence localization of the 67 kDa protein on the surface of the lactose treated cells showed the protein to be distributed in an abnormal pattern (Hinek et al., 1988). The coincidental effects of altered 67 kDa protein distribution and abnormal elastic fiber formation in the presence of lactose

provides evidence that the assembly of elastic fibers at the cell surface is not a random event but is mediated by the elastin receptor complex.

The specific role of the elastin receptor complex in elastic fiber assembly remains to be established. It has been suggested that the 67 kDa protein may present the tropoelastin molecules on the cell surface in a manner conducive to elastic fiber assembly (Hinek et al., 1988). With multiple binding sites, the 67 kDa protein may also direct some specific interaction between the tropoelastin molecule and the highly glycosylated microfibrils (Hinek et al., 1988, Mecham et al., 1989a). Since the 67 kDa protein is critical for elastic fiber assembly but does not appear to be part of the final structure, the 67 kDa protein can be termed a "molecular chaperon" (Ellis, 1987). As a molecular chaperon, the 67 kDa protein may provide targeting signals for the intracellular sorting and secretion of tropoelastin, facilitate the correct folding of the molecule, present it on the cell surface in the correct orientation and assist in assembly of the elastic fiber (Hinek and Mecham, 1990). Although such a role for the 67 kDa protein is plausible from the existing evidence, in depth investigation of the individual steps involved in the secretion and ultimate assembly of tropoelastin must be examined.

Another function of the elastin receptor may involve cell movement and/or cell adhesion. Skin fibroblasts and aortic smooth muscle cells have been shown to strongly adhere to purified elastic fibers in culture (Hornebeck et al., 1986). In addition, lactose added to cultured fibroblasts can inhibit chemotaxis to elastin peptides suggesting a possible association of the receptor with cytoskeletal elements (Mecham et al., 1989a). This view is supported by the copurification of actin with the elastin receptor proteins

(Wrenn et al., 1988; Mecham et al., 1989a), although no direct interaction between actin and the receptor has been demonstrated.

Recently, additional evidence for an association of the elastin receptor complex with the cytoskeleton has come from observations of the movements of elastin-coated gold particles bound to the surface of live cells using video-enhanced microscopy (Mecham et al., 1991a). The elastin-coated particles were shown to undergo random motion after initial binding which was suddenly followed by a directed rearward transport towards the cell nucleus. The retrograde transport was shown to be in alignment with intracellular stress fibers, thus providing evidence that the elastin receptor complex has both a physical and functional relationship with the cytoskeleton. In addition, the elastin-coated particles associated with the cytoskeleton are unaffected by the presence of lactose, whereas those particles undergoing random motion show an increased dissociation from the cell surface (Mecham et al., 1991a). The fact that the cytoskeleton may provide information to the receptor complex that causes a deactivation of the carbohydrate binding site and a resultant increased affinity of the receptor for the ligand is suggestive of a bidirectional transfer of signals characteristic of a true receptor.

#### **1.4.2 OTHER ELASTIN-BINDING PROTEINS**

In addition to the 67 kDa elastin-binding protein (Hinek et al., 1988; Mecham et al., 1989a), two other cell surface proteins have been identified to bind elastin; a 120 kDa protein found on fibroblasts and smooth muscle cells that has been named

"elastonectin" (Hornebeck et al., 1986) and a 59 kDa protein found on a tumor cell line of the Lewis lung carcinoma (Blood et al., 1988).

Elastonectin is one of four proteins in the cell membrane of cultured human skin fibroblasts that adheres to purified elastic fibers added to the culture (Hornebeck et al., 1986). When isolated, these four elastin-binding proteins were shown to have molecular weights of 120, 67, 60 and 45 kDa. Although the 120 kDa protein was proposed to be directly responsible for elastin binding, specific binding properties of the protein have not been established. The later identification of four proteins involved in elastin binding in nuchal ligament fibroblast cell membranes (Wrenn et al., 1988) appeared consistent with those of Hornebeck and colleagues (1986). As described above, Wrenn and coworkers (1988) isolated proteins of 67, 61, 55 and 43 kDa. However, a 120 kDa could not be detected and further studies showed the 67 kDa protein to be the protein responsible for the elastin binding (Hinek et al., 1988; Mecham et al., 1989a).

The 59 kDa elastin-binding protein was identified on the cell surface of an invasive, metastatic tumor cell line by binding and subsequently cross-linking a radiolabeled tyrosinated VGVAPG peptide (the elastin recognition sequence) to the cell surface (Blood et al., 1988). Using elastin-affinity chromatography on solubilized tumor cell membranes, two other elastin-binding proteins were identified having molecular weights of 67 and 47 kDa. Only the 59 kDa protein was detected at VGVAPG concentrations appropriate for the binding and cross-linking studies; thus, the 59 kDa protein was suggested to either have a higher affinity for the VGVAPG peptide or be the only elastin-binding protein that can bind the peptide in its iodinated, tyrosinated form.

(Blood et al., 1988). Further studies showed that both the binding affinity of the 59 kDa protein and the chemotactic responsiveness of the tumor cells to the VGVAPG peptide is affected by levels of active membrane-associated protein kinase C (Blood and Zetter, 1989). In addition, a cytosolic rise in protein kinase C activity was observed when the tumor cells were exposed to the VGVAPG peptide, thus indicating that the 59 kDa protein had the ability of signal transduction. How the tumor cell 59 kDa elastin-binding protein relates to the 67 kDa protein aforementioned remains unclear.

## 1.5 ELASTIN KINETICS

The kinetics of a protein involve processes of turnover, degradation, remodeling and repair. Although each can be described individually, it is difficult to discuss these processes separately with respect to the properties of a particular protein since they often occur in conjunction.

Studies of elastin turnover have primarily involved measurements of changes in specific activity of radiolabeled elastin with respect to time. In early development, the specific activity is often seen to decrease due to dilution of the radiolabel by the addition of newly synthesized elastin. Whether the decrease is due entirely to growth or whether some turnover of elastin occurs during post-natal development, remains to be established. In the adult, elastin synthesis in most tissues has ceased and thus predictions of elastin turnover can be made with more accuracy. Increasing evidence suggests that elastin is remarkably stable with minimal new synthesis and turnover throughout adult life (Rucker and Tinker, 1977; Lefevre and Rucker, 1980; Dubick et al., 1981; Shapiro et al., 1991).

Degradation of elastin occurs by elastolytic proteinases (elastases) that have the ability to solubilize mature cross-linked elastin (Bieth, 1986). Since elastin appears to undergo little or no turnover in the adult, the physiological function of elastases is poorly understood. Under normal conditions, elastases may be utilized by phagocytic cells to break down foreign substances prior to ingestion, be secreted into the duodenum to aid in digestion, and play a role in wound repair after acute injury (Bieth, 1986). In most

cases, however, elastin degradation from the actions of elastases appears to result in pathological conditions. This can occur either by the release of elastases from inflammatory cells, or by a genetic deficiency in the physiological regulator of elastases,  $\alpha_1$ -antiprotease, which leads to pulmonary emphysema (Gadek et al., 1981).

Some degradation of elastin may be important in vascular remodeling of elastic fibers as a normal process during development. In the aorta, elastic laminae form complete rings around the circumference of the vessel prior to the completion of vessel diameter growth (Karrer, 1961; Gerrity and Cliff, 1975). Clearly, for the vessel to enlarge in diameter, the elastic laminae would have to stretch or break with the accretion or insertion of new elastin, respectively (Mecham et al., 1991b). Recently, *in situ* hybridization techniques have been used to demonstrate foci of cells that exist in the vessel wall that surround broken or fragmented ends of elastic laminae (Prosser et al., 1989). The smooth muscle cells that surround these cell nests show a positive reaction for the presence of tropoelastin; thus, these areas may be localized regions in the vessel wall where the elastic laminae are cut and newly synthesized elastin is added to allow for expansion of the elastic laminae during growth of the vessel (Mecham et al., 1991b).

Although remodeling of elastic fibers and elastic laminae plays an important role during normal development, vascular remodeling also occurs in a number of vascular diseases, such as atherosclerosis and hypertension. In atherosclerosis, elastase content is increased, the content of cross-linked elastin is decreased (Hornebeck et al., 1978) and fragmentation of elastic fibers within the media of arterial walls is observed (Bieth, 1986). Concomitant with these changes, is a proliferation of smooth muscle cells in the vessel

intima and an accumulation of extracellular matrix proteins, including elastin, which results in the formation of an atherosclerotic plaque (Ross, 1981). In hypertension, there is a thickening of the vessel wall due to an increased production of elastin and other extracellular matrix proteins (Wolinsky, 1970).

Remodeling changes in vascular architecture appear to be at least partially in response to changes in arterial blood pressure. The mechanical force of stretch alone has been shown to provide a signal to smooth muscle cells which is transduced into expression of the elastin gene and reproducible stimulation of tropoelastin synthesis (Sutcliffe and Davidson, 1990). In addition, increased blood pressure may result in vascular damage leading to leakage of cellular or plasma factors into the vessel wall (Mecham et al., 1991b). Pulmonary artery smooth muscle cells isolated from hypertensive animals have been shown to produce one or more elastogenic factors which can stimulate the production of elastin in both fibroblasts and smooth muscle cells from normotensive animals (Mecham et al., 1987).

The fact that smooth muscle cells can be reactivated to commence elastin synthesis in a mature vessel, suggests the potential for elastin fiber repair following injury. However, the smooth muscle cells that produce excess elastin in both atherosclerosis and hypertension are phenotypically altered cells which produce different connective tissue components than do the normal cells (Mecham et al., 1991b). In addition, the elastin produced in response to injury is often morphologically disorganized and may be inappropriate for, or even impair, normal function (Kuhn et al., 1976; Rucker and Dubick, 1984; Prosser and Mecham, 1988).

## **1.6 THESIS OBJECTIVES**

### **1.6.1 HYPOTHESIS**

The fundamental hypothesis of this thesis is that aortic endothelial cells and smooth muscle cells are intimately associated with elastic laminae with structural connections that are functionally important to cope with the mechanical stresses imposed upon the vessel wall. Since microfibrils have been implicated to have a role in cell anchorage, are located in tissues subjected to mechanical tension, and are predominant structures in the developing aortic wall, it is hypothesized that microfibrils are a major component involved in cell to elastic lamina attachments in the aortic media and intima. Finally, since smooth muscle cell to elastic lamina connections are important for the normal dynamics of the vessel, it is proposed that the connections formed during development are metabolically stable, and thus, aortic elastin undergoes little or no turnover.

### **1.6.2 PLAN OF THE THESIS**

Chapter one is an extensive literature review on elastic fiber components, organization and formation. It is intended to provide the reader with a background on elastin, microfibrils and the process of elastogenesis. Chapters two to five each contain an introduction, methods, results, figures and discussion.



Chapter two provides a detailed investigation of aortic smooth muscle cell ultrastructure and specifically deals with the association of elastic laminae with the smooth muscle cells. The attachment of the smooth muscle cells to the interposed elastic laminae is studied throughout development and the structural and functional implications of such attachments are discussed. The relationship of extracellular matrix components and intracellular structures is addressed with respect to overall structural organization of the aortic media. A schematic model of this organization is presented.

Chapter three describes ultrastructural features of the aortic endothelial cells and extracellular structures in the subendothelial matrix. The association of the endothelial cells with the subjacent elastic lamina in the developing aortic wall is investigated in detail. Distinct bundles of filaments, seen to connect the abluminal membrane of the endothelial cell to the surface of the underlying elastic lamina early in development, are studied with respect to morphology and relationship with intracellular structures. The functional implications of endothelial cell connecting filaments are discussed.

Chapter four presents immunoelectron microscopic localization of microfibril and microfibril-associated proteins in the aortic intima in the attempt to identify the nature of the endothelial cell connecting filaments. The immunolabeling results are discussed with respect to the known composition of microfibrils and the role of microfibrils in cell anchorage and tissue stability.

Chapter five provides information concerning the stability of aortic elastin based on longterm radioautographic experimentation. Radiolabel incorporated into the elastic laminae early in post-natal development and investigated at progressively older ages

provides qualitative and quantitative information concerning distribution and turnover of elastin. Elastin synthesis and stability are discussed with respect to elastic lamina growth and normal development.

Chapter six provides a summary of the results obtained from the individual chapters. The results are related to one another to provide an overview concerning the association of endothelial cells and smooth muscle cells to elastic laminae in the mouse aortic wall, the structures involved in these associations and the role and stability of such associations in the developing and mature vessel.

References for all chapters are assembled at the end of the thesis.

***CHAPTER TWO***

***ULTRASTRUCTURAL FEATURES OF THE DEVELOPING MOUSE AORTIC  
MEDIA: SMOOTH MUSCLE CELL - ELASTIC LAMINA ASSOCIATION***

## 2.1 INTRODUCTION

The aortic wall is subjected to changing mechanical stresses both in development and throughout adult life. Within the vessel wall, smooth muscle cells provide an active contractile component, while elastin and collagen form stress distributing and stress bearing systems, respectively (Wolinsky and Glagov, 1964; Gerrity and Cliff, 1975). How these components are structurally and functionally integrated to provide the necessary stability and resilience of the vessel remains to be established.

Aortic media structural components are organized in an orderly manner; circumferential smooth muscle cell layers alternating with interposing elastic laminae. Wolinsky and Glagov (1964) demonstrated that under increasing intraluminal distending pressures the elastic laminae undergo uniform progressive straightening throughout the aortic wall. Further studies showed that the average tension per elastic lamina is nearly constant regardless of animal weight, aortic diameter or medial thickness (Wolinsky and Glagov, 1967). The constant tension and ability of the aortic media to respond in a coordinated manner to mechanical stress suggests that some system of organized connections likely exists between smooth muscle cells and elastic laminae.

Early studies of aortic media ultrastructure showed that smooth muscle cells in one cell layer are arranged parallel to one another and that the orientation of the cells changes direction from one cell layer to the next (Pease and Paule, 1960). Relatively few models, however, have been proposed to describe any detailed organization of the overall arrangement of the cell layers and interposing elastic laminae. Wolinsky and Glagov

(1967) suggested that the aortic media was composed of concentric "lamellar units"; each consisting of an elastic lamina and immediately adjacent interlamellar structures. In a later study, the lamellar unit was redefined and a model was described depicting the aortic wall organized into repeating "musculo-elastic fascicles"; with each smooth muscle cell layer and adjacent elastic laminae representing one fascicle (Clark and Glagov, 1985). Although such models have provided some information concerning the overall structural organization of the aortic media, specific ultrastructural details concerning smooth muscle cell to elastic lamina attachments are lacking.

A close association of elastin and filamentous material with the smooth muscle cell membrane was noted by early investigators of aortic wall ultrastructure (Karrer, 1960; Pease and Paule, 1960; Paule, 1963). One interpretation of this observation was that the regions of close apposition of elastic fibers to the cell membrane represented sites of elastic fiber formation (Karrer, 1960). However, the observation of elastic fibers at a distance from the smooth muscle cell, that appeared to develop independent of the cell surface, raised some question as to the method of elastic fiber assembly. A second interpretation suggested that elastic fibers adjacent to the smooth muscle cells were physically attached to the cell membrane (Pease and Paule, 1960). Within the smooth muscle cell, contractile filaments were observed to anchor in "patches" of enhanced electron density along the inner surface of the cell membrane (Pease and Paule, 1960; Wolinsky and Glagov, 1964). These membrane-associated dense plaques were suggested to be areas of specialization for adhesion of the cell to the elastic fibers (Fahrenbach et al., 1966). Such an association was confirmed by studies of aortic medial integrity under

conditions of hyperdistension which showed the adhesion of smooth muscle cells to elastic laminae at membrane-associated dense plaques to be even stronger than the forces of cell membrane cohesion (Clark and Glagov, 1979). Furthermore, it was proposed that these connection sites were responsible, at least in part, for the transmission of tensile stresses throughout the vessel wall (Clark and Glagov, 1979). Thus, it is generally accepted that aortic smooth muscle cells form a structural association with adjacent elastic laminae; however, to date, no extensive morphological studies have been undertaken to investigate the development or ultrastructural components involved in such associations.

In the present chapter, general ultrastructural features of the developing mouse aortic smooth muscle cell are described. In particular, connections between smooth muscle cells and elastic laminae are investigated with respect to structural development and overall organization within the adult vessel wall. Results from this study demonstrate that the association of smooth muscle cells to elastic laminae commences early in development with the formation "contractile-elastic units". These units span from one elastic lamina to the next and remain as functional tension-bearing structures in the adult vessel. The ordered arrangement of contractile-elastic units observed in the present study provides evidence for aortic medial organization.

## **2.2 MATERIALS AND METHODS**

### **2.2.1 TISSUE DISSECTION**

Thoracic aortae from C57/BL mice were used for all ultrastructural studies. Due to the need to examine structures in both cross-sectional and longitudinal planes, the vessel was dissected so that these planes could be easily identified. Each aorta was dissected free of any extraneous tissue and cut into 4 - 8 segments depending on the length of the vessel. For the purpose of orientation, these initial segments were cut so that the length of each segment was greater than the width. Each segment was then cut in half along the longitudinal axis of the vessel. This resulted in the formation of two rectangular pieces of tissue; the short edge of which was the cross-sectional surface of the vessel and the long edge was the longitudinal surface.

### **2.2.2 PREPARATION OF EPON EMBEDDED TISSUE**

Mice of post-natal ages 1 day, 5 days, 21 days and 3 months were anaesthetized with sodium pentobarbital and prepared for cardiac perfusion. Each mouse was perfused through the left ventricle with lactated Ringer's until the liver was cleared of blood. Immediately, the perfusing solution was changed to 3% glutaraldehyde buffered with 0.1

M sodium cacodylate (pH 7.4) at a pressure in the physiological range. After 5 minutes of perfusion, the thoracic aorta was removed and dissected as previously described. The tissue pieces were then placed in fresh fixative at room temperature for an additional 2 hours.

Pre-natal mice aortae were also prepared for Epon embedding. Pregnant C57/BL mice, at 15d gestation, were anaesthetized with sodium pentobarbital and the mouse pups were removed. Thoracic aortae were dissected from the pups, cut into segments and placed in 3% glutaraldehyde buffered with 0.1 M sodium cacodylate (pH 7.4) for 2 hours at room temperature.

The tissue pieces were rinsed, following fixation, in several changes of 0.1 M sodium cacodylate (pH 7.4) and stored overnight at 4°C in a fresh change of buffer. The following day, the tissue pieces were post-fixed for 1 hour in 1% osmium tetroxide buffered with 0.1 M sodium cacodylate, rinsed in 3 changes of cacodylate buffer over 30 minutes and treated for 1 hour with 2% tannic acid in 0.1 M sodium cacodylate to enhance electron density and contrast (Wagner, 1976). After 3 washes of 10 minutes each in double distilled water, the tissue pieces were stained en bloc with 2% aqueous uranyl acetate for 1 hour. The post-fixation steps involving osmium tetroxide, tannic acid and uranyl acetate were all carried out at 4°C.

Following post-fixation, the tissue pieces were rinsed in several changes of double distilled water for a total of 10 minutes. The tissue pieces were then dehydrated in a graded series of methanol which involved 5 minutes in each of the following methanol dilutions: 10%, 20%, 40%, 60%, 80%, 90%, 95%, 2x100% methanol. After the last

rinse in 100% methanol, the tissue pieces were rinsed twice in 100% propylene oxide for 5 minutes each.

Infiltration of the tissue with Epon (M.E.C.A. Lte., Montreal, Que.) involved 3 changes of propylene oxide:Epon mixtures; a 3:1 ratio mixture for 1 hour, a 1:1 ratio mixture for 2 hours and a 1:3 ratio mixture overnight. The Epon solution consisted of 23.0 gm of Epon 812, 14 gm of nadic methyl anhydride (NMA), 13 gm of dodecenyl succinic anhydride (DDSA) and 1.0 ml of DMP-30. All infiltration steps were carried out at room temperature on a rotating device. The next day, the tissue was placed in a pure solution of Epon and left for 6 hours under vacuum. The tissue pieces were then embedded in fresh Epon with either the cross-sectioned or longitudinal surface of the vessel at the face of each block.

For light microscopy, 0.5  $\mu\text{m}$  sections were cut with a glass knife on a Reichert ultracut microtome and placed on a clean, bare glass slide. The slide was placed on a hot plate until the water surrounding the sections had completely evaporated and the sections were dry. The warm slide was then stained with toluidine blue for 10 seconds, rinsed under a stream of distilled water and left to air dry.

Straw to silver thin sections, cut with a diamond knife on a Reichert ultracut ultramicrotome, were placed on 200-mesh copper grids. Sections were counterstained to contrast elastin according to the method of Franc and colleagues (1984). Briefly, the grids were immersed in 7% uranyl acetate in absolute methanol for 2 - 5 minutes. This solution could be stored for several weeks protected from the light at 4°C. The grids were then gently rinsed in 3 successive baths of absolute methanol; approximately 10 dips in each

bath over a total of 45 seconds. This step is critical as excessive or rapid dipping results in a loss of sections from the grid. Excess methanol was removed from the grids by touching the edge of the grid to filter paper after each bath. After drying, the sections were further contrasted by staining for 2 minutes with lead citrate (Reynolds, 1963).

The thin sections were examined in a Philips 301 transmission electron microscope at an accelerating voltage of 80 kV.

## 2.3 RESULTS

### 2.3.1 DEVELOPING MOUSE AORTIC WALL - 5-DAY POST-NATAL AGE

#### *2.3.1.1 General histological features*

The wall of the developing aorta consists of an endothelium, tunica media and tunica adventitia; typical of mature blood vessels (Fig. 2-1).

The endothelium is characterized by a single layer of squamous cells (Fig. 2-1). The cells are roughly ovoid in shape with the long axis parallel to the long axis of the vessel. Details concerning endothelial cell organization and ultrastructure will be dealt with in Chapter 3.

The tunica media is composed of usually four, but occasionally five, smooth muscle cell layers; each one cell thick, interposed with concentric elastic laminae. Smooth muscle cells characteristically "wrap around" the lumen of blood vessels, thus a vessel cut in longitudinal section reveals cross-sectional profiles of the smooth muscle cells (Fig. 2-2), whereas a vessel cut in cross-section reveals smooth muscle cells cut in longitudinal section (Figs. 2-1, 2-3). The smooth muscle cells are rectangular in shape; although the ends are tapered and overlap so as to form a continuous layer of relatively uniform thickness around the circumference of the vessel (Figs. 2-1, 2-3). At this stage of development, smooth muscle cells are occasionally seen in contact across the intercellular region by small projections that extend through gaps in the incomplete elastic laminae

(Fig. 2-3). Dividing cells are not uncommon within the smooth muscle cell layer (Fig. 2-3).

Thin elastic laminae surrounded by connective tissue elements separate the adjacent smooth muscle cell layers. Although the elastic laminae clearly demarcate distinct smooth muscle cell layers, the laminae adjacent to the adventitia occasionally branch causing the formation of an additional layer (Fig. 2-3). Less commonly, elastic laminae may terminate resulting in the unification of two smooth muscle cell layers; often this occurs in association with a dividing cell (Fig. 2-4). The elastic laminae have an irregular outline with extensions of elastin and discrete elastin deposits being common in the intercellular region between the laminae and adjacent smooth muscle cells (Figs. 2-3, 2-4). The first elastic lamina, in the subendothelial region, appears most advanced in development with regard to thickness and uniformity; those in successive layers become progressively thinner and discontinuous (Figs. 2-1, 2-2). No extensions of elastin are seen to transect the smooth muscle cell layers to join successive elastic laminae.

The tunica adventitia consists of a thin layer of randomly arranged stellate-shaped fibrocytes interposed with bundles of collagen fibers and elastin deposits (Fig. 2-5). The collagen bundles are most often oriented parallel to the long axis of the vessel and are thus seen as bundles of cross-sectioned collagen profiles when observed in the adventitia of a vessel cut in cross-section. Subjacent to the last smooth muscle cell layer of the tunica media, the final elastin lamina is usually not well formed, thus making the border of the tunica media and tunica adventitia difficult to distinguish (Fig. 2-5). Occasionally, nerve bundles can be seen among the fibrocytes in the adventitia (Fig. 2-5).

### **2.3.1.2 Smooth muscle cell ultrastructure**

The smooth muscle cells of the 5-day old mouse aortic media are rectangular in shape with tapering ends that overlap to form a continuous single layer of cells interposed between two elastic laminae (Fig. 2-1). The nucleus occupies the center of the cell where it fills much of the intracellular region (Figs. 2-1, 2-2). Along the cell membrane, membrane-associated dense plaques and caveolae, inpocketings of the cell membrane, are observed (Fig. 2-6). Dense plaques and caveolae are common features of all smooth muscle cells.

The smooth muscle cells are somewhat atypical in that they generally lack a well defined basement membrane. In some regions, no basement membrane can be seen apposed to the plasma membrane (Fig. 2-6a). In other regions, a typical basement membrane may be seen associated with the cell surface; however, often at some point it will leave the cell surface and extend into the extracellular matrix or will appear to disintegrate into a fine network of basement membrane-like material (Fig. 2-6b). A complete basement membrane that associates with the plasma membrane for any considerable length is rarely observed (Fig. 2-6c). Regions of the plasma membrane that are devoid of basement membrane are often occupied by membrane-associated dense plaques with contractile filaments present in the adjacent cytoplasm (Fig. 2-6a). Those regions possessing a basement membrane usually contain groups of caveolae (Figs. 2-6b and c).

At this stage of development, the intracellular features of the smooth muscle cells consist of an extensive Golgi apparatus with associated rough endoplasmic reticulum,

secretory vesicles, mitochondria and developing bundles of contractile filaments.

The Golgi apparatus is located at either pole of the nucleus; often in a triangular region bordered by microfilaments, mitochondria, and cisternae of rough endoplasmic reticulum (Fig. 2-7). In this region, several Golgi stacks are usually seen situated among a multitude of small vesicles that vary in diameter from 40 - 60 nm (Figs. 2-7, 2-8a). Also included within this area are numerous vesicles, approximately 140 nm in diameter, with electron-dense cores (Figs. 2-7, 2-8a and b). These small dense core vesicles are frequently seen adjacent to the trans face of the Golgi stack. Within the stack, the saccules often have dilated ends that contain electron dense material similar in appearance to that of the dense core material within the small vesicles (Figs. 2-8a and b).

Small dense core vesicles in the vicinity of the plasma membrane are not uncommon (Figs. 2-9a and b); however, exocytic profiles of such vesicles have not been observed. At the cell membrane, numerous coated pits in various stages of endocytosis are frequently seen (Figs. 2-9b and c). In the adjacent cytoplasm and throughout the cell, electron lucent coated vesicles are evident (Fig. 2-9d). Thus, the coated pits and vesicles may be remnants from exocytosis of the small dense core vesicles.

Large dense core vesicles, similar to the small dense core vesicles, are seen in the Golgi region and elsewhere throughout the smooth muscle cell cytoplasm (Fig. 2-10). These vesicles are 350 - 400 nm in diameter and may be found alone or in small groups. Occasionally, a small dense core vesicle may be observed near or in contact with a large dense core vesicle (Fig. 2-11).

The developing contractile system within the smooth muscle cell consists of

discrete bundles of microfilaments interposed with glycogen granules and cell organelles (Fig. 2-12). The microfilament bundles are almost exclusively oriented oblique to the long axis of the cell. Individual bundles can be traced, in entirety, from one side of the cell to the other (Fig. 2-12). Although regions of enhanced electron density can occasionally be observed among the microfilaments, no organization as well defined as striated muscle sarcomeres is evident. At the cell membrane, the contractile filaments insert and anchor in membrane-associated dense plaques (Figs. 2-13a and b). On the extracellular face of the dense plaques, connective tissue elements form a close association with the cell surface.

#### *2.3.1.3 Intercellular features*

The most prominent feature of the intercellular region in the aortic media is the elastic laminae. However, between the elastic laminae and the cell surface numerous other structures are evident. These include small elastin deposits, isolated collagen fibers, collagen bundles, microfibrils and a delicate network of small filaments.

The appearance of the elastic laminae seen in cross-sections of the aortic wall, is notably different than that observed in longitudinal sections of the vessel. In cross-section (Fig. 2-14a), the border of the elastic lamina appears relatively smooth. Small extensions of elastin are often seen to project obliquely from the surface of the elastic lamina towards the smooth muscle cell (Figs. 2-14a, 2-18a). The intercellular region between the elastic laminae and the smooth muscle cell surface contains relatively few isolated elastin deposits.

In sections of the aortic wall cut parallel to the longitudinal axis of the vessel, the surface of the elastic laminae has an irregular appearance (Fig. 2-14b). Rather than a solid band of elastin, the elastic lamina appears to be composed of a multitude of elastin deposits that have merged to give the lamina a distinctive lobular appearance. Due to the highly irregular border of the elastic laminae, extensions of elastin towards the smooth muscle cells are difficult to distinguish. No extensions are observed to extend obliquely towards the smooth muscle cell; however, some extensions, that appear as merged elastin deposits, can be observed to extend perpendicularly from the elastic laminae towards the smooth muscle cell (Fig. 2-14b).

Isolated collagen fibers and collagen bundles are frequently observed between the elastic laminae and the smooth muscle cell surface (Figs. 2-15a and b). Considerable variation is seen in the size of the collagen bundles and in the diameter of individual collagen fibers. In between the collagen fibers composing a bundle, small filaments are observed which appear to link the collagen fibers together (Figs. 2-15a and b). The majority of individual collagen fibers and bundles are oriented parallel to the cross-sectioned surface of the vessel. Thus, like the smooth muscle cells, the collagen fibers appear to "wrap around" the circumference of the vessel. Isolated collagen fibers and bundles are most often observed in the intercellular region between the elastic laminae and the cell surface (Fig. 2-15a). However, collagen bundles and individual collagen fibers can also be seen embedded within the amorphous elastin of the elastic laminae (Fig. 2-15b).

At the surface of the elastic laminae, elastin associated microfibrils are frequently

observed (Figs. 2-16a and b). The microfibrils appear to be oriented in a similar manner to that of the smooth muscle cells and collagen fibers, such that they extend along the surface of the elastic laminae around the circumference of the vessel. From this mantle of microfibrils, a delicate network of small filaments extends to the cell surface and encompasses all the structures located between the cell and the elastic lamina (Fig. 2-17).

#### ***2.3.1.4 Smooth muscle cell - elastic lamina association***

The site of association of the smooth muscle cells and the elastic laminae is at the region of membrane occupied intracellularly by membrane-associated dense plaques. The extracellular face of the dense plaques forms an intimate association with bundles of microfibrils that extend from the elastic lamina to the cell surface. At this point in development, the microfibril bundles are infiltrated with elastin so as to form extensions of elastin from the surface of the laminae (Fig. 2-18a). However, the microfibrils at the distal end of the extensions often remain free of elastin. Within the cell, the contractile filaments that anchor in the plaque have the same orientation as the extracellular elastin extensions and microfibrils (Fig. 2-18a). All contractile filament bundles within one cell have the same orientation. The intracellular contractile filaments and extracellular elastin extensions that attach the cell on either side to adjacent elastic laminae form a "contractile-elastic unit".

The contractile-elastic units are oriented in the circumferential plane of the vessel. Thus, when the longitudinal axis of vessel wall is observed, the elastin extensions and contractile filaments are seen in cross-section. The elastin extensions observed in cross-

section appear as isolated elastin deposits. However, the microfibrils at the cell surface do not appear as a round bundle, rather they appear spread out in a layer that covers the surface of the cell membrane in the region that overlies a dense plaque (Fig. 2-18b). In addition to forming a lateral association with the cell surface in this region, the microfibrils also appear to have extensive lateral associations between one another. This association appears to involve the electron-dense material that coats the microfibrils.

### **2.3.2 DEVELOPMENTAL CHANGES IN THE SMOOTH MUSCLE CELL - ELASTIC LAMINA ASSOCIATION**

#### ***2.3.2.1 Fetal aorta - 15-days gestation***

The aortic wall at 15 days of gestational age has already developed the three regions characteristic of the mature vessel; tunica intima, tunica media and tunica adventitia (Fig. 2-19). The differentiating smooth muscle cells in the tunica media are organized in circumferential layers. In most areas, the four smooth muscle cell layers observed in the adult are already present. Each layer is only one smooth muscle cell thick, with the longitudinal axis of the cells oriented perpendicular to the long axis of the vessel. Subjacent to the endothelial cells, the first elastic lamina consists of numerous bands of elastin separated by small gaps (Fig. 2-19). Although very thin, this first elastic lamina is almost continuous, even at this early stage of development. Between the successive smooth muscle cell layers, the elastic laminae are progressively less developed; increasing

elastin deposits rather than bands of elastin and larger gaps between the amorphous elastin are evident.

The smooth muscle cells in the fetal aorta appear relatively undifferentiated. Within the cells, only a few bundles of contractile filaments can be observed. These bundles often terminate at the cell membrane and appear to anchor in membrane-associated dense plaques (Fig. 2-20). On the extracellular face of the dense plaque, microfibrils form a close lateral association with the cell surface. Microfibrils are also seen at the periphery of the bands of elastin and often extend across gaps between two elastin bands. The microfibrils that form the association with the smooth muscle cell membrane at the dense plaque appear to be an extension of the those surrounding the developing elastic lamina (Fig. 2-20). These microfibrils thus form link from the elastic lamina to the cell surface.

#### *2.3.2.2 Post-natal aorta - 1-day*

The four circumferential layers of smooth muscle cells are well defined in the 1 day post-natal aortic wall (Fig. 2-21). Interposed between these cell layers, the elastic laminae are almost complete. Although there are still numerous gaps along the length of the elastic laminae, the laminae are thicker and more regular in appearance than those observed in pre-natal aortae.

The smooth muscle cells still contain an abundance of organelles and vesicles, however, characteristic features typical of smooth muscle cells are more evident. Bundles of contractile filaments oriented obliquely to the longitudinal axis of the cell are observed

(Fig. 2-21). These bundles terminate at the cell membrane where they anchor in membrane-associated dense plaques. As in pre-natal aortae, extracellular bundles of microfibrils extend from the developing elastic laminae to the cell surface in this region (Fig. 2-22). The microfibrils form a lateral association with the cell membrane on the extracellular face of the dense plaque. At this stage of development, amorphous deposits of elastin have infiltrated the microfibril bundle (Fig. 2-22).

### *2.3.2.3 Post-natal aorta - 21-days*

The smooth muscle cells in the aortic media of the 21-day old mouse appear fully differentiated. The cytoplasm is almost exclusively filled with contractile filaments. Individual contractile filament bundles are now difficult to discern; however, large groups of filaments are often separated by mitochondria and the few organelles that remain in the cytoplasm. (Fig. 2-23a). The surface of the smooth muscle cell, occupied by caveolae and membrane-associated dense plaques, is usually serrated in appearance. The contractile filaments of the cell obliquely cross the longitudinal axis of the cell and anchor in the dense plaques distributed along either side. The microfibril bundles are almost completely infiltrated with elastin to form elastin extensions that radiate from the elastic laminae to the cell surface (Fig. 2-23a). Some variation as to the degree of infiltration exists; often microfibrils can be observed to extend to the cell surface from the distal end of the elastin extension (Fig. 2-23b). In the regions of the membrane occupied by the dense plaques, both microfibrils (Fig. 2-23b) and/or elastin (Fig. 2-23c) can be seen to associate with the cell surface. The contractile-elastic units, formed by elastin extensions, associated

microfibrils, and the intracellular contractile filaments, are always aligned in the same direction.

#### *2.3.2.4 Adult aorta - 3 months*

At the level of the light microscope, extensive areas of the aortic wall can be examined. In the cross-sectional plane of the vessel (Fig. 2-24), elastin extensions radiate out from each elastic lamina towards the interposing smooth muscle cells. On either side of one elastic lamina, the elastin extensions radiate in the same circumferential direction. This orientation of elastin extensions alternates in direction from one elastic lamina to the next thus forming a herringbone-like pattern.

Ultrastructural details of the arrangement of the elastin extension attachments to the smooth muscle cells can be seen by electron microscopy. Within the smooth muscle cells, the contractile filaments traverse the cell obliquely and anchor in membrane-associated dense plaques on either side of the cell. Continuing in the same oblique direction from the extracellular face of the dense plaques, the elastin extensions link the cell on either side to the adjacent elastic laminae. A continuous line of structures is thus formed which extends from one elastic lamina to the next. This line of structures represents a contractile-elastic unit. Due to the orientation of the elastin extensions on either side of one elastic lamina, the contractile-elastic units alternate in direction in successive smooth muscle cell layers (Fig. 2-25).

Since the elastin extensions are all oriented in the circumferential plane of the vessel, only cross-sectioned elastin extensions are seen when the longitudinal plane of the

vessel wall is examined. At the light microscope level, no elastin extensions are seen to radiate from the elastic laminae in the longitudinally sectioned aortic wall (Fig. 2-26). Instead, the border of the elastic lamina appears irregular and numerous isolated elastin deposits are observed adjacent to the smooth muscle cell membrane and in the extracellular matrix between the elastic lamina and the cell surface. By electron microscopy, the highly irregular nature of the border of the elastic lamina is more evident (Fig. 2-27). Isolated elastin deposits are observed both in the extracellular matrix and apposed to the smooth muscle cell surface. These isolated elastin deposits likely represent the elastin extensions that have been cut in cross-section at various levels from the elastic lamina to the cell surface.

**FIGURE 2-1:** Cross-section through the wall of a 5-day old mouse aorta. The wall consists of an endothelial cell layer (E), a tunica media usually composed of 4 smooth muscle cell layer (SM), however, 5 layers are not uncommon, and a tunica adventitia (A). Thin elastic laminae (EL) separate the smooth muscle cell layers. In this plane of section, the endothelial cells are cut in cross-section while the smooth muscle cells are cut in longitudinal section. The smooth muscle cell layers are one cell thick and are relatively uniform due to overlapping of the tapered ends of the cells (arrows). L, lumen; F, fibrocyte. x4,180.

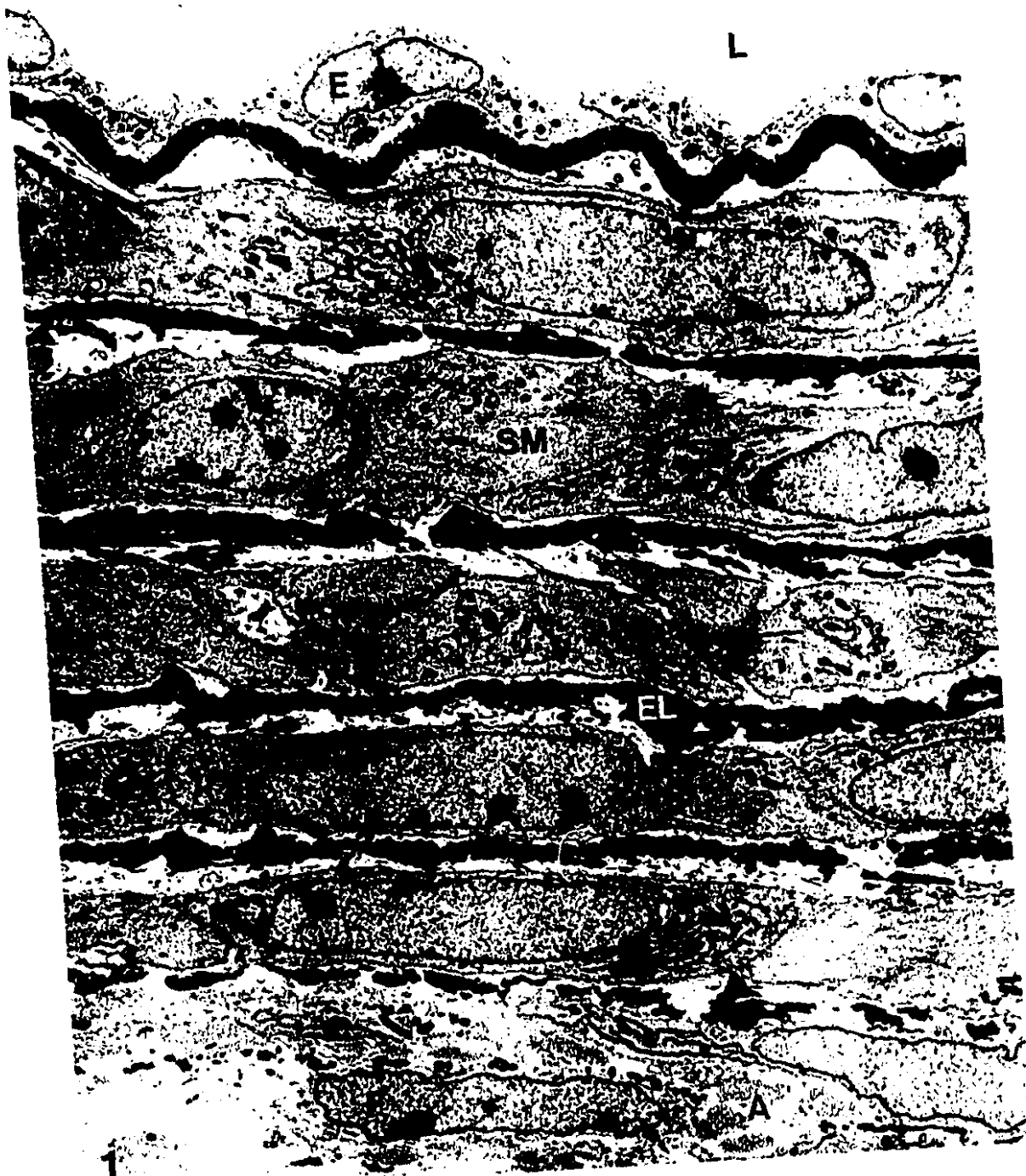


**FIGURE 2-2:** Longitudinal section through the wall of a 5-day old mouse aorta. In this plane of section, the smooth muscle cells (SM) are cut in cross-section. Note that the elastic laminae (EL) are less developed and appear less complete from the luminal side of the vessel to the adventitia. Among the elastic laminae in the intercellular space are numerous collagen bundles (coll). L, lumen; E, endothelial cell. x4,180.

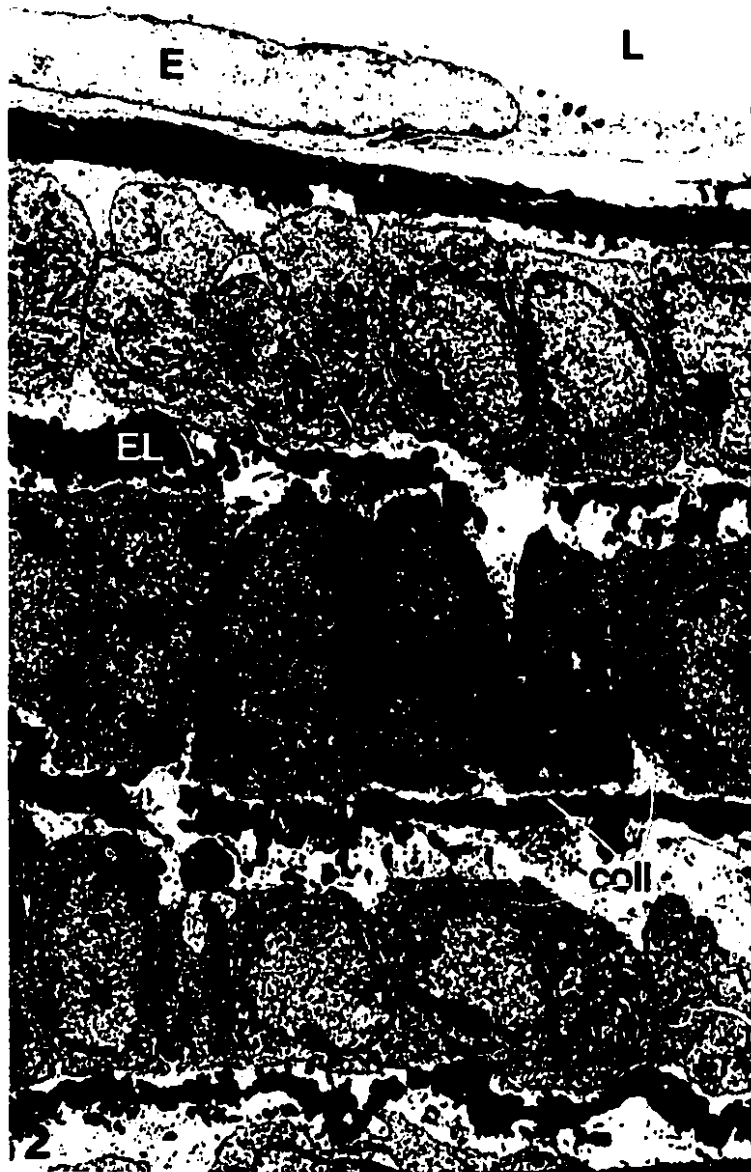


**FIGURE 2-3:** Cross-section of a 5-day old mouse aortic wall showing developmental features. **Box A:** Smooth muscle cells (SM) from adjacent cell layers occasionally remain in contact through gaps in the elastic laminae (EL). **Box B:** At this stage of development, dividing smooth muscle cells within the media are occasionally seen. **Box C:** Although the elastic laminae clearly delimit individual cell layers, the laminae closest to the adventitia (A) frequently merge or branch to form a total of 4 or 5 smooth muscle cell layers, accordingly. E, endothelial cell. x4,180.



**FIGURE 2-4:** Cross-section of a 5-day old mouse aorta showing a portion of the aortic wall where an elastic lamina (EL), next to a dividing smooth muscle cell (SM), appears to terminate. L, lumen; E, endothelial cell. x6,300.



**FIGURE 2-5:** Cross-section of a 5-day old mouse aorta showing the tunica adventitia underlying the outermost smooth muscle cell layer (SM) and elastic lamina (EL). Stellate-shaped fibrocytes (F), with highly attenuated cytoplasm, are seen dispersed among large bundles of collagen (coll), elastin deposits (ed) and the occasional nerve bundle (NB). x9,900.



**FIGURE 2-6:** The edge of smooth muscle cells (SM) and the adjacent elastic lamina (EL) in the aortic media of a 5-day old mouse showing variations in basement membrane organization. **(a)** In some areas, the plasma membrane of the smooth muscle cell appears completely devoid of basement membrane. This appears to occur most often along regions of the plasma membrane that are associated with dense plaques (dp) and adjacent contractile filaments (cf). **(b)** Some regions of the plasma membrane are associated with basement membrane (BM), however, the basement membrane often either deviates from the cell surface or breaks up to form a diffuse network (asterisk). **(c)** Only on a rare occasion will a basement membrane be seen in association with the cell surface for any considerable length. Most often, regions of the smooth muscle cell membrane that are associated with basement membrane are occupied by caveolae (cav). x47,200.

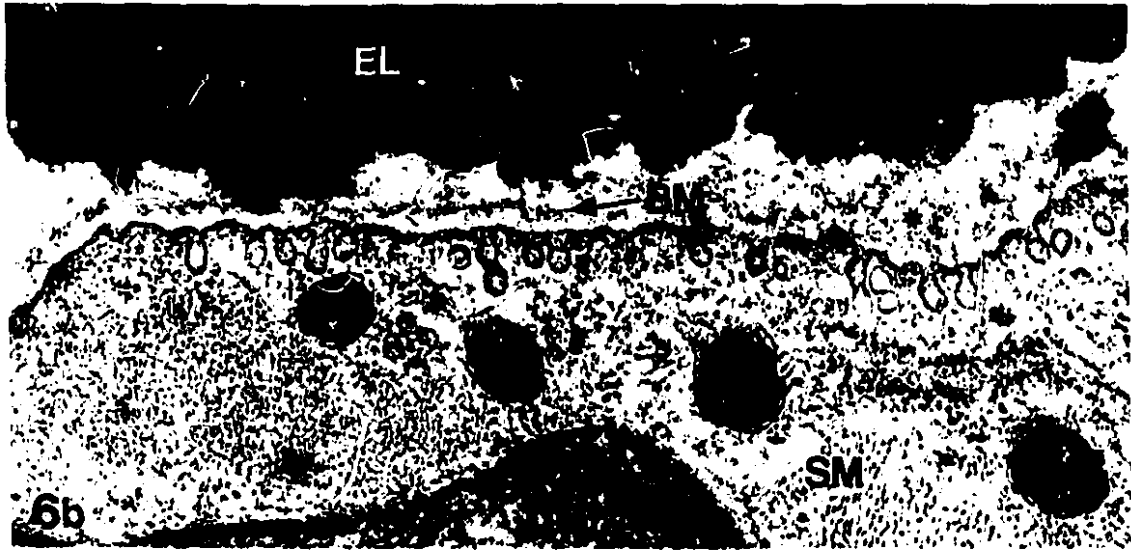
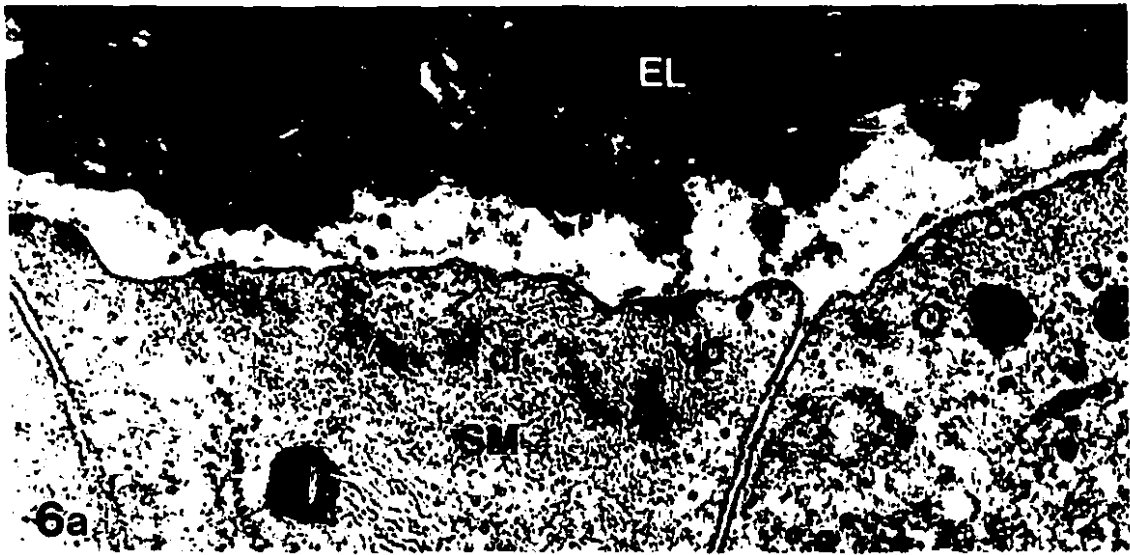


**FIGURE 2-7:** Longitudinal section through a portion of a smooth muscle cell in a 5-day old mouse aorta. An extensive Golgi region (G) is located at the pole of the nucleus (N). The Golgi region contains several Golgi stacks and a multitude of coated and uncoated small vesicles. Some dense core vesicles (dcv) can also be observed close to the Golgi stacks. At the perimeter of the Golgi region are cisternae of rough endoplasmic reticulum (rER), mitochondria (m) and contractile filaments (cf). Note the lack of a well defined basement membrane surrounding the smooth muscle cell. EL, elastic lamina. x24,200.

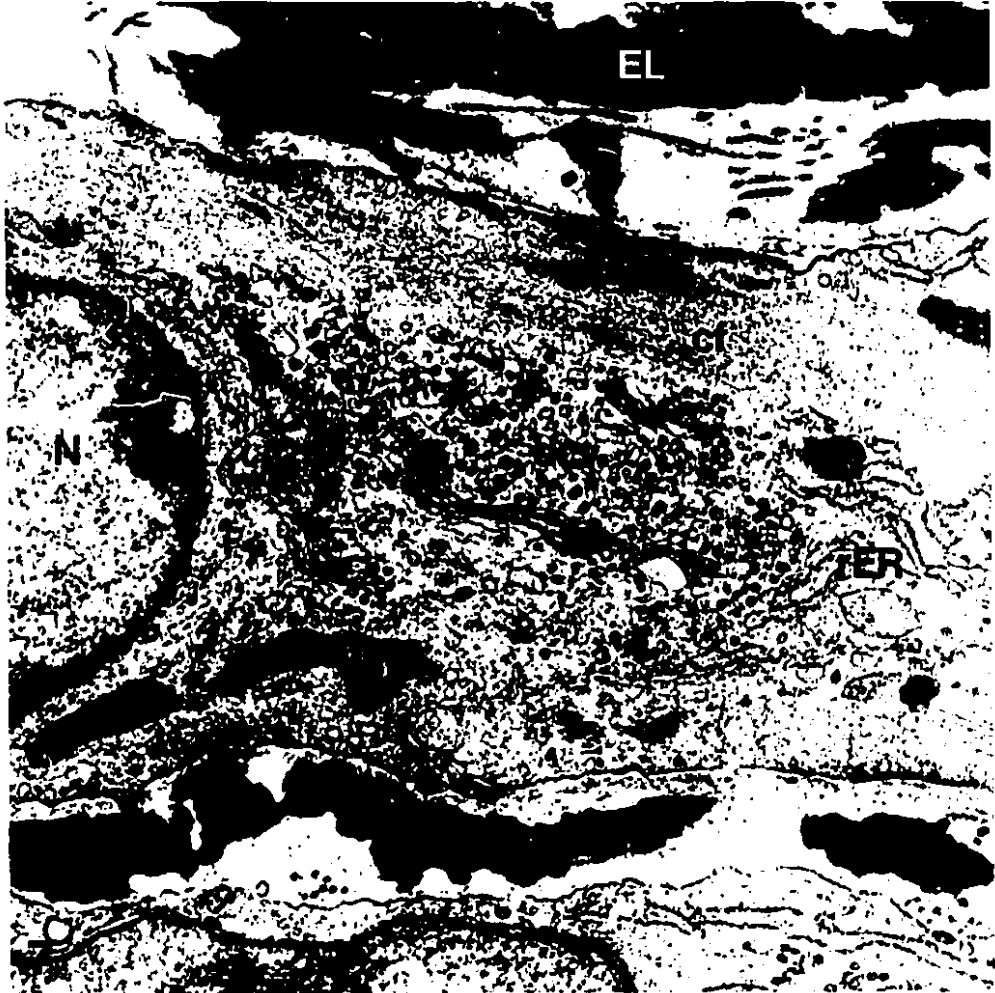


**FIGURE 2-8:** Two Golgi regions in cross-sectioned smooth muscle cells in a 5-day old mouse aorta. (a) Many small vesicles and several dense core vesicles (dcv) can be seen in an area surrounded by three Golgi stacks (G). Within the dilated ends of the Golgi saccules, electron dense material is evident (arrowheads). Some dense core vesicles appear to be budding from portions of the Golgi saccules (bv). In the extracellular space, numerous elastin deposits (ed) can be seen. (b) The Golgi stack (G) is surrounded by dilated cisternae of rough endoplasmic reticulum (rER). A dense core vesicle (dcv) is seen in close association with the adjacent Golgi saccule. EL, elastic lamina; cf, contractile filaments; m, mitochondria. x43,750.

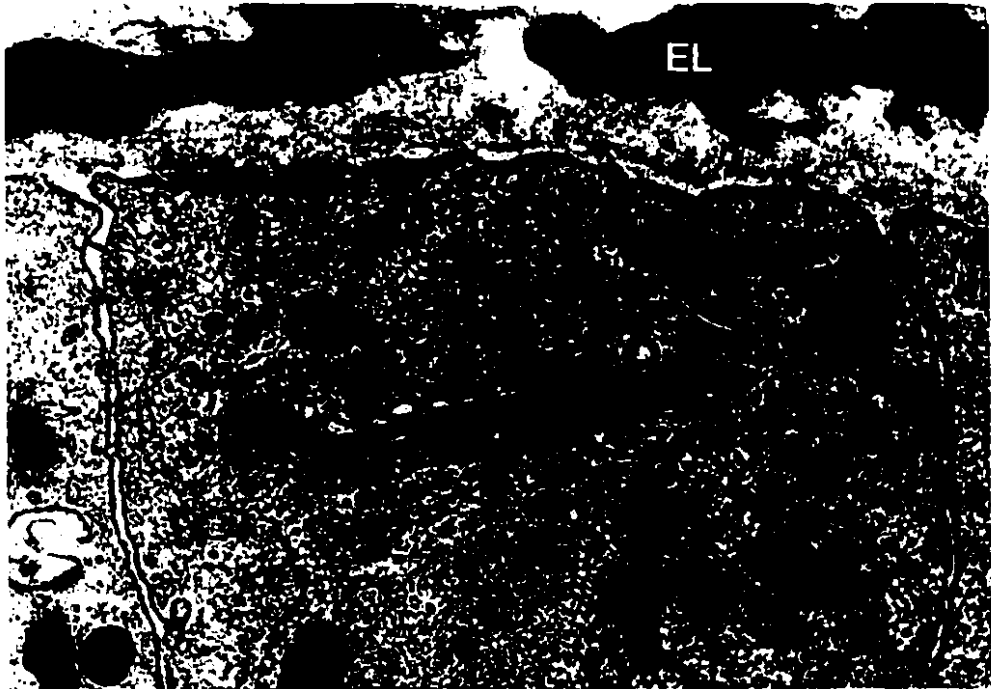
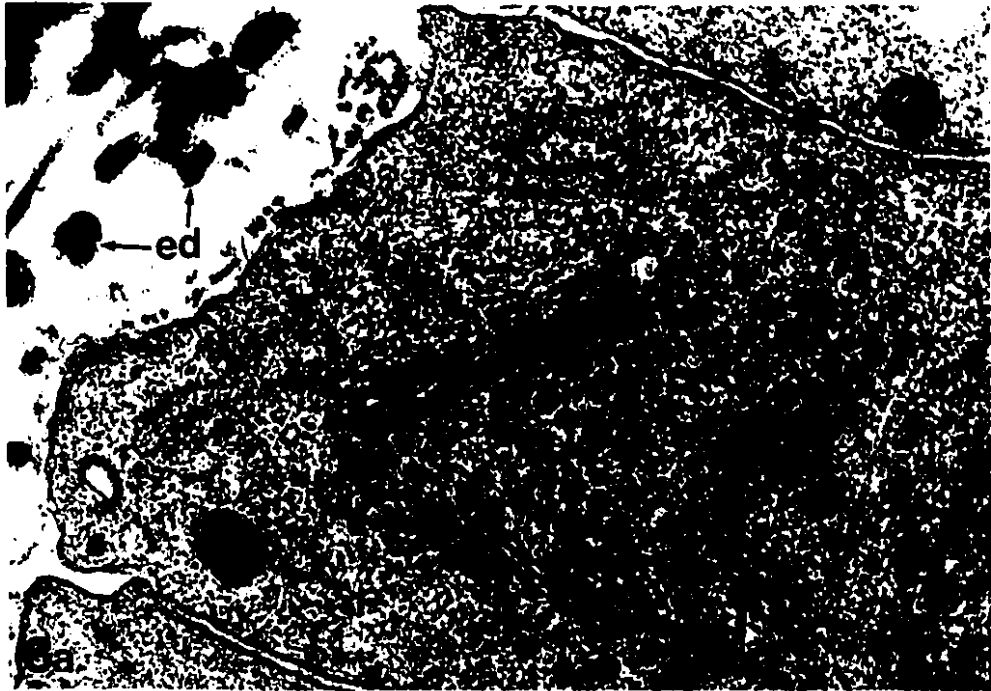
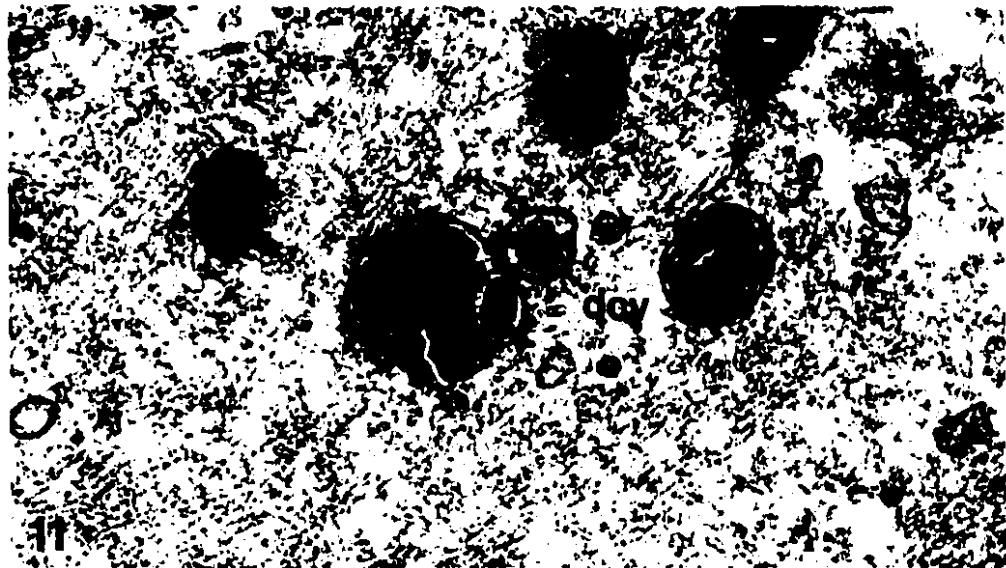
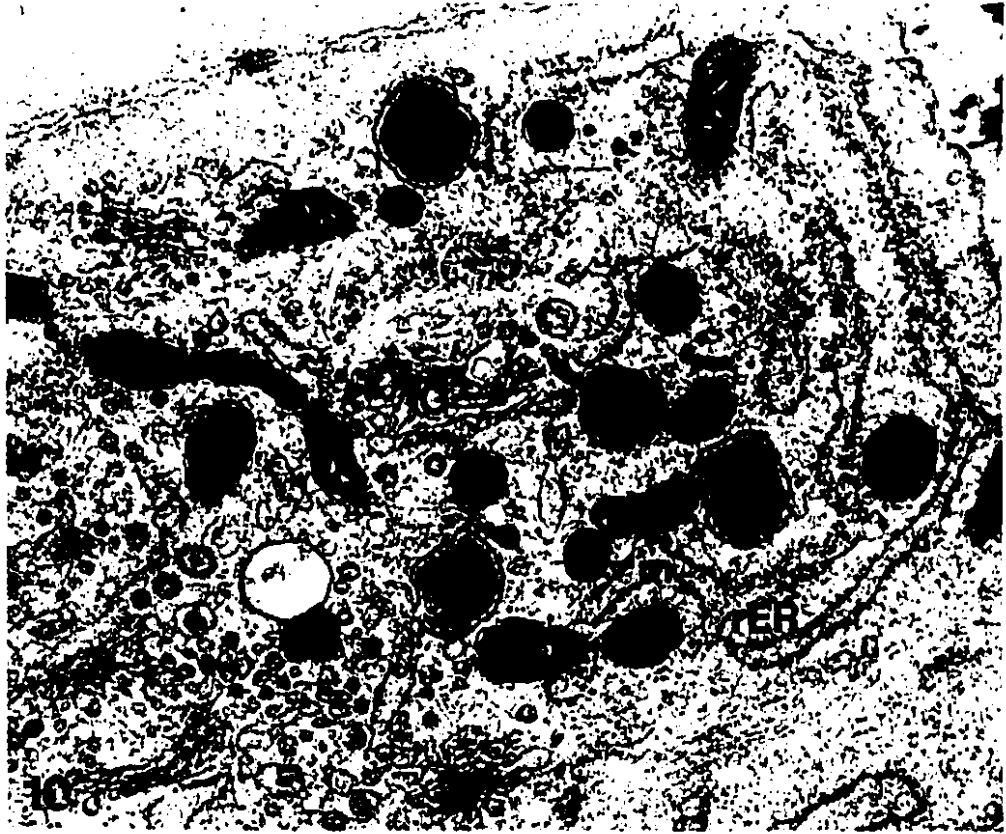


**FIGURE 2-9:** Four regions of smooth muscle cells in a 5-day old mouse aorta showing structures present at the plasma membrane. **(a)** A dense core vesicle (dcv) among caveolae (cav) and microtubules (mt) at the plasma membrane (arrowheads). **(b)** A coated pit (cp) at the plasma membrane closely associated with an extracellular amorphous elastin deposit (ed) and microfibrils (mf). Note the presence of a dense core vesicle (dcv) close to the plasma membrane. **(c)** A coated pit (cp) in the final stage of endocytosis. **(d)** Two coated vesicles (cv) near the plasma membrane; one is sectioned through the electron lucent center and the other has only been grazed along the surface by the plane of section. These four micrographs present a credible series of events for the exocytosis of the content of the dense core vesicles into the extracellular matrix: **(a)** dense core vesicles approach the plasma membrane; **(b)** release their contents and the vesicle membrane becomes coated to form a coated pit; **(c)** the coated pits are drawn into the cell; **(d)** which results in the intracellular presence of an electron lucent coated vesicle. mvb, multivesicular body; m, mitochondria. x61,200.



**FIGURE 2-10:** At the perimeter of the Golgi region, in a 5-day old mouse aortic smooth muscle cell, large dense core vesicles (asterisks) are not uncommon. m, mitochondria; rER, rough endoplasmic reticulum. x34,200.

**FIGURE 2-11:** A small dense core vesicle (dcv) in close apposition to a large dense core vesicle (asterisk) in a 5-day old mouse aortic smooth muscle cell. Within the large dense core vesicle, a separate mass can be seen (arrowhead). This may be as a result of prior fusion with another small dense core vesicle. m, mitochondria. x61,200.



11

**FIGURE 2-12:** Longitudinal section of a smooth muscle cell in the aortic media of a 5-day old mouse. Organelles occupy much of the cytoplasm, however, a bundle of contractile filaments (cf) can be seen oriented oblique to the long axis of the cell. The bundle traverses the cell to anchor on either side in membrane-associated dense plaques (dp). Another bundle, with similar orientation, can also be seen (small arrows), although the entire bundle is not completely within the plane of section. EL, elastic lamina. x12,990.

**FIGURE 2-13:** Membrane-associated dense plaques in 5-day old mouse aortic smooth muscle cells. (a) High magnification of a membrane-associated dense plaque (dp) at the surface of a smooth muscle cell cut in longitudinal section. Contractile filaments (cf) can be seen to penetrate and anchor within the plaque. (b) In cross-section, numerous cross-sectioned profiles of contractile filaments (cf) are observed near the dense plaque (dp). In both sections, connective tissue elements form a close association with the cell surface on the extracellular face of the plaque (arrows). EL, elastic lamina. (a) x43,700; (b) x78,200.

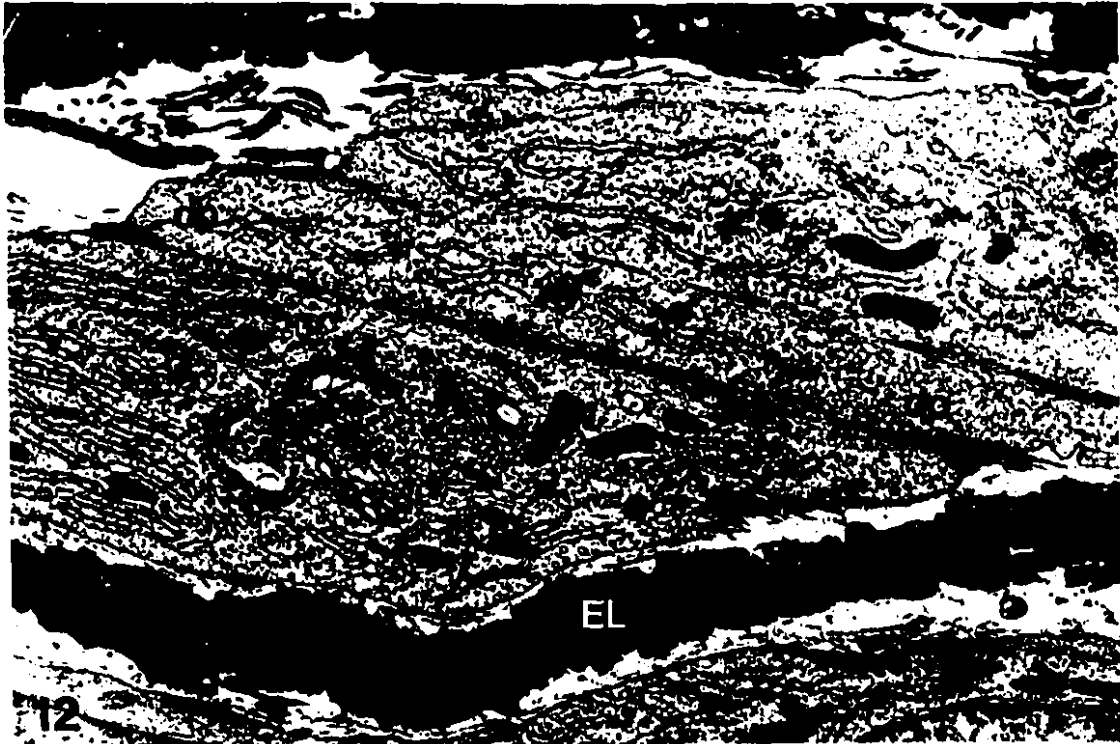


**FIGURE 2-14:** (a) Cross-section through a 5-day old mouse aortic media showing the appearance of the elastic lamina (EL). In this plane of section, the surface of the elastic lamina is relatively smooth. Occasionally, small elastin extensions may project obliquely from the lamina towards the cell surface (arrow). (b) In a longitudinal section of the aortic media, the surface of the elastic lamina (EL) is highly irregular and is lobular appearance. Numerous elastin deposits (ed) are observed between the elastic lamina and the cell surface. (SM) smooth muscle cell. x18,565.

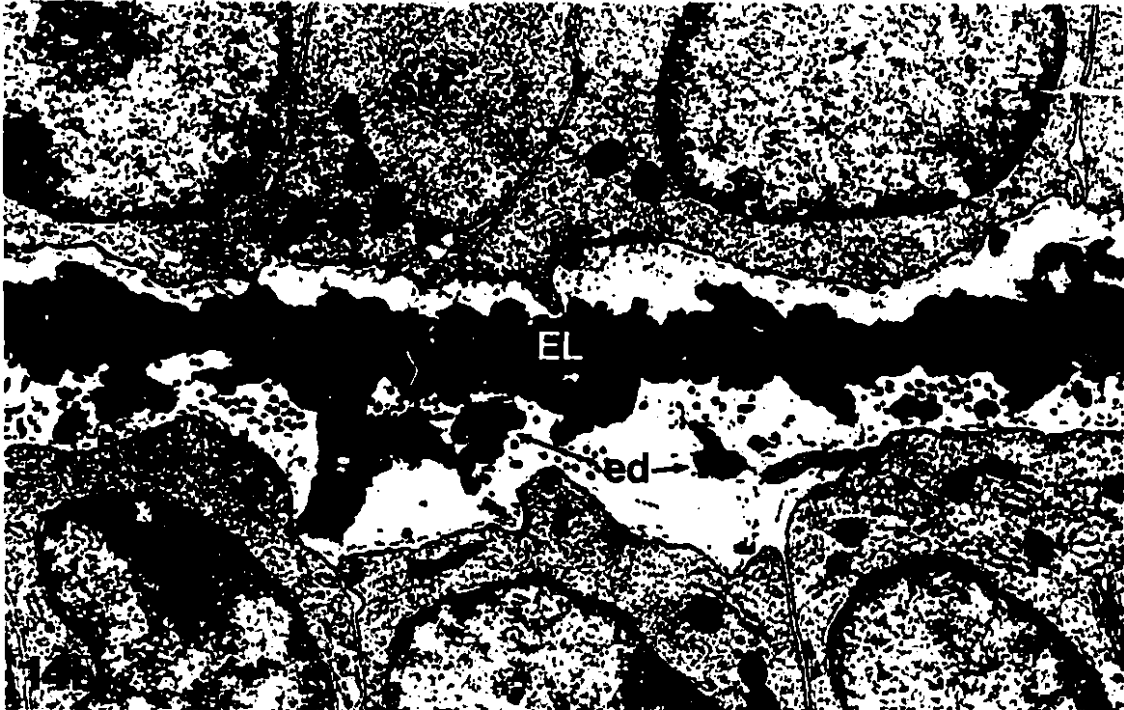
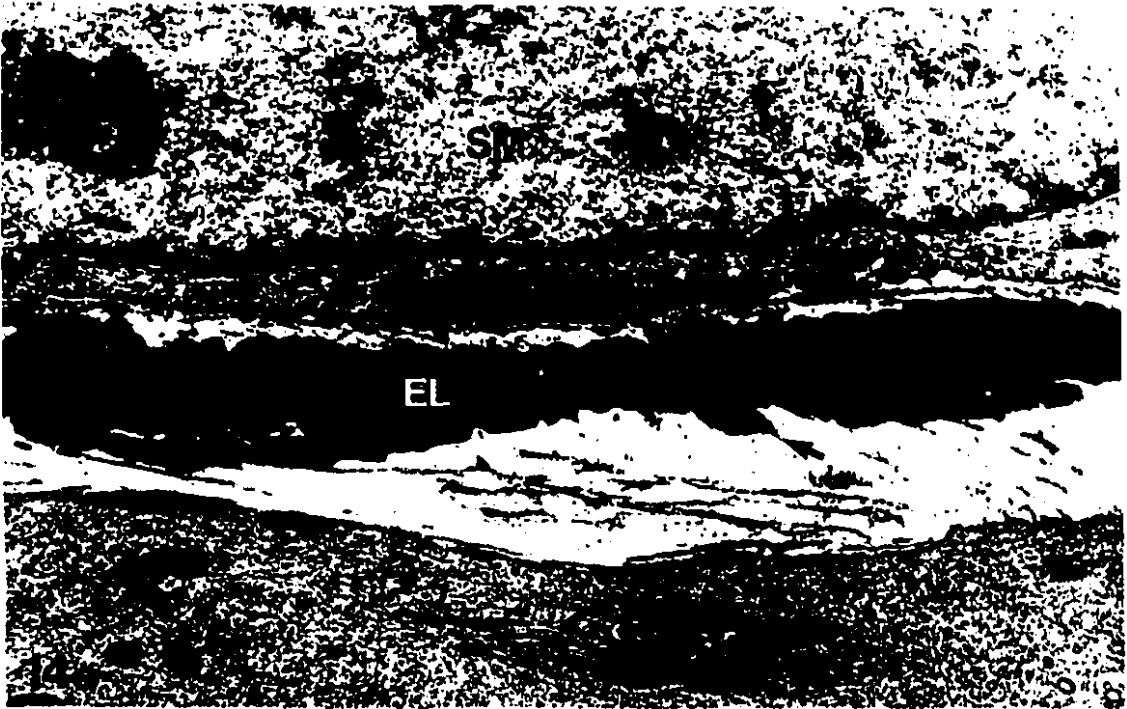


**FIGURE 2-15:** Longitudinal sections of a 5-day old mouse aortic media showing the organization of collagen fibers in the intercellular space. In this plane of section, the collagen fibers appear most often as cross-sectional profiles and are thus oriented around the circumference of the vessel. **(a)** A collagen bundle (coll) and isolated collagen fibers (arrows) in the intercellular space between the elastic lamina (EL) and the cell surface. **(b)** A collagen bundle (coll) and isolated collagen fibers (arrows) embedded within the substance of the elastic lamina (EL). Note the variation in collagen fiber diameter. x27,300.

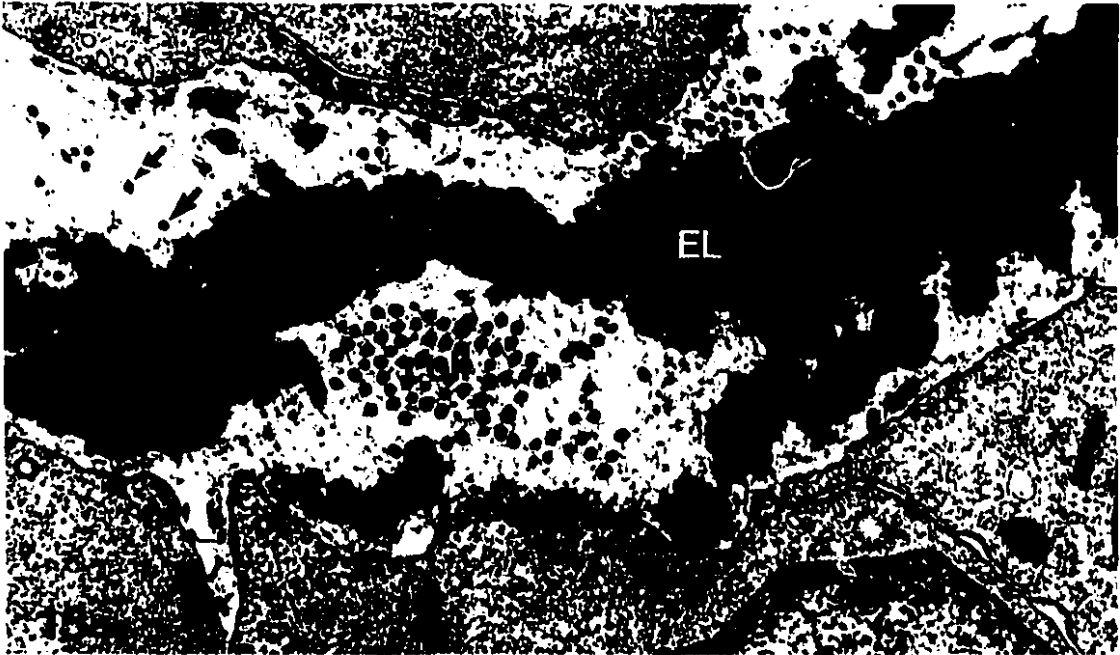


**FIGURE 2-16:** Elastic laminae in a 5-day old mouse aorta. **(a)** The surface of an elastic lamina (EL), seen in a cross-section of the aortic media, is occupied by a mantle of elastin-associated microfibrils (mf). In this plane of section, the microfibrils and adjacent collagen fibers (coll) are observed in longitudinal section and thus are oriented circumferentially around the vessel. **(b)** The surface of the elastic lamina (EL) in a longitudinal section of the vessel wall shows cross-sectional profiles of microfibrils (mf) and collagen fibers (coll) at the periphery. x68,000.

**FIGURE 2-17:** A delicate network of fine filaments (f) spans the intercellular space between the elastic lamina (EL) and the surface of the smooth muscle cell (SM) in a 5-day old mouse aorta. The network of filaments appears to anchor the structures in the space, such as collagen fibers (coll). x62,900.

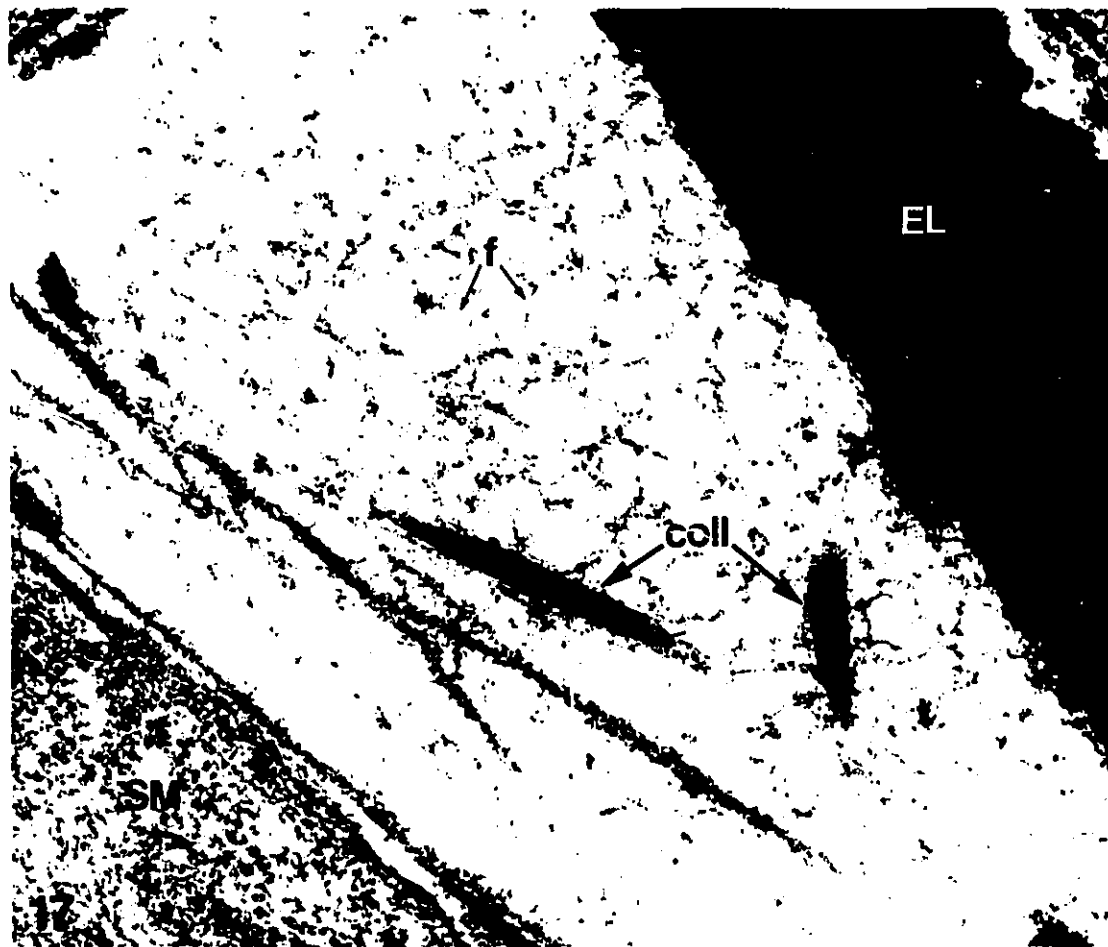
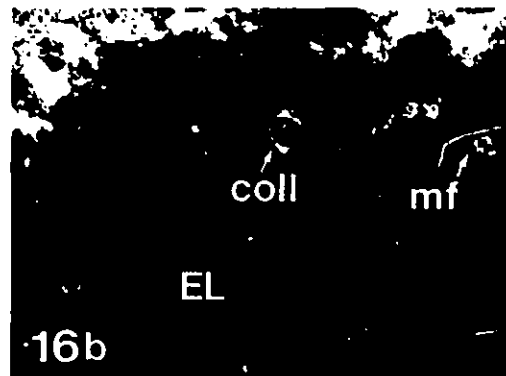


**FIGURE 2-18:** Aortic media of a 5-day old mouse showing the association of a smooth muscle cell (SM) with the adjacent elastic lamina (EL). (a) In a cross-section of the media, a bundle of microfibrils (mf) extending from the elastic lamina is observed that has become infiltrated with elastin proximal to the elastic lamina so as to form an elastin extension (ee). At the distal end, the microfibrils remain free of elastin and form a lateral association with the cell surface in a region overlying a membrane-associated dense plaque (dp). The contractile filaments (cf) anchored to the dense plaque have the same orientation as the elastin extension and microfibrils. The dashed line represents the plane of section seen in Figure 18b. (b) Cross-section of a membrane-associated dense plaque (dp) seen in a longitudinal section of the vessel wall. Within the smooth muscle cell, cross-sectional profiles of contractile filaments (cf) can be seen. Extracellular to the dense plaque, the cross-sectioned microfibrils (mf) appear coated with electron-dense material and seem to laterally associate with each other in addition to the cell membrane. In this plane of section, individual elastin deposits (ed) likely represent elastin extensions cut in cross-section. (a) x43,700; (b) x69,360.

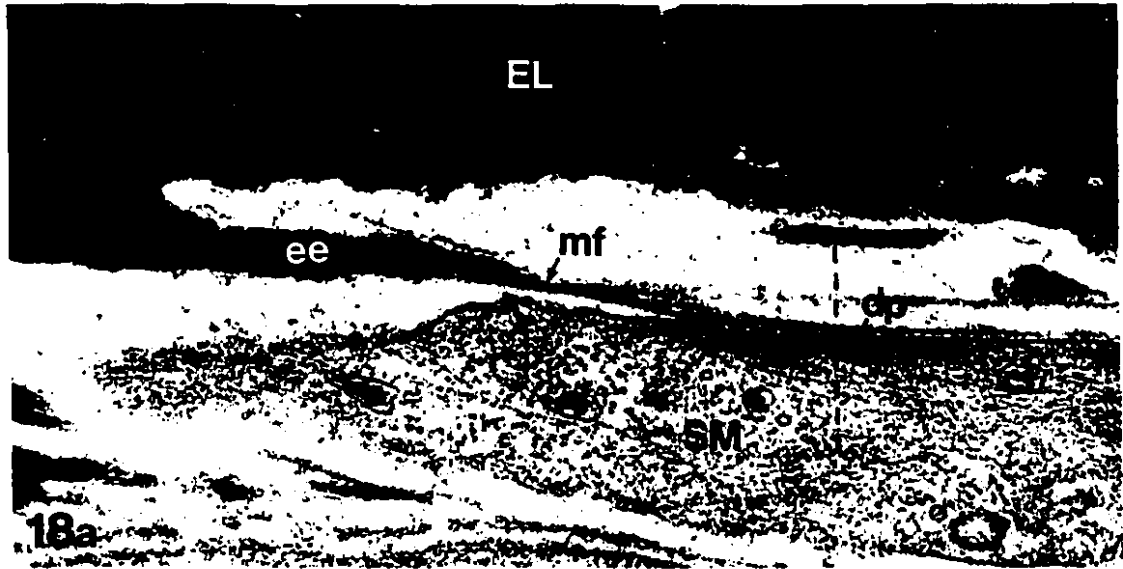


**FIGURE 2-19:** Cross-section of a mouse aortic wall at 15-days gestational age. The smooth muscle cells (SM) are already organized into circumferential layers. Between the cell layers, isolated elastin deposits (ed) are observed. In some areas, the deposits have merged to form small bands of elastin (eb). These bands will eventually join to form complete elastic laminae. E, endothelial cell; L, lumen. x6,000.



**FIGURE 2-20:** Intercellular region between two smooth muscle cell layers (SM) in a cross-section of the aortic wall from a 15-day gestational mouse. A small group of contractile filaments (cf), within the smooth muscle cell, penetrates a membrane-associated dense plaque (dp) which anchor the filaments to the cell surface. On the extracellular face of the dense plaque, microfibrils (mf) form a close lateral association with the cell membrane. The microfibrils extend from the developing elastic lamina (EL) and thus form a link from the elastic lamina to the cell surface. Note that the extracellular microfibrils and the intracellular contractile filaments have a similar orientation (arrows). x64,600.



**FIGURE 2-21:** Cross-section of an aortic wall from a 1-day post-natal mouse. At this stage of development, the four layers of smooth muscle cells (SM) are well defined. Much of the cytoplasm is occupied by organelles, however, contractile filaments (cf) can be seen to obliquely traverse the long axis of the cell. Interposed between the smooth muscle cell layers, the elastic laminae (EL) are almost complete. L, lumen; E, endothelial cell; A, adventitia. x8,160.



**FIGURE 2-22:** Intercellular region between two smooth muscle cell layers (SM) in a cross-section of the aortic media from a 1-day old mouse. A bundle of microfibrils (mf) extends from the developing elastic lamina (EL) to the smooth muscle cell surface. Although the elastic lamina is not yet continuous, elastin deposits (ed) appear to have infiltrated the microfibrils of the bundle. At the cell surface, the microfibrils form a close lateral association with the cell membrane in a region occupied by a membrane-associated dense plaque (dp). The dense plaque provides an anchoring point for the contractile filaments (cf) developing within the cell. Note that the extracellular microfibril bundle and the intracellular contractile filaments have a similar linear orientation. x39,900.



**FIGURE 2-23:** Cross-section of the aortic media from a 21-day post-natal mouse showing the association of the smooth muscle cells to the adjacent elastic lamina. **(a)** At this stage of development, the cytoplasm of the smooth muscle cell (SM) is filled with contractile filaments. The microfibril bundles, seen to link the smooth muscle cells to the elastic laminae at earlier developmental ages, are now almost completely infiltrated with elastin so as to form elastin extensions (ee). The elastin extensions link the elastic lamina (EL) to the cell surface in a similar orientation to that of the contractile filaments within the cell (arrows). **(b)** Often the end of the elastin extension (ee) is not completely infiltrated with elastin and the microfibrils (mf) extend past the elastin to form an association with the cell surface. **(c)** Other microfibril bundles appear to be completely infiltrated with elastin; the elastin itself forms the association with the cell surface in the region occupied intracellularly by a membrane-associated dense plaque (dp). Note that the dense plaques are penetrated by contractile filaments (cf). **(a)** x19,565; **(b)** x45,750; **(c)** x62,220.

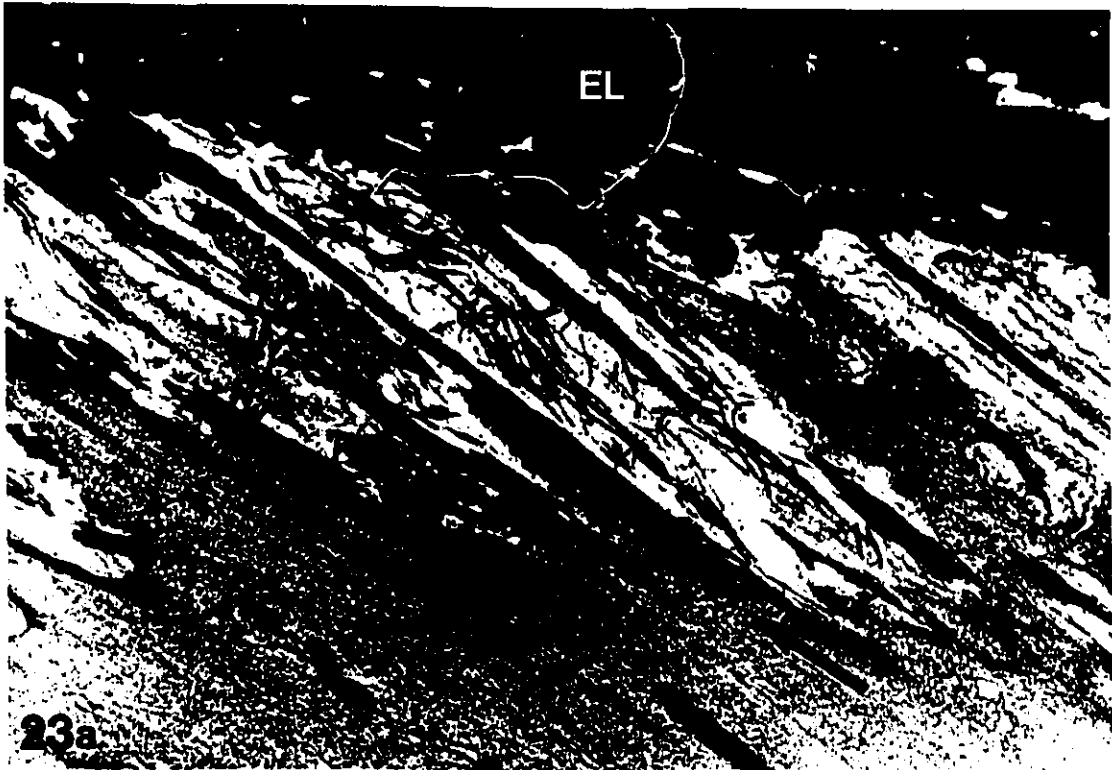


**FIGURE 2-24:** Light micrograph of the entire thickness of an adult mouse aortic wall cut in cross-section. Four layers of longitudinally sectioned smooth muscle cells and five elastic laminae can be seen. On either side of each elastic lamina, elastin extensions (arrowheads) radiate obliquely towards the smooth muscle cells in the same circumferential direction. Tension applied to the extensions by the smooth muscle cells will result in a uniform directional force being exerted on the elastic lamina (arrows). Note that the orientation of elastin extensions and the resultant force exerted on the elastic laminae alternates from one elastic lamina to the next. L, lumen; A, adventitia. x2,000.



24

**FIGURE 2-25:** Electron micrograph of the outer three elastic laminae and interposing smooth muscle cells in an adult mouse aortic wall seen in cross-section. Elastin extensions (ee) radiate from each side of the elastic laminae so as to form a herringbone-like pattern. Within the smooth muscle cell, the contractile filaments traverse the cell obliquely (two-headed arrows) and anchor in membrane-associated dense plaques on either side of the cell. Continuing in the same linear direction from the extracellular face of the dense plaques, elastin extensions link the cell to the elastic laminae. Thus, between adjacent elastic laminae, "contractile-elastic units" exist which form a continuous line of tension from one elastic laminae to the next. Note that the orientation of the contractile-elastic units alternates in direction in successive smooth muscle cell layers. A, adventitia. x13,300.



**FIGURE 2-26:** Light micrograph of the entire thickness of an adult mouse aortic wall cut in longitudinal section. Four layers of cross-sectioned smooth muscle cells and five elastic laminae can be seen. At the surface of the smooth muscle cells, numerous elastin deposits are observed (arrowheads). Since the elastin extensions are oriented around the circumference of the vessel in the cross-sectional plane, these elastin deposits likely represent the elastin extensions cut in cross-section. L, lumen; A, adventitia. x2,000.

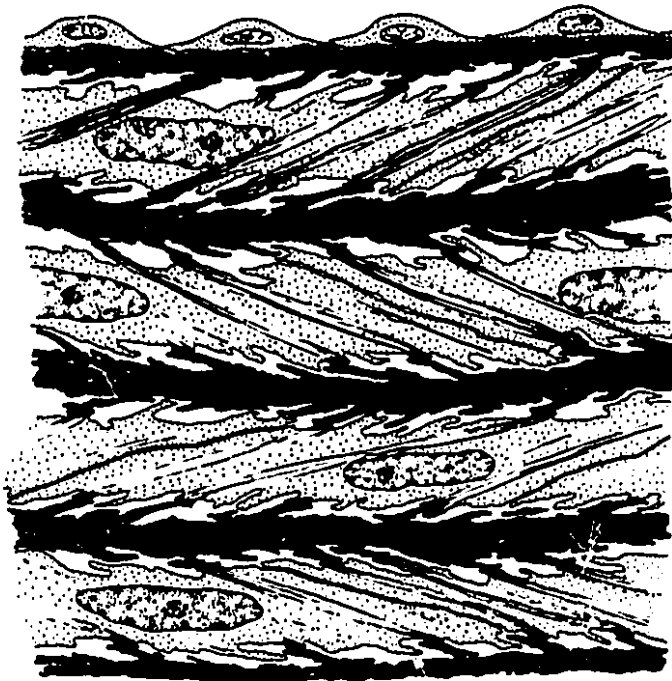
26



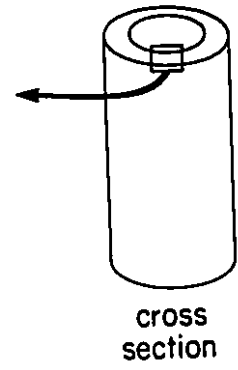
**FIGURE 2-27:** Electron micrograph of the outer three smooth muscle cell layers and interposing elastic laminae in an adult mouse aortic wall seen in longitudinal section. Bundles of contractile filaments within the cell are not evident since the cell and thus the filaments are cut in cross-section. The elastic laminae are highly irregular in appearance due to numerous elastin extensions cut in cross-section associated with the surface of the laminae. Elastin deposits (ed) seen between the elastic laminae and the surface of the cells are also likely cross-sectioned elastin extensions. x7,000.



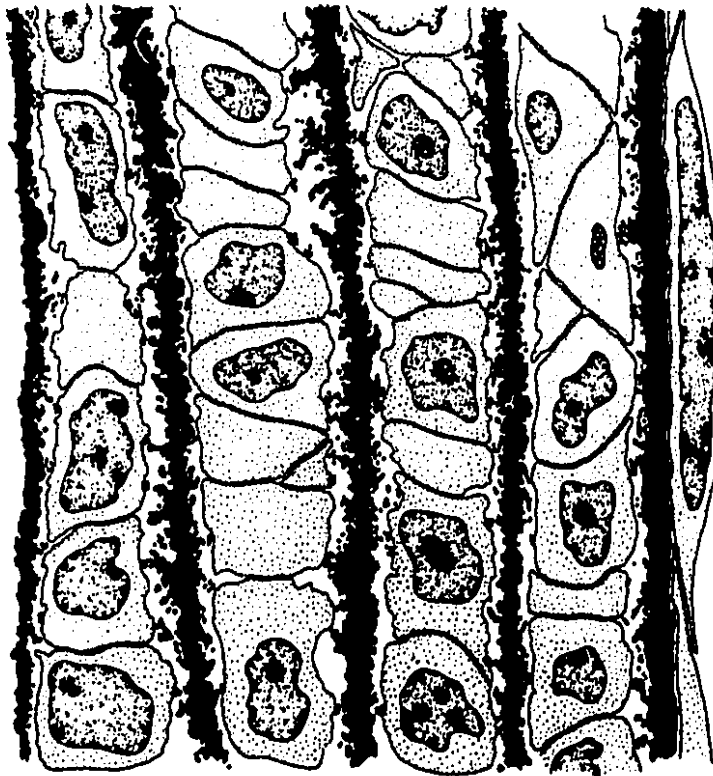
**FIGURE 2-28:** Schematic models illustrating the interrelationships between smooth muscle cells and elastic laminae in an adult mouse aortic media. **(a)** Cross-section. Contractile filaments within the cells traverse the long axis of the cell obliquely to anchor in membrane-associated dense plaques on either side. From these sites, elastin extensions continue in the same direction to link the cell to adjacent elastic laminae. Any tension generated by the intracellular contractile filaments will be transmitted to the elastic laminae such that the force exerted on adjacent elastic laminae will be in opposite circular directions. **(b)** Longitudinal section. The smooth muscle cells are seen in cross-section since the cells are oriented around the circumference of the vessel. No elastin extensions are seen to radiate from the elastic laminae to the surface of the cells. Instead, the elastin extensions are seen in cross-section and appear as elastin deposits at the cell surface, in the intercellular space, and at the edge of the elastic laminae. The elastin extensions seen in cross-section at the surface of the elastic laminae give the laminae a highly irregular appearance.



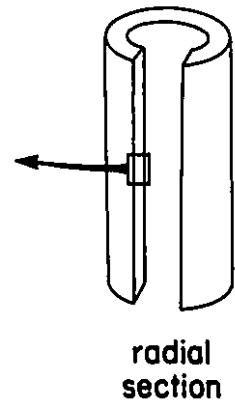
**28a**



**cross  
section**



**28b**



**radial  
section**

## 2.4 DISCUSSION

### 2.4.1 SMOOTH MUSCLE CELL MORPHOLOGY

The general features of mouse aortic smooth muscle cell ultrastructure observed in the present study are consistent with early investigations of aortic media structure in developing mice (Karrer, 1961), rats (Cliff, 1967; Berry et al., 1972a; Gerrity and Cliff, 1975) and chick embryo (Karrer, 1960). In these studies, however, many morphological features were difficult to discern due to the tissue preparation techniques employed at that time.

Smooth muscle cells of the developing aortic wall appear largely involved in the synthesis of proteins due to the abundance of rough endoplasmic reticulum and Golgi stacks. Of particular interest in the present study, is the appearance of numerous dense core vesicles, approximately 140 nm in diameter, in the vicinity of the smooth muscle cell Golgi apparatus and near the cell membrane. Thyberg and colleagues (1979) noted the presence of similar vesicles, 100 - 300 nm in diameter, in the cytoplasm of rat aortic smooth muscle cells. The dense core vesicles were found to be distinct from lysosomes both morphologically and by their negative cytochemical reaction for acid phosphatase activity. Due to the similar appearance of the dense core vesicle content with that of the amorphous elastic laminae, the dense core vesicles were suggested to be secretory vesicles involved in the production of elastin (Thyberg et al., 1979). Immunolabeling results later

confirmed this hypothesis by identifying the presence of tropoelastin, the elastin precursor, in the Golgi apparatus and electron dense vesicles of embryonic chick aortic smooth muscle cells (Damiano et al., 1984; Daga-Gordini et al., 1987).

The observation of both large and small dense core vesicles in the present study corroborates similar findings by Thyberg and colleagues (1979). The larger dense core vesicles have been suggested to play a role in tropoelastin storage due to their appearance and close association with small dense core vesicles (Thyberg et al., 1979; Damiano et al., 1984; Daga-Gordini et al., 1987). Observations from the present study show both large and small dense core vesicles close to the smooth muscle cell surface in the mouse aortic media; however, neither vesicle type was observed in the process of exocytosis. At the cell membrane, numerous coated pits and vesicles were observed. Previous investigations of elastin-producing cells have also revealed an abundance of coated pits and vesicles along the cell membrane (Fahrenbach et al., 1966). From this observation, Fahrenbach and colleagues (1966) thought that the coated vesicles were elastin-containing secretory vesicles; however, immunolabeling results have shown the coated pits and coated vesicles to only weakly label for the presence of tropoelastin (Daga-Gordini et al., 1987). Thus, it appears possible that following exocytosis of the dense core vesicle content, the membrane is coated and the coated pits endocytosed to form electron-lucent coated vesicles. Although this is only speculative, such a process may play a role in membrane retrieval and the maintenance of membrane integrity during this actively synthesizing period.

## 2.4.2 DEVELOPMENT OF SMOOTH MUSCLE CELL TO ELASTIC LAMINA CONNECTIONS

Results from the present study demonstrate that connections of smooth muscle cells to elastic laminae form early in neo-natal aortic wall development, prior to the formation of complete elastic laminae. Similar early attachments of smooth muscle cells to elastic laminae have been observed in the aortic media of growing rats as "fine fibrillar material" merging with the smooth muscle cell basement membrane (Cliff, 1967). In the present study, fibrillar material associated with the cell membrane consist of microfibrils that are morphologically similar to those associated with the elastic laminae. The development of extracellular connections of microfibrils to the smooth muscle cell surface was coordinated with the formation of intracellular contractile filament bundles anchored to the cell surface. Consistent with the present study, membrane-associated dense plaques have been reported to provide the anchoring site for the contractile filaments and underlie the region of membrane where the microfibrils connect to the cell membrane (Keech, 1960; Bierring and Kobayasi, 1963; Cliff, 1967; Clark and Glagov, 1979). Whether initial contact of the microfibrils with the cell surface signals dense plaque formation or whether some specialization of the smooth muscle cell membrane at the dense plaque site influences microfibril attachment remains to be established.

The anchorage of cells to elastic fibers, mediated by microfibrils, has been well documented in several tissues. In the skin (Cotta-Pereira et al., 1976; Tsuji, 1980; Dahlbäck et al., 1990), epidermal cells are linked to elastic fibers in the dermis by

1 bundles of microfibrils, termed oxytalan fibers (Fullmer and Lillie, 1958). Elaunin fibers, microfibril bundles partially infiltrated with elastin, form an intermediate link between the oxytalan fibers and the elastic fibers (Gawlik, 1965). Cotta-Pereira and colleagues (1977) suggested the term "elastic system fibers" for the oxytalan, elaunin and elastic fibers of the skin. A similar network of elastic system fibers is also involved in anchoring lymphatic endothelial cells to elastic fibers in the surrounding matrix (Leak and Burke, 1968; Gerli et al., 1990), myoid cells to elastic fibers surrounding seminiferous tubules (Herms et al., 1977) and is present in human gingiva (Chavrier et al., 1988) and rat tail tendon (Caldini et al., 1990). In the present study, the connection of the smooth muscle cells to the elastic laminae by microfibril bundles that progressively become infiltrated with elastin provides strong evidence that elastic system fibers may provide a common mechanism for the attachment of cells to elastic fibers or laminae.

The degree of elastin infiltration of the microfibril bundles of elastic system fibers appears to vary depending on the tissue location. In the skin, large oxytalan fiber can be identified subjacent to the epidermis (Dahlbäck et al., 1990), whereas in the aorta, the microfibril bundles were observed to become almost completely infiltrated with elastin from the elastic lamina to the cell surface. Since microfibrils appear to serve as a scaffolding for the deposition of elastin during elastic fiber assembly (Fahrenbach et al., 1966), Cotta-Pereira and colleagues (1977) proposed that the oxytalan and elaunin fibers result from an interruption of elastogenesis. Although the mechanism responsible for the control of elastin deposition among the microfibrils is unknown, the degree of infiltration may be partially in response to the tensile demands imposed upon the elastic system fibers

and the cell types that they anchor. This suggestion is supported by the fact that oxytalan fibers, which consist solely of microfibrils, do not stretch under mechanical stress (Ross, 1973), whereas elastin and elastic fibers stretch in proportion to the amount of elastin they contain (Cotta-Pereira, 1984). Thus, the microfibrils anchored to the smooth muscle cell surface may become infiltrated with elastin as a result of the tensions imposed upon them by the changing mechanical stresses that occur during development of the vessel.

The early connections of smooth muscle cells to elastic laminae may also be important for normal development of aortic medial architecture. Mechanical stretch of cultured smooth muscle cells has been shown to be a signal that is transduced by the cells into expression of the elastin gene (Sutcliffe and Davidson, 1990). During post-natal development, increases in intraluminal blood pressure and tangential tension of the vessel wall coincide with the production of elastin (Gerrity and Cliff, 1975). In hypertension, morphological changes in aortic medial organization result from an increase in vessel wall tension (Wolinsky, 1970). These changes include an increased accumulation of elastin that is both coincidental and proportional to the elevation in blood pressure (Keeley and Alatawi, 1991). Treatment of rats with colchicine during the development of hypertension has been shown to inhibit the increase in elastin production thus providing evidence that the perception of stress by the smooth muscle cell cytoskeleton is an important factor in elastin synthesis (Keeley and Alatawi, 1991). The connections observed in the present study between elastic laminae and smooth muscle cells may therefore play a vital role in early aortic medial development by the transmission of tension to the smooth muscle cells.

### 2.4.3 AORTIC MEDIA ORGANIZATION IN THE ADULT VESSEL

Relatively few studies have provided any information concerning the organization of smooth muscle cell to elastic lamina attachments in the adult vessel. Pease and Paule (1960) described the smooth muscle cell layers of the rat aortic media as a single layer of obliquely oriented cells with each cell extending from one elastic lamina to the next; the orientation of the smooth muscle cells changed direction in successive layers. Several investigators have presented similar representations of aortic medial architecture (Keech, 1960; Wolinsky and Glagov, 1964; Cliff, 1967). However, specific details concerning the attachment of smooth muscle cells to elastic laminae and their orientation from one smooth muscle cell layer to the next were not illustrated.

The present study has shown that smooth muscle cell to elastic lamina attachments form early in development, establishing "contractile-elastic units" which remain as organized functional structures in the adult vessel. A schematic model of the ultimate organization of the contractile-elastic units in the mouse aortic media is presented in Figure 2-28. In this model, a continuous line of tension is exerted between one elastic lamina and the next due to the oblique orientation of the contractile-elastic units. Since this line of tension alternates in successive smooth muscle cell layers, the resultant force on one elastic lamina is in one circumferential direction while that on adjacent elastic laminae is in the opposite direction. This system of organized connections would allow the "elastic tension" generated by the elastic laminae and the "active tension" generated by the smooth muscle cells to act in a coordinated manner. The cooperation between the

smooth muscle cells and the elastic laminae is thought to be important in maintaining an equilibrium in vessel wall tension (Burton, 1954). According to the 1841 law of Laplace, tangential wall stress in a vessel is directly proportional to the pressure and radius of the lumen and inversely proportional to wall thickness (Burton, 1954; Peterson et al., 1960). The organization of the contractile-elastic units in the vessel wall may therefore be important for the balance of normal changes in luminal pressure and wall stress. From the proposed model, one could speculate that a slight increase in luminal pressure would cause a proportional increase in wall stress that would be transmitted to the smooth muscle cells through their connections with the elastic laminae. In response, the smooth muscle cells would generate an active tension that would be transmitted back to the elastic laminae. Due to the orientation of the contractile-elastic units, an increase in wall thickness would result causing a decrease the tangential wall stress. Although the vasomotor function of smooth muscle cells in large vessels is not clear, this organized system of contractile-elastic units may allow vessel wall tangential stress to remain relatively constant during normal fluctuations of blood pressure. In cases of chronic or severe wall tension increases, such as in hypertension, the smooth muscle cells would not be able to generate enough active tension to counteract the luminal pressure elevation; thus, the increase in wall tension causes morphological changes which increase vessel wall thickness to reduce wall stress (Keeley and Alatawi, 1991).

In the present study, the basic structural unit of the aortic media is the contractile-elastic unit; involving the contractile filaments of the cell and the elastin extensions that anchor the cell to the adjacent elastic laminae. Wolinsky and Glagov (1967) proposed the

aortic media to consist of concentric "lamellar units"; each composed of one elastic lamina and immediately adjacent interlamellar components. The lamellar unit was later redefined based on the observation that between two smooth muscle cell layers, two elastic laminae separated by collagen bundles, appear to exist (Clark and Glagov, 1985). Thus, the aortic mediae of the rabbit and pig were reported to be comprised of a repeating sequence of elastic lamina-cells-elastic lamina-collagen bundles. Each smooth muscle cell layer and its associated elastic laminae, termed a "musculo-elastic fascicle", was implied to be the structural and functional unit of the media (Clark and Glagov, 1985). In the present study, only one elastic lamina separates the smooth muscle cell layers in the mouse aortic media; and although there may be collagen bundles embedded within the lamina, these bundles do not divide the laminae into two distinct elastic laminae. Since the mouse aortic media is only four layers thick, the interrelationships of medial components in aortae of larger animals may be more complex than that reported in the present study for the mouse aorta. Although the formation of two elastic laminae between smooth muscle cell layers may be a feature of larger animal aortae where the media consists of more smooth muscle cell layers, the same basic structural unit of organization may exist.

One of the few studies that deals with specific details of the relationships and attachments of smooth muscle cells to elastic laminae (Clark and Glagov, 1979) presents a number of observations that are in direct contrast with those of the present study and of the majority of past studies on aortic medial ultrastructure (Smith et al., 1951; Keech, 1960; Pease and Paule, 1960; Karrer, 1961; Bierring and Kobayasi, 1963; Cliff, 1967). Clark and Glagov (1979) reported that the smooth muscle cells and contractile filaments

are parallel and not oblique to the elastic laminae and that the contractile filaments do not anchor in the membrane-associated dense plaques but pass directly through them. These contradictory results were stated to represent the true ultrastructural arrangement of aortic medial components since the aortae examined were perfused in situ rather than removed and fixed by immersion as had been done previously (Clark and Glagov, 1979). However, aortae in the present study were also perfused in situ and the ultrastructural results obtained corroborate the earlier findings, in that, the smooth muscle cells and intracellular contractile filaments span from one elastic laminae to the next. Both arrangements of smooth muscle cell orientation have been previously described. Benninghoff (1928) termed the cells that join concentric elastic laminae, "spann-muskeln", and the cells that connect end to end in continuous rings that lie parallel to the elastic laminae, "ring-muskeln". Consistent with the present study, spann-muskeln have been predominately described in the aorta and large conducting arteries, whereas distributing arteries and arterioles usually contain ring-muskeln (Dobrin, 1978).

In summary, the present study demonstrates the presence of connections from smooth muscle cells to elastic laminae in the mouse aortic media. These connections form early in development as contractile-elastic units. These units are proposed to be the basic structural unit of aortic medial architecture which remain in the adult media as functional tension-bearing structures. The organization of the contractile-elastic units from one smooth muscle cell layer to the next provides evidence for an organized arrangement of aortic medial components and a possible mechanism for the transmission of tension throughout the vessel wall.

*CHAPTER THREE*

*ULTRASTRUCTURAL FEATURES OF THE DEVELOPING AORTIC INTIMA:*

*ENDOTHELIAL CELL - ELASTIC LAMINA ASSOCIATION*

### 3.1 INTRODUCTION

A physical attachment of the endothelial cells to the subendothelial matrix must exist to maintain the structural integrity of the aortic intima. Ts'ao and Glagov (1970) described focal adhesion sites on the abluminal endothelial cell surface in regions of the membrane occupied by cytoplasmic "dense zones". These sites proved resistant to mechanical detachment and remained firmly attached to the subendothelial matrix even under disruptive hypotonic conditions (Ts'ao and Glagov, 1970). In cultured cells, adhesion of the cell to the underlying substrate has been shown to involve membrane-associated dense plaques which provide anchoring points for intracellular microfilament bundles or "stress fibers" (Abercrombie and Dunn, 1975; Lloyd et al., 1977). Antibody staining has demonstrated that the stress fibers contain actin (Lazarides and Weber, 1974) and myosin (Weber and Groschel-Stewart, 1974). Similar stress fibers have been demonstrated in vascular endothelial cells *in vivo*, with an orientation parallel to the direction of blood flow (Gabbiani et al., 1983; Wong et al., 1983). The expression and distribution of stress fibers appears greatly influenced by a number of factors including, anatomical location and hemodynamic forces (White et al., 1983).

The structural components, distribution and expression of endothelial cell stress fibers have been extensively studied and specific proteins, such as vinculin and talin, have been localized to the membrane-associated dense plaques (Geiger et al., 1984). Relatively few studies, however, have dealt with the nature of structures located extracellular to the dense plaques and the relationship of these structures to the intracellular

stress fibers. Extracellular "anchoring filaments" have been reported to attach to the abluminal endothelial cell membrane at the extracellular face of membrane-associated dense plaques (Gerrity and Cliff, 1972; Yohro and Burnstock, 1973; Buck, 1979). These filaments are oriented in a direction that is continuous with that of the intracellular stress fibers and are thus aligned parallel to the direction of blood flow (Buck, 1979). Anchoring filaments, in association with intracellular dense plaques and stress fibers, have also been noted in the pre-natal rat aortic subendothelial matrix (Nakamura, 1988); however, no elucidation as to the structural features or functional implications of these filaments was given.

Anchoring filaments similar to those observed in the subendothelium of blood vessels have been described to be involved in anchoring lymphatic endothelial cells to surrounding connective tissue elements (Leak and Burke, 1966, 1968). Ultrastructural studies of lymphatic endothelial cell anchoring filaments have revealed features similar to those of "elastin-associated microfibrils" (Böck, 1978).

In this chapter, endothelial cell ultrastructure in the developing aortic intima is investigated. Specific attention is given to the structural associations of the endothelial cells and extracellular matrix components with the aim to provide a better understanding of the relationship of these cells with the elastic lamina. The results of this study demonstrate that extensive bundles of filaments connect the endothelial cell layer to the underlying elastic lamina during early development of the aortic wall. In accordance with studies on the fibrillar elastic apparatus around lymphatic vessels (Gerli et al., 1990), the endothelial cell connecting filaments of the aorta show features that are appear



morphologically similar to elastin-associated microfibrils, and thus suggest that microfibrils may play a functional role in cell anchorage.

## 3.2 MATERIALS AND METHODS

Thoracic aortae from C57/BL mice of post-natal ages of 1 day, 5 days, 10 days and 3 months were prepared for electron microscopy. Aortae from fetal mice of a gestational age of 15 days were also prepared. Animals and tissues were handled as previously described (see section 2.2)

Thin electron microscope sections were examined in a Philips 301 transmission electron microscope at an accelerating voltage of 80 kV.

### 3.3 RESULTS

#### 3.3.1 DEVELOPING MOUSE AORTIC INTIMA - 5-DAY POST-NATAL AGE

##### *3.3.1.1 General histological features*

The endothelium is a single layer of ovoid shape squamous cells oriented with their long axis parallel to the long axis of the vessel (Fig. 3-1). The endothelial cell nuclei are also ovoid and similarly oriented. Due to the attenuation of the endothelial cell cytoplasm, the nuclei bulge into the lumen forming ridges on the vessel wall that parallel the direction of blood flow. In cross-section, the surface of the endothelial cell apposed to the subendothelial matrix often has an undulating appearance as it conforms to the contours of the first elastic lamina (Fig. 3-1a). In longitudinal section, this abluminal surface appears relatively smooth (Fig. 3-1b). On a rare instance, an endothelial cell can be seen in the process of cell division (Fig. 3-2). Other features of the endothelial cells at this stage of development include contact with underlying smooth muscle cells through gaps in the elastic lamina (Fig. 3-3) and the presence of primary or rudimentary cilia (Fig. 3-4).

##### *3.3.1.2 Endothelial cell ultrastructure*

The endothelial cells of the developing aortic wall have features common to all endothelial cells; such as a prominent nucleus surrounded by an attenuated cytoplasm,

numerous transcytotic vesicles and oblique cell to cell junctions with characteristic marginal folds (Fig. 3-1).

The Golgi region is located in the proximity of the nucleus and appears well developed and highly active (Fig. 3-5). Many small Golgi stacks are observed together surrounded by an extensive, dilated rough endoplasmic reticulum. The stacks usually consist of four or five short saccules that often appear distended at either end. Within these distensions, electron dense flocculent material is frequently seen (Figs. 3-5, 3-6).

The Golgi region contains a number of vesicles that range in size and electron density. The most abundant are small vesicles, approximately 40 - 60 nm in diameter, situated in the vicinity of the Golgi stacks (Figs. 3-5, 3-6). These vesicles are likely involved in a number of different functions since they vary somewhat in size and considerably in electron density. Some of the more electron dense vesicles appear to be coated (Figs. 3-5, 3-6). Similar coating is occasionally observed on the distended ends of the Golgi saccules that contain electron dense material (Fig. 3-5). Since this region of the saccule appears to be budding from the rest of the saccule, it may be the origin of the small electron dense coated vesicles.

Another type of vesicle, also in close proximity of the Golgi saccules, averages 140 nm in diameter and contains an electron dense core (Figs. 3-5, 3-6). The dense core is separated from the vesicle membrane by a distinct electron lucent margin that is periodically crossed by fine filaments. The electron dense material within these vesicles is similar in appearance to that of the elastic laminae. Although these vesicles are frequently observed, only 2 or 3 are usually evident in one sectioned endothelial cell

Golgi region. These vesicles are usually seen adjacent to the trans face of the Golgi stack (Figs. 3-5, 3-6); however, small dense core vesicles observed next to the abluminal endothelial cell membrane are not uncommon (Fig. 3-7).

At the perimeter of the Golgi region and elsewhere in the cytoplasm, other dense core vesicles are occasionally seen (Fig. 3-8). However, these vesicles are considerably larger in size than the small dense core vesicles, being approximately 450 nm in diameter, and are less frequently observed. Although identical in appearance to the small dense core vesicles, these larger dense core vesicles may represent a separate population of vesicles, in respect to content and/or function, since vesicles of an intermediate size are not seen.

Another vesicle type, of moderate electron density, is occasionally seen in the vicinity of the Golgi region but more often in the perinuclear or attenuated cytoplasm. These vesicles, called Weibel-Palade bodies after the investigators that first described them (Weibel and Palade, 1964), are distinctive in appearance as they contain numerous small circular profiles with electron lucent centers, embedded in a dense amorphous matrix (Figs. 3-9a and b). Also observed within these vesicles, sometimes in the absence of circular profiles, are sets of parallel lines (Figs. 3-9b, 3-10). Both the diameter of the circular profiles and the distance between the parallel lines measures 20 nm; thus, the vesicles likely contain tube-like structures that appear as circles or parallel lines depending on the plane of section. The actual size and shape of the vesicle is difficult to ascertain. Vesicles have been observed with circular shapes of 130 - 210 nm in diameter (Fig. 3-11), but more common is an oval shape with an average dimension of 150 by 215 nm (Figs. 3-9a and b). Within these vesicles there is a predominance of the 20 nm circular

profiles. In addition, elongated oval shaped vesicles, with a long axis of 600 - 800 nm, have also been observed (Fig. 3-10). These vesicles contain exclusively the sets of parallel lines. Thus, although a definitive vesicle shape remains somewhat obscure, the circular vesicles may be cross-sections, and the various oval vesicles may be oblique sections, through an elongated ellipsoidal shaped vesicle; the tubular structures within the vesicle being oriented parallel to the long axis of the vesicle. This vesicle type is most frequently observed directly adjacent to, or in the vicinity of, the adluminal plasma membrane of the endothelial cell.

Finally, a vesicle has been observed on occasion that appears to be a composite of several of the vesicle types (Fig. 3-12). This vesicle is of similar size as the large dense core vesicles, being approximately 430 nm in diameter, but contains both electron dense material and the circular or linear profiles of the Weibel-Palade bodies aforementioned. The two materials appear to remain separate; the electron dense material is en masse and often eccentrically located, whereas the remainder of the vesicle is filled with the moderately dense tube-like structures. Similar to the dense core vesicles, an electron lucent region is also observed around the inside perimeter of this vesicle.

Another feature of the endothelial cells is distinctive bundles of microfilaments, termed stress fibers, present in the basal region of the cytoplasm (Fig. 3-13). The microfilaments are oriented parallel to the long axis of the endothelial cell and thus parallel to the long axis of the entire vessel. The stress fibers are straight and occasionally show faint electron dense striations that traverse the fiber along its length (Fig. 3-13a). The termini of the microfilaments penetrate discrete regions of enhanced electron density

along the basal surface of the cell (Figs. 3-13a and c). These membrane-associated dense plaques appear to anchor the microfilaments to the abluminal cell membrane.

### ***3.3.1.3 Endothelial cell - elastic lamina association***

The endothelial cells of the 5-day old mouse aortic intima are separated from the underlying elastic lamina by the subendothelial matrix. Although the subendothelial matrix may be quite small, the abluminal membrane of the endothelial cell is usually not in direct contact with the surface of the elastic lamina. The endothelial cells appear to be connected to the subjacent elastic lamina by extensive bundles of filaments. These filaments cross the subendothelial matrix in an orientation parallel to the long axis of the vessel. Thus, in longitudinal sections of the aortic wall (Fig. 3-14a), the entire extent of the filament bundles can be seen (Fig. 3-14b). The filaments within the bundle are anchored at the surface of the endothelial cell at a region of the membrane occupied on the intracellular face by a membrane-associated dense plaque. The plaque provides an anchoring point for the intracellular microfilaments of a stress fiber (Fig. 3-13). Both the intracellular microfilaments and the extracellular endothelial cell connecting filaments are aligned in the same direction thus forming a continuous linear unit from within the cell to the elastic lamina. At the edge of the elastic lamina, the connecting filaments appear to either penetrate and merge with the elastin or travel along the surface of the elastic lamina forming a lateral association with the elastin (Fig. 3-14b).

In cross-sections of the aortic wall, the endothelial cell connecting filaments appear as electron dense foci distributed in small groups under the endothelial cell layer (Fig. 3-

15a). Since the bundle of connecting filaments may have been sectioned at any point along its length, the cross-sectioned filaments do not always appear associated with a membrane-associated dense plaque. In many instances a relatively large group of cross-sectioned filaments can be observed which likely represents a complete connecting bundle (Fig. 3-15b). Individual connecting filaments are often difficult to distinguish due to a heavy coating of electron dense material around each filament, as well as, an extensive array of fine thread-like fibers that appear to link the filaments together to form the bundle. Similar lateral associations can be observed between the filaments and the endothelial cell membrane and between the filaments and the surface of the elastic lamina (Fig. 3-15b).

At higher magnification, the lateral association of cross-sectioned filaments can be seen to involve not only the thread-like fibers but also the electron dense coating; often to such an extent that the individual filaments are almost unrecognizable (Fig. 3-16). On occasion, however, an individual filament may be observed if it appears in a location where it is isolated somewhat from the other filaments. The isolated filaments vary in overall diameter due to the irregularity of the electron dense coat. The center of each filament consists of a 6 nm electron lucent core. With this observation, similar cross-sectional profiles are more readily observed within the rest of the bundle (Fig. 3-16).

Longitudinal sections of the connecting filaments at high magnification reveal the linear core of the filament only in extremely rare instances due to the unlikelihood of obtaining a perfect longitudinal section along the center of the 6 nm core. However, occasionally a longitudinal section through a connecting filament core is observed (Fig. 3-17). If the plane of section grazes the edge of the filament, only the electron dense

coating would be seen. Often when this occurs, a periodicity of approximately 35 nm is revealed (Fig. 3-17).

Cross-sectional profiles of individual connecting filaments studied at very high magnification reveal the filament to be roughly pentagonal in shape with an approximate diameter of 9.5 nm (Figs. 3-18a and b). Within the center of the filament the 6 nm electron lucent core can be seen. Often the core appears to contain a centrally located electron dense dot. From the edges of the filament, spike-like projections extend and associate with a network of fine thread-like fibers (Figs. 3-18a and b). The projections and fine fibers are likely the structures responsible for giving the filament the appearance of being heavily coated.

In longitudinally sectioned connecting filaments, sets of three parallel lines can occasionally be distinguished (Fig. 3-18c). These lines likely represent the outer limits of the filament and a row of centrally located dots. On the surface of the two outer lines, extending away from the center of the filament, spike-like projections and fine filaments can be seen.

### **3.3.2 DEVELOPMENTAL CHANGES IN THE ENDOTHELIAL CELL - ELASTIC LAMINA ASSOCIATION**

#### ***3.3.2.1 Fetal aorta - 15-days gestation***

The endothelial cell layer in the fetal aorta is separated from the developing first

elastic lamina by a considerable subendothelial matrix. Although this matrix can be as small as  $0.2 \mu\text{m}$ , the bands of elastin developing into the first elastic lamina are usually up to  $1.0 \mu\text{m}$  away from the abluminal endothelial cell membrane. Within the subendothelial matrix small elastin deposits and the occasional collagen fiber can be seen. Associated with the surface of the developing elastic lamina, are numerous 10 nm microfibrils. The most notable structure present in the subendothelial matrix, however, is the developing endothelial cell connecting filament bundles. The bundles appear as extensive networks of electron dense foci that span from the abluminal membrane of the endothelial cell to the edge of the underlying elastic lamina (Fig. 3-19a). In some sections, the network appears to consist of filamentous structures rather than individual foci (Fig. 3-19b). Therefore, the electron dense foci actually represent the individual cross-sectioned filaments of the bundle that laterally associate to appear as a network. Cross-sectioned filaments, seen as electron dense foci, are most often observed in sections of the aorta cut perpendicular to the long axis of the vessel. Thus, similar to those observed in the 5-day old aorta, the filaments extend along the subendothelial matrix parallel to the longitudinal axis of the endothelial cell and to the direction of blood flow.

The filaments in the subendothelial matrix connect to the abluminal endothelial cell membrane in regions occupied intracellularly by membrane-associated dense plaques (Figs. 3-19a and b). As was previously described, the dense plaques are anchoring sites for intracellular stress fibers. At 15-days gestational age, both the dense plaques and the intracellular stress fibers do not appear as extensive in number or size as those observed in the 5-day post-natal aorta.

### *3.3.2.2 Post-natal aorta - 1-day*

The first elastic lamina in the aortic intima of the 1-day post-natal mouse is no longer composed of individual bands of elastin but has developed into a continuous lamina with only a few gaps remaining. With the growth of the elastic lamina, the distance across the subendothelial matrix has reduced in size to approximately 0.3  $\mu\text{m}$  in width (Fig 3-20a). Within this matrix, a multitude of connecting filaments can be seen in association with both the abluminal endothelial cell membrane and the underlying elastic lamina (Figs. 3-20a and b). Similar to that observed in fetal aorta, extensive lateral associations exist between the filaments giving them the appearance of a network when seen in cross-section (Fig. 3-20b). Occasionally, cross-sectional profiles similar to those of elastin-associated microfibrils can be seen among the endothelial cell connecting filaments (Fig. 3-20b). More often, however, the filaments appear heavily coated making even individual filaments difficult to distinguish.

Within the cytoplasm along the abluminal endothelial cell membrane, stress fibers are abundant and appear more condensed and well defined than those observed in the fetal aorta (Figs. 3-20a and b). Each stress fiber anchors in a membrane-associated dense plaque which is linked extracellularly to the connecting filaments in the subendothelial matrix.

### *3.3.2.3 Post-natal aorta - 10-days*

The distance across the subendothelial matrix in the aortic wall of a 10-day old mouse is considerably smaller than that of earlier post-natal and fetal ages. In general, the

elastin of the first elastic laminae is now less than 100 nm from the abluminal endothelial cell membrane (Fig. 3-21). Within the subendothelial matrix only a few connecting filaments remain. The filaments often appear as a single row immediately subjacent to the endothelial cell membrane. Stress fibers can still be seen in the abluminal endothelial cell cytoplasm but they are notably smaller in size and less frequent (Fig. 3-21).

#### ***3.3.2.4 Adult aorta - 3 months***

In the adult aorta, the first elastic lamina is separated from the abluminal endothelial cell membrane by a small subendothelial matrix similar to that observed in the aortic intima of the 10-day old mouse (Fig. 3-22). No connecting filaments are evident in the subendothelial matrix. In addition, stress fibers within the endothelial cell cytoplasm are scarce. However, the abluminal endothelial cell membrane shows the presence of peg-like projections extending towards the underlying elastic lamina (Fig. 3-22). The elastic lamina follows the contour of the endothelial cell, including the endothelial pegs. Intracellularly, the pegs appear electron dense, similar to the membrane-associated dense plaques observed in aortae of young mice. On the extracellular face of the pegs, flocculent material is often observed which appears to extend between the peg and the elastic lamina (Fig. 3-22). The endothelial pegs are most frequently observed in cross-sections of the vessel wall and are not often seen in longitudinal sections of the aorta. Thus, the pegs may actually be small ridges oriented parallel to the long axis of the vessel.

**FIGURE 3-1: Cross-section and longitudinal section of the aortic endothelium (E). (a)** In cross-section, the regions of the endothelial cells containing nuclei bulge into the lumen (L) of the vessel. The nuclei are oval shaped and oriented parallel to the long axis of the vessel. **(b)** In longitudinal section, the nuclei form ridges on the adluminal surface of the endothelial cell that parallel the direction of blood flow. EL, elastic lamina; SM, smooth muscle cell. x4,940.

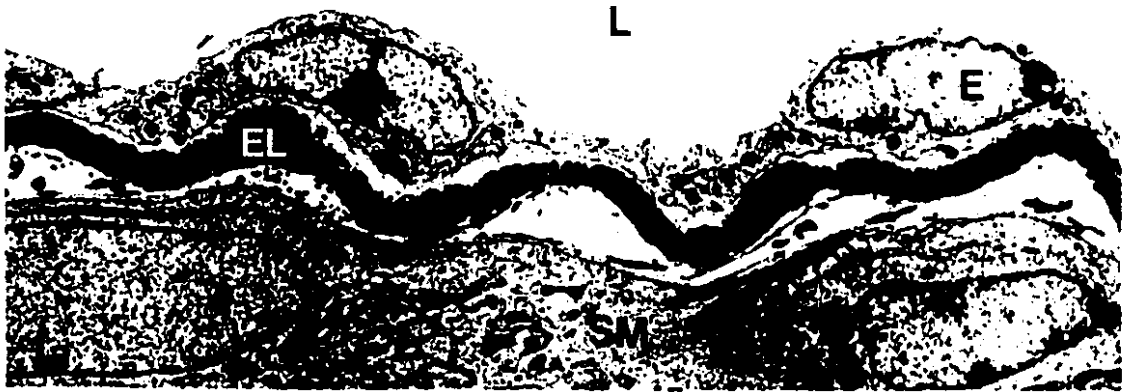


**FIGURE 3-2:** A rare instance of an endothelial cell (E) undergoing cell division. L, lumen; EL, elastic lamina; SM, smooth muscle cell. x11,400.



**FIGURE 3-3:** A small projection (arrow) from an endothelial cell (E) remains in contact with the underlying smooth muscle cell layer (SM) through a gap in the elastic lamina (EL). L, lumen. x12,780.

**FIGURE 3-4:** Cross-section through an endothelial cell Golgi region (G). On the adluminal surface of the endothelial cell is a rudimentary cilium (arrow) produced from one of the pair of centrioles (c). L, lumen; EL, elastic lamina. x19,800.

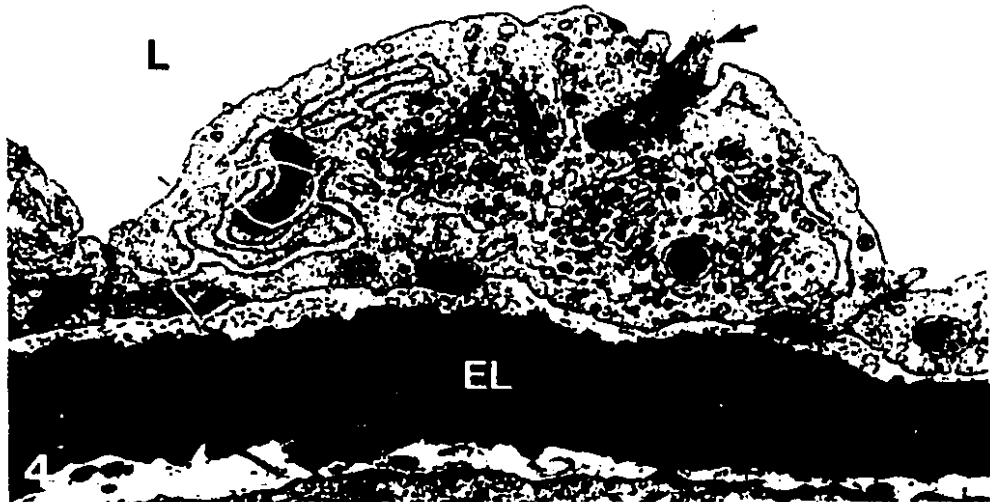


**FIGURE 3-5:** Endothelial cell Golgi region showing numerous Golgi stacks (G) surrounded by an extensive dilated rough endoplasmic reticulum (rER). In the vicinity of the Golgi stacks, a multitude of small vesicles (sv) that range in size and density are observed. Some of the vesicles appear to be coated (cv), as are regions of membrane budding from the Golgi saccules (cb). Pinocytotic or transcytotic vesicles (tv), seen at the endothelial cell membrane, may give rise to some of the electron lucent small vesicles. Also near the Golgi stacks are dense core vesicles (dcv); the content of which appears similar to that of the elastic lamina (EL). L, lumen; m, mitochondria. x32,300.

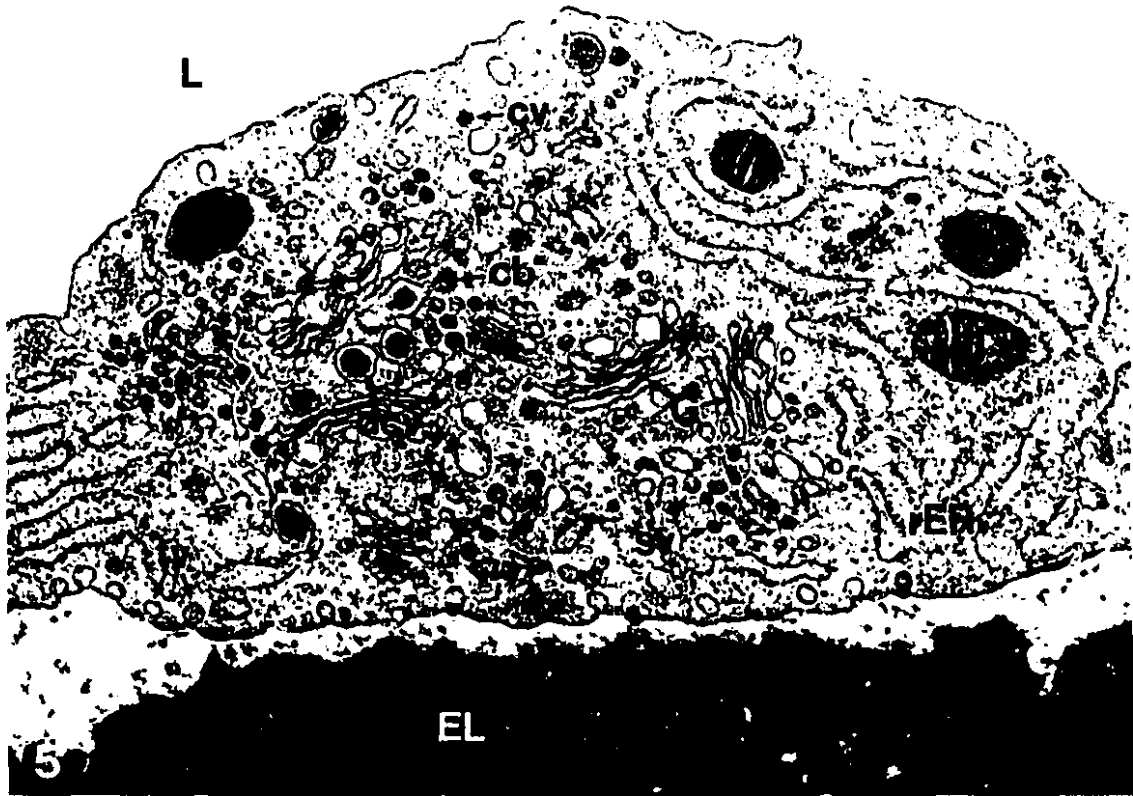


**FIGURE 3-6:** Endothelial cell Golgi region showing 5 small Golgi stacks (G) and associated vesicles. In the vicinity of the Golgi stacks are numerous small vesicles (sv) that vary in size and electron density. Some of the vesicles appear coated with flocculent material (cv). Dense core vesicles (dcv) are observed adjacent to one face of the Golgi stack; the core of which appears similar in consistency to that of the elastic lamina (EL). L, lumen; mvb, multivesicular body; m, mitochondria; tv, transcytotic vesicles. x42,500.

**FIGURE 3-7:** Dense core vesicles (dcv) are frequently observed near the abluminal endothelial cell membrane. L, lumen; EL elastic lamina. x42,500.

**FIGURE 3-8:** Similar to the dense core vesicles seen adjacent to the Golgi apparatus, large dense core vesicles are also observed in the endothelial cell cytoplasm. Often these large dense core vesicles are seen in the perinuclear space or attenuated cytoplasm. L, lumen; N, nucleus. x42,500.

**NOTE:** Figures 6, 7, 8, 11 and 12 are of the same magnification for comparative purposes.

I

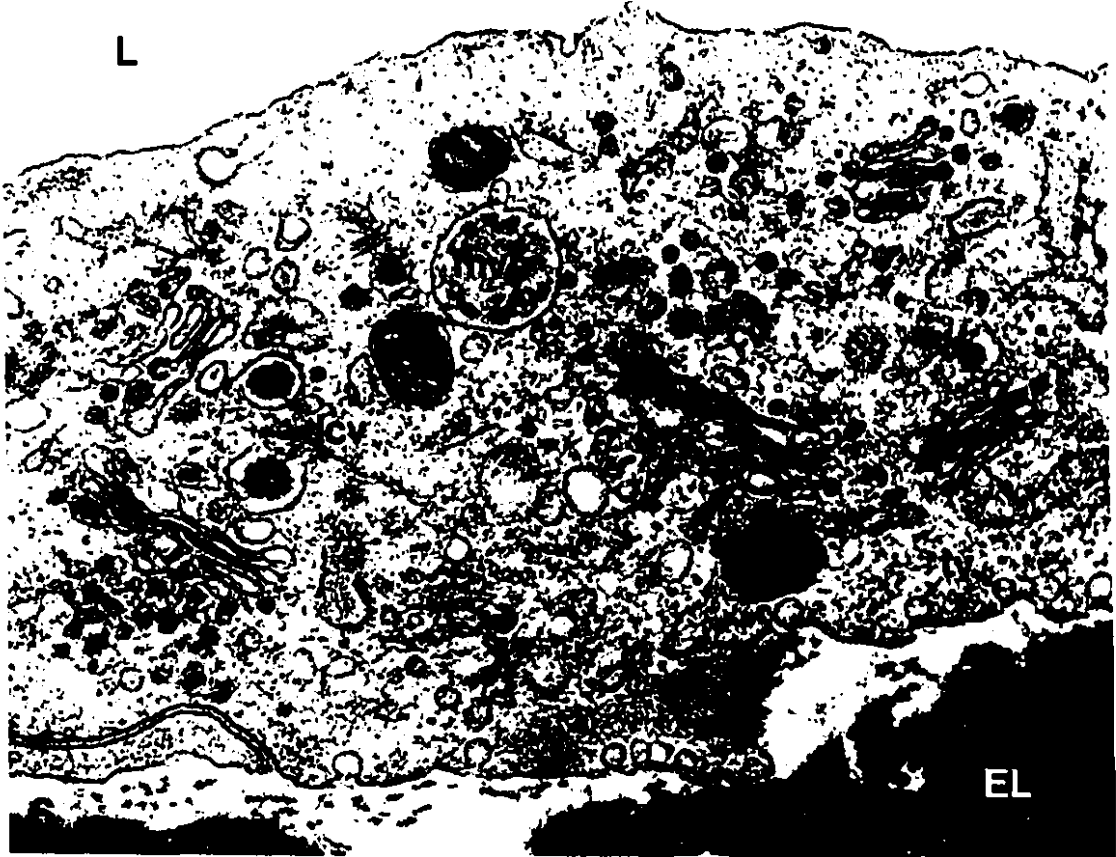


**FIGURE 3-9:** Distinctive oval shaped vesicles are observed in the endothelial cell cytoplasm that contains many small circular profiles, cross-sectioned tubules (t), embedded in an amorphous matrix. This type of vesicle is most frequently seen adjacent to the adluminal plasma membrane. (a) Occasionally, small densities can be seen to span from the vesicle to the plasma membrane (arrows). (b) Often the vesicle displays sets of parallel lines (arrowheads) as well as circular profiles. The distance between the parallel lines is identical to the diameter of the circular profiles. L, lumen; N, nucleus. x125,000.

**FIGURE 3-10:** Extended oval shaped vesicle that contains sets of parallel lines (arrowheads) similar in appearance to those seen in Figure 3-9b. This vesicle is also in close association with the adluminal plasma membrane (arrow). L, lumen; mvb, multivesicular body. x125,000.

**FIGURE 3-11:** Two round shaped vesicles containing circular profiles are seen adjacent to the adluminal plasma membrane (arrows). L, lumen; N, nucleus. x42,500.

**FIGURE 3-12:** Mixed vesicle containing an eccentrically located electron dense core (dc) and less dense material containing sets of parallel lines (arrowheads) observed in the endothelial cell cytoplasm. L, lumen. x42,500.

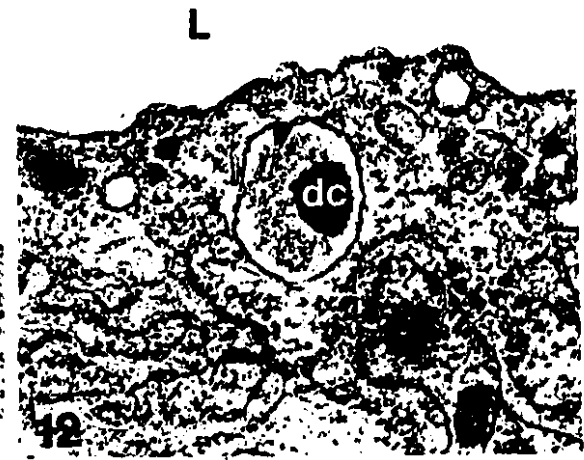
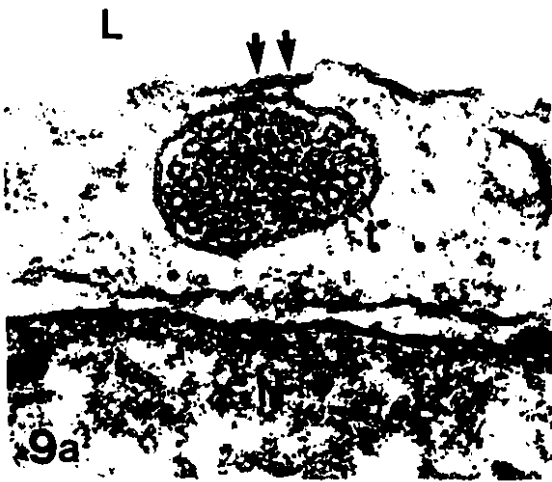


**FIGURE 3-13: (a)** Longitudinal section through a portion of an endothelial cell showing a linear bundle of microfilaments, which constitutes a stress fiber (sf), inserting into a membrane-associated dense plaque (dp). On the extracellular face of the dense plaque, connective tissue components extend in a similar orientation to that of the microfilaments within the cell (arrow). Cross-sections of the microfilament bundle at the dashed lines B and C are represented in Figures 13b and 13c, respectively. The microfilaments of the stress fiber (sf) seen in cross-section appear as a collection of small dots. L, lumen; mt, microtubule; EL, elastic lamina. x35,000.

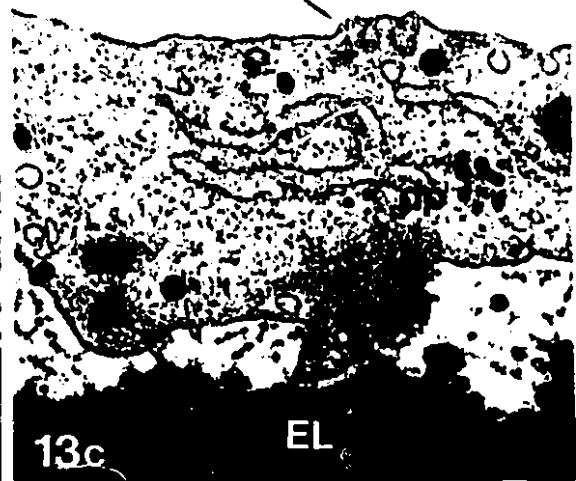
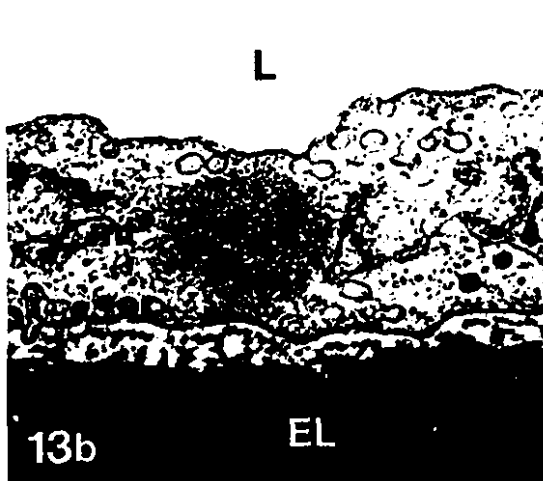
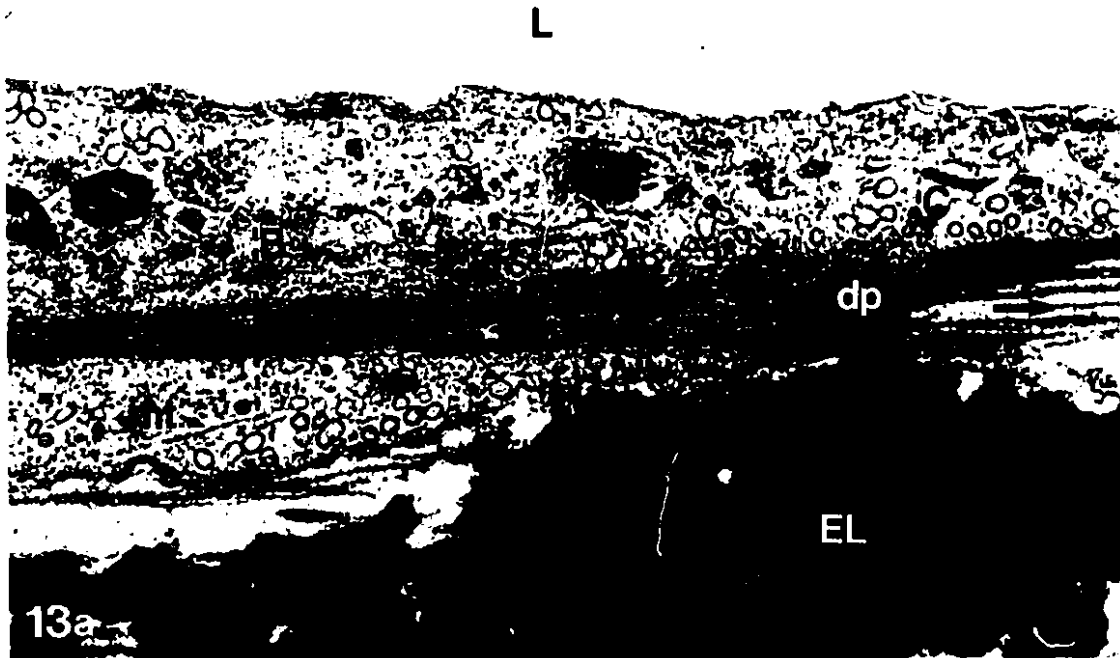


**FIGURE 3-14:** Longitudinal section of the aortic intima of a 5-day old mouse. (a) Endothelial cells (E) are seen in longitudinal section while the underlying smooth muscle (SM) cells are in cross-section. (b) Higher magnification of the endothelial cell (E) and subjacent first elastic lamina (EL). A membrane-associated dense plaque (dp), situated on the abluminal cell membrane, provides an anchor for a bundle of intracellular microfilaments; a stress fiber (sf). On the extracellular face of the plaque, a bundle connecting filaments (CF) anchors the endothelial cell to the surface of the underlying elastic lamina (white arrows). Note that both the intracellular stress fiber and the extracellular connecting filaments are aligned in the same direction (black arrows). L, lumen.  $\times 33,000$ .

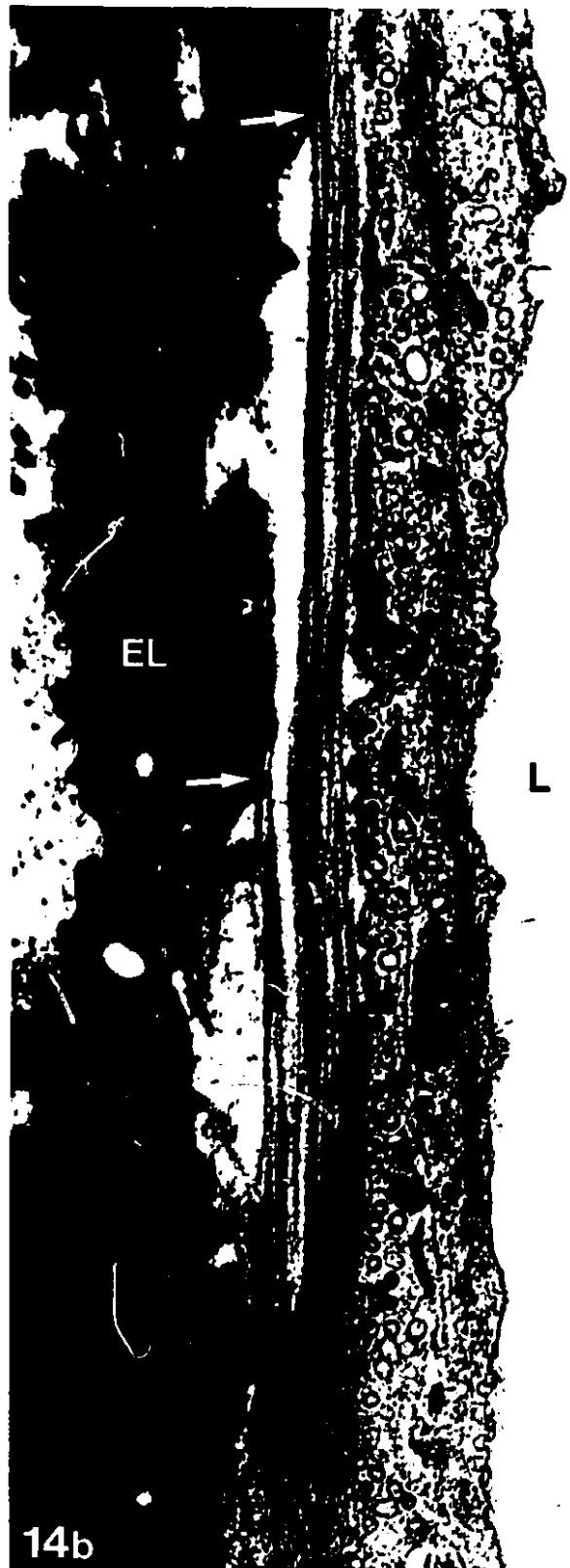
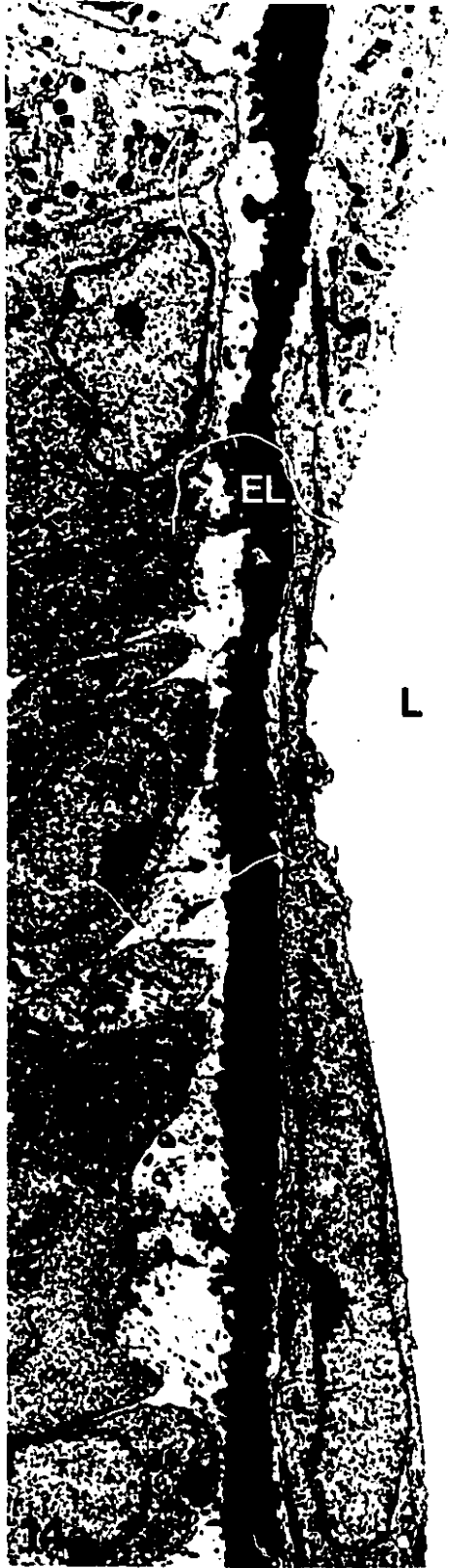
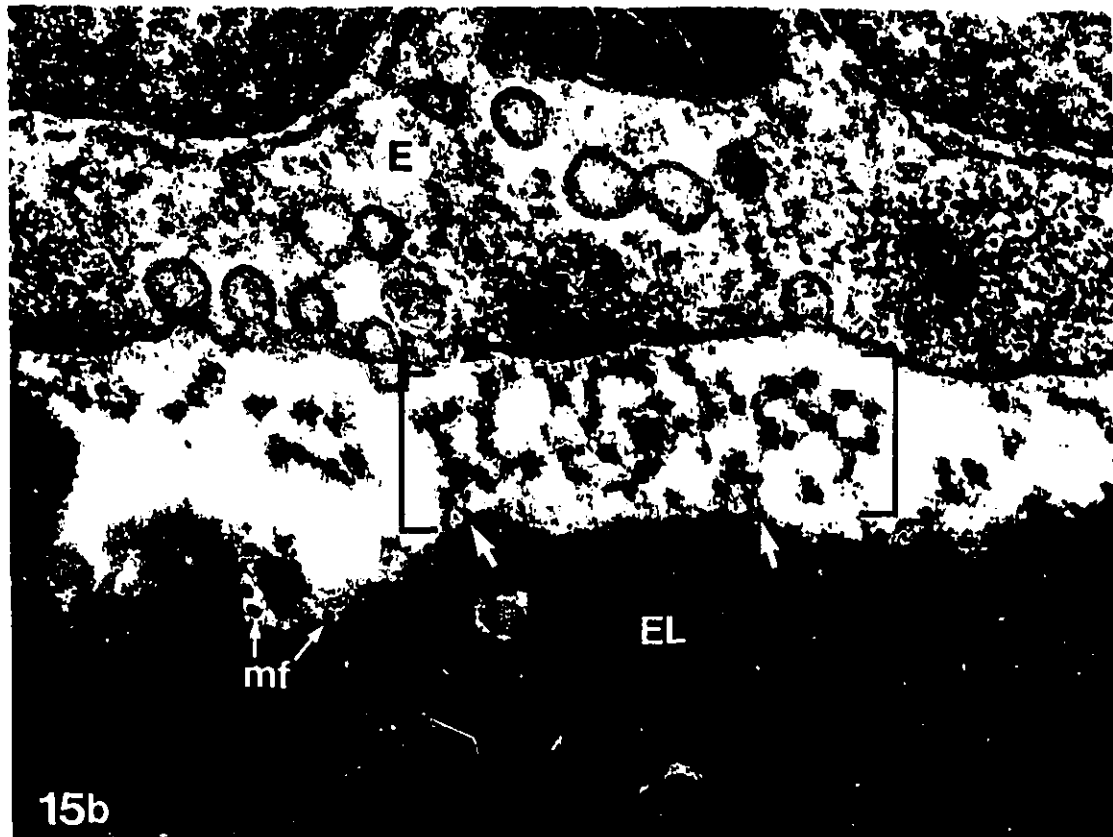
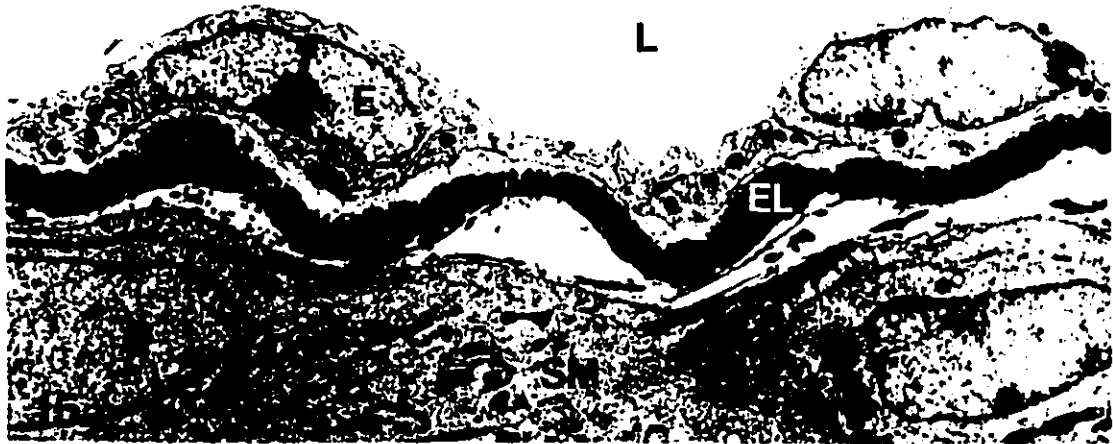


**FIGURE 3-15:** Cross-section of the aortic endothelium of a 5-day old mouse. **(a)** Endothelial cells (E) are seen in cross-section while the underlying smooth muscle cells (SM) are in longitudinal section. The abluminal surface of the endothelial cell follows the contour of the first elastic lamina (EL). **(b)** Higher magnification of the abluminal surface of an endothelial cell (E) and subendothelial matrix. Numerous membrane-associated dense plaques (dp) along the cell membrane are penetrated by the microfilaments of stress fibers (sf). Extracellular to the plaque, a bundle of connecting filaments (bracketed), can be seen in cross-section. The filaments appear heavily coated with electron dense material, with a fine network of thread-like fibers laterally linking the filaments together to form the bundle. A similar lateral association exists between the connecting filaments of the bundle and the endothelial cell membrane in the region of the dense plaque (arrowheads) and with the adjacent elastic lamina (arrows). Note the appearance of the elastin associated microfibrils (mf). L, lumen; EL, elastic lamina. **(a)** x5,700; **(b)** x102,000.



15b

**FIGURE 3-16:** High magnification view of a bundle of connecting filaments cut in cross-section in the subendothelial matrix. Extensive lateral associations and heavy coatings of electron-dense material make individual filaments difficult to discern. On occasion, however, individual filaments may be observed (black arrows - these filaments have been enlarged in Figures 18a and 18b to show ultrastructural details). The filament appears to be approximately 9.5 nm in diameter with an electron lucent core. With this observation, similar cross-sectional profiles can be identified within the bundle itself (arrowheads). Note that fine thread-like fibers (white arrows) laterally connect the filaments within the bundle to the endothelial cell membrane in the region of the dense plaque (dp) and to the surface of the elastic lamina (EL). E, endothelial cell; sf, stress fiber. x202,300.

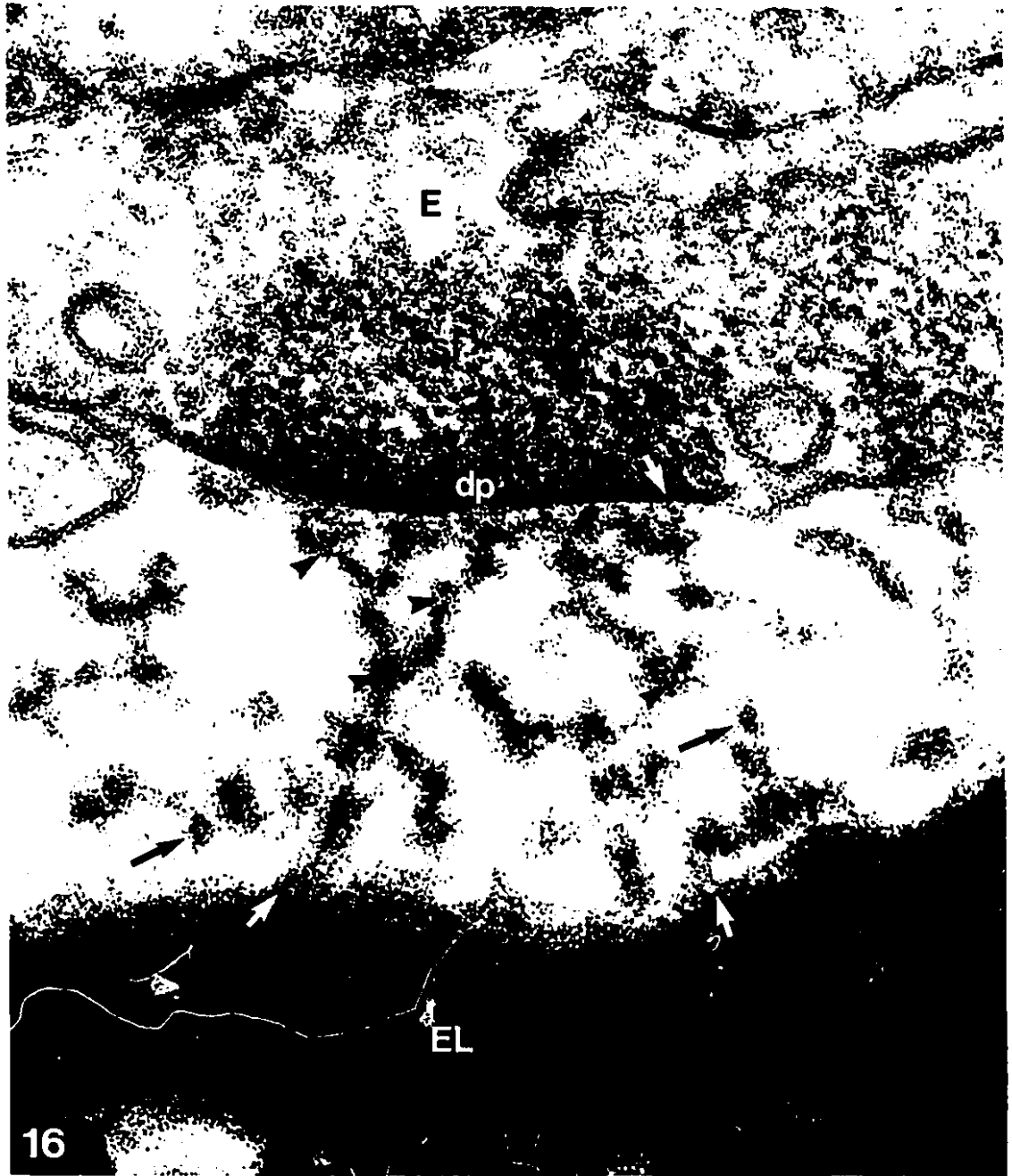


**FIGURE 3-17:** High magnification view of connecting filaments cut in longitudinal section in the subendothelial matrix. The linear core of the filament (large arrows - this filament has been enlarged in Figure 18c to show ultrastructural details) is difficult to observe due to the heavy coating on the filaments and the rarity of a perfect longitudinal section through the filament core. A grazing section of a filament reveals a periodicity of approximately 35 nm of electron dense material along its length (vertical bars). In a slightly deeper plane of section, the filament appears to be wrapped by electron-dense material with a similar 35 nm periodicity (small arrows). E, endothelial cell; EL, elastic lamina. x202,300.



**FIGURE 3-18:** High magnification micrographs of connecting filaments in the subendothelial matrix. **(a and b)** Two individual cross-sectioned connecting filaments enlarged from Figure 3-16. Each filament is approximately 9.5 nm in diameter and roughly pentagonal in shape. The filaments contain a 6 nm electron lucent core that appears to have a centrally located electron dense dot. Spike-like projections (arrowheads) extend from the filament and associate with a network of fine thread-like fibers (arrows). **(c)** Two longitudinally sectioned connecting filaments enlarged from Figure 3-17. The upper filament appears to have been sectioned through the core. Sets of three horizontal arrows mark the outer limits of the filament and a row of centrally located dots. Spike-like projections can be seen to extend from the sides of the filament (arrowheads). The lower filament appears to have been sectioned closer to the edge of the filament. Electron dense material wraps around the filament with an irregular periodicity of approximately 35 nm (large arrows). x550,800.



**FIGURE 3-19:** Cross-sections of the aortic intima of a 15-day gestational mouse showing features of the subendothelial matrix. The endothelial cell (E) is connected to the developing elastic lamina (EL) by an extensive bundle of connecting filaments (CF). The connecting filaments are oriented parallel to the long axis of the vessel, thus appear as electron-dense foci in cross-section. Due lateral associations among the filaments, they appear as an elaborate network. The lateral associations extend from the filaments to the surface of the elastic lamina (large arrowheads) and to the endothelial cell membrane (small arrowheads) in the regions occupied by dense plaques (dp). Note the appearance of elastin-associated microfibrils (mf) at the surface of the elastic lamina. (a) Within the endothelial cell cytoplasm a dense core vesicle (dcv) can be seen close to the abluminal cell membrane. (b) Since this section is slightly oblique, the connecting filaments appear as short filaments rather than foci (arrows). ed, elastin deposit. x88,400.

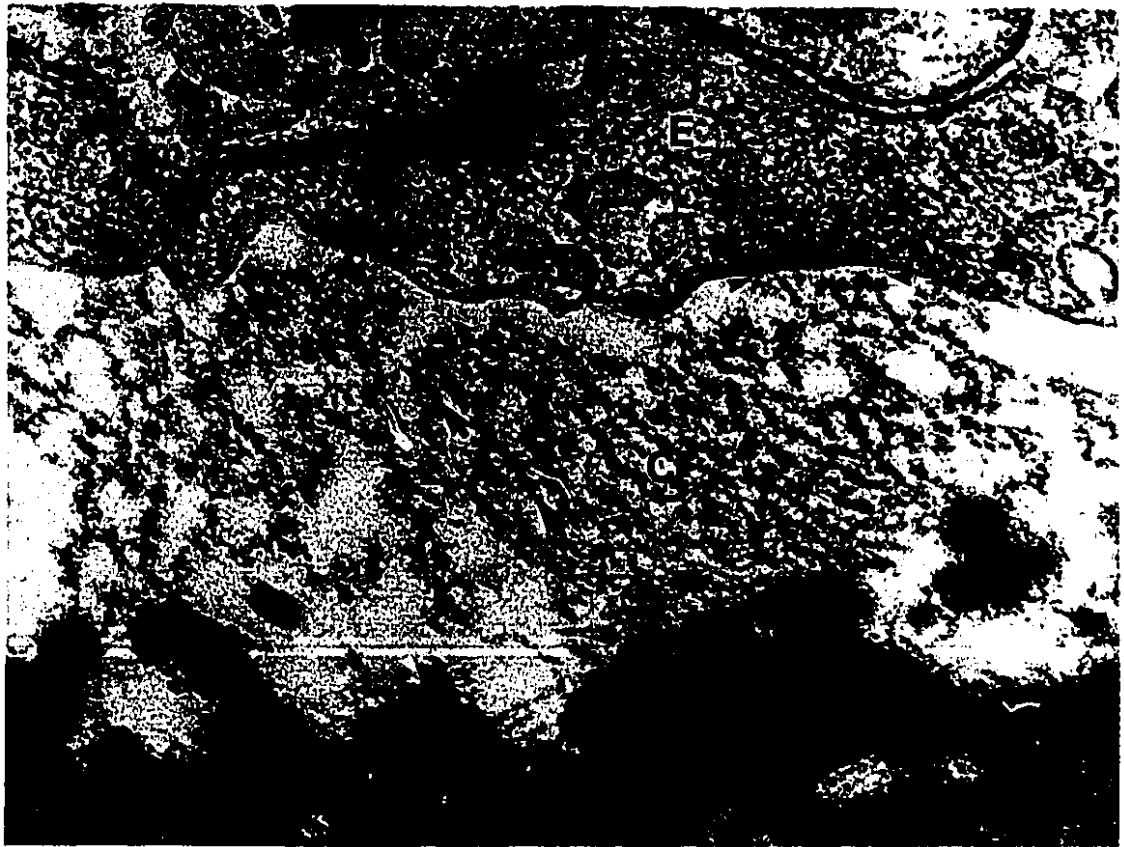


**FIGURE 3-20:** Cross-sections of the aortic wall of a 1-day old post-natal mouse showing features of the subendothelial matrix. (a) Numerous membrane-associated dense plaques, with associated stress fibers (sf), are distributed along the abluminal membrane of the endothelial cell (E). In the adjacent subendothelial matrix, large bundles of connecting filaments (CF) can be seen. (b) At higher magnification, individual connecting filaments are easier to discern. Cross-sectioned filaments (arrowheads) within the connecting filament bundles (CF) show structural features similar to elastin-associated microfibrils. EL, elastic lamina; SM, smooth muscle cell; L, lumen; dp, dense plaque. (a) x21,840; (b) x39,900.

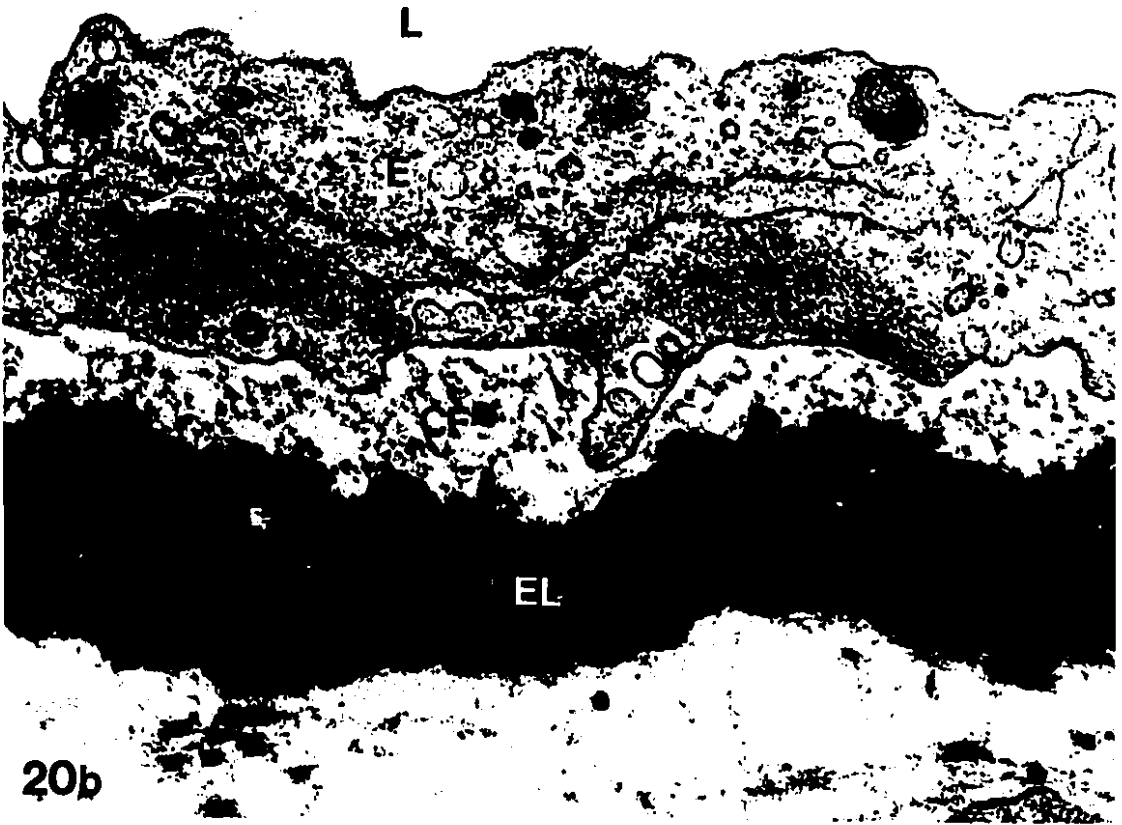
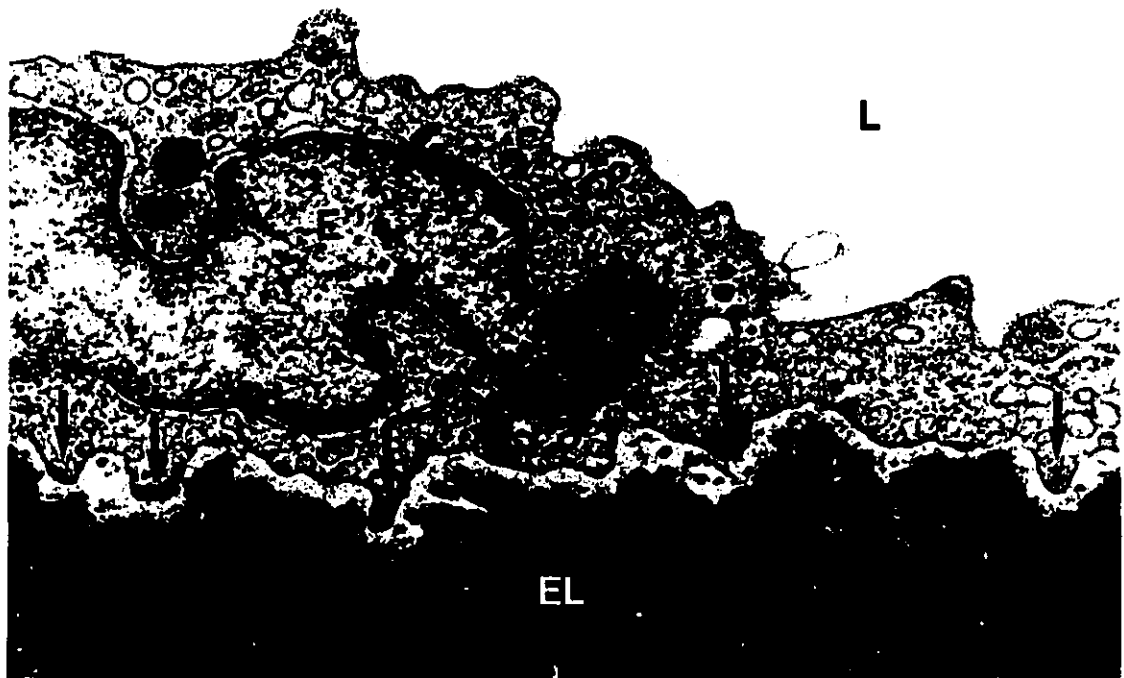
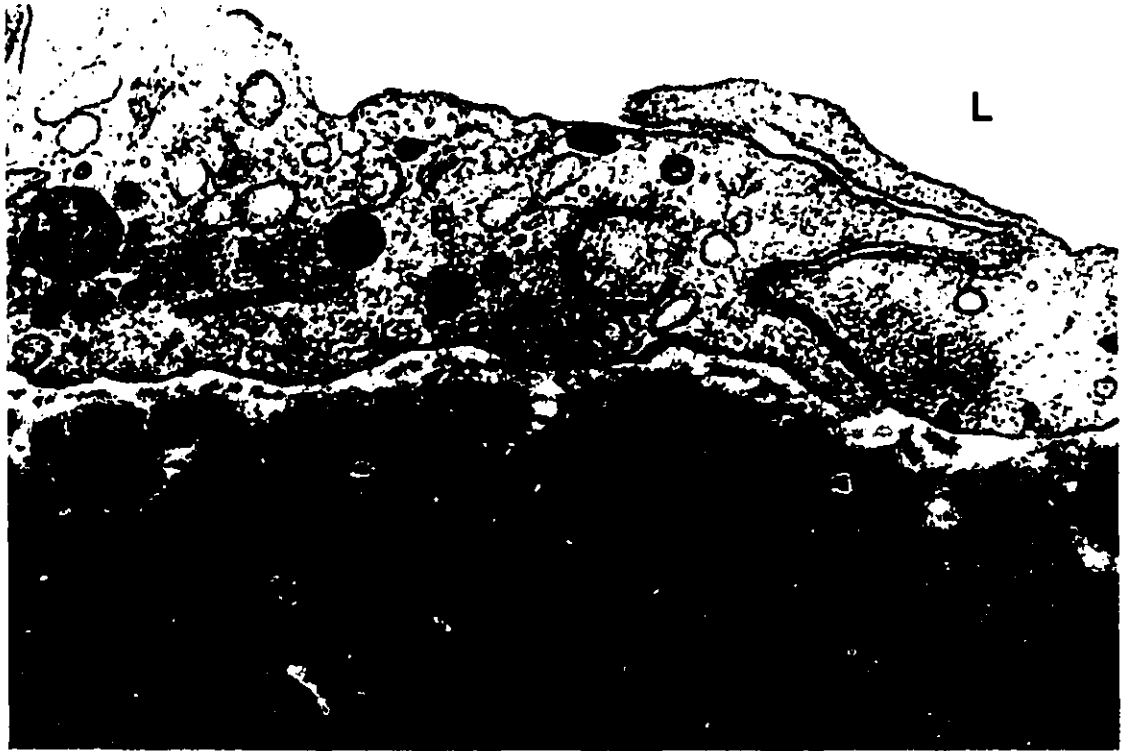


**FIGURE 3-21:** Cross-section of a portion of an endothelial cell (E) and subjacent elastic lamina (EL) of a 10-day old mouse aortic intima. The subendothelial matrix appears considerably smaller than that from younger post-natal and fetal mice. Along the abluminal endothelial cell membrane, bundles of intracellular stress fibers (sf) are still present. Within the narrow subendothelial matrix, small groups of connecting filaments (CF) remain in association with the endothelial cell and elastic lamina. L, lumen. x65,000.

**FIGURE 3-22:** Cross-section of a portion of an endothelial cell (E) and subjacent elastic lamina (EL) of an adult mouse aortic intima. In the adult aorta, the elastin is in close proximity to the abluminal endothelial cell membrane. No connecting filaments are observed between the two structures. A characteristic feature of the abluminal cell membrane in the adult aortic intima is pegs which extend towards the underlying elastic lamina (arrows). Within the pegs, electron-dense material is frequently observed. The pegs are most notable in this plane of section and thus may actually represent small ridges rather than peg. Note that large bundles of intracellular stress fibers and connecting filaments are not evident. L, lumen. x39,140.





## 3.4 DISCUSSION

### 3.4.1 ENDOTHELIAL CELL MORPHOLOGY

The morphological features of endothelial cells of the mouse aorta presented in this study provide an overview of endothelial cell structure in the developing aortic intima. Although many of these features have been previously described in early studies of aortic ultrastructure (Karrer, 1960, 1961; Pease and Paule, 1960; Paule 1963), these studies were hampered by the tissue preservation techniques available at the time for electron microscopy.

The endothelial cells of the developing mouse aortic intima were shown to contain numerous organelles; especially those involved in protein synthesis and secretion. Of particular interest were vesicles with dense cores of amorphous material that appeared morphologically similar to the substance of the elastic laminae. As was observed in the smooth muscle cell (see section 2.3.1.2), both large and small dense core vesicles were seen in the endothelial cell cytoplasm. Small dense core vesicles, 100 - 300 nm in diameter, have also been observed within the Golgi region, in the cytoplasm and near the cell surface of rat aortic endothelial cells (Thyberg et al., 1979). Based on the morphological appearance of the dense core material, the endothelial cell dense core vesicles were thought to contain precursor molecules of elastin, and were thus suggested to participate in the formation of the subendothelial elastic lamina (Thyberg et al., 1979).

The involvement of large and small dense core vesicles in elastin synthesis and secretion has been previously discussed in accordance with observations of similar vesicles in the aortic smooth muscle cells (see section 2.4.1). In the present chapter, the observation of similar vesicles in the endothelial cell provides evidence that the same processes of elastin synthesis and secretion takes place in both smooth muscle cells and endothelial cells. The involvement of endothelial cells in the production of elastin is supported by the demonstration of intracellular labeling of elastin precursor molecules within cisternae of rough endoplasmic reticulum, Golgi saccules and vesicles of aortic endothelial cells (Damiano et al., 1984; Daga-Gordini et al., 1987).

Another type of vesicle observed in the mouse aortic endothelial cell cytoplasm was Weibel-Palade bodies. Although these vesicles are not involved in elastin synthesis, they are distinctive features of endothelial cells. Weibel-Palade bodies have been described to be elongated vesicles, approximately 100 nm thick and up to 3  $\mu\text{m}$  in length, containing tubular structures, 15 - 20 nm in diameter, embedded in a dense matrix (Weibel and Palade, 1964). Sengel and Stoebner (1970) showed that the tubular inclusions were assembled and possibly synthesized in the endothelial cell Golgi apparatus. Later studies showed that endothelial cells have the capacity to synthesize von Willebrand factor (Jaffe et al., 1973, 1974). von Willebrand factor mediates the attachment of platelets to the subendothelium after injury to the vessel wall (Sakariassen et al., 1979). Subsequent studies in both cultured endothelial cells (Wagner et al., 1982) and endothelial cells in vivo (Warhol and Sweet, 1984) demonstrated that Weibel-Palade bodies were the storage sites of von Willebrand factor.

### 3.4.2 ENDOTHELIAL CELL TO ELASTIC LAMINA CONNECTIONS

The present study reveals that extensive filament bundles connect endothelial cells to the underlying elastic lamina in the developing aortic intima. The connecting filaments anchor to the abluminal surface of the endothelial cell in regions of membrane occupied intracellularly by membrane-associated dense plaques. Similar dense plaques have been observed along the basal surface of endothelial cells of the frog heart (Stehbens and Meyer, 1965) and in lymphatic and vascular endothelial cells (Stehbens, 1966). In these cells, the dense plaques were thought to represent structures similar to dermoepidermal hemidesmosomes and thus provide basal attachment of the endothelial cell to the basement membrane and surrounding matrix (Stehbens, 1966). To examine the structural basis of endothelial cell attachment, Ts'ao and Glagov (1970) subjected rabbit aortic endothelial cells to mechanical injury in vivo or hypotonic solutions in vitro. Despite these disruptive conditions, the endothelial cells remained attached to the underlying matrix, however, only in the regions of the cell membrane occupied by "dense zones".

In the present study, endothelial cell connecting filaments were shown to be most prominent during early development of the vessel wall; becoming increasingly inconspicuous as the vessel grows and the subendothelial elastic lamina approaches the endothelial cell surface. Although Paule (1963) noted irregularly distributed diffuse material in the subendothelial matrix of the newborn rat aorta, most early ultrastructural studies of developing aortae (Karrer, 1960, 1961) were hampered by poor techniques for tissue preservation and thus failed to show any subendothelial specializations.

Extracellular filaments that connect endothelial cells to the surrounding matrix were first shown in association with lymphatic capillaries (Leak and Burke, 1968). The filaments were suggested to be responsible for maintaining a firm attachment of the lymphatic capillary wall to the surrounding connective tissue elements and were thus termed "anchoring filaments". Consistent with the present study, Gerrity and Cliff (1972) described similar filaments in the vascular subendothelial matrix of aortae from young rats. These investigators retained the term "anchoring filaments"; however, in the present study, these structures have been renamed "endothelial cell connecting filaments" to avoid possible confusion with the term "anchoring fibrils" used for type VII collagen (Keane et al., 1987).

The ultrastructure details of endothelial cell connecting filaments presented in this study provide morphological evidence that the connecting filaments are microfibrillar in nature; either as direct extensions of elastin-associated microfibrils or as modified microfibrils specific for the function of endothelial cell anchorage. Consistent with the present findings, Gerrity and Cliff (1972) reported that connecting filaments in the subendothelial matrix of young rats are 9 - 10 nm in diameter and appear identical to elastin-associated microfibrils. Ultrastructural studies on lymphatic endothelial cell connecting filaments have also provided evidence for the microfibrillar nature of connecting filaments (Leak and Burke, 1968; Böck, 1978; Gerli et al., 1990). Typical of microfibrils, the lymphatic endothelial cell connecting filaments have a diameter of approximately 12 nm with a central electron-lucent core and peripheral electron-dense subunits, some with spike-like projections (Gerli et al., 1990). In addition, the filaments

were shown by specific histochemical stains to react in an identical manner to that of both elastin-associated microfibrils and microfibril bundles free of elastin (Böck, 1978; Gerli et al., 1990). The fact that lymphatic endothelial cells appear to be anchored by microfibrils to elastic fibers in the surrounding matrix provides credibility to the hypothesis that microfibrils are involved in vascular endothelial cell anchorage to the elastic lamina.

The proposed role of connecting filaments in endothelial cell anchorage to the underlying matrix has been based on observations of the organization of the connecting filaments in the vessel wall and their relationship to adjacent structures. Connecting filaments anchor on the abluminal endothelial cell membrane in regions of membrane occupied by intracellular dense plaques. The dense plaques are attachment points for a bundles of intracellular filaments, termed stress fibers (Wong et al., 1983). The stress fibers and the extracellular connecting filaments are aligned in the same direction, parallel to the long axis of the vessel, and are thus parallel to the direction of blood flow (Gerrity and Cliff, 1972; Yohro and Burnstock, 1973; Buck, 1979). In contrast to the present findings and those of Gerrity and Cliff (1972), Buck (1979) reported that the connecting filaments usually appear to terminate prior to reaching the surface of the first elastic lamina. However, the aortae examined were sectioned parallel to the endothelial cell layer and thus the association of the connecting filaments with the underlying elastic lamina may have been difficult to discern.

The appearance of endothelial cell connecting filaments early in development of the aortic intima and their relative disappearance in adult life suggest that the filaments

are primarily involved in the maintaining the structural integrity of the endothelial cell layer during vessel formation. Since the subendothelial elastic lamina is not fully formed during pre-natal and neo-natal life, and is separated from the endothelial cells by a considerable distance, the connecting filaments may provide a means to anchor the endothelial cells to the lamina in order to protect the cells from the hemodynamic stresses imposed upon the vessel wall during development. Although no studies on connecting filament expression in response to mechanical stress have been reported, considerable work has been carried out on the expression and distribution of the intracellular stress fibers. Stress fibers are more prominent and more often observed in endothelial cells that are next to branch points in vessels (White et al., 1983; Kim et al., 1989a). In addition, a higher proportion of stress fibers has been observed in endothelial cells of hypertensive rats as compared with normotensive controls (White et al., 1983; White and Fujiwara, 1986). The increased expression of stress fibers is thought to be due to elevated fluid shear force (White et al., 1983; Herman et al., 1987); the frictional force created by blood flow (Dewey, 1979). This suggestion is supported by the observation that stress fibers can be induced to form in cultured vascular endothelial cells exposed to fluid shear stress (Franke et al., 1984) and appear enhanced in aortic endothelial cells exposed in vivo to experimentally elevated shear stress (Kim et al., 1989b). These studies suggest that stress fibers play an important role in the maintenance of endothelial cell integrity under conditions of increased hemodynamic stress by providing increased cell to substrate adhesion. Although these studies did not report on subendothelial structures, the results argue a priori for the involvement of endothelial cell connecting filaments in this function

since they are directly associated with the intracellular stress fibers. Furthermore, stress fibers have been shown to reorganize during endothelial cell adaptation and regeneration following injury (Gabbiani et al., 1983). Thus, endothelial cell connecting filaments may also be able to redistribute and reform in pathological situations.

The relative disappearance of the connecting filaments as the vessel matures may be due to their incorporation into the expanding elastic lamina. In the pre-natal aorta, the endothelial cells are separated from the subjacent elastic lamina by a considerable subendothelial matrix. The distance from the abluminal cell membrane to the elastic lamina diminishes in size until the elastic lamina is almost directly apposed to the cell surface. In the adult vessel, the basal attachment of the endothelial cells to the underlying elastic lamina has been suggested to consist of two modes of adhesion: one, fine diffuse contacts over the entire surface of the membrane; and the other, strong focal contacts at regions of the membrane occupied by dense plaques (Ts'ao and Glagov, 1970). The fine diffuse contacts may not be well established or sufficient enough to support the endothelium in the developing vessel, especially since the subendothelial structures are still forming. Thus, the connecting filaments may be vital for the maintenance of endothelial cell attachment until the subendothelial structures develop and the fine contacts are fully formed. Although the endothelial cell connecting filaments disappear, the dense plaques to which they anchor appear to remain as endothelial pegs on the abluminal endothelial cell surface and may provide the strong focal contacts. These results are consistent with the observation of endothelial pegs in the rat aorta (Gerrity and Cliff, 1972; Buck, 1979) where they are thought to provide enhanced adhesion of the endothelial

cells to the subendothelial matrix through increased surface contact (Buck, 1979).

The present study has demonstrated filamentous connections from the abluminal endothelial cell surface to the subjacent elastic lamina that appear morphologically similar to elastin-associated microfibrils. The connecting filaments, together with intracellular stress fibers, appear to play an important role in maintaining the structural integrity of the aortic intima against the shear stress exposed to the endothelium during early development of the vessel wall.



***CHAPTER FOUR***

***IMMUNOLOCALIZATION OF MICROFIBRIL AND MICROFIBRIL-  
ASSOCIATED PROTEINS ON ENDOTHELIAL CELL  
CONNECTING FILAMENTS***



## 4.1 INTRODUCTION

Elastic fibers consist of two morphologically distinct components; an amorphous core of elastin and a peripheral mantle of 10 - 12 nm microfibrils (Low, 1961, 1962; Greenlee et al., 1966; Ross and Bornstein, 1969). The microfibrils appear first in development and are subsequently infiltrated with elastin to form mature elastic fibers (Fahrenbach et al., 1966; Albert, 1972). Morphologically similar microfibrils have also been described that remain completely devoid of elastin. These microfibrils, termed "oxytalan fibers" by Fullmer and Lillie (1958), appear to predominate in areas subjected to mechanical stress such as skin (Cotta-Pereira et al., 1976), periodontal ligament (Carmichael and Fullmer, 1966) and tendon (Rodrigo et al., 1975). This suggests that in addition to their involvement in elastogenesis, microfibrils may play an important role in cell anchorage and tissue stability.

In skin, oxytalan fibers anchor the epidermal cells to elastic fibers in the dermis by forming a continuous link with the elastin-associated microfibrils (Cotta-Pereira et al., 1976; Dahlbäck et al., 1990). Similarly, "anchoring filaments" have been identified in subendothelial matrix of lymphatic capillaries where they appear to connect lymphatic endothelial cells to surrounding elastic fibers (Leak and Burke, 1968; Böck, 1978; Gerli et al., 1990). Based on ultrastructural similarities and histochemical staining properties, these anchoring filaments were identified as microfibrils typical of oxytalan fibers (Böck, 1978; Gerli et al., 1990). Oxytalan fibers have also been identified in association with endothelial cells of bone marrow sinusoids on the basis of morphology; although the

microfibrils of the oxytalan fibers were wrongly identified as type III collagen (Campbell, 1987).

Gerrity and Cliff (1972) described anchoring filaments which apparently connected endothelial cells to the subjacent elastic lamina in the aorta of young rats. Similar anchoring filaments were observed in the subendothelial matrix of coronary vessels (Yohro and Burnstock, 1973). In both studies, the anchoring filaments were suggested to be synonymous with microfibrils based on morphological similarities. In a later study on subendothelial matrix structures in the rat aorta, Buck (1979) described anchoring filaments and microfibrils as distinct filamentous components. Furthermore, the anchoring filaments were reported to terminate prior to reaching the surface of the elastic lamina (Buck, 1979). Recently, studies of the developing mouse aorta have demonstrated the presence of extensive filament bundles that extend from the abluminal membrane of the endothelial cell to the surface of the subjacent elastic lamina (see Chapter 3). Detailed morphological investigation of these endothelial cell connecting filaments has provided evidence for their ultrastructural similarity to microfibrils; however, further characterization of these filaments is necessary to establish their relationship to elastin-associated microfibrils and oxytalan fibers.

Specific localization of antibodies directed against microfibrils provides one means to identify filamentous structures as microfibrils. At least two glycoproteins have been isolated and characterized that appear to be constituents of microfibrils: microfibril-associated glycoprotein (MAGP), a 31 kDa protein isolated from reductive guanidine-hydrochloride extracts of fetal bovine ligamentum nuchae (Gibson et al., 1986, 1991); and

fibrillin, a 350 kDa glycoprotein isolated from the medium of human fibroblast cultures (Sakai et al., 1986). Gibson and colleagues (1989) also identified a 340 kDa glycoprotein component of microfibrils (MP340) in the reductive guanidine-hydrochloride extracts; however, this protein was found to be the bovine homologue of fibrillin (M.A. Gibson, personal communication). Immunolocalization studies using specific antibodies to MAGP (Gibson and Cleary, 1987; Kumaratilake et al., 1989) and fibrillin (Sakai et al., 1986; Dahlbäck et al., 1990) have shown the presence of the two glycoproteins in both elastin-associated microfibrils and oxytalan fibers. These findings provide strong evidence that microfibrils of different tissues have some ultrastructural similarity; although, it still remains uncertain as to whether microfibrils are a single structural entity or constitute a family of filamentous structures.

In the present study, the composition of endothelial cell connecting filaments in the developing mouse aorta was investigated by immunohistochemistry. Antibodies specific for the microfibril proteins, MAGP and MP340 were used. Since endothelial cell connecting filaments appear coated with electron-dense material (see Chapter 3), the immunolocalization of fibronectin, amyloid P component (AP) and heparan sulfate proteoglycan (HSPG) were also examined. Both fibronectin (Krauhs, 1983; Fleischmajer and Timpl, 1984; Schwartz et al., 1985; Inoue et al., 1989) and amyloid P component (Breathnach et al., 1981, 1989; Khan and Walker, 1984; Inoue et al., 1986a; Dahlbäck et al., 1990) have been shown by immunohistochemistry to localize to microfibrils in a number of tissues. Although HSPG is not specifically recognized as a microfibril-associated protein, HSPG has been immunolocalized on the surface of fibronectin-

containing fibers in the extracellular matrix of fibroblast cultures (Singer et al., 1987).

The results from this study indicate that endothelial cell connecting filaments of the mouse aortic intima are microfibrillar in nature, and thus provides evidence for the additional role of microfibrils as anchoring components in tissues.

## 4.2 MATERIALS AND METHODS

### 4.2.1 PREPARATION OF LOWICRYL EMBEDDED TISSUE

C57/BL mice, 5-day post-natal age, were anaesthetized with sodium pentobarbital and prepared for cardiac perfusion. Each mouse was perfused through the left ventricle with lactated Ringer's until the liver was cleared of blood. Immediately, the perfusing solution was changed to 4% paraformaldehyde in 0.1 M Sorensen's buffer (pH 7.4). Alternatively, some animals were perfused with 4% paraformaldehyde and 0.25% glutaraldehyde in 0.1 M Sorensen's buffer. After 5 minutes of perfusion, the thoracic aorta was removed and dissected as previously described (see section 2.2.1). All tissue pieces, with and without initial glutaraldehyde fixation, were placed separately in 4% paraformaldehyde in 0.1 M Sorensen's buffer containing 4% sucrose for an additional 2 hours at room temperature.

Pre-natal mice aortae were also prepared for Lowicryl embedding. Pregnant C57/BL mice, at 15 days of gestation, were anaesthetized with sodium pentobarbital and the mouse pups were removed. Thoracic aortae were dissected from the pups, cut into segments and placed in either 4% paraformaldehyde in 0.1 M Sorensen's buffer without glutaraldehyde or in 4% paraformaldehyde in 0.1 M Sorensen's buffer with 0.25% glutaraldehyde. After 10 minutes, all tissue pieces were placed separately in 4% paraformaldehyde in 0.1 M Sorensen's containing 4% sucrose for an additional 2 hours

at room temperature.

Following fixation, half of each sample was removed and placed in new vials containing 20 mM Tris (pH 8.0) in preparation for reductive denaturing treatment according to Gibson and colleagues (1989). After 2 minutes, the tissue pieces were treated with 6 M guanidine-hydrochloride and 5 mM dithiothreitol in 20 mM Tris for 15 minutes. The tissue pieces were then rinsed briefly in 20 mM Tris and placed in 100 mM iodoacetamide in Tris buffer for an additional 15 minutes. All samples, treated and untreated, were then rinsed several times in 0.15 M Sorensen's buffer (pH 7.4) containing 4% sucrose and left overnight at 4°C in a fresh change of buffer.

The following morning methanol and Lowicryl solutions were prepared for dehydration and infiltration. Methanol dilutions of 30%, 50%, 75% and 90% were made and placed at 4°C, -10°C, -20°C and -20°C, respectively. Lowicryl (M.E.C.A. Ltd., Montreal, Que.) was prepared by mixing 17.3 gm of monomer B, 2.7 gm of cross-linker A and 0.109 gm of initiator C in a 100 ml plastic beaker covered with parafilm and wrapped with foil. Nitrogen gas was bubbled through the solution for several minutes before it was drawn into a 20 ml syringe and wrapped in foil to protect the solution from light exposure. Lowicryl:90% methanol mixtures of 1:1 and 2:1 were made and placed at -20°C with the remaining pure Lowicryl left in the syringe.

After several hours to allow all solutions to reach their appropriate temperatures, the tissue pieces were dehydrated for 5 minutes in 30% methanol at 4°C, 10 minutes in 50% methanol at -10°C, 10 minutes in 75% methanol at -20°C and 2 changes for 15 minutes each in 90% methanol at -20°C. Following dehydration, the tissue pieces were

infiltrated at -20°C with 1:1 Lowicryl:90% methanol for 1 hour, 2:1 Lowicryl:90% methanol for 2 hours and finally placed in pure Lowicryl at -20°C overnight. All dehydration and infiltration steps were carried out on a rotator placed inside the freezer.

The next day, a fresh solution of pure Lowicryl was prepared and placed in the -20°C freezer. The temperature was immediately lowered to -35°C. After several hours to allow for temperature equilibration, samples were removed from the freezer one at a time and individual tissue pieces were placed in 250  $\mu$ l ultracentrifuge tubes filled with cold Lowicryl and capped. During embedding, all solutions and tubes were kept in a fume hood on crushed ice supercooled with sodium chloride. The ultracentrifuge tubes were placed back in the -35°C freezer in a methanol sink and left for 3 hours to ensure that the Lowicryl in the tubes had equilibrated to -35°C. The methanol sink is critical as it aids in heat dissipation during polymerization. Two ultraviolet lights were then placed in the freezer approximately 10 cm away from either side of the tubes and turned on. After 24 hours, the temperature of the freezer was turned up to -10°C and left for an additional 48 hours. Polymerized Lowicryl blocks were stored indefinitely at -20°C in vials containing a drying agent.

#### 4.2.2 ANTIBODIES

Control Lowicryl sections were incubated either with non-immunized rabbit serum as the primary antibody or with no primary antibody. Experimental Lowicryl sections were incubated with either anti-MP340, anti-microfibril-associated glycoprotein (MAGP),

anti-fibronectin, anti-heparan sulfate proteoglycan (HSPG) or anti-amyloid P component (AP). The anti-MP340 and anti-MAGP antibodies were affinity purified polyclonal antibodies raised in rabbits. The MP340 and MAGP antigens were isolated and purified from reductive guanidine-hydrochloride extracts of fetal bovine ligamentum nuchae. These antibodies were generously donated by Dr. Mark Gibson, University of Adelaide. Since MP340 has been shown to be the bovine homologue of fibrillin (M.A. Gibson, personal communication), MP340 will hereafter be referred to as fibrillin. The anti-fibronectin antibody, a rabbit polyclonal antibody raised against rat plasma fibronectin, was commercially purchased (Calbiochem, San Diego, CA). The anti-HSPG antibody was a rabbit polyclonal antibody raised against HSPG isolated from murine Engelbreth-Holm-Swarm tumor. This antibody was generously donated by Dr. Hynda Kleinman, NIH. Several polyclonal anti-AP antibodies were used: a rabbit anti-mouse serum AP antibody generously donated by Dr. Martha Skinner, Boston University; a rabbit anti-mouse serum AP antibody and a rabbit anti-Syrian hamster female AP antibody generously donated by Dr. John Cole, NIH; and a commercially purchased rabbit anti-mouse serum AP antibody (Calbiochem, San Diego, CA).

The anti-fibrillin and anti-MAGP antibodies were used as provided at a concentration of approximately 60  $\mu\text{g/ml}$ . The anti-fibronectin, anti-HSPG and anti-AP antibodies were diluted 1:50 in 50 mM Tris (pH 7.6) with 0.1 M sodium chloride and 1% bovine serum albumin (BSA).

The secondary antibody was goat anti-rabbit IgG conjugated to 8 nm colloidal gold diluted 1:15 in 50 mM Tris (pH 7.6) with 0.1 M sodium chloride and 1% BSA.

### 4.2.3 IMMUNOLABELING PROCEDURE

Lowicryl thin sections were cut with a diamond knife on a Reichert ultracut microtome and placed on formvar coated nickel grids. The grids were stored overnight at 4°C.

The following day, the grids were incubated face down on drops of blocking solution consisting of 50 mM Tris (pH 7.6) with 0.1 M sodium chloride and 1% BSA. After 15 minutes, the grids were removed from the blocking solution, touched to filter paper to remove the excess solution and immediately transferred face down to 15  $\mu$ l drops of primary antibody for 1 hour. Following the 1 hour incubation, the grids were washed by floating face down on wells of washing solution in a multiwell plate for 3 changes of 10 minutes each. The washing solution consisted of 50 mM Tris (pH 7.6) with 0.1 M NaCl and 0.1% Tween-20. The grids were then placed on fresh drops of blocking solution for 15 minutes prior to being transferred to 15  $\mu$ l drops of secondary antibody. After 1 hour, the grids were washed on 3 changes of washing solution, followed by 3 changes of double distilled water, for a total of 30 minutes then let air dry. All incubations were carried out in a humidity chamber at room temperature.

The immunolabeled sections were counterstained with methanolic uranyl acetate for 2 minutes followed by lead citrate for 30 seconds as previously described (see section 2.2.2). The stained sections were examined in a Philips 301 transmission electron microscope at an accelerating voltage of 80 kV.

## 4.3 RESULTS

### 4.3.1 TECHNICAL DETAILS

#### *4.3.1.1 Appearance of Lowicryl embedded tissue*

The tissue embedded in Lowicryl and stained with methanolic uranyl acetate followed by lead citrate appears different from that routinely prepared for Epon embedding. Lowicryl embedded tissue is usually prepared for immunolabeling, thus the tissue is fixed with little or no glutaraldehyde and no en bloc stains are used during tissue processing. This results in reduced preservation of cytoplasmic components and less general tissue contrast (Fig. 4-1). Specifically, cell and organelle membranes are difficult to distinguish and, in the aorta, the elastic laminae are electron lucent. Elastin-associated microfibrils at the periphery of the elastic laminae appear electron dense and thus the borders of the laminae can be recognized in the intercellular region (Fig. 4-1). In higher magnification micrographs of the subendothelial matrix, endothelial cell connecting filaments are easily recognized, usually in association with membrane-associated dense plaques (Fig. 4-2). The morphological appearance of endothelial cell connecting filaments as observed in Epon embedded tissue will not be discussed in this chapter as ultrastructural features of the connecting filaments have already been covered in detail (see Chapter 3).

#### ***4.3.1.2 Effects of fixation on immunolabeling***

Immunolabeling with each antibody was conducted on tissues fixed in paraformaldehyde only, as well as, tissues fixed in paraformaldehyde with a low concentration of glutaraldehyde during perfusion. Following perfusion, all tissues were transferred to fixative containing only paraformaldehyde. Tissues briefly exposed to glutaraldehyde during perfusion demonstrated better preservation and tissue contrast over those fixed in paraformaldehyde only. However, when these tissues were used for immunolabeling, a slight increase in non-specific background labeling over the aortic cells was occasionally observed. For all antibodies used in the present study, comparison between tissues fixed by the two different methods during perfusion showed that the specific distribution and relative intensity of labeling was not affected by the addition of glutaraldehyde to the perfusing solution.

#### ***4.3.1.3. Effects of reductive guanidine-hydrochloride on immunolabeling***

One half of all tissue samples prepared for immunolabeling was treated with the chaotropic agent, guanidine-hydrochloride together with the reducing agent, dithiothreitol, followed by alkylation with iodoacetamide. Anti-fibronectin, anti-HSPG and anti-AP antibodies reacted with approximately the same affinity on both treated and untreated tissue. Little or no reaction was observed on untreated tissues with anti-MAGP antibody; however, a good reaction was seen on treated tissue. With anti-fibrillin antibody, no reaction was observed on untreated tissue; whereas treated tissue showed a very strong reaction. Due to these observations, all immunolabeling electron micrographs presented

in this study are from tissue treated with reductive guanidine-hydrochloride following fixation.

#### ***4.3.1.4 Immunolabeling control***

Control sections were prepared from each different tissue sample for every separate immunolabeling experiment. Immunolabeling with non-immunized rabbit serum as the primary antibody followed by colloidal gold conjugated to goat anti-rabbit IgG as the secondary antibody resulted in only a few non-specific background gold particles bound to the tissue (Fig. 4-2). A similar amount of background labeling was observed on tissue sections treated with the secondary antibody alone (not shown). In general, little qualitative difference in background labeling was seen between sections from tissues exposed to glutaraldehyde in the perfusing fixative as opposed to those fixed only in paraformaldehyde.

### **4.3.2 IMMUNOLABELING OF THE DEVELOPING AORTIC INTIMA - 5-DAY POST-NATAL AGE**

#### ***4.3.2.1 Fibrillin***

Immunolocalization of fibrillin in the aortic intima showed extensive labeling in the subendothelial matrix. The strongest reaction was observed over the peripheral mantle of elastin-associated microfibrils that surrounds the elastic lamina (Fig. 4-3). Microfibrils

embedded within the elastin lamina were also labeled. Between the elastic lamina and the abluminal surface of the endothelial cell, the endothelial cell connecting filaments were easily recognized; often in association with a membrane-associated dense plaque. The connecting filaments showed a moderate reaction to the anti-fibrillin antibody; although the immunoreaction observed over the elastin-associated microfibrils was so strong that this labeling was often difficult to appreciate (Fig. 4-3). The positive immunolocalization of fibrillin associated with the connecting filaments appeared more evident in longitudinal sections of the filaments (Fig. 4-4). Individual gold particles could often be seen along the length of a single connecting filament.

Immunolabeling with anti-fibrillin appeared to result in slight intracellular non-specific background labeling (Fig. 4-3). However, some electron-dense vesicles within the endothelial cell cytoplasm showed a positive reaction for the presence of fibrillin (Fig 4-4b); thus, if the cell was actively involved in the synthesis of fibrillin, some intracellular labeling of structure such as rough endoplasmic reticulum and Golgi saccules, would be expected. Since these membranous structures are difficult to recognize in Lowicryl sections, the labeling that appears as background labeling may actually be within these structures. Although not easily distinguished, cisternae of rough endoplasmic reticulum were often seen in areas that appeared to show background labeling (Fig. 4-3).

#### ***4.3.2.2 Microfibril-associated glycoprotein (MAGP)***

Anti-MAGP showed a moderate immunoreaction periodically distributed along the edge of the elastic lamina in the area occupied by elastin-associated microfibrils (Fig. 4-

5). Gold particles were also observed in association with microfibrils within the elastic lamina. Little or no immunolabeling was observed in association with the endothelial cell connecting filaments either in cross-section (Fig. 4-5a) or in longitudinal section (Fig. 4-5b). Although a few gold particles were occasionally seen on connecting filaments, the immunolabeling was not consistent enough, nor abundant enough, to indicate the presence of MAGP associated with the connecting filaments. No immunolabeling of endothelial cell vesicles was observed.

#### **4.3.2.3 *Fibronectin***

Immunolabeling with anti-fibronectin revealed a strong positive reaction associated with the endothelial cell connecting filaments (Fig. 4-6). In cross-section, gold particles were observed over the entire area occupied by the connecting filaments (Fig. 4-6a); while in longitudinal section, the gold particles appeared evenly distributed along their lengths (Fig. 4-6b). Relatively little immunolabeling was observed at the edges of the elastic lamina in association with the elastin-associated microfibrils; any labeling that was observed, appeared more concentrated on the adluminal side of the lamina as opposed to the abluminal side (Fig. 4-6a). A small amount of labeling was also seen within the elastic lamina, often over electron dense foci, indicating the presence of fibronectin on microfibrils embedded within the amorphous elastin.

#### **4.2.3.4 *Heparan sulfate proteoglycan (HSPG)***

Immunolabeling of the aortic intima with anti-HSPG revealed the presence of

HSPG on endothelial cell connecting filaments (Fig. 4-7). Both in cross-section (Fig. 4-7a) and in longitudinal section (Fig. 4-7b), the gold particles appeared directly over the connecting filaments. Only the occasional gold particle was observed in association with the elastin-associated microfibrils, either at the periphery or within the elastic lamina.

#### ***4.2.3.5 Amyloid P component (AP)***

Immunolocalization with all anti-AP antibodies resulted in diffuse labeling over all tissue within the section, regardless of the fixative used or tissue treatment (not shown). Although gold particles were occasionally observed over elastin-associated microfibrils and endothelial cell connecting filaments, approximately the same number of particles were observed over the cytoplasm and nuclei of the endothelial cells and smooth muscle cells. Since the immunolabeling appeared non-specific due to high background labeling, localization of AP to either elastin-associated microfibrils or connecting was inconclusive.

### **4.3.3 IMMUNOLABELING OF THE FETAL AORTIC INTIMA - 15-DAYS GESTATIONAL AGE**

#### ***4.3.3.1 Fibrillin***

Extensive bundles of endothelial cell connecting filaments were easily recognized in the subendothelial matrix in the 15-day gestation aortic intima. Immunolabeling with anti-fibrillin showed a moderate reaction associated with the connecting filaments and a

heavy reaction over the elastin-associated microfibrils at the edges of the developing elastic lamina (Fig. 4-8a). In addition, some electron-dense vesicles within the endothelial cell cytoplasm showed a strong reaction for the presence of fibrillin (Fig. 4-8b).

#### **4.3.3.2 *Microfibril-associated glycoprotein (MAGP)***

Immunolocalization of MAGP showed a moderate distribution of the protein at the edges of the elastic lamina in association with elastin-associated microfibrils (Fig. 4-9). Endothelial cell connecting filaments, however, showed no immunolabeling with anti-MAGP in either cross-section (Fig. 4-9a) or longitudinal section (Fig. 4-9b). No intracellular labeling of endothelial cell vesicles was observed.

#### **4.3.3.3 *Fibronectin***

The anti-fibronectin antibody showed the a strong immunoreaction over the region of subendothelial matrix occupied by the endothelial cell connecting filaments (Fig. 4-10). Little or no immunolabeling of elastin-associated microfibrils was apparent.

#### **4.3.3.4 *Heparan sulfate proteoglycan (HSPG)***

A diffuse immunolabeling reaction was observed over the endothelial cell connecting filaments with anti-HSPG (Fig. 4-11). This reaction was relatively weak as compared to the immunoreaction of the connecting filaments to anti-fibrillin or anti-fibronectin. The elastin-associated microfibrils showed little or no labeling for the presence of HSPG.

#### **4.3.3.5 Amyloid P component (AP)**

Due to the results obtained with the anti-AP antibodies on the 5-day old mouse aortic intima, immunolocalization of AP in the 15-day gestational mouse aortic intima was not attempted.

#### **4.3.4 IMMUNOLABELING SUMMARY**

Each antibody appeared to label the endothelial cell connecting filaments and the elastin-associated microfibrils with relatively the same affinity in both the 5-day old aortic intima and the 15-day gestational aortic intima. The overall intensity of immunolabeling, in relative terms, is summarized in Figure 4-12. The table represents both 15-day gestational and 5-day post-natal results since no qualitative difference was observed between the two ages. The intensity of the immunoreaction should only be compared between the two different fibrillar structures when labeled with the same antibody since the affinity of the individual antibodies for their epitopes may not be the same.

In summary, immunolabeling of the elastin-associated microfibrils demonstrated the presence of both fibrillin and MAGP. The presence of fibronectin and HSPG on these microfibrils was difficult to determine, although they appeared to show a small amount of immunolabeling with anti-fibronectin and anti-HSPG.

The endothelial cell connecting filaments showed strong labeling for fibronectin as compared to the elastin-associated microfibrils. In addition, the connecting filaments

also labeled weakly with anti-HSPG. Immunolabeling with anti-fibrillin demonstrated the presence of fibrillin on the connecting filaments; however, in contrast to the elastin-associated microfibrils, no labeling of the connecting filaments with anti-MAGP antibody was observed.

No conclusion as to the presence of AP associated with either elastin-associated microfibrils or endothelial cell connecting filaments could be made due to the apparent non-specific labeling observed over the entire tissue section.

All immunolabeling micrographs are from tissues fixed with paraformaldehyde and glutaraldehyde in the perfusing solution followed by treatment with reductive guanidine-hydrochloride, except Figures 4-4a, 4-4b and 4-7a, in which no glutaraldehyde was used in the perfusing solution.

**FIGURE 4-1:** Low magnification of the tunica intima from a 5-day old post-natal mouse showing the general appearance of Lowicryl embedded tissue. The cell nuclei (N) have relatively good contrast; however, within the cytoplasm, cell organelles are difficult to discern. Due to the lack of en bloc staining, membranous components of the cell, such as the cisternae of rough endoplasmic reticulum, Golgi saccules and the cell membrane are not easily identified. In contrast to Epon embedded material counterstained in a similar manner, the elastic lamina (EL) appears electron lucent rather than electron dense. The borders of the lamina are distinguished by the electron dense appearance of the elastin-associated microfibrils (mf). Electron dense foci within the elastic lamina are microfibrils "trapped" within the amorphous elastin (arrowheads). L, lumen; E, endothelial cell; SM, smooth muscle cell. x24,140.



**FIGURE 4-2:** High magnification of the abluminal surface of an endothelial cell (E) and subjacent elastic lamina (EL) in a 5-day old post-natal mouse aorta. Endothelial cell connecting filaments (CF) are easily recognized in the subendothelial matrix associated with a membrane-associated dense plaque (dp). This section is a control section incubated with non-immunized rabbit serum as the primary antibody. Very little background non-specific gold label is observed (arrows). x68,000.

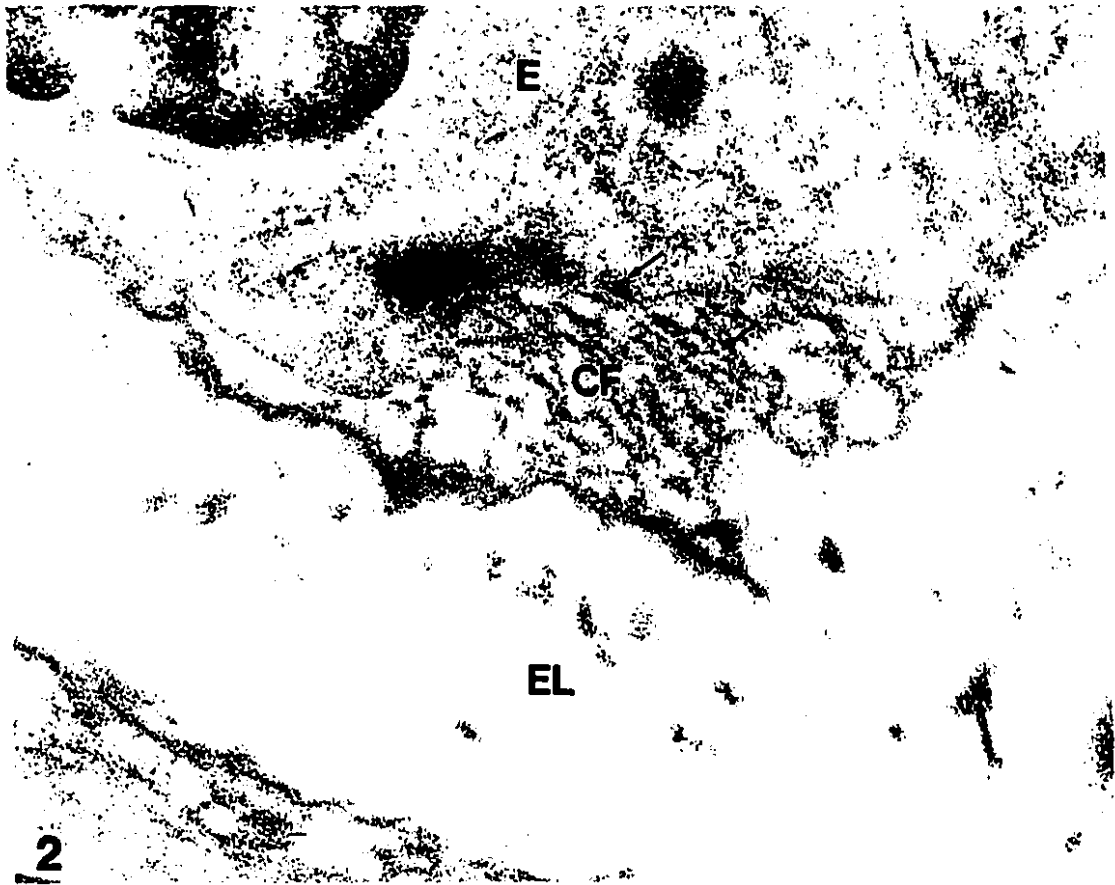
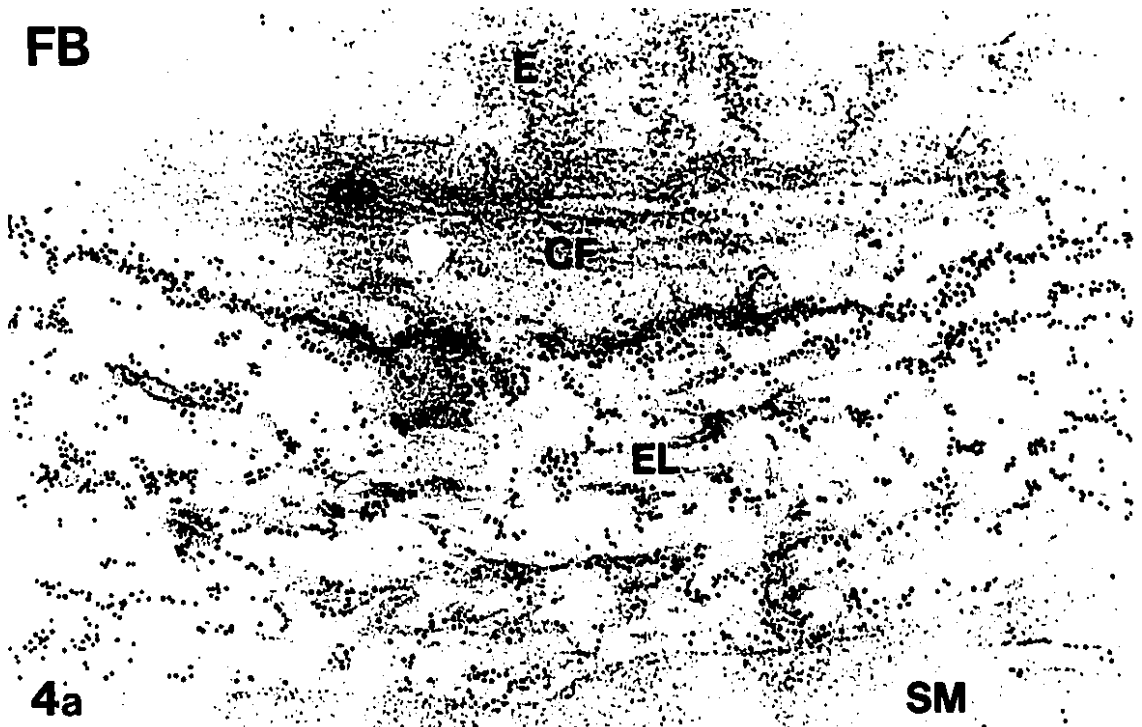


**FIGURE 4-3:** Immunolocalization of fibrillin (FB) in the subendothelial matrix of a 5-day old mouse aorta. Heavy labeling is observed in association with the elastin-associated microfibrils at the edges of the elastic lamina (EL) and with the microfibrils embedded within the lamina (arrows). Endothelial cell connecting filaments (CF), seen in cross-section, are moderately labeled, although slightly overshadowed by the degree of labeling on the adjacent elastin-associated microfibrils. Some labeling is observed within the endothelial cell cytoplasm (E), possibly in association with cisternae of rough endoplasmic reticulum (rER). dp, dense plaque; SM, smooth muscle cell. x63,750.

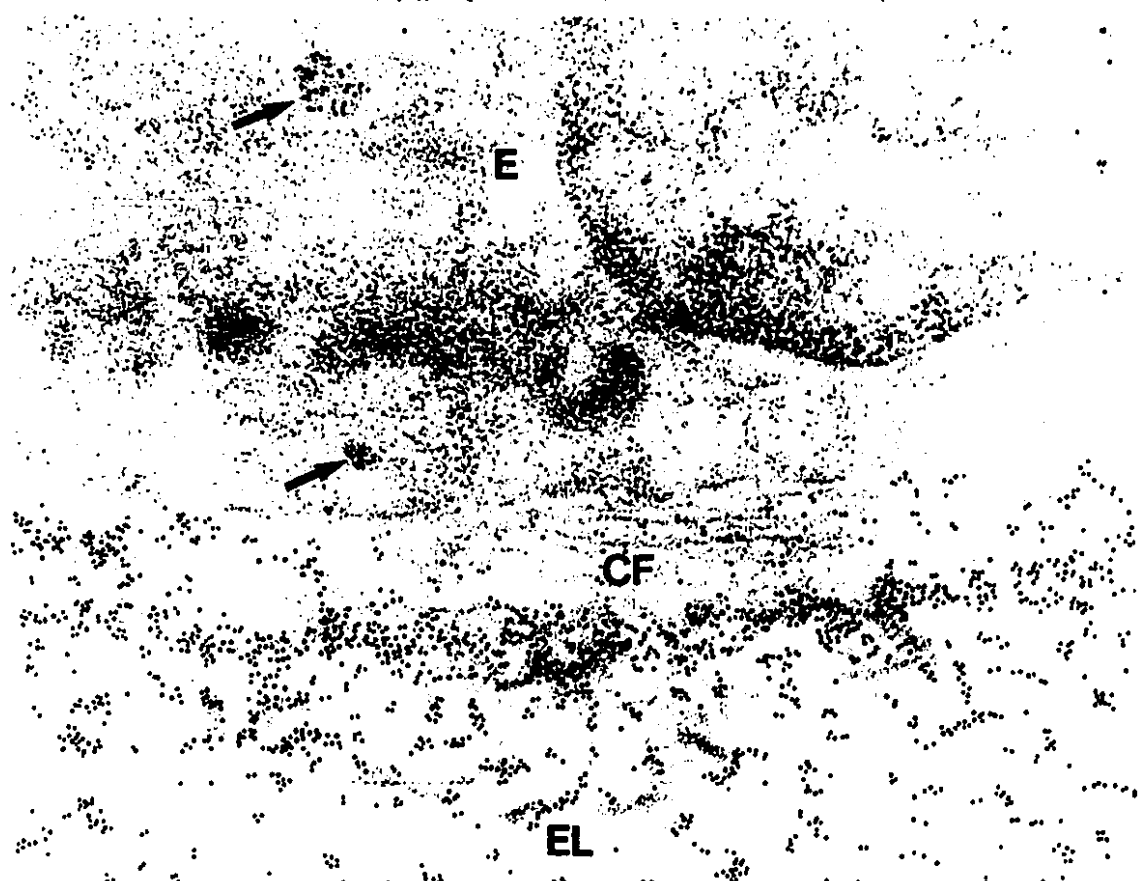


**FIGURE 4-4:** Immunolocalization of fibrillin (FB) in the subendothelial matrix of a 5-day old mouse aorta. As observed in Figure 4-3, anti-fibrillin heavily labels the elastin-associated microfibrils at the periphery of the elastic lamina (EL) (a) Subjacent to the endothelial cell membrane, longitudinally sectioned connecting filaments (CF) can be seen in association with a membrane-associated dense plaque (dp). A moderate distribution of label is seen along the length of the connecting filaments. (b) In addition to the labeling of endothelial cell connecting filaments and elastin-associated microfibrils, some electron dense vesicles within the endothelial cell cytoplasm show strong labeling for the presence of fibrillin. E, endothelial cell; SM, smooth muscle cell. (a) and (b) x41,800.

**FB**



**4a**



**4b**

**FIGURE 4-5:** Immunolocalization of microfibril-associated glycoprotein (MAGP) in the subendothelial matrix of a 5-day old mouse aorta. In both cross-section (a) and longitudinal section (b), endothelial cell connecting filaments (CF) do not appear to label with anti-MAGP. The distribution of label along the periphery of the elastic lamina (EL) and on electron dense foci within the lamina indicates the presence of MAGP on elastin-associated microfibrils. No intracellular labeling of vesicles is observed. L, lumen; E, endothelial cell; N, nucleus; dp, dense plaque; SM, smooth muscle cell. (a) x62,500; (b) x42,000.



**MAGP**

**L**

**E**

**CF**

**EL**

**5a**

**E**

**EL**

**EL**

**5b**

**SM**



**FIGURE 4-6:** Immunolocalization of fibronectin (FN) in the subendothelial matrix of a 5-day old mouse aorta. **(a)** In cross-section, the endothelial cell connecting filaments (CF) are heavily labeled over the entire extent of the filament bundle. Only a few gold particles can be seen in association with the elastin-associated microfibrils; most of these are on the adluminal side (arrowheads) or within the lamina. **(b)** In longitudinal section, the anti-fibronectin labeling shows the distribution of fibronectin along the length of the connecting filaments (CF). Note again the relative lack of label in association with the elastin-associated microfibrils at the edge of the elastic lamina (EL). E, endothelial cell; N, nucleus; dp, dense plaque. **(a)** x50,160; **(b)** x31,350.

**FN**



**6a**

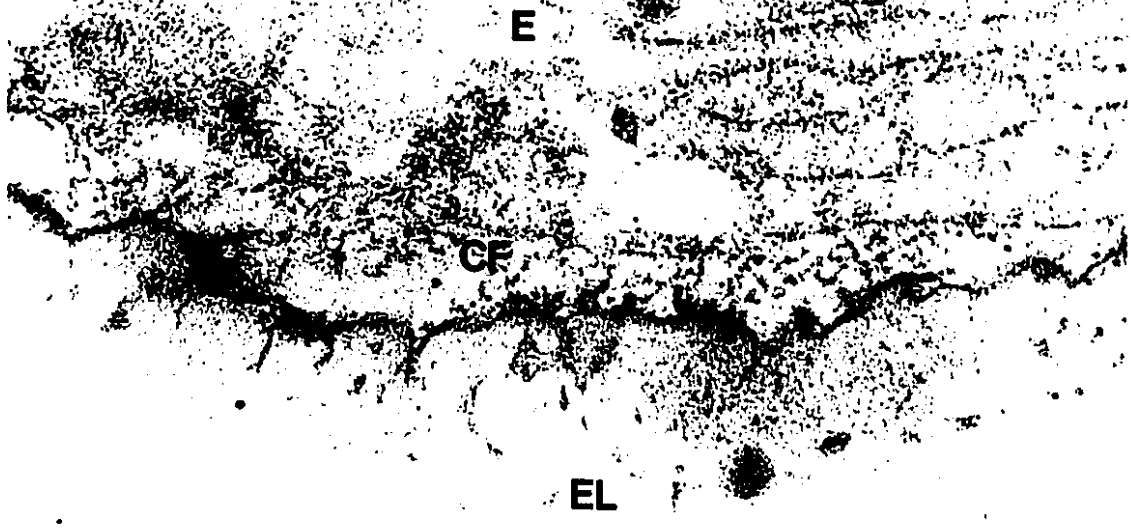


**EL**

**6b**

**FIGURE 4-7:** Immunolocalization of heparan sulfate proteoglycan (HSPG) in the subendothelial matrix of a 5-day old mouse aorta. In both cross-section (a) and longitudinal section (b), a relatively weak reaction is seen in association with the endothelial cell connecting filaments (CF). Elastin-associated microfibrils show little or no labeling for the presence of HSPG. L, lumen; E, endothelial cell; EL, elastic lamina. (a) and (b) x47,500.

**HSPG**

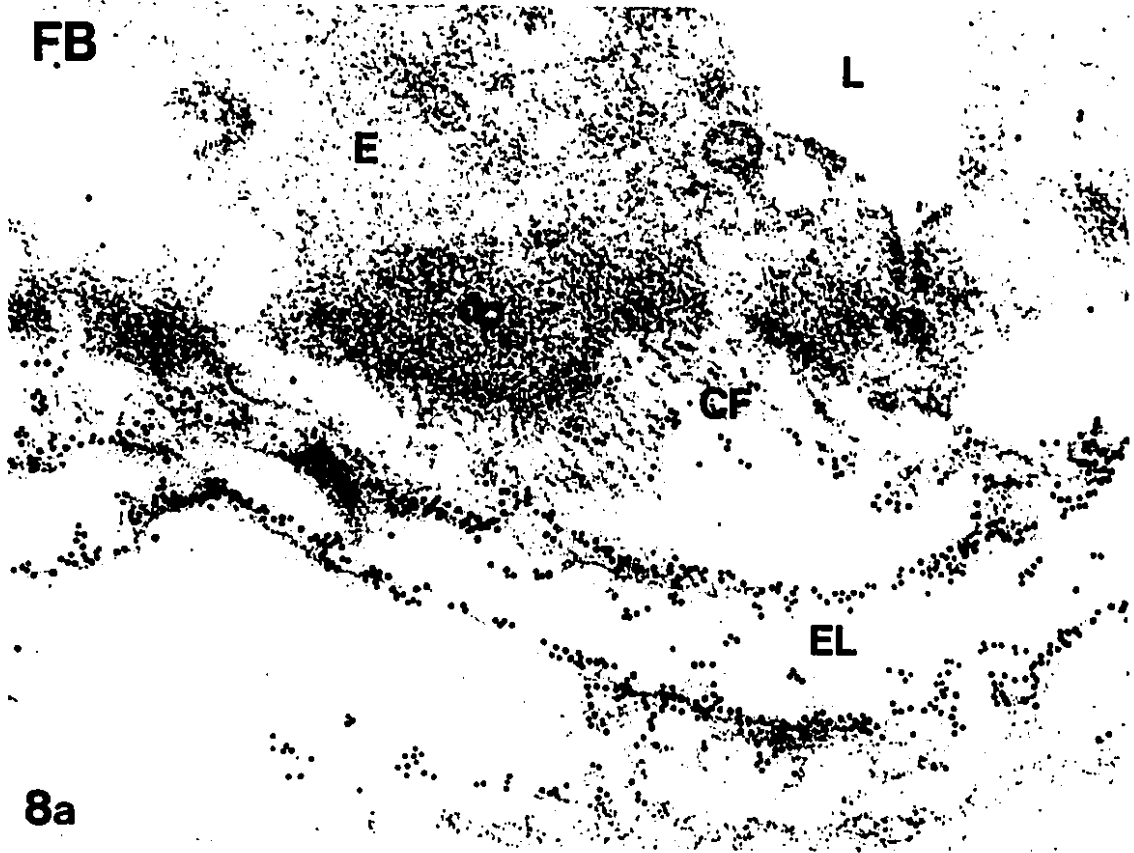


**7a**



**7b**

**FIGURE 4-8:** Immunolocalization of fibrillin (FB) in the subendothelial matrix of a 15-day gestational mouse aorta. **(a)** Elastin-associated microfibrils along the periphery of the developing elastic lamina (EL) show heavy labeling with anti-fibrillin. In comparison, the endothelial cell connecting filaments (CF) appear moderately labeled for the presence of fibrillin. **(b)** Similar to that observed in the 5-day old post-natal mouse aorta, some electron dense cytoplasmic vesicles within the endothelial cell (E) are heavily labeled with anti-fibrillin. L, lumen; dp, dense plaque. **(a)** and **(b)** x57,000.



8a



8b

**FIGURE 4-9:** Immunolocalization of microfibril-associated glycoprotein (MAGP) in the subendothelial matrix of a 15-day gestational mouse aorta. In both cross-section (a) and longitudinal section (b), endothelial cell connecting filaments (CF) do not appear to label with anti-MAGP. A punctate distribution of label is observed along the periphery of the elastic lamina (EL) indicating the presence of MAGP on elastin-associated microfibrils. No intracellular labeling is seen. L, lumen; E, endothelial cell; dp, dense plaque; SM, smooth muscle cell. (a) and (b) x57,000.

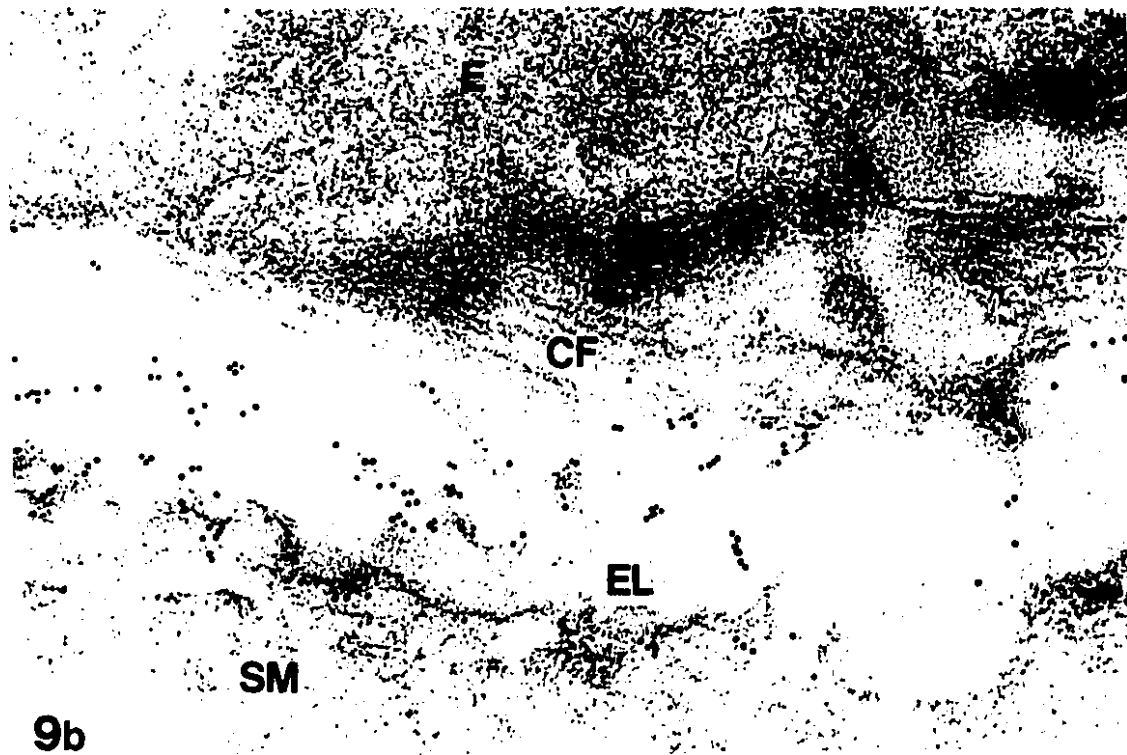
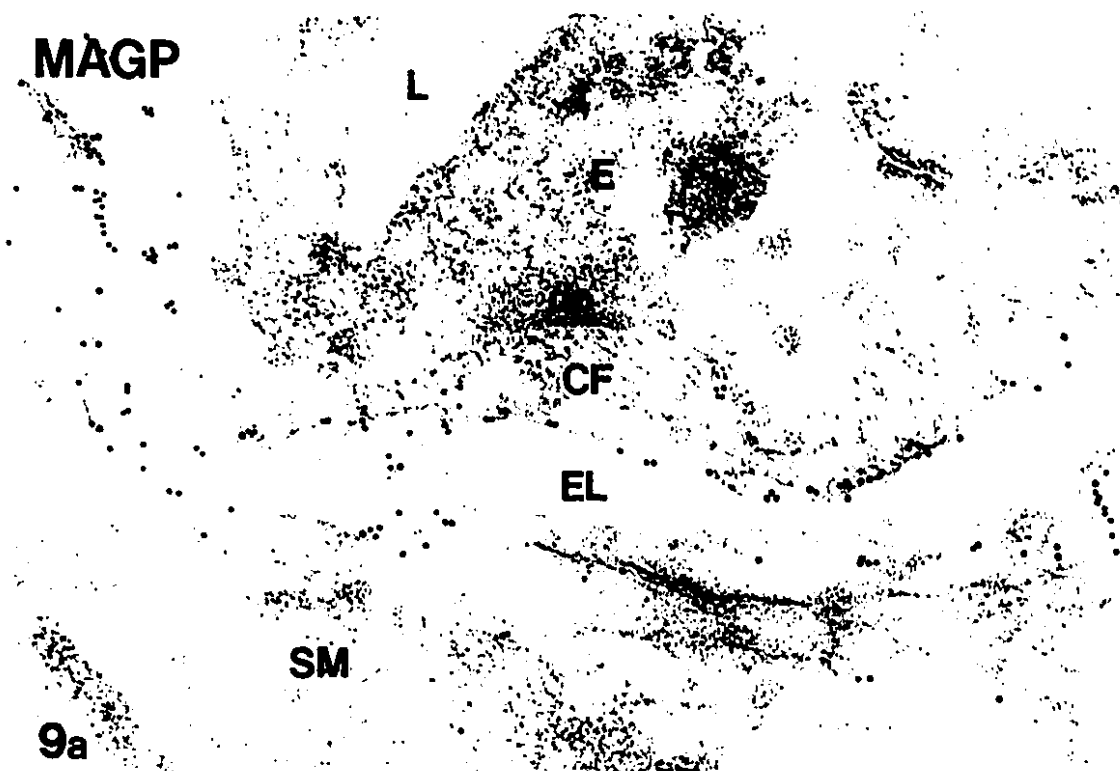


**FIGURE 4-10:** Immunolocalization of fibronectin (FN) in the subendothelial matrix of a 15-day gestational mouse aorta. Endothelial cell connecting filaments (CF) are heavily labeled as seen in both cross-section **(a)** and oblique section **(b)**. Elastin-associated microfibrils at the periphery of the elastic lamina (EL) show little or no labeling for the presence of fibronectin. L, lumen; E, endothelial cell; dp, dense plaque; SM, smooth muscle cell. **(a)** and **(b)** x57,000.

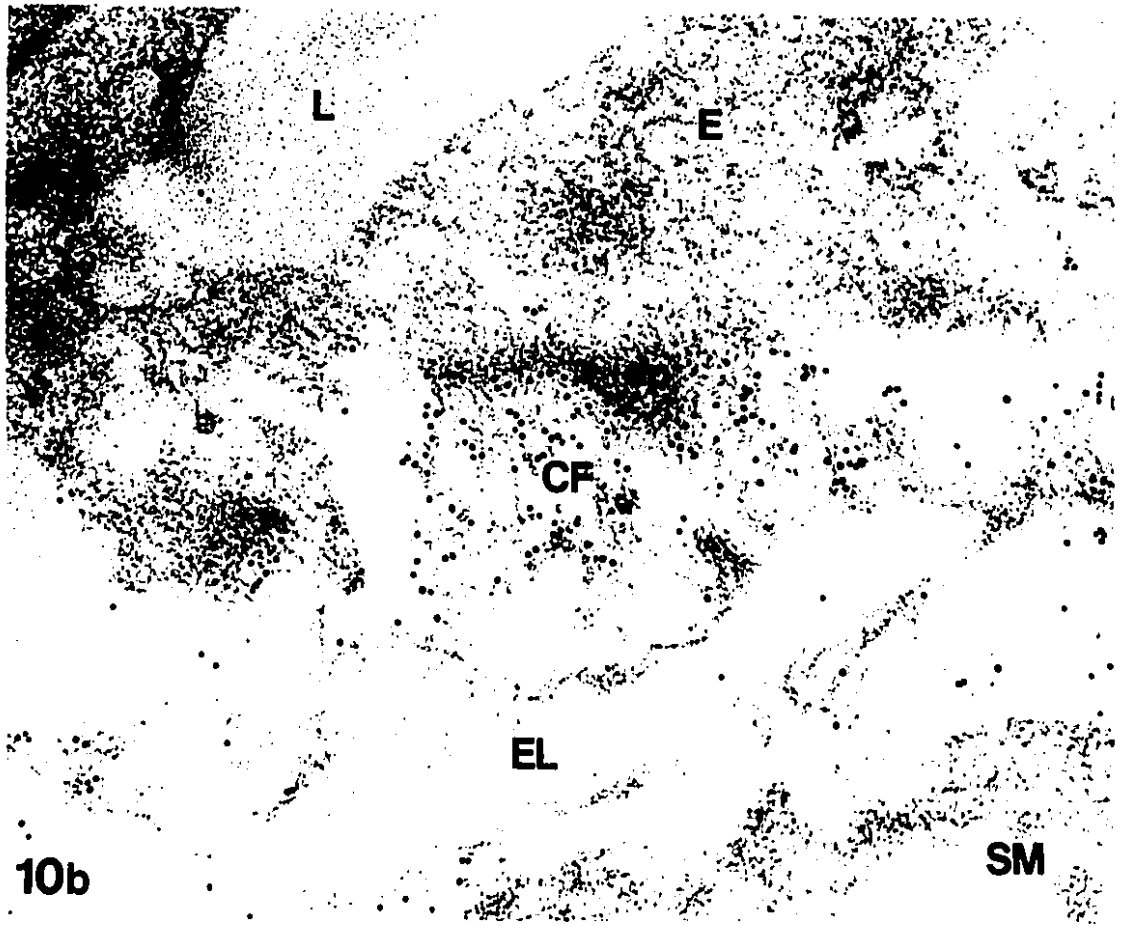
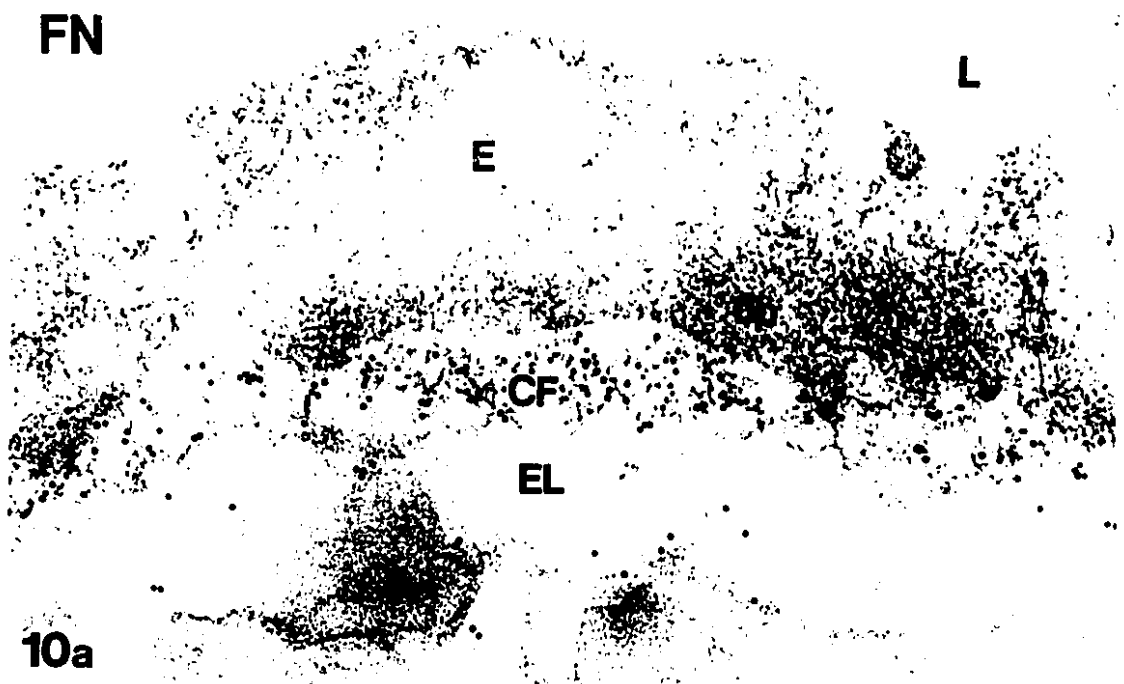
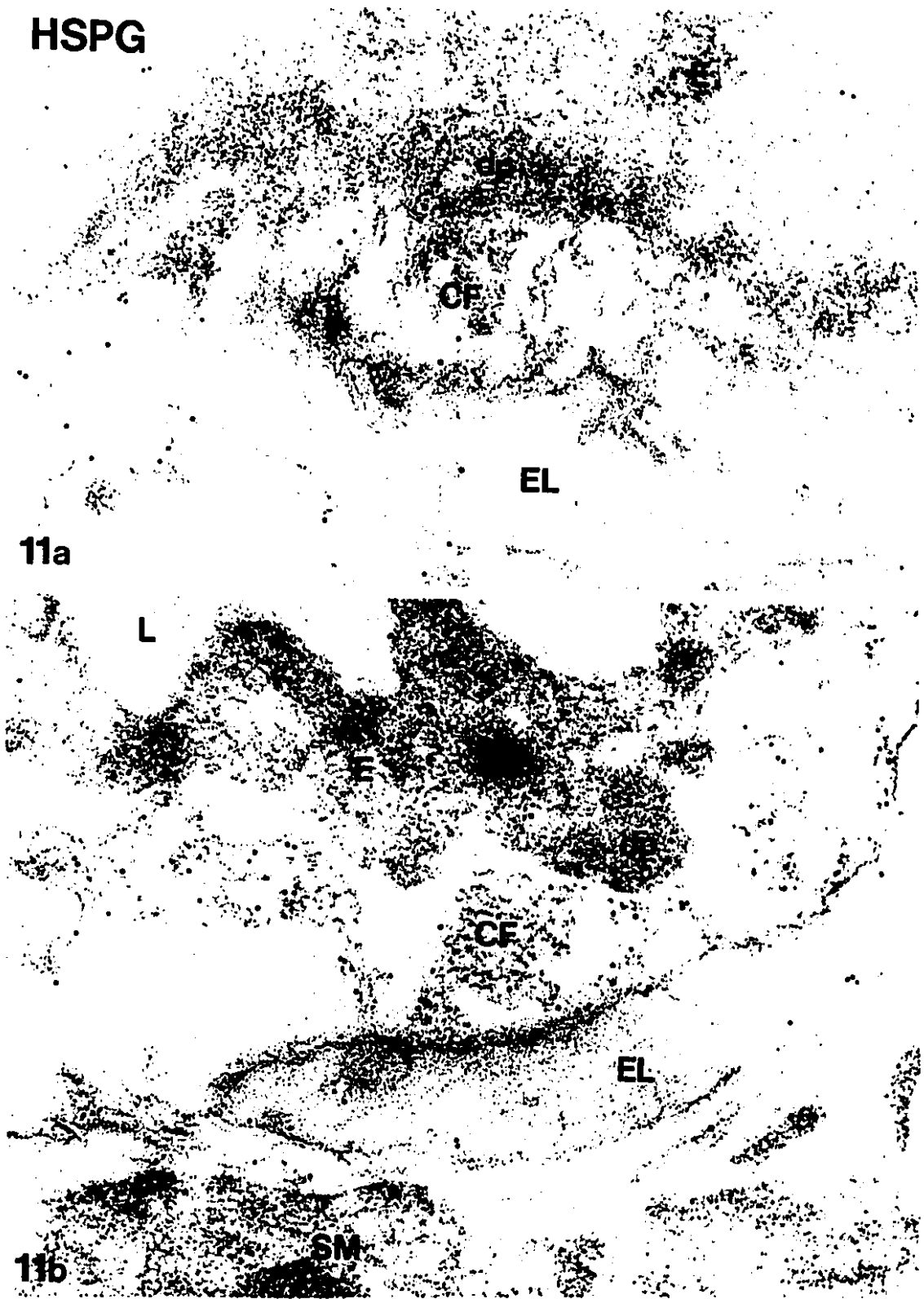


**FIGURE 4-11:** Immunolocalization of heparan sulfate proteoglycan (HSPG) in the subendothelial matrix of a 15-day gestational mouse aorta. Two examples of the relatively weak labeling for HSPG observed in association with the endothelial cell connecting filaments (CF). Elastin-associated microfibrils at the edges of the elastic lamina (EL) show no labeling with anti-HSPG. L, lumen; E, endothelial cell; dp, dense plaque; SM, smooth muscle cell. (a) and (b) x57,000.

HSPG



11a

L

CF

EL

CF

EL

11b

SM

**FIGURE 4-12:** Summary table of the relative immunolabeling observed over elastin-associated microfibrils and endothelial cell connecting filaments. In general, the intensity of label associated with these two fibrillar structures did not appear considerably different between the 15-day gestational animals and 5-day post-natal animals for any of the antibodies. Thus, the table represents the overall labeling trends observed at both ages. Note that FB represents fibrillin and FN represents fibronectin. Very heavy labeling = + + + + ; heavy labeling = + + + ; moderate labeling = + + ; weak labeling = + ; little or no labeling = +/- ; no labeling = - ; inconclusive = IC.

	FB	MAGP	FN	HSPG	AP
Elastin - associated microfibrils	++++	++	+/-	+/-	IC
Endothelial cell connecting filaments	++	-	+++	+	IC

Fig. 4-12

#### 4.4 DISCUSSION

The detection of fibrillin immunoreactivity on endothelial cell connecting filaments in the developing mouse aortic intima provides evidence that the filaments are microfibrillar in nature. Fibrillin has been demonstrated by immunofluorescence localization to be present in both elastin-associated microfibrils and microfibril bundles devoid of amorphous elastin, termed oxytalan fibers (Sakai et al., 1986). In skin, fibrillin immunoreactivity has been shown to be specifically associated with oxytalan fibers in the subepidermal region (Dahlbäck et al., 1990). These oxytalan fibers have been proposed to provide a role in anchoring the epidermal cell layer to dermal elastic fibers. Similarly, the endothelial cell connecting filaments observed in the present study appear to anchor the endothelial cell to the subjacent elastic lamina during early development of the vessel (see Chapter 3). Thus, the identification of the endothelial cell connecting filaments as microfibrils supports the hypothesis that microfibrils function in cell anchorage to elastic elements and aid in tissue stability.

In addition to fibrillin, MAGP has also been identified to be a constituent of microfibrils (Gibson et al., 1986, 1991) with a widespread distribution on both elastin-associated microfibrils and oxytalan fibers (Kumaratilake et al., 1989). However, in the present study, MAGP immunoreactivity could not be demonstrated on endothelial cell connecting filaments. Although from this observation it appears that MAGP is not present as a component of the connecting filaments, negative immunolabeling results must be interpreted with caution. The ubiquitous distribution of MAGP on microfibrils from a

wide variety of tissues (Kumaratilake et al., 1989), as well as, the difficulties occasionally encountered with anti-MAGP immunolocalization (White et al., 1988; Fanning et al., 1991) suggests the possibility that the negative immunoreaction observed with anti-MAGP may be a false-negative result.

The lack of MAGP immunoreactivity observed on endothelial cell connecting filaments may be due to a number of reasons. Firstly, the anti-MAGP antibody, which was raised against a bovine antigen from fetal tissue, may not cross-react with mouse tissue. However, MAGP immunoreactivity of the elastin-associated microfibrils at the periphery of the elastic lamina was observed. This immunoreaction was not as strong as that observed with anti-fibrillin antibodies, thus the species difference may have had some effect on anti-MAGP binding due to low cross-reactivity. This is supported by the fact that the anti-MAGP immunolabeling is best observed in fetal bovine tissue, more limited in adult bovine tissue and fetal tissue from other species, and only seen after enhancement procedures in adult tissue from other species (White et al., 1988).

A second reason for the lack of MAGP immunoreactivity of the endothelial cell connecting filaments may be due to the antigenic epitope being inaccessible or masked. Although the tissue treatment of reductive guanidine-hydrochloride followed by alkylation is apparently unnecessary to obtain positive immunolabeling with anti-MAGP antibodies (Kumaratilake et al., 1989), a significant improvement in specific microfibril labeling has been observed following reduction and alkylation of tissue sections prior to immunolabeling (Fanning et al., 1991). This enhanced immunoreaction has been suggested to be related to a conformational change of the MAGP molecule (Fanning et al., 1991).

Since the MAGP used for antibody production was reduced and alkylated during the process of isolation from ligamentum nuchae tissue (Gibson et al., 1986), a conformational change of the MAGP molecule may be necessary to expose immunoreactive epitopes prior to labeling with anti-MAGP antibodies. In the present study, even though mouse aortic tissue was treated with reductive guanidine-hydrochloride followed by alkylation during tissue processing, immunolabeling failed to demonstrate the presence of MAGP in endothelial cell connecting filaments. However, the connecting filaments were shown to be strongly associated with fibronectin; thus, the actions of the chaotropic and reducing agents may have been restricted by the fibronectin fixed to the surface of the connecting filaments. In addition, HSPG immunolocalized on the connecting filaments may have further limited agents by linking to heparan-binding domains of fibronectin (Singer et al., 1987). This may have resulted in the antigenic epitopes being inaccessible for antibody binding.

Fibronectin on the surface of the connecting filaments may have also masked the immunoreactive epitopes on the molecule or blocked penetration of the anti-MAGP antibody. Using cultured calf aortic smooth muscle cells, Schwartz and colleagues (1985) demonstrated that microfibrils, which predominate in the extracellular matrix of such cultures (Goldfischer et al., 1983), consist of core proteins that become coated with fibronectin as a function of time. In young cultures, the microfibrils showed immunoreactivity to both fibronectin and an antibody raised against "insoluble microfibrillar" proteins (MFP). As the cultures grew to confluency, the immunoreaction observed with anti-MFP diminished, whereas that of fibronectin increased. Treatment of

confluent cultures with urea, to dissociate the fibronectin from the microfibril surface, restored the immunoreactivity of the anti-MFP antibody (Schwartz et al., 1985). These results suggest that microfibril-associated proteins may have the ability to block immunoreactive epitope on the core of the microfibril.

The studies of Schwartz and colleagues (1985) demonstrated that fibronectin was deposited on the surface of microfibrils with respect to time. Thus, in the present study, fetal tissue was examined with the premise that the fibronectin accumulation on the surface of the endothelial cell connecting filaments would be minimal in fetal tissues thus allowing exposure of epitopes recognized by anti-MAGP. However, endothelial cell connecting filaments in the fetal aortic intima showed similar immunoreactivity as those from a 5-day old post-natal aorta for all antibodies examined. Although these results do not provide information concerning the localization of MAGP, they do support previous observations suggesting that endothelial cell connecting filaments are well established early in fetal development as supporting elements of the endothelial cell layer (see Chapter 3).

The aforementioned evidence suggests that the immunoreactive epitopes of MAGP on endothelial cell connecting filaments may be unaccessible or blocked by associated proteins. However, the negative immunolabeling results may be correct; in that, MAGP may not present in these structures even though the positive immunoreaction for fibrillin demonstrates that the connecting filaments are microfibrils. The relationship between MAGP and fibrillin remains to be resolved. MAGP has been shown to immunologically cross-react with fibrillin (Gibson et al., 1989); however, the size of the mRNA for MAGP determined by cDNA cloning has demonstrated that MAGP is a discrete component of

microfibrils and not a degradation product of fibrillin (Gibson et al., 1991). If the endothelial cell connecting filaments observed in the present study contain fibrillin and not MAGP, then the two proteins must be structurally distinct components of microfibrils.

The lack of MAGP in the fibrillin-containing connecting filaments would also provide evidence that microfibrils consist of a family of filamentous structures that may vary depending on location and functional requirements. The ubiquitous immunolabeling of elastin-associated microfibrils and oxytalan fibers observed with anti-MAGP (Gibson et al., 1987; Kumaratilake et al., 1989) and anti-fibrillin (Sakai et al., 1986) suggests that all microfibrils are members of a single system of structures; however, some differences must exist since not all microfibrils become infiltrated with elastin to form elastic fibers and elastic laminae.

In skin, oxytalan fibers at the dermal-epidermal junction remain as microfibril bundles free of elastin, whereas in the dermis, the microfibrils become either partially or completely infiltrated with elastin to form elaunin or elastic fibers, respectively (Cotta-Pereira et al., 1976). Even though the microfibrils of oxytalan, elaunin and elastic fibers all immunolabel positively for the presence of MAGP (Kumaratilake et al., 1989) and fibrillin (Dahlbäck et al., 1990), only those of elaunin and elastic fibers demonstrate the presence of amyloid P component and vitronectin (Dahlbäck et al., 1990). Furthermore, a 36 kDa microfibril-associated protein (36-kDa MAP), purified from porcine aorta, has been shown to have a restricted immunolocalization to microfibrils in the aortic adventitia with no immunoreactivity detectable in a number of other tissues known to contain elastic fibers, including skin, liver, placenta and esophagus (Kobayashi et al.,

1989). In the present study, both fibronectin and HSPG localize on the endothelial cell connecting filaments but not on the elastin-associated microfibrils. These findings suggest that some constituent(s) of microfibrils may vary to allow for their differential association with both elastin and other extracellular matrix proteins.

The immunolabeling results obtained with the anti-AP antibodies were inconclusive, thus further experimentation is required to determine the precise location of amyloid P component in the developing aortic wall. Amyloid P component has been shown to be associated with elastin-associated microfibrils in human skin and aorta (Breathnach et al., 1981) and with ciliary zonular fibrils in the mouse (Inoue et al., 1986a). Thus, the lack of specific labeling observed in the present study may be due to technical difficulties of the immunolabeling procedure. Some evidence also suggests that amyloid P component is deposited on microfibrils with respect to age (Khan and Walker, 1984; Gibson et al., 1986; Gibson and Cleary, 1987). Since the aortic tissue examined in the present study was from 5-day old mice, there may not have been a sufficient amount of amyloid P component associated with the elastin-associated microfibrils or connecting filaments to give a strong enough immunoreaction to be recognized over the diffuse intracellular labeling. Amyloid P component has been shown to bind to both fibronectin (de Beer et al., 1981; Rostagno et al., 1986) and glycosaminoglycans (Hamazaki, 1987). Since both fibronectin and HSPG were shown to be associated with endothelial cell connecting filaments, it is possible that some amyloid P component may be bound or become bound to the connecting filaments.

In summary, the results from the present study provide the first evidence that

endothelial cell connecting filaments are microfibrillar in nature. Since similar connecting filaments have been observed in association with endothelial cells of lymphatic capillaries (Leak and Burke, 1968; Böck, 1978; Gerli et al., 1990) and sinusoids (Campbell, 1987), it appears that microfibrils may play a widespread role in endothelial cell anchorage. The connecting filaments also appear to be heavily coated with fibronectin. Fibronectin has high-affinity binding sites for cell surfaces and other extracellular matrix molecules (Hynes, 1985; Yamada et al., 1985), thus the fibronectin on the surface of the connecting filaments may provide an important structural link between the filaments and endothelial cell surface. This link may be further stabilized by associated proteins such as HSPG (Singer et al., 1987) and possibly amyloid P component (Inoue et al., 1989). The negative immunolabeling results obtained with anti-MAGP on the connecting filaments require further investigation; however, the possibility that MAGP may be absent from these structures has emphasized that it still remains to be established as to whether microfibrils are a single structural element or represent a family of filamentous structures with common properties.

***CHAPTER FIVE***

***RADIOAUTOGRAPHIC STUDY OF ELASTIN STABILITY  
AND ELASTIC LAMINA GROWTH IN THE MOUSE AORTA***

## 5.1 INTRODUCTION

Elastin accumulates rapidly in the aortic wall during peri-natal development in response to changing hemodynamic factors (Bendeck and Langille, 1991). In the rat aorta, elastic fibers are first observed at a gestational age of 13 days (Nakamura, 1988). These fibers continue to develop until complete elastic laminae are formed at a post-natal age of approximately 4 weeks (Gerrity and Cliff, 1975). Similarly, a rapid synthesis of elastin during early development has been reported for human (Berry et al., 1972b), pig (Davidson et al., 1986), chick (Lee et al., 1976; Keeley, 1979), quail (Lefevre and Rucker, 1980) and rat aortae (Looker and Berry, 1972). Following maturation, however, little new elastin synthesis is apparent (Keeley, 1979; Lefevre and Rucker, 1980; Davidson et al., 1986). These results imply that little or no turnover of elastin occurs in the mature vessel. Thus, elastin synthesized early in development must remain intact and functional throughout life.

Elastogenesis in the aorta not only involves the formation of elastic laminae, but also elastin-containing connections that attach the laminae to smooth muscle cells (see Chapter 2). These connections appear to persist in the adult vessel as functional stress-bearing structures; thus, one would predict that once these connections are formed, they would remain relatively stable in the vessel wall.

Most previous estimates of elastin turnover in the aorta have been based on measurements of specific activity of radiolabeled elastin isolated from vessels at various times following injection. This has produced conflicting reports of turnover times that

range from several weeks (Fischer, 1971; Fischer and Swain, 1978) to several years (Slack, 1954; Walford et al., 1964; Rucker and Tinker, 1977; Lefevre and Rucker, 1980; Dubick et al., 1981). The discrepancy in turnover times appears to be due, in the most part, to contamination of elastin fractions with collagen. Other difficulties in an accurate prediction of elastin turnover have been due to inappropriate labeling techniques and inadequate experimental time periods.

The present study was designed to investigate the turnover of elastin in the aorta by radioautography and thus circumvent the problems encountered by biochemical methods. By light and electron microscope radioautography, Ross and Klebanoff (1971) demonstrated the uptake of  $^3\text{H}$ -proline into aortic smooth muscle cells and the subsequent incorporation and deposition of the radiolabel in elastin laminae of prepubertal rats. Similar radioautographic results were obtained by Gerrity and colleagues (1975); however, since both studies were primarily concerned with the synthesis of connective tissue proteins, the longest time points examined were in terms of hours and the fate of the radiolabel was not determined.

In theory, the radiolabeled amino acids that become incorporated into the elastic laminae during development should remain evident throughout life if little or no turnover of elastin occurs. Based on this premise, aortae of animals injected early in development and killed at subsequent time points up to 4 months of age were prepared for light and electron microscope radioautography. The radioautographic observations presented herein provide both qualitative and quantitative evidence for the long-term stability of elastin in the aorta.

In addition to elastin turnover, the incorporation of radiolabel into elastic laminae early in development of the aorta has provided information concerning elastic lamina growth. During development, elastic laminae must continue to enlarge in circumference as the vessel matures and diameter of the lumen increases. This presents an interesting problem since the elastic laminae are completely formed as continuous concentric rings prior to full maturation of the vessel (Karrer, 1961; Gerrity and Cliff, 1975). In the present study, radioautographs of aortae from animals injected soon after birth and killed 4 months later have allowed the location of elastin synthesized early in development to be identified in the adult vessel. In addition, radioautographs from aortae of young animals injected in the later stages of post-natal growth have allowed the subsequent incorporation of elastin into the completely formed elastic laminae to be investigated.

## 5.2 MATERIALS AND METHODS

### 5.2.1 EXPERIMENTAL DESIGN

Two experimental groups were designed to investigate elastin kinetics in the mouse aorta (Fig. 5-1). The first experimental group consisted of 18 C57/BL mice given a single injection of radiolabel at 3 days post-natal age. Two mice were subsequently killed at 4, 7, 10, 14, 21, 28, 54, 84, 118 days post-natal age. This experimental design allows the fate of the radiolabel incorporated into the elastic laminae to be followed over the course of development. The second experimental group consisted of 20 C57/BL mice; 4 mice at each of the following post-natal ages: 3 days, 14 days, 21 days, 28 days and 8 months. Each animal received a single injection of radiolabel. Two mice were subsequently killed from each age group 1 day after injection. The remaining two mice from the first 4 age groups were killed at 4 months of age and the two mice from the last age group were killed at 12 months of age. This experimental design allows the synthesis and deposition of elastin to be investigated at different developmental ages.

As a control, two additional animals were injected at 3 days post-natal age with buffer containing no radiolabel. One mouse was killed at 4 days old and the other at 4 months old.

### 5.2.2 PREPARATION AND ADMINISTRATION OF RADIOLABEL

All radiolabeling experiments were performed using L-[3,4-<sup>3</sup>H]-valine in 0.01 N hydrochloric acid purchased at a concentration of 1 mCi/ml (NEN Research Products, Du Pont, Mississauga, Ont.). Immediately prior to use, 1 ml samples of radiolabel were concentrated to 0.5 ml in a Savant Speed Vac Concentrator. This was necessary in order to reduce the volume needed to inject into each animal. To buffer the solution, 62  $\mu$ l each of 1.5 M sodium chloride and 0.5 M phosphate buffer (pH 7.5) was added to the concentrated radiolabel. Each mouse, at the appropriate age for injection, was individually weighed and given a single subcutaneous injection on the back with radiolabel at a level of 50  $\mu$ Ci per 1 gm body weight.

### 5.2.3 PREPARATION OF TISSUE FOR RADIOAUTOGRAPHY

Tissues prepared for radioautography involved the preparation of Epon embedded tissue. All animals were handled and tissues were treated as previously described (see section 2.2). Care was taken to ensure that both cross-sections and longitudinal sections were prepared from each aorta. Tissue from the two different animals killed at one time point were kept separate and labeled accordingly.

#### 5.2.4 LIGHT MICROSCOPE RADIOAUTOGRAPHY

Epon blocks from each animal were trimmed and sectioned for toluidine blue staining as previously described (see section 2.2.2). Two blocks from each animal were selected for radioautography based on the quality and plane of section; one cross-section and one longitudinal section. From each block selected, 0.5  $\mu\text{m}$  sections were cut with a diamond knife on a Reichart ultracut microtome and placed in a row on a bare glass slide. Three slides were made for each block with 5 sections per slide.

Following sectioning, the slides were placed on a heater block and warmed to 85°C. The slides were then covered with filtered iron alum solution for 7 minutes, rinsed in several changes of distilled water and returned to the heater. After the slides were dry and warm, they were covered with filtered hematoxylin for an additional 7 minutes, rinsed and again returned to the heater to dry and warm. To enhance the blue tones of the stain, the slides were covered with tap water for 3 minutes, then rinsed in distilled water and left to dry.

Each slide was dipped by hand in Kodak NTB-2 emulsion and placed in a light proof box in the presence of calcium sulfate. The box was stored standing on edge so that the slides were in a horizontal position. After 12 weeks of exposure at 4°C, the radioautographic slides were developed in freshly prepared Kodak D-170 developer (pH 7.1) for 6 minutes at 18°C. After a brief rinse in distilled water, the slides were transferred to 24% sodium thiosulfate (pH 6.7) and fixed for 3 minutes. The radioautographic slides were then washed in running tap water at 18°C for 10 minutes, rinsed briefly in distilled

water and left to air dry.

Light microscope radioautographs were photographed with an Ultraphot II camera light microscope (Zeiss, Toronto, Ont.) for qualitative analysis.

#### 5.2.5 ELECTRON MICROSCOPE RADIOAUTOGRAPHY

Electron microscope radioautographs were prepared as described by Kopriwa (1973). Glass slides were dipped in 1.0% celloidin in isoamylacetate and left to dry overnight in a vertical position. From the blocks previously chosen for light microscope radioautography, sections were cut of a straw interference color (90 nm thick) and placed on the celloidin coated slides. Three slides were prepared from each block with 3 groups of several sections per slide.

Prior to the application of emulsion, the sections were coated with a thin layer of carbon to prevent displacement of the silver grains following development. An Edwards 306 carbon evaporator, modified to permit control of carbon deposition, was used to apply a thin uniform layer of carbon to each slide.

For the application of Ilford L4 emulsion, a semi-automatic dipping apparatus was used. This allowed the speed of dipping to be controlled, which together with the dilution and temperature of the emulsion, is critical in determining the emulsion thickness. After the emulsion was dry, the slides were stored as described above.

For quantitative analysis, radioautographic slides were developed after 6 months

exposure with D-19b developer for 1 minute at 20°C to produce large filamentous grains. For qualitative analysis, radioautographic slides were developed after 11 months exposure with gold thiocyanate for 1 minute followed by Agfa-Gevaert developer for 7 minutes at 20°C. This developing procedure produces fine rather than filamentous grains. After development by either method, the slides were rinsed briefly in distilled water, fixed for 2 minutes in 24% sodium thiosulfate, washed in 5 changes of distilled water for 1 minute each and left to dry.

To transfer the sections from the slides to electron microscope grids, the celloidin was scored and floated off the slide onto the surface of distilled water. Grids were then placed over the sections and the celloidin film together with the grids was aspirated onto moistened filter paper and left to dry.

Prior to counterstaining, the celloidin film was removed from the surface of the grid by agitating the grid in glacial acetic acid for 3 - 8 seconds. The grid was then dipped quickly into distilled water followed by a thorough wash under a flow of distilled water. If the celloidin was not completely removed, the procedure was repeated. The surface of the grid appears purple or green when covered by celloidin as opposed to gold or yellow when the celloidin is removed.

All grids were counterstained with methanolic uranyl acetate for 2 minutes followed by lead citrate as previously described (see section 2.2.2). The stained sections were examined in a Philips 301 transmission electron microscope at an accelerating voltage of 80 kV.

## 5.2.6 QUANTITATION AND STATISTICS

Electron microscope radioautographs from the first experimental group of animals injected with radiolabel at 3 days post-natal age and killed at 9 subsequent time points were used for quantitation. A total of 4 different blocks were used from each time point; a cross-section and a longitudinal section from each of the two animals. Ten micrographs were taken from each of the 4 different sections, giving a total of 40 micrographs per time point. All micrographs were taken at the same magnification from a minimum of 2 different grids. Portions of the elastic laminae were selected from several different sections on each grid based on the quality of the preparation (i.e. lack of folds, knife marks, and other artifacts of section preparation). The 10 micrographs for each time point included an even distribution from all 4 elastic laminae. The micrographs were enlarged to a final magnification of 19,252 times.

For each micrograph, the regions occupied by elastin and cells were traced individually using a Kontron MOP-Videoplan image analysis system and the areas ( $\mu\text{m}^2$ ) were recorded. The area of the extracellular matrix not occupied by elastin was separately quantified by tracing around the perimeter of all the tissue on the micrograph and subtracting the areas occupied by elastin and cells from this value. Within each area, the number of silver grains was counted and recorded as grains per  $\mu\text{m}^2$  of elastin, cell or extracellular matrix. The average grains per  $\mu\text{m}^2$  of each area was calculated for each of the 4 sets of 10 micrographs and for the entire 40 micrographs as a whole. A total of 360 micrographs were quantified; 4 sets of 10 micrographs for each of 9 time points. A

Fisher PLSD one factor analysis of variance at a confidence level of 0.05 was used to ensure that there was no consistent significant difference either between the two animals or between cross-sections and longitudinal sections at any one time point.

The average grains per  $\mu\text{m}^2$  of elastin, cell and extracellular matrix were plotted against the age of the animal. The data was divided into two phases based on the appearance of the graph: one phase, from 4 - 21 days, where the grains per  $\mu\text{m}^2$  were obviously decreasing; and the other phase, from 28 - 118 days, where the grains per  $\mu\text{m}^2$  were apparently constant with respect to the age of the animal. The difference between the mean values for the nine time points was tested for significant difference using a Fisher PLSD one factor analysis of variance at a confidence level of 0.05. For each phase, a simple linear regression was computed by the principle of least-squares to enable a prediction of growth and turnover.

## 5.3 RESULTS

### 5.3.1 ELASTIN STABILITY

#### *5.3.1.1 Light microscope radioautography*

Light microscope radioautography of aortic tissue from animals injected with  $^3\text{H}$ -valine at 3 days post-natal age and subsequently killed at 4, 7, 10, 14, 21, 28, 54, 84, and 118 days of age allows the fate of elastin synthesized at 3 days of age to be followed through the course of development (Fig. 5-2). At 4 and 7 days post-natal age, the silver grains are localized over the entire vessel wall (Figs. 5-2a and b). Through ages 10 - 21 days, the grains over the smooth muscle cells become progressively less evident causing those over the elastic laminae to appear more prominent as the vessel develops (Figs. 5-2c - e). By 28 days post-natal age, very few grains remain over the cells, however, the distribution of grains associated with the elastic laminae appears relatively unchanged (Fig. 5-2f). At 54, 84 and 118 days, the distribution of grains remains the same; little or no grains are observed over the cells while a continuous line of grains can be seen associated with each elastic lamina (Figs. 5-2g - i).

Animals injected at ages ranging from 3 days to 8 months allows the synthesis of elastin at different post-natal ages to be investigated by examining the aortae 4 months post-injection for the presence of radiolabeled elastic laminae (Fig. 5-3). Animals injected with radiolabel at 3 days of age (Fig. 5-3a) or 14 days of age (Fig. 5-3b) and killed 1 day

later show silver grains distributed over the entire vessel wall. The smooth muscle cells of aortae from animals injected at 21 days of age and killed 1 day later appear similarly labeled with grains; however, relatively few grains overlie the center of the elastic laminae and thus they can be recognized between the cell layers (Fig. 5-3c). The elastic laminae are even more conspicuous in aortae of animals injected at 28 days of age (Fig. 5-3d) or 8 months of age (Fig. 5-3e) and killed 1 day later since no grains overlie the laminae and fewer grains are evident over the cells. Aortae from animals injected at 3 days and killed at 4 months of age show very few grains over the smooth muscle cells, whereas a continuous line of grains can be seen over the elastic laminae (Fig. 5-3f). A similar distribution of grains is observed in aortae of animals injected at 14 days and killed at 4 months of age, except that, the majority of grains appear to be located on either side of each elastic lamina thus giving the appearance of two parallel lines of grains rather than a single central line (Fig. 5-3g). In aortae of animals injected at 21 days and killed at 4 months of age (Fig. 5-3h), silver grains were only distributed over the elastic laminae in a similar manner to that of aortae from animals injected at 14 days of age and killed at 4 months (Fig. 5-3g). Aortae of animals injected at 28 days and killed at 4 months of age (Fig. 5-3i) show almost no grains over the smooth muscle cells and considerably fewer grains over the elastic laminae as compared to animals injected at younger ages. Very few grains are observed in aortae of animals injected at 8 months and killed at 12 months (Fig. 5-3j).

### ***5.3.1.2 Electron microscope radioautography, quantitation and statistical analysis***

Electron microscope radioautographs of aortae from animals injected at 3 days post-natal age and killed at 4, 7, 10, 21, 28, 54, 84 and 118 days of age show silver grain distributions similar to that observed by light microscope radioautography. Aortae from animals injected at 3 days and killed at 4 days of age show silver grains over both the smooth muscle cells and the elastic laminae (Fig. 5-4). The grains located on the cells are frequently observed over the nucleus and cell membrane; those on the elastic laminae are seen most often at the edges of the laminae. Radioautographs from animals injected at 3 days and killed at 7, 10, 14 or 21 days appear similar to those from animals killed at 4 days, although, progressively fewer grains appear to be located over the smooth muscle cells. By 28 days of age, very few grains remain associated with the smooth muscle cells; whereas silver grains can still be seen over the elastic laminae. In contrast to the grains observed over the elastic laminae from animals killed at 4 days, most grains at 28 days lie over the center of the elastic laminae (Fig. 5-5). Aortae from animals injected at 3 days of age and killed at ages older than 28 days have silver grain distributions that appear identical to that observed at 28 days.

In order to quantitatively assess the distribution of silver grains from these animals (i.e. animals injected at 3 days and killed at 4, 7, 10, 14, 21, 28, 54, 84, and 118 days of age), silver grains per unit area of elastin, cell and extracellular matrix were calculated by individually tracing each of the three areas on radioautographs and counting the number of grains associated with each area. An example showing a tracing of the area occupied by elastin on a radioautograph from an animal injected at 3 days and killed at

4 days of age is represented in Figure 5-6. For each of the 9 time points a total of 40 radioautographs were quantified: 10 cross-sections and 10 longitudinal sections from each of 2 different animals. Figure 5-7 represents the data from each of the 40 radioautographs quantified from the 9 time points. The individual values for grains per  $\mu\text{m}^2$  of elastin appear to vary considerably for the first 2 time points; however, by 10 to 14 days of age the values appear more consistent. An analysis of variance between the each set of 10 radioautographs quantified for each time point showed a significant difference ( $p \leq 0.05$ ) in only 5 analyses out of a total of 54. Since no consistent significant difference was shown between the values for cross-sections as compared to those for longitudinal sections, all values were included for further statistical analysis. No significant difference was shown to exist between the values from the two different animals from any one time point. A separate analysis of variance at each time point showed the values for grains per  $\mu\text{m}^2$  of elastin to be significantly higher ( $p \leq 0.05$ ) than those for the cell and extracellular matrix. There was no significant difference between the values for grains per  $\mu\text{m}^2$  of cell and those for extracellular matrix.

As was observed qualitatively from the radioautographs, the grains per  $\mu\text{m}^2$  of cell and extracellular matrix steadily decrease until the average number of grains over the cells and extracellular matrix is almost negligible by 28 days of age and remains at this level thereafter (Fig. 5-8). The average grains per  $\mu\text{m}^2$  of elastin also decreases until around 21 to 28 days of age at which time the density of grains appears to remain constant (Fig. 5-8). The line for the average grains per  $\mu\text{m}^2$  of elastin can thus be divided into two phases: one phase, from 4 to 21 days, when the values are continually decreasing; and

the other phase, from 28 to 118 days, when the values are relatively constant. Analysis of variance between the values for grains per  $\mu\text{m}^2$  of elastin at the different time points shows a significant difference ( $p \leq 0.05$ ) between the values at 4, 7, 10, 14 and 21 days of age, whereas between the values at 21, 28, 54, 84 and 118 days of age, no significant difference ( $p \leq 0.05$ ) was shown.

The first phase of the graph, when average grains per  $\mu\text{m}^2$  of elastin are continually decreasing, was analyzed with respect to elastic lamina growth. Since this phase corresponds to a time of post-natal development, the assumption was made that the observed decrease in grains per  $\mu\text{m}^2$  of elastin was actually due to a dilution of the grains as a result of growth. Although a decrease in grains per  $\mu\text{m}^2$  of elastin could also be as a result of elastin turnover, for the purpose of analysis, it was assumed that there was no turnover of elastin. With the assumption that the number of grains over the elastin do not change over time, one can plot the inverse of grains per  $\mu\text{m}^2$  of elastin to represent growth since the amount of elastin per grain will increase as the elastic lamina grows (Fig. 5-9a). The linear regression of the graph of elastin per grain (Fig. 5-9b) shows a high correlation between animal age and growth of elastin ( $r^2 = 0.997$ ). Thus, there appears to be constant growth of elastin during this phase; the slope of the regression line indicates the rate of growth to be 4.3% per day. At this growth rate, the elastic laminae double in size in approximately 23 days ( $1/0.043$ ).

During the second phase of the graph, grains per  $\mu\text{m}^2$  of elastin appear to remain constant with increasing age of the animal (Fig. 5-10a). No turnover or growth of elastin can be said to occur during this time period since there is no significant difference

between any of the time points from 28 to 118 days. Accordingly, the slope of the regression line is not statistically different than zero (Fig. 5-10b).

### 5.3.2 ELASTIC LAMINA GROWTH

#### 5.3.2.1 *Light microscope radioautography*

The distribution pattern of silver grains over the elastic laminae in aortae of animals injected at early ages and killed at 4 months of age allows the fate of the elastin synthesized in the developing aortic wall to be investigated. Light microscope radioautographs of aortae from animals injected at 3 days and killed at 4 months of age show a relatively uniform distribution of grains along the entire length of the elastic laminae (Figs. 5-11a and 5-12a). The grains appear to be located approximately along the center of the elastic laminae. No large areas of elastic laminae were seen to be devoid of silver grains in either cross-sections (Fig. 5-11a) or longitudinal sections (Fig. 5-12a) of the vessel wall. Some areas of the laminae do appear to have slightly higher densities of grains than others and some areas have no grains; however, these areas are relatively small being only a fraction of the length of one smooth muscle cell.

A similar even distribution of silver grains is observed around the circumference of aortae from animals injected at 14 days and killed at 4 months of age (Figs. 5-11b and 5-12b). In contrast to the central location of grains observed along the elastic laminae in animals injected at 3 days of age, most grains appear to be located at the edges of the

laminae. Some areas appear to have higher densities of silver grains than others; however, these areas are very small with respect to the entire diameter of the vessel (Figs. 5-11b and 5-12b). In aortae of animals injected at 21 days and killed at 4 months of age (Figs. 5-11c and 5-12c), the distribution of silver grains along the elastic laminae appears very similar to that of animals injected at 14 days of age. Many grains appear close to the edges of the smooth muscle cells and in some areas a higher concentration of grains is observed along the elastic laminae (Fig. 5-12c).

#### *5.3.2.2 Electron microscope radioautography*

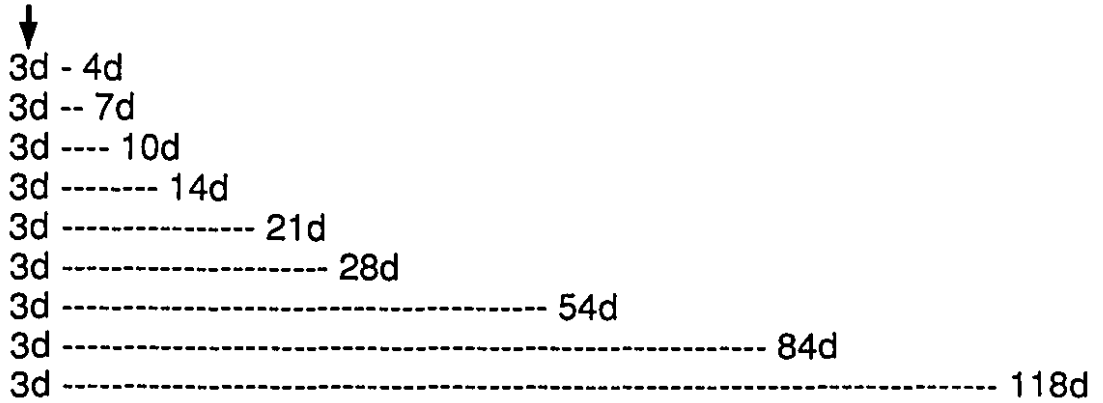
Radioautographs developed to produce fine silver grains as opposed to filamentous grains were used to identify with more precision the location of the radiolabel over specific structures by electron microscopy. In aortae from animals injected at 3 days and killed at 4 days of age, silver grains are seen over the elastic laminae, extracellular matrix, and smooth muscle cells; including the nucleus, cytoplasm and cell membrane (Figs. 5-13a and b). Of these three areas, most grains appear to be located over the edges of the developing elastic laminae. In many areas, silver grains can be seen in regions where the elastic laminae form a close association with the cell surface (Figs. 5-13a and b). The elastic laminae at this early age of development are often incomplete, in that, small gaps can be seen along their length. In these areas, silver grains appear especially numerous around the edges of the elastic lamina (Fig. 5-14). In aortae of animals injected at 3 days and killed at 4 months of age, almost all the silver grains are observed in association with the elastic laminae. Of these grains, most are over the center of the

elastic laminae (Figs. 5-15a and b).

Similar to that of animals injected at 3 days and killed one day later, aortae of animals injected at 14 days and killed at 15 days of age show silver grains distributed over the smooth muscle cells, extracellular matrix and elastic laminae (Figs. 5-16a and b). The grains associated with the elastic laminae are most often seen along the edges of the laminae; both in regions where the elastic lamina is at a distance and where closely apposed to the cell surface. Occasionally, silver grains are seen along the edges of openings in the elastic laminae resulting in the presence of grains near the center of the elastic laminae (Fig. 5-16b). In aortae of animals injected at 14 days and killed at 4 months of age, most silver grains appear distributed along the edges of the elastic laminae (Figs. 5-17a and b).

**FIGURE 5-1:** Schematic representation of the two experimental groups as described in the materials and methods (see section 5.2.1). The numbers refer to the animal's age in days (d) or months (m). The first number in each series represents the animal's age at the time of injection of the radiolabel, as indicated by the arrow. The second number represents the animal's age when killed.

**EXPERIMENTAL GROUP #1**



**EXPERIMENTAL GROUP #2**

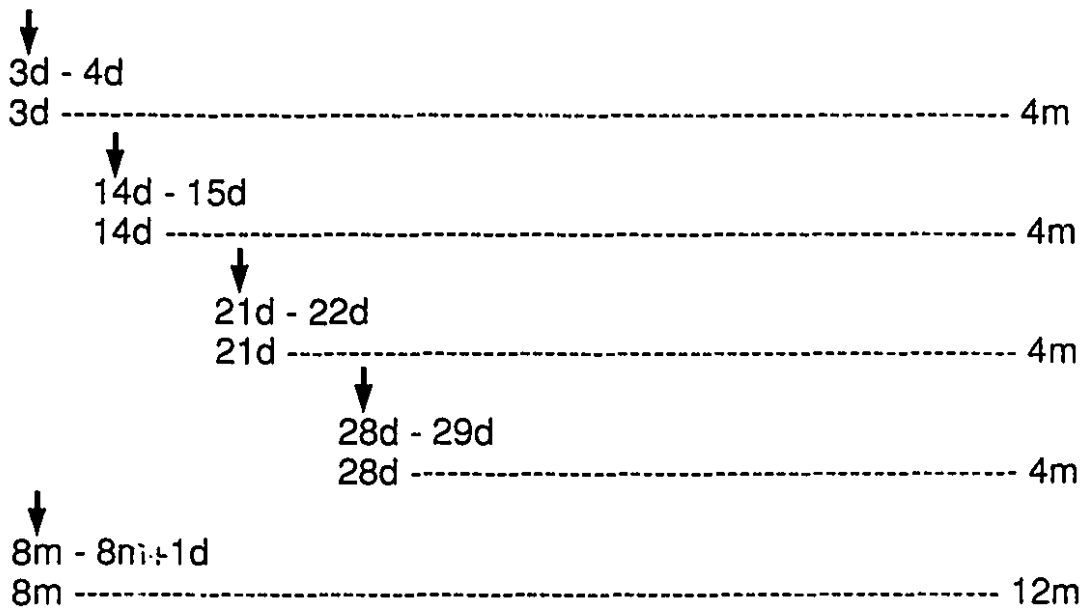


Fig. 5-1

**FIGURE 5-2:** Light microscope radioautographs from experimental group #1 showing the fate of radiolabel over time. All animals were injected with radiolabel at 3 days of age. The number in the upper right hand corner of each panel denotes the age in days of the animal when killed. Initially, silver grains overlies the entire vessel wall (panels a and b). As the number of grains over the smooth muscle cell layers decrease with respect to time, those over the elastic laminae become more evident (panels c-f). Qualitatively, the number of silver grains over the elastic laminae appears relatively unchanged from 54 days of age onward (panels g-i); thus, it appears that there is little or no turnover of elastin upon maturation of the vessel. The lumen of the vessel is at the top of each panel. x480.



4



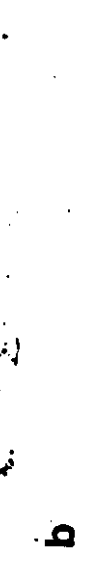
7



10



12a



14



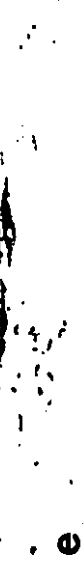
21



28



54



84



118



9



h



i

**FIGURE 5-3:** Light microscope radioautographs from experimental group #2 showing incorporation of radiolabel at different ages. In the upper right hand corner of each panel, the first number denotes the animal's age when injected with radiolabel and the second number is the animal's age when killed. One day following injection, silver grains can be seen over the smooth muscle cells after injection at any age (panels a-e); however, more grains are seen over the cells in the younger animals. By 4 months of age, the aortae from animals injected at 3 days of age show silver grains along the center of the elastic laminae (panel f); whereas the grains appear located more at the edges of the elastic laminae in aortae from animals injected at 14 and 21 days of age (panels g and h). Animals injected at 28 days and killed at 4 months of age (panel i) show that considerably less elastin is synthesized at 28 days as opposed to at earlier ages. Animals injected at 8 months and killed at 12 months of age show that relatively no elastin is synthesized at this time (panel j). The lumen of the vessel is at the top of each panel. x600.

3d/4d



3a

3d/4m



f

14d/15d



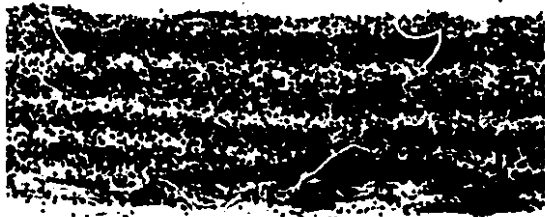
b

14d/4m



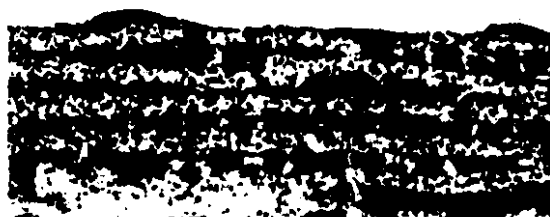
g

21d/22d



c

21d/4m



h

28d/29d



d

28d/4m



e

8m/8m+1d



e

8m/12m



f

**FIGURE 5-4:** Electron microscope radioautograph of a portion of the vessel wall from an animal injected with radiolabel at 3 days and killed at 4 days of age. Silver grains can be seen over the endothelial cells (E), smooth muscle cells (SM) and elastic laminae (EL). Within the smooth muscle cells, the silver grains are often located over the nuclei (N). Thus, at one day following injection, the radiolabel appears to have been incorporated into both elastin and cellular proteins. L, lumen. x10,965.



**FIGURE 5-5:** Electron microscope radioautograph of a portion of the vessel wall from an animal injected with radiolabel at 3 days and killed at 28 days of age. By 28 days of age, almost all silver grains are over the center of the elastic laminae (EL). Only the occasional grain is seen over the extracellular matrix (arrow) or the smooth muscle cells (SM, arrowhead). Thus, the radiolabel incorporated into elastin appears to have remained within the elastic laminae; whereas that utilized for cellular proteins appears to have turned over. L, lumen; E, endothelial cell. x15,140.



5

**FIGURE 5-6:** Electron microscope radioautograph of a portion of the vessel wall from an animal injected with radiolabel at 3 days and killed at 4 days of age. The area of the micrograph occupied by elastin has been outlined to demonstrate how the area is traced and quantified using a Kontron MOP-Videoplan image analysis system. The number of silver grains within the area would be counted and recorded as grains per  $\mu\text{m}^2$  of elastin. Similarly, the area occupied by cells and that occupied by the remaining extracellular matrix would be quantified and the silver grains over each area counted. SM, smooth muscle cell; EL, elastic lamina; EC, extracellular matrix. x14,400.



**FIGURE 5-7:** Graphic representation of the silver grains per  $\mu\text{m}^2$  of elastin (●), cell (■) and extracellular matrix (▲) quantified from each of 40 micrographs at nine different time points following injection of radiolabel at 3 days of age. The number in the upper left hand side of each graph denotes the animal's age in days when injected followed by the animal's age in days when killed. The graphs show that variability between individual values is high initially but decreases progressively with the age of the animal. From 21 to 28 days onwards, there appears to be little change in the distribution of individual values.

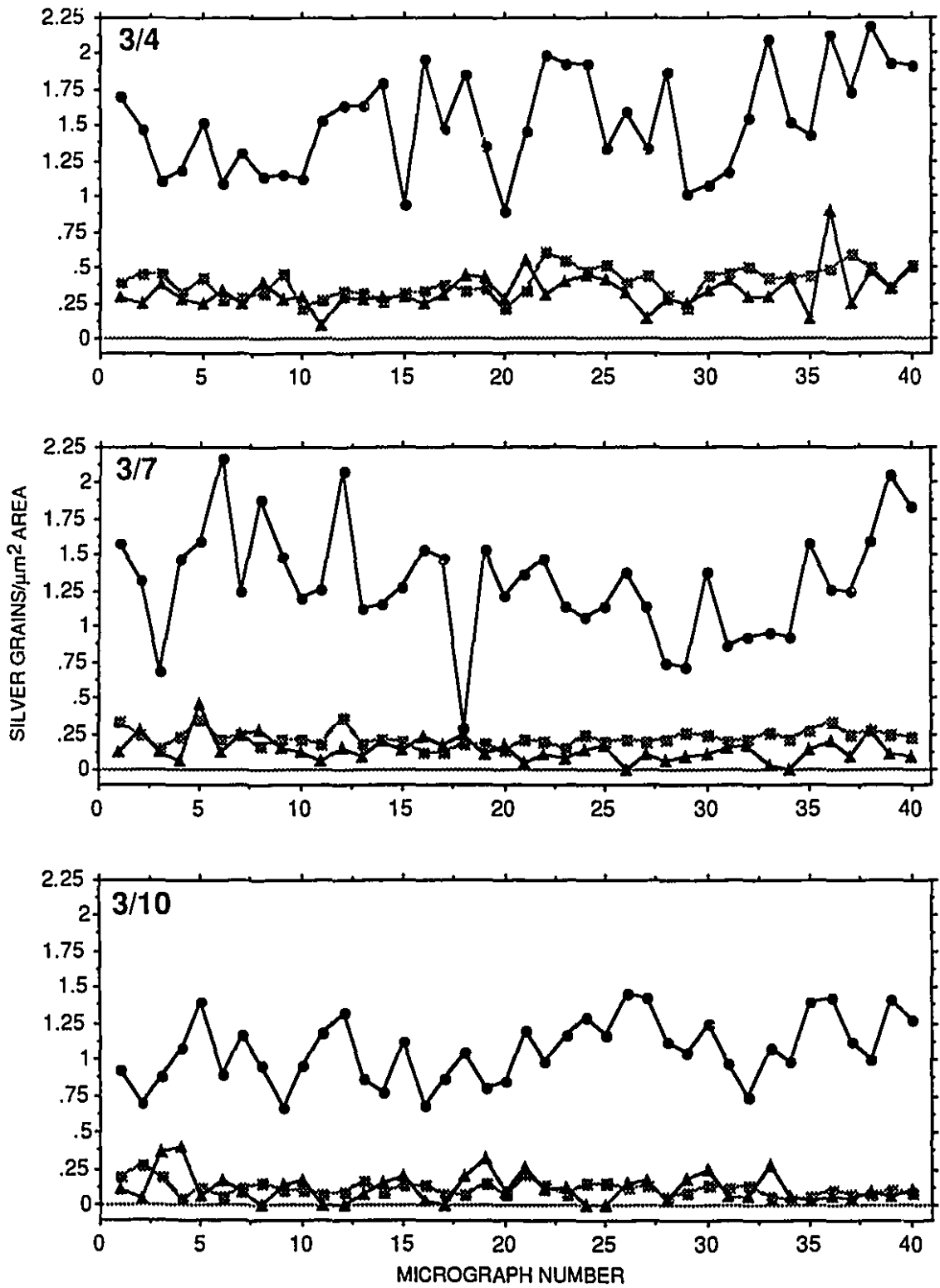


Fig. 5-7

● SILVER GRAINS/ $\mu\text{m}^2$  ELASTIN  
 ■ SILVER GRAINS/ $\mu\text{m}^2$  CELL  
 ▲ SILVER GRAINS/ $\mu\text{m}^2$  EC MATRIX

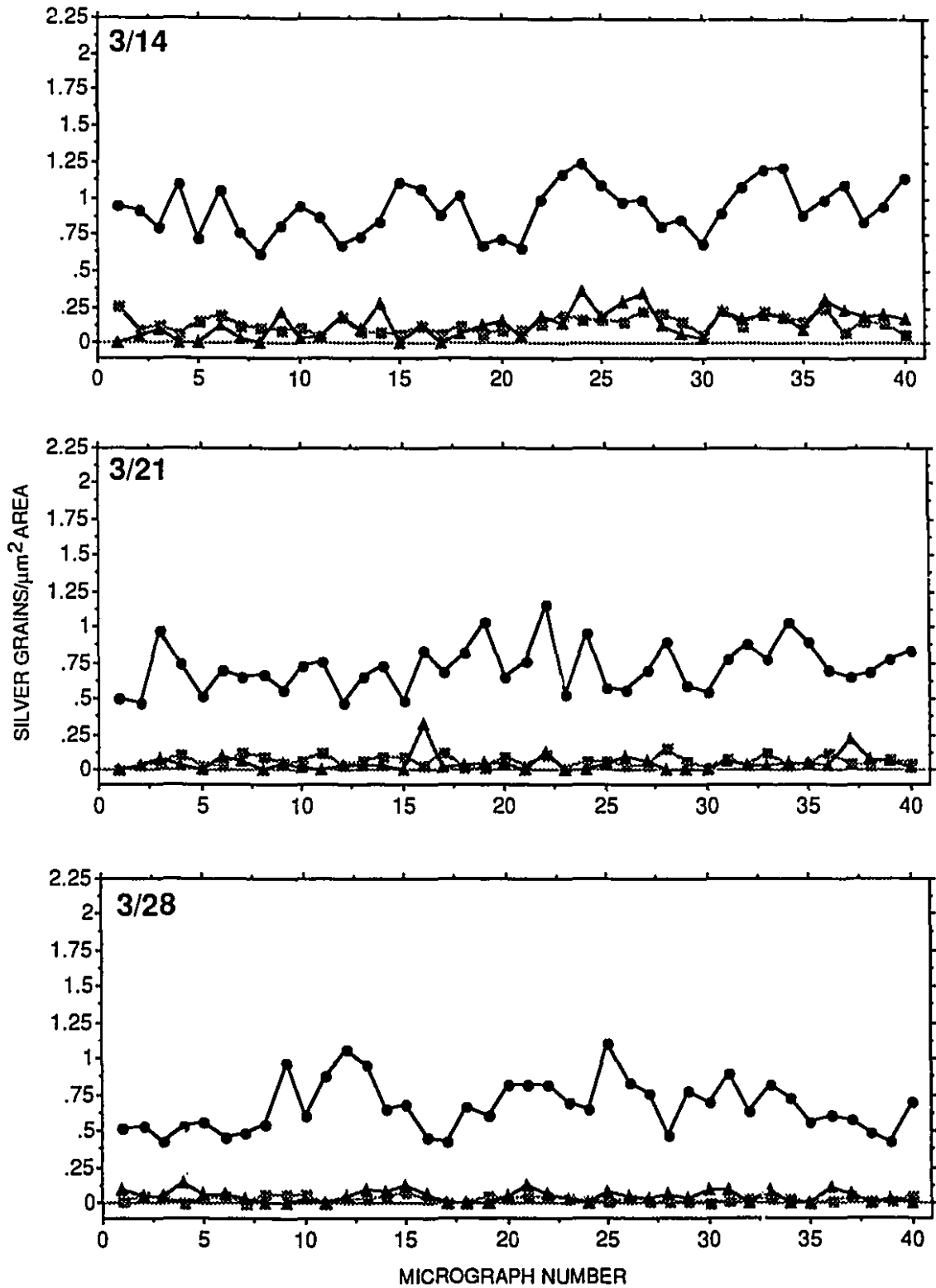


Fig. 5-7 (cont.)

- SILVER GRAINS/μm² ELASTIN
- SILVER GRAINS/μm² CELL
- ▲ SILVER GRAINS/μm² EC MATRIX

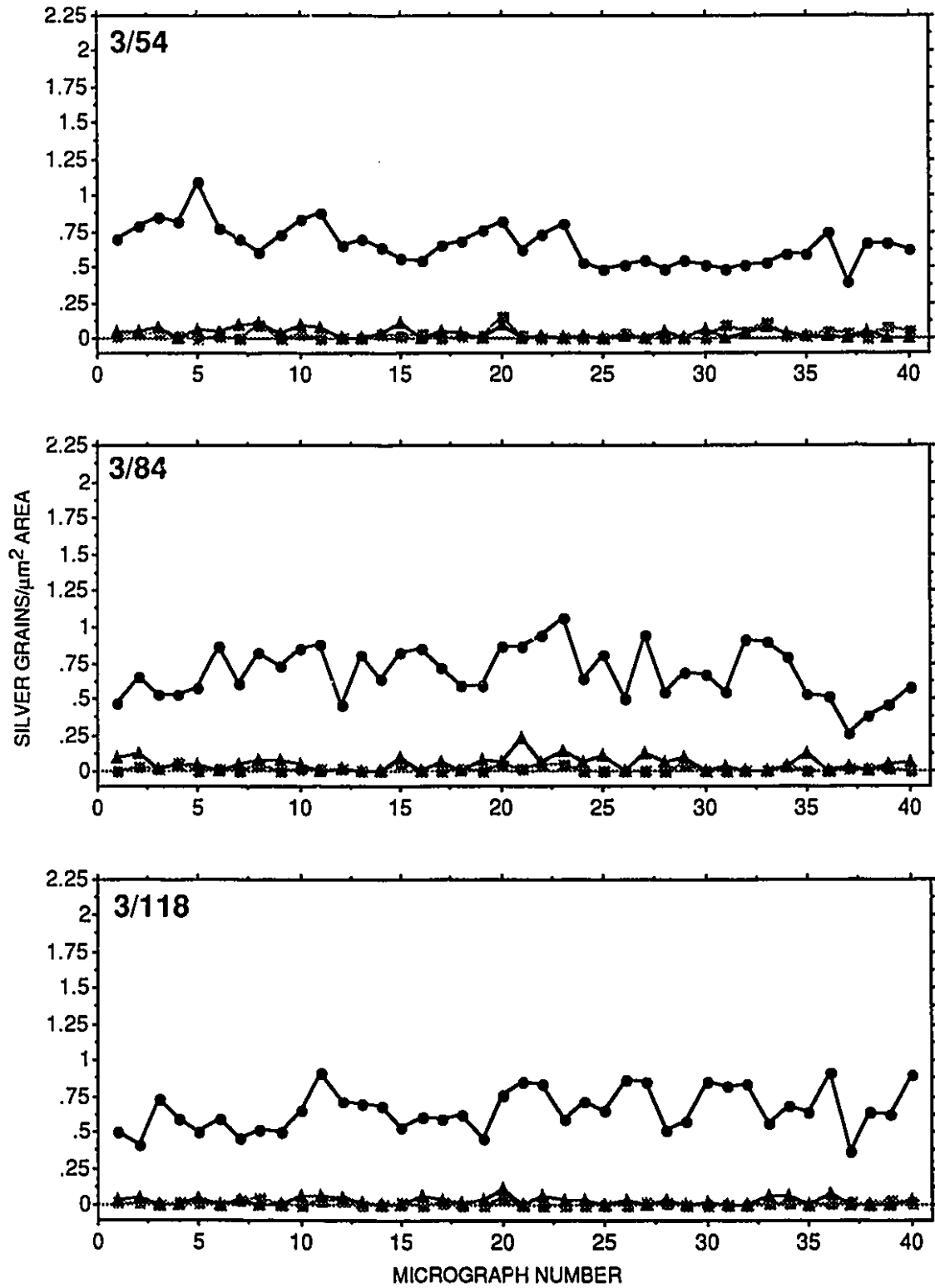


Fig. 5-7 (cont.)

- SILVER GRAINS/ $\mu\text{m}^2$  ELASTIN
- SILVER GRAINS/ $\mu\text{m}^2$  CELL
- ▲ SILVER GRAINS/ $\mu\text{m}^2$  EC MATRIX

I

**FIGURE 5-8:** Changes in silver grains per area of elastin, cell and extracellular matrix with respect to time following an injection of radiolabel at 3 days of age (mean  $\pm$  SEM). Grains per area of elastin apparently decrease until approximately 28 days of age; after which time, they appear to remain constant. The grains per area of cell and extracellular matrix also decrease until approximately 28 days of age at which time they approach a value close to zero. The silver grains per area of elastin can be divided into two phases: one, from 4 days to 21 days of age, where the density of grains is obviously decreasing; and the other, from 28 days to 118 days of age, where the density of grains appears constant.

3

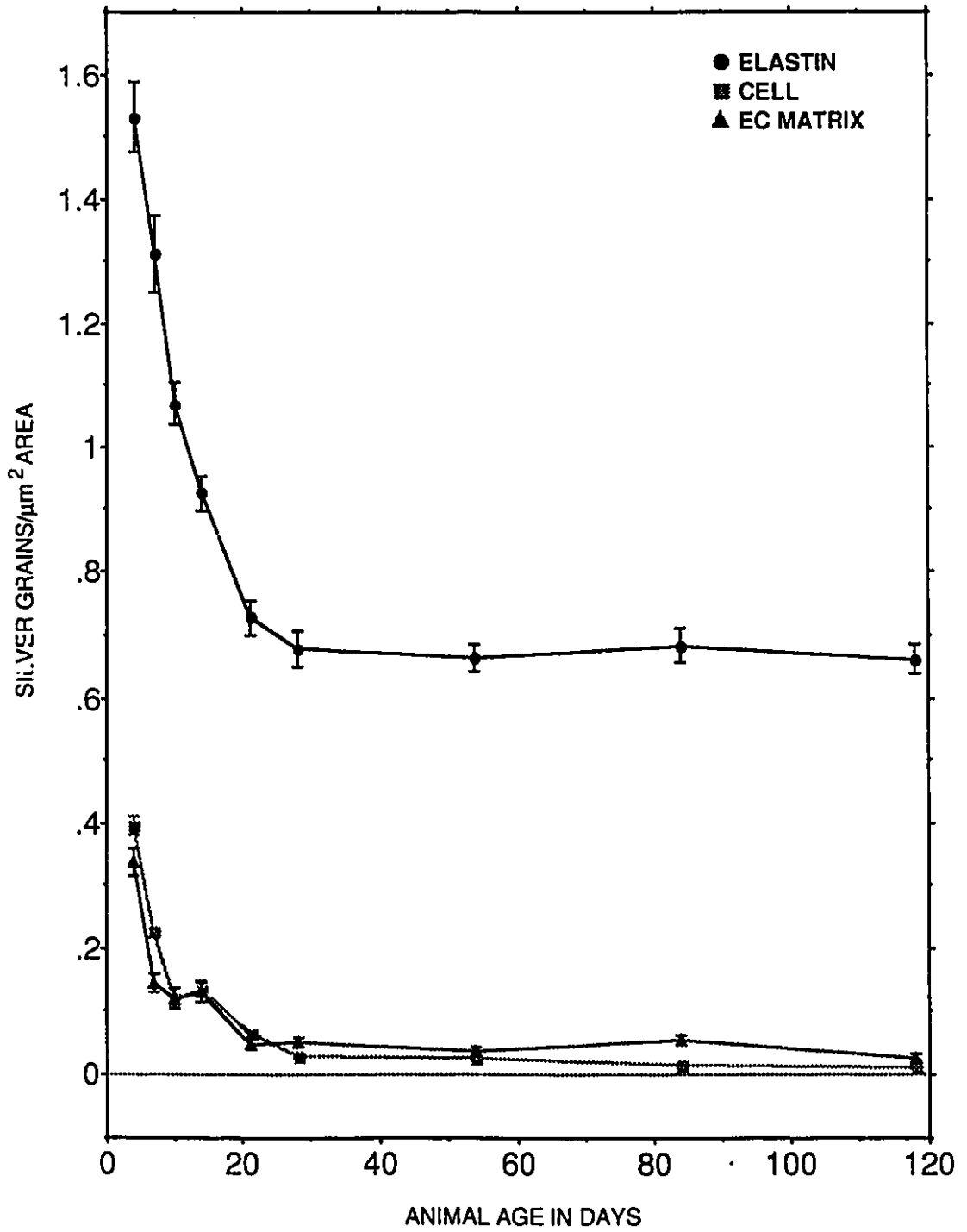


Fig. 5-8

**FIGURE 5-9:** (a) Change in amount of elastin per grain in animals from 4 days to 21 days of age following an injection of radiolabel at 3 days of age (mean  $\pm$ SEM). Since the absolute number of silver grains over the elastic laminae is assumed to be constant, the graph is plotted as amount of elastin per grain rather than grains per area of elastin to illustrate growth of the elastic laminae. (b) Regression line of the plot shown in Figure 5-9a. The high correlation ( $r^2 = 0.997$ ) between amount of elastin per grain and animal's age provides evidence for a constant rate of growth during this time period. The slope of the line predicts the rate of growth to be 4.3% per day. Thus, during this time period, the amount of elastin in the elastic laminae can be said to double in approximately 23 days ( $1/0.043$ ).

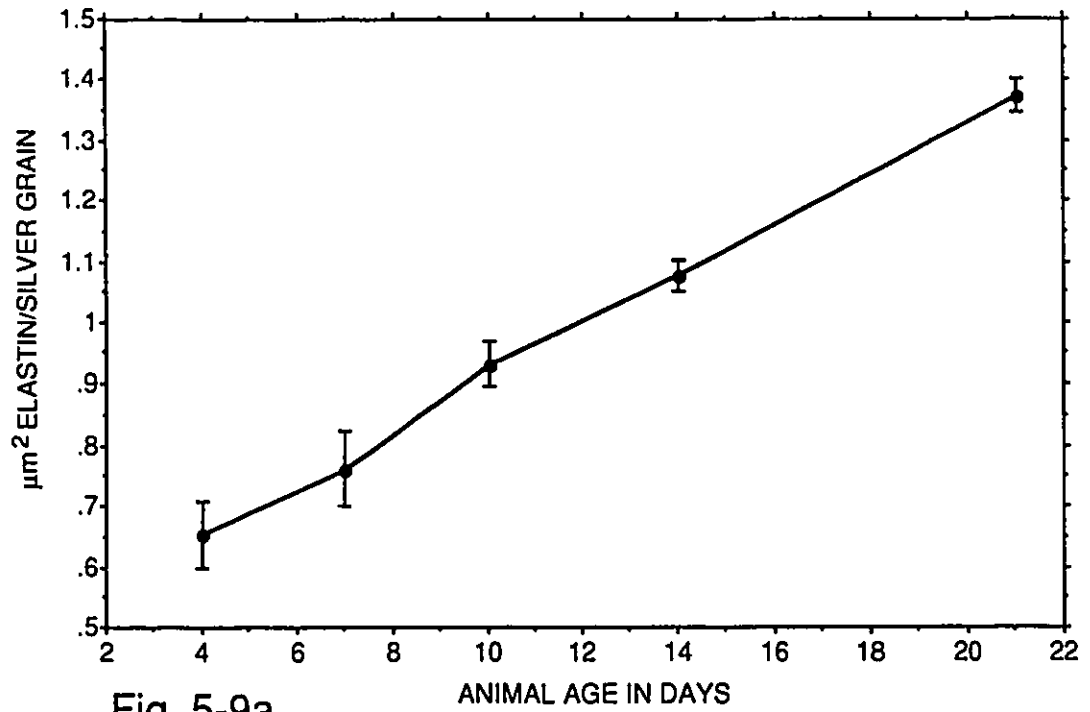


Fig. 5-9a

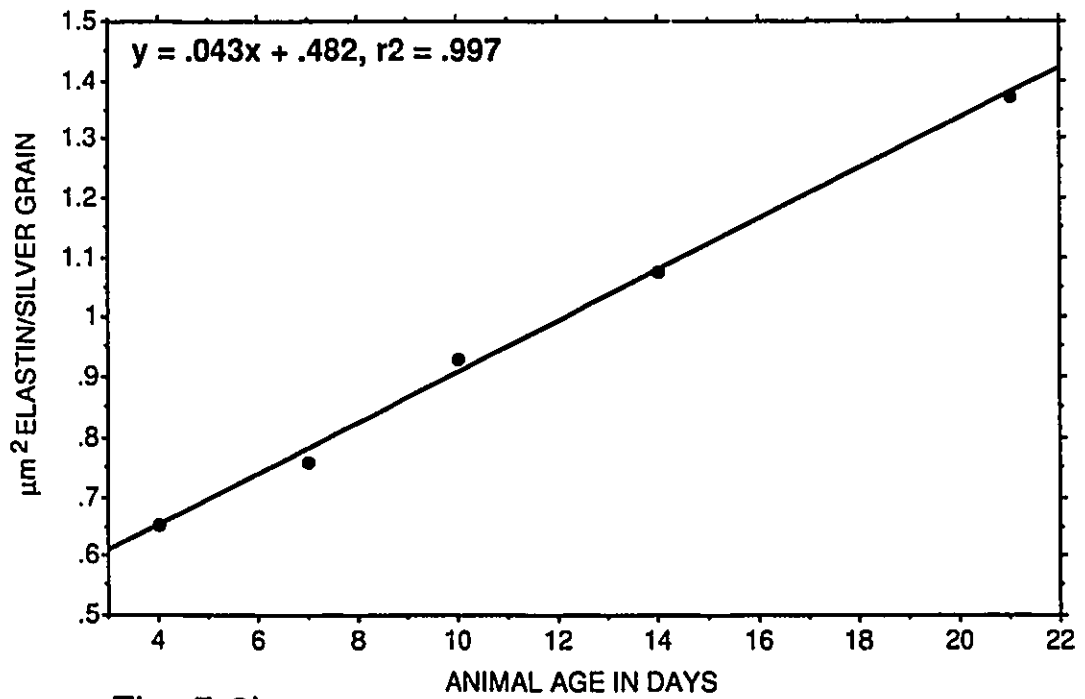


Fig. 5-9b

**FIGURE 5-10:** (a) Change in silver grains per area of elastin in animals from 28 days to 118 days of age following an injected with radiolabel at 3 days of age (mean  $\pm$ SEM). Since there is no significant difference ( $p \leq 0.05$ ) between the density of grains at any of the 4 time points, the silver grains per area of elastin can be said to be unchanged during this time period. (b) Regression line of the plot shown in Figure 5-10a. Although the line has a slight negative slope (-0.0001), statistically the line is no different than zero because of the lack of significant difference between the individual points.

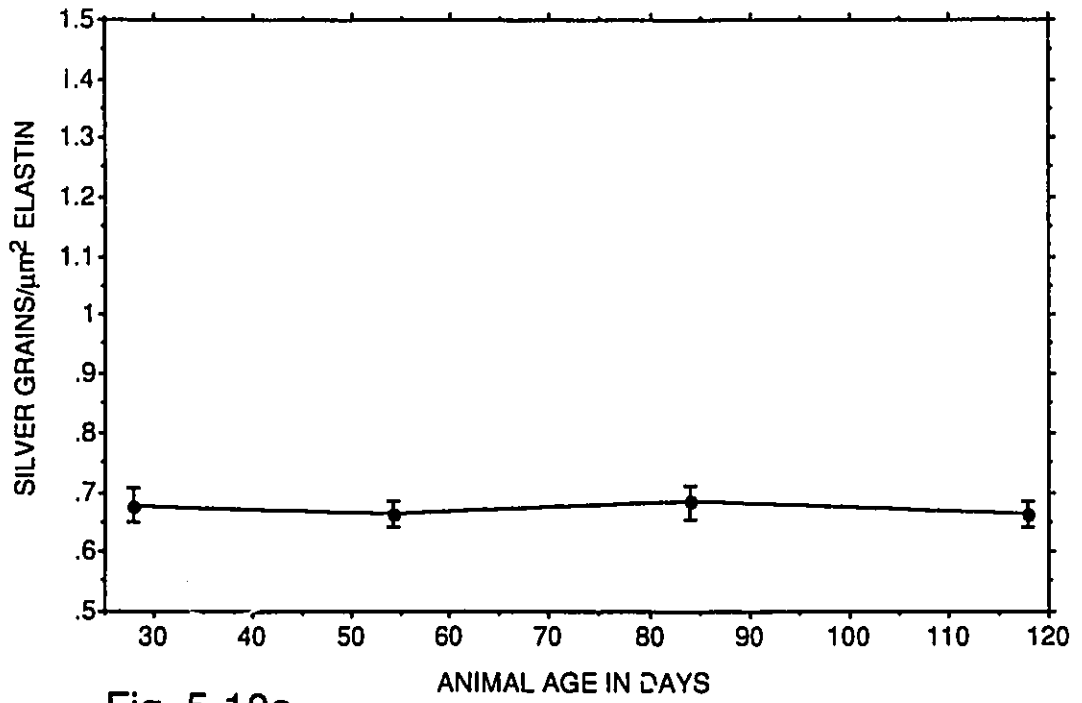


Fig. 5-10a

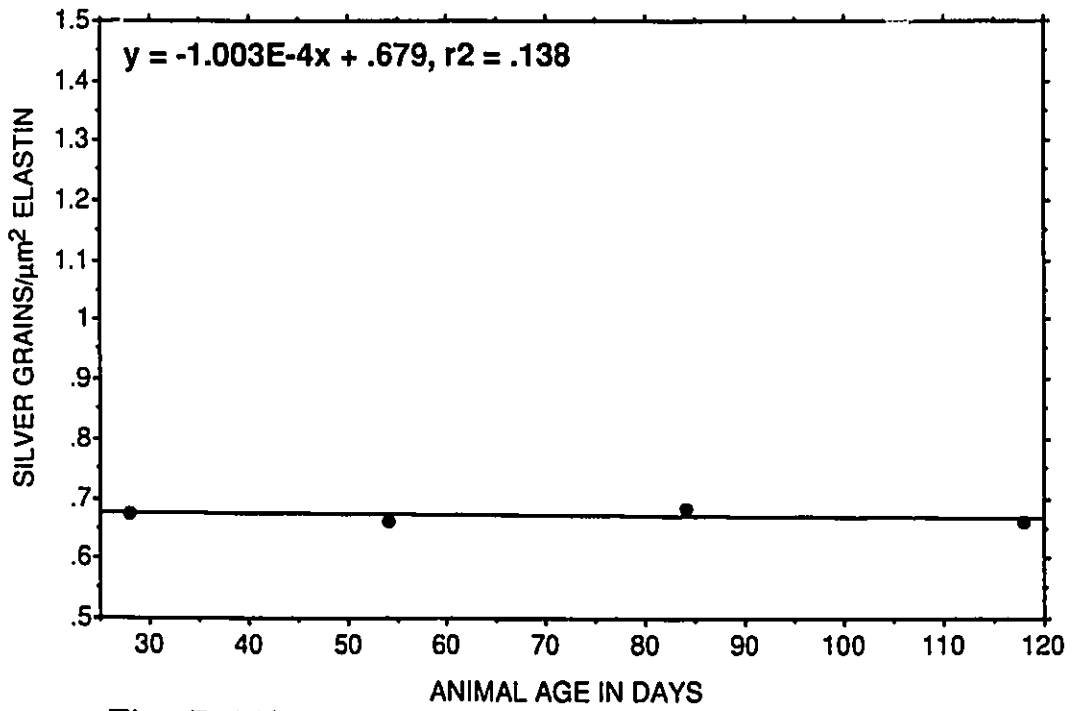


Fig. 5-10b

I

**FIGURE 5-11:** Light microscope radioautographs of a portion of the vessel wall seen in cross-section from animals injected with radiolabel at young ages and killed at 4 months of age. The number in the upper right hand corner denotes the animal's age when injected followed by the animal's age when killed. In aortae of animals injected at 3 days and killed at 4 months of age (a), the silver grains appear evenly distributed approximately over the center of each elastic lamina. Only very small regions of the elastic laminae can be seen to be devoid of grains (arrowheads). In animals injected at 14 days (b) or 21 days (c) and killed at 4 months of age, the silver grains are also evenly distributed along the elastic laminae; however, the grains appear less concentrated in the center of the elastic laminae and are often seen closer to the surface of the smooth muscle cells (arrows). The lumen is at the top of each panel. x1,000.

0

3d/4m



11a

14d/4m



11b

21d/4m



11c

I

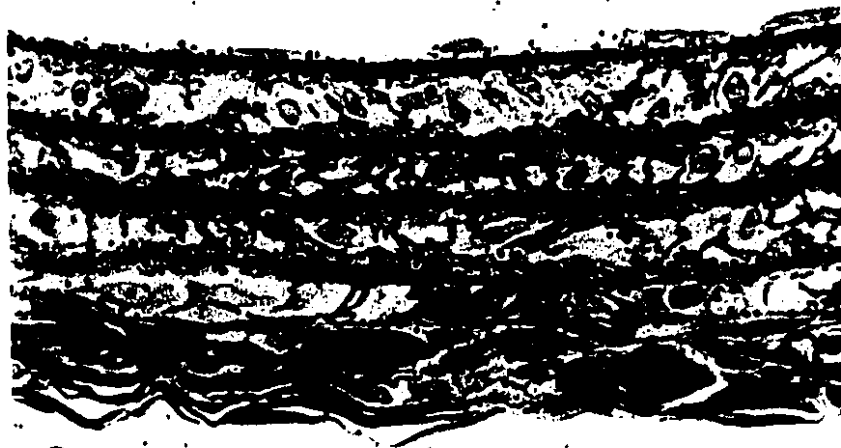
**FIGURE 5-12:** Light microscope radioautographs of a portion of the vessel wall seen in longitudinal section from animals injected with radiolabel at different ages and killed at 4 months of age. The number in the upper right hand corner denotes the animal's age when injected followed by the animal's age when killed. In aortae of animals injected at 3 days and killed at 4 months of age (a), the silver grains appear evenly distributed approximately along the center of the elastic laminae. Similar to that of Figure 5-11a, only small areas of the elastic laminae are devoid of grains (arrowheads). In aortae of animals injected at 14 days (b) or 21 days (c) and killed at 4 months of age, the silver grains are also evenly distributed along the elastic laminae; however, the grains are more often observed at the edges of the elastic laminae rather than in the center (arrows). The lumen is at the top of each panel. x1,000.

3d/4m



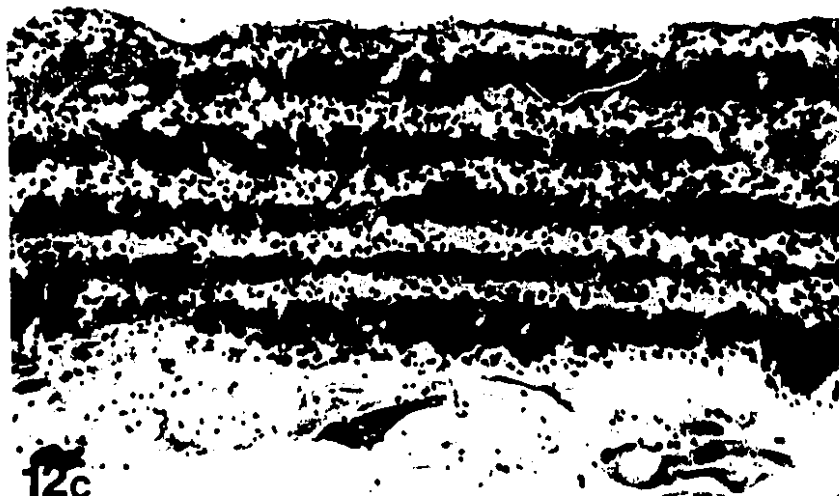
12a

14d/4m



12b

21d/4m



12c

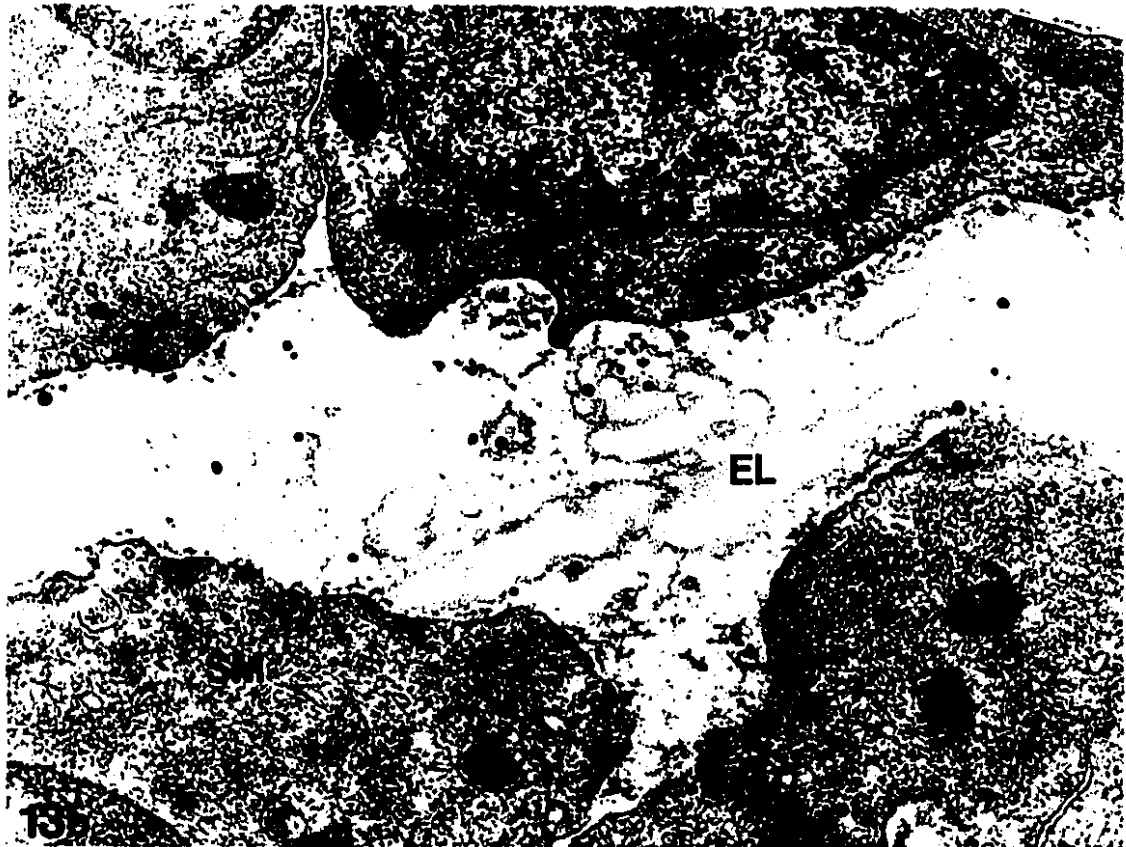
**FIGURE 5-13:** Two electron microscope radioautographs from aortae of animals injected with radiolabel at 3 days and killed at 4 days of age showing an elastic lamina (EL) between two smooth muscle cells (SM). The radioautographs were developed to produce fine silver grains rather than filamentous grains. Many silver grains can be seen along the edges of the elastic laminae. In addition, silver grains are seen over the cells and extracellular matrix. Often, the developing elastic lamina, which is incomplete at this age, and associated silver grains are seen close to the surface of the smooth muscle cells (arrows). (a) x23,100; (b) x31,500.



EL



13a



EL

13b

**FIGURE 5-14:** Electron microscope radioautograph from an aorta of an animal injected with radiolabel at 3 days and killed at 4 days of age showing an elastic lamina (EL) between two layers of smooth muscle cells (SM) in longitudinal section. Silver grains are observed over the smooth muscle cells, extracellular matrix and elastic lamina. In the center of the micrograph, a gap in the elastic lamina can be seen (arrow). In this region, a large number of silver grains are located, whereas in the area of the elastic lamina distant from the gap, fewer grains are observed. This suggests that the newly secreted elastin may be directed to certain areas during growth and completion of the elastic laminae. x19,170.



**FIGURE 5-15:** Electron microscope radioautographs of (a) a subendothelial elastic lamina (EL) and (b) an elastic lamina between two smooth muscle cells (SM) from an animal injected with radiolabel at 3 days and killed at 4 months of age. At this age, silver grains are observed in the center of the elastic laminae. The silver grains represent the location of radiolabel that was incorporated into the elastic laminae early in development. The presence and location of the grains suggests that there was little or no turnover or remodeling from the time of injection until 4 months of age. L, lumen; E, endothelial cell. (a) x31,900; (b) x26,390.

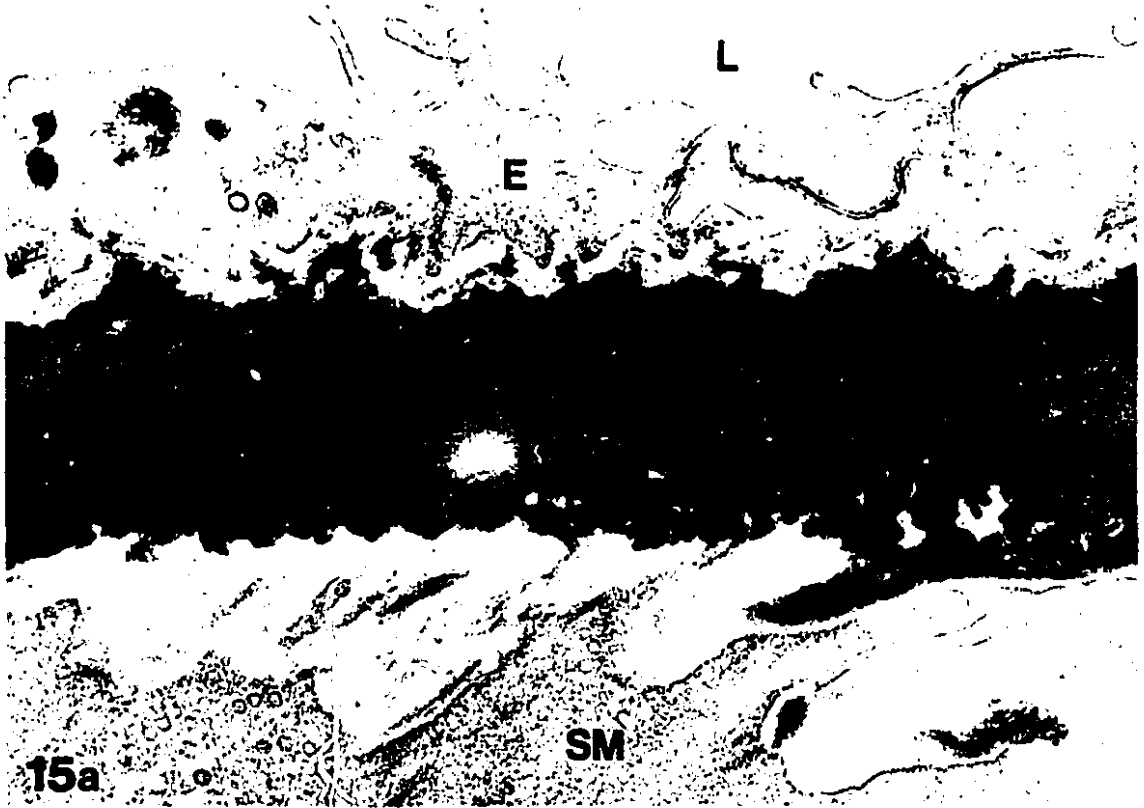
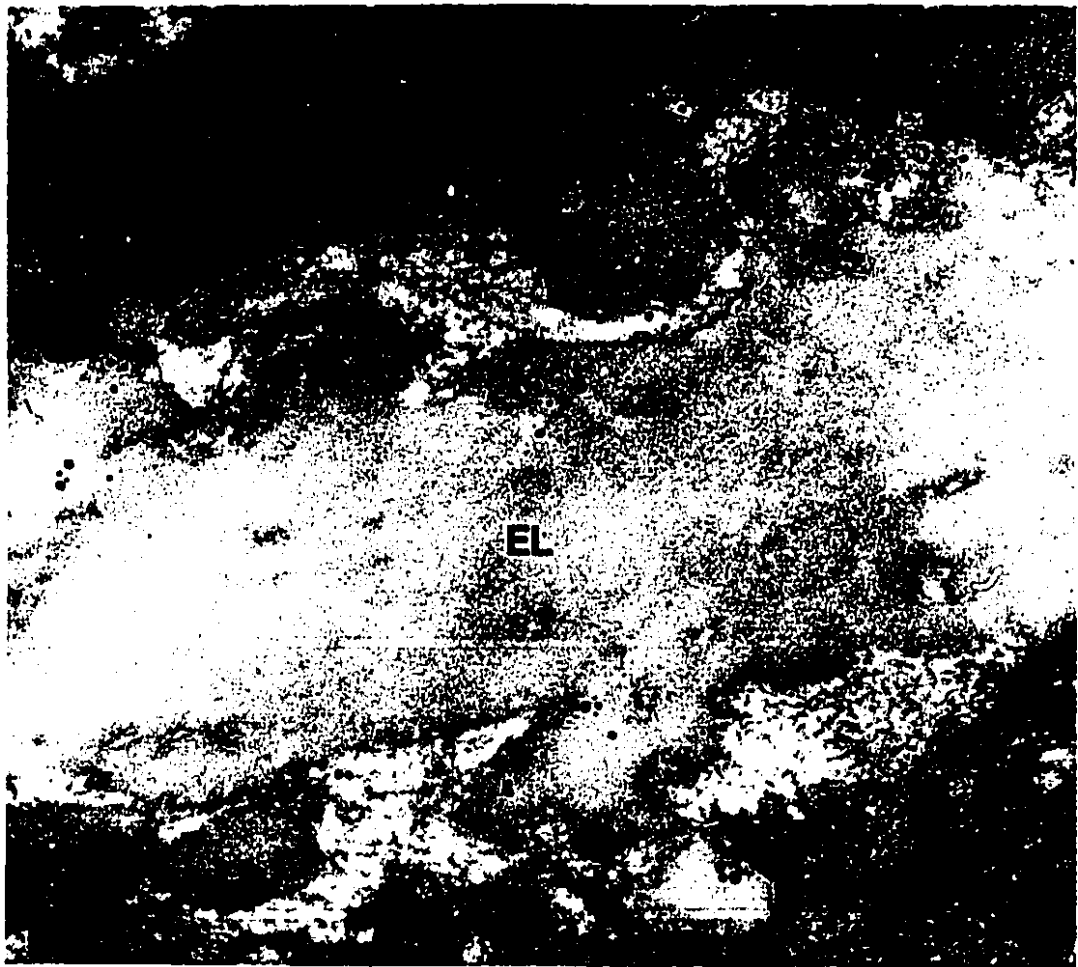


**FIGURE 5-16:** Electron microscope radioautographs of aortae from animals injected with radiolabel at 14 days and killed at 15 days of age. At this age, the elastic laminae (EL) are almost completely formed. (a) Silver grains appear to be primarily located along the edges of the elastic laminae. Some elastin and associated silver grains can be seen close to the smooth muscle cell surface (arrows). (b) A considerable number of silver grains are observed over the smooth muscle cells (SM). Occasionally, silver grains appear to be located toward the center of the elastic lamina along edges of openings in the lamina (arrowheads). This suggests that newly synthesized elastin may be "channeled" into such areas during final completion of elastic lamina formation. (a) x14,910; (b) x13,680.



**FIGURE 5-17:** Electron microscope radioautographs of (a) a subendothelial elastic lamina (EL) and (b) an elastic lamina between two smooth muscle cells (SM) from an animal injected with radiolabel at 14 days and killed at 4 months of age. In both areas, the silver grains are seen predominantly over the edges of the elastic laminae. These observations suggest that growth of the elastic laminae at 14 days of age is by accretion of newly synthesized elastin onto the edges of the laminae. The presence of the silver grains at the edges of the laminae at 4 months of age suggests that little or no remodeling of the laminae has taken place. L, lumen; E, endothelial cell. (a) x23,660; (b) x34,100.





## 5.4 DISCUSSION

The observations reported in the present study represent the first information regarding turnover of elastin in the aorta from long-term radioautographic quantitation. The results indicate that aortic elastin is remarkably stable with little or no new elastin synthesis or turnover following maturation.

The present results corroborate several prior studies in rodents and birds that demonstrate an extremely slow rate of elastin turnover in the adult aorta (Kao et al., 1961; Walford et al., 1964; Lefevre and Rucker, 1980); however, in other studies, a significant turnover of elastin has been reported (Fischer, 1971; Fischer and Swain, 1978). All of these studies have primarily involved the injection of a radiolabeled amino acid and the subsequent determination of the specific activity of the radiolabel in elastin fractions isolated from the aorta. The conflicting results of elastin turnover observed with this methodology appear to be due to the choice of radiolabeled amino acid used for experimentation and the ability to obtain a pure elastin fraction for analysis.

In studies where elastin turnover was found to be significant (Fischer, 1971; Fischer and Swain, 1978), the analyses of turnover were based on measurements of the specific activity of [<sup>14</sup>C]-hydroxyproline in elastin fractions after injection of young rats with [<sup>14</sup>C]-proline. The use of hydroxyproline as a marker of elastin turnover is not ideal since elastin fractions are often contaminated with collagen; in which proline is extensively hydroxylated. In addition, the degree of hydroxylation of prolyl residues in elastin is not consistent and thus even pure elastin fractions may vary in their

hydroxyproline content (Rucker and Tinker, 1977). In contrast to the results obtained with [<sup>3</sup>H]-proline, the use of L-[<sup>14</sup>C]-lysine and the subsequent measurement of <sup>14</sup>C-labeled desmosine and isodesmosine in elastin fractions has shown that there is no significant turnover of elastin in the aorta (Lefevre and Rucker, 1980). Desmosines and isodesmosines are crosslinking amino acids derived from lysyl residues and are unique to elastin as compared to other aortic proteins (Rucker and Tinker, 1977). For this reason, the measurement of these proteins may provide a more accurate estimate of elastin turnover.

In the present study, [<sup>3</sup>H]-valine was used as the radiolabel and its incorporation into the elastic laminae was investigated by radioautography. The choice of valine was based on its abundance in elastin, where it comprises approximately 14% of the amino acids (data in Rucker and Tinker, 1977). In addition, a high percentage of [<sup>3</sup>H]-valine has been shown to become incorporated into both soluble and insoluble elastin fractions from chick aortae (Lee et al., 1976). Previous radioautographic studies that demonstrate radiolabel incorporation into elastic laminae have used [<sup>3</sup>H]-proline (Ross and Klebanoff, 1971; Gerrity et al., 1975). However, these studies were interested in the synthesis of both elastin and collagen and thus proline, which is abundant in both proteins, was more suitable than valine.

The ability to quantitate silver grains directly associated with elastic laminae by radioautography has provided a means to circumvent the problems encountered by collagen contamination which have lead to inaccurate estimates of elastin turnover. Although microfibrils and occasionally isolated collagen fibers become embedded in the

elastic laminae during development, an inaccurate estimate of elastin turnover due to silver grains being associated with these structures rather than elastin appears unlikely due to the small area that they occupy within the laminae in relation to that of the elastin. In addition, microfibrils appear to be synthesized and deposited in the extracellular matrix prior to that of elastin (Fahrenbach et al., 1966; Daga-Gordini et al., 1987; Nakamura, 1988). Furthermore, Shapiro and colleagues (1991) have reported that the age of microfibrils and other non-elastic components of elastic fibers are highly correlated with that of elastin and that both elastin and non-elastin components appear equally stable.

In most studies of elastin turnover, measurements of specific activity of radiolabel during the immediate post-natal time period are disregarded due to dilution of the radiolabel as a result of growth. In the present study, the decrease in silver grains per  $\mu\text{m}^2$  of elastin from 4 to 21 days of age following injection of [ $^3\text{H}$ ]-valine at 3 days of age was analysed with respect to growth. During post-natal development, aortic elastin is known to be rapidly synthesized (Gerrity and Clif, 1975; Lee et al., 1976; Keeley, 1979; Davidson et al., 1986), whereas turnover of elastin at this time is uncertain. Since the proportion of the decrease in grains per  $\mu\text{m}^2$  of elastin due to growth as opposed to turnover cannot be distinguished, it was assumed that the decrease was due entirely to growth for the purpose of analysis. Since the number of grains over the elastic laminae is assumed to be constant, area of elastin per grain was plotted to show the increase in elastin over time. The high correlation ( $r^2 = 0.997$ ) observed for the amount of elastin per silver grain from 4 to 21 days of age indicates that during this time period there is a constant rate of elastin accumulation. The rate of elastin growth was computed at 4.3%

per day which converts to a doubling time of approximately 23 days. Thus, from birth to the time when elastin synthesis arrests, the amount of elastin approximately doubles in the mouse aorta. If some turnover of elastin is occurring during this time period, however, then this estimate of growth would be an overestimate since turnover would have reduced the number of grains thus resulting in a higher percentage of elastin per grain than would be expected by the dilution effect of growth alone. The rapid and constant rate of elastin synthesis following birth observed in the present study is consistent with determinations of elastin synthesis rates in rodents (Looker and Berry, 1972; Gerrity and Cliff, 1975), birds (Lee et al., 1976, Lefevre and Rucker, 1980; Keeley and Johnson, 1983), pigs (Davidson et al., 1986) and humans (Berry et al., 1972b).

The present study reveals no significant difference between the number of silver grains per  $\mu\text{m}^2$  of elastin from 28 days to 4 months of age; thus, no growth or turnover of elastin can be said to occur during this time period. Since the slope of the regression line of grains per  $\mu\text{m}^2$  of elastin is extremely small (-0.0001), it is unlikely that the data points would be significantly different unless a very large number of samples were taken to reduce the variance or the time period was sufficiently extended to result in two points that were far enough apart to be statistically different. Although not statistically significant, the slight negative slope observed in the present study represents a 0.01% decrease in silver grains per  $\mu\text{m}^2$  of elastin per day from 28 days to 4 months. Based on this rate of decrease, the estimated turnover time of elastin would be approximately 27 years in the mouse aorta. This estimate, although speculative, is consistent with results obtained by J.P. Bentley and A. Hanson (data in Rucker and Tinker, 1977) which

estimate the half-life of aortic elastin in the rat to be approximately 40 years. In addition, recent studies of the prevalence of D-aspartate and nuclear weapons-related  $^{14}\text{C}$  in human lung elastin have indicated that lung parenchymal elastic fibers persist for a life-time with minimal new elastin synthesis (Shapiro et al., 1991).

The longevity of elastin and relative absence of new elastin synthesis upon maturation implies that accumulation and proper organization of elastin in the developing vessel is critical since any remodeling of elastin would have to occur at an incredibly slow rate. This presents an interesting problem with respect to vascular growth during development (Mecham et al., 1991b). Gerrity and Cliff (1975) have shown that elastic laminae in the rat aorta are essentially complete by 4 weeks of age; however, the radius of the aortic lumen continues to increase until approximately 8 weeks of age. Since the elastic laminae form complete rings around the circumference of the vessel, there must be a concomitant enlargement of the rings of elastin with the increase in lumen diameter. Either, the elastic laminae must stretch with subsequent accretion of elastin on the sides of the laminae or the elastic laminae must "break" with new elastin inserted in the opening. The even distribution of silver grains observed along the elastic laminae in the present study, from aortae of animals injected at 3 days and killed at 4 months of age, suggests that the elastic laminae may stretch as the vessel grows in diameter. This is further emphasized by the observation of silver grains on either side of the elastic laminae in aortae of animals injected at 14 days and killed at 4 months of age. Stretching of the vessel wall during growth may even be important for elastin production since it has been shown that stretching of cultured aortic smooth muscle cells stimulates tropoelastin

synthesis (Sutcliffe and Davidson, 1990). Since the smooth muscle cells appear to be connected to the elastic laminae early in development (see Chapter 2), stretching of the laminae during growth may be responsible, at least in part, for the transmission of tension to the smooth muscle cells.

Although the silver grains appear evenly distributed along the elastic laminae, aortae from animals injected at 14 days and killed at 4 months show that the relative concentration of grains over the elastic laminae does appear to vary somewhat around the circumference of the vessel; thus, there may be small regions where the elastic laminae are "cut" and new elastin is added. Recently, evidence of such a process of elastic laminae remodeling has been reported using *in situ* hybridization techniques (Prosser et al., 1989; Mecham et al., 1991b). Within the vessel wall, foci of cells were observed that had few intervening elastic laminae; any laminae within the foci appeared fragmented. Although these cell nests were negative for the presence of tropoelastin, the adjacent surrounding cells showed a strong positive reaction (Prosser et al., 1989). This suggests that the cells within these nests may degrade the elastin while the surrounding cells would contribute new elastin to fill the breaks, thus resulting in an enlargement of the elastic lamina (Mecham et al., 1991b). These findings, together with the present radioautographic results, suggest that remodeling of the elastic laminae during normal development may involve a combination of stretching the existing laminae with elastin accretion and cutting the elastic laminae with insertion of newly synthesized elastin.

The fact that there appears to be little new synthesis or turnover of elastin does not imply that elastin is not damaged or modified in normal aging and disease (Rucker and

Tinker, 1977; Robert, 1977; Sandberg et al., 1981; Davidson and Giro, 1986; Bieth, 1986). For example, hypertension induces the vessel wall to thicken with an increase production of elastin (Wolinsky and Glagov, 1970) and atherosclerosis causes fraying or fragmentation of elastic laminae (Bieth, 1986). Clearly, age-related and pathological changes to the amount or organization of elastin may be of severe consequence because of the inert and long-lived nature of this protein.

In summary, results from the present study have provided corroborating evidence for the longevity and stability of elastin in the aortic media by the use of radioautographic techniques. Since elastin undergoes little or no turnover in the vessel wall, the injection of radiolabel and the subsequent observation of its distribution in elastic laminae has provided a valuable method to study elastic lamina growth and development.

***CHAPTER SIX***

***SUMMARY***

## 6.1 GENERAL DISCUSSION

The aortic wall consists of alternating layers of smooth muscle cells and elastic laminae; an organization that develops early in fetal life (Nakamura, 1988). Studies of the mechanical properties of the aorta have suggested that these two layers are structurally and functionally interrelated (Burton, 1954; Wolinsky and Glagov, 1964; Dobrin, 1978). A number of studies have examined morphological aspects of the developing aortic wall (Cliff, 1967; Berry et al., 1972a; Gerrity and Cliff, 1975); however, these studies have provided little information concerning the association of smooth muscle cells and elastic laminae. The work of this thesis was thus intended to provide a detailed investigation concerning interrelationships of aortic cells with elastic lamina during development and the ultimate fate of the associations between the two structures in the adult vessel.

The study of smooth muscle cell to elastic lamina connections in the mouse aortic wall revealed the presence of "contractile-elastic units" consisting of bundles of contractile filaments within the smooth muscle cells and associated elastin extensions that anchor the cells to adjacent elastic laminae (Fig. 2-18a). Contractile-elastic units commence formation in early fetal life and remain as functional structures in the adult vessel. Wolinsky and Glagov (1967) described the aortic media to be composed of "lamellar units"; each consisting of one elastic lamina and the adjacent interlamellar components. The lamellar unit was later redefined to consist of one smooth muscle cell layer and the elastic laminae on either side and was termed a "musculo-elastic fascicle" (Clark and Glagov, 1985). Musculo-elastic fascicles and contractile-elastic units represent different structural units

within the aortic wall. Since musculo-elastic fascicles represent entire smooth muscle cell layers, numerous contractile-elastic units can be said to be contained within one fascicle. The contractile-elastic unit thus represents the basic structural unit of the aortic media. In the adult vessel wall, the contractile-elastic units were shown to be oriented in alternating directions from one smooth muscle cell layer to the next (Figs. 2-24, 2-25). This observation has provided evidence for an ordered arrangement of aortic medial components and has allowed a new model for aortic medial architecture to be proposed (Fig. 2-28).

In addition to connections between smooth muscle cells and elastic laminae, a structural association between endothelial cells and the subjacent elastic lamina was also revealed. The presence of "anchoring filaments" in the subendothelial matrix, that appear structurally related to bundles of endothelial cell cytoplasmic filaments, has been previously reported (Gerrity and Cliff, 1972; Yohro and Burnstock, 1973; Buck, 1979). These studies, however, present conflicting observations concerning the association of the anchoring filaments with the surface of the underlying elastic lamina. Observations from the present study demonstrate that the anchoring filaments, renamed "endothelial cell connecting filaments", merge with the elastic lamina and thus form a structural link from the abluminal endothelial cell membrane to the elastic lamina surface (Fig. 3-14b). This link is continued within the endothelial cell by bundles of similarly aligned cytoplasmic filaments, termed stress fibers, that anchor in the same region of membrane (Fig. 3-13a). Endothelial cell connecting filaments were observed predominately in the developing aortic intima parallel to the direction of blood flow; thus, these structures, together with

the intracellular stress fibers, were proposed to play a role in the maintenance of endothelial cell integrity. This hypothesis is supported by previous studies which show induction of stress fiber formation by fluid shear stress (Franke et al., 1984) and appearance of extensive stress fibers in areas of blood vessels subjected to high shear forces due to blood flow (Kim et al., 1989a). Endothelial cell connecting filaments may therefore be important to protect the endothelial cells from the shear force of blood flow, and possibly to transmit tension to underlying layers, during early development of the vessel wall.

Morphological and immunohistochemical results presented in this study provide evidence that the endothelial cells connecting filaments are microfibrillar in nature. Previous morphological observations of endothelial cell connecting filaments presented conflicting results concerning their structural composition (Gerrity and Cliff, 1972; Buck, 1979). In the present study, immunolabeling results demonstrated that the connecting filaments contain fibrillin (Figs. 4-3, 4-4), a component of microfibrils (Sakai et al., 1986), and are heavily coated with fibronectin (Fig. 4-5). Attempts to immunolocalize another microfibril protein, microfibril-associated glycoprotein (MAGP) (Gibson et al., 1986, 1991), to the connecting filaments failed (Fig. 4-5). The negative immunolabeling results with MAGP may be a false-negative result in that the reactive epitope could have been inaccessible or blocked. This suggestion is supported by the demonstration that fibronectin on the surface in microfibrils produced by cultured smooth muscle cells can block immunolocalization of microfibril associated antigens (Schwartz et al., 1985). One must also consider the possibility that MAGP may not be present as a component of

connecting filaments. This would provide the first evidence that microfibrils may be a family of filamentous structures and not a single structural entity. It has yet to be established why microfibrils show various degrees of association with elastin (Cotta-Pereira et al., 1976, 1977) and other extracellular matrix proteins, such as vitronectin and amyloid P component (Dahlbäck et al., 1990); thus the possibility exists that some component(s) of microfibrils may vary depending on location or function to allow for this difference. In any event, the identification of endothelial cell connecting filaments as microfibrillar provides evidence that beside the possible roles of microfibrils in elastogenesis (Cleary et al., 1981), microfibrils may be important for cell anchorage and tissue stability.

The study of elastin stability in the mouse aortic wall in this work provides the first long-term radioautographic investigation of elastin turnover. Previous studies have shown the incorporation of radiolabel into developing elastic laminae (Ross and Klebanoff, 1971); however, no long-term studies were carried out to determine the fate of the radiolabel. Elastin turnover studies based on measurements of specific activity have produced turnover rates that range from several weeks (Fischer, 1971; Fischer and Swain, 1978) to several years (Lefevre and Rucker, 1980; Dubick et al., 1981). Technical problems associated with contamination of elastin samples, thought to produce the discrepancy of these results, were circumvented in the present radioautographic study by the ability to directly observe and quantitate the radiolabel associated with elastin. The present results provide evidence for the remarkable longevity of elastin in the aorta (Fig. 5-2) and support the hypothesis that the connections between aortic smooth muscle cells

to elastic laminae are metabolically stable and thus remain throughout development as important functional structures.

In addition to elastin turnover, the radioautographic results have provided novel information concerning elastic lamina growth and development. Morphological studies have shown that the lumen of the aorta continues to increase in diameter after complete formation of the elastic laminae (Gerrity and Cliff, 1975). Since the elastic laminae form continuous concentric rings around the lumen of the vessel, an increase in lumen diameter upon their completion presents an interesting problem (Mecham et al., 1991b). Recent evidence suggests that the elastic laminae may be "cut" and new elastin inserted to increase the diameter of the laminae and thus allow the lumen diameter to increase (Prosser et al., 1989; Mecham et al., 1991b). The observations of the present radioautographic work, showing an even distribution of silver grains in elastic laminae from adult animals that were injected with radiolabel at early in post-natal ages (Figs. 5-11, 5-12), suggest that, if such a mechanism of elastic lamina growth occurs, it must take place in many small localized area throughout the vessel wall.

In summary, the results from this thesis have provided a better understanding of the interrelationships of endothelial and smooth muscle cells with elastic laminae in the developing and adult aorta. Both new and corroborating evidence concerning aortic structure and elastin stability has been presented.

## 6.2 CONTRIBUTIONS TO ORIGINAL KNOWLEDGE

The work of this thesis has provided information concerning the relationships of endothelial cells and smooth muscle cells to elastic laminae in the developing mouse aorta. In addition, qualitative and quantitative data on elastin stability and elastic lamina growth in the aorta was presented. Original contributions from chapter two through chapter five of this work are as follows:

**Chapter Two:** The work from this chapter has provided the first ultrastructural information concerning the development of smooth muscle cell to elastic lamina connections in the aortic media. Results from this study have provided evidence for a new basic unit of structural organization in the aortic media; the "contractile-elastic unit". Observations of the orientation of contractile-elastic units in the adult media have allowed for the proposal of a new model concerning the aortic media organization. The early development and ultimate organization of contractile-elastic units in the mouse aortic media stresses the importance of the association of smooth muscle cells to elastic laminae in vessel wall structure.

**Chapter Three:** In this chapter, detailed information concerning the structure of filaments that anchor endothelial cells to the underlying elastic lamina was presented. These filaments, termed endothelial cell connecting filaments, were studied for the first time with respect to development and ultimate fate in the aortic intima. The observations from this

study provide the first specific ultrastructural evidence that endothelial cell connecting filaments are related to microfibrils and suggest that the connecting filaments function to protect the aortic endothelial cells from the mechanical stresses of development.

**Chapter four:** Immunolocalization of microfibril and microfibril-associated proteins to endothelial cell connecting filaments was presented in this chapter. This is the first attempt to identify the structural components that form these filaments. The results demonstrate that the connecting filaments are microfibrillar in nature and are heavily coated with fibronectin. These findings provide evidence for the role of microfibrils in cell anchorage and in the maintenance tissue integrity.

**Chapter five:** This is the first long-term radioautographic study of elastin stability in the aortic wall. The quantitative results provide evidence for the longevity of aortic elastin and support the findings from Chapter two that suggest that connections of smooth muscle cells to elastic laminae, which form early in development, remain as permanent structures in the adult vessel. Furthermore, observations concerning the fate of radiolabel incorporated early in development have provided novel information in regard to elastic lamina growth.

***REFERENCES***



Abercrombie M, Durn GA (1975) Adhesions of fibroblasts to substratum during contact inhibition observed by interference-reflection microscopy. *Exp Cell Res* 92:57-62

Albert EN (1972) Developing elastic tissue. An electron microscope study. *Am J Pathol* 69:89-102

Almassian BJ, Trackman PC, Iguchi H, Boak A, Calvaresi D, Kagan HM (1990) Induction of lung lysyl oxidase activity and lysyl oxidase protein by exposure of rats to cadmium chloride: properties of the induced enzyme. *Connect Tiss Res* 25:197-208

Arbeille BB, Fauvel-Lafeve FMJ, Lemesle MB, Tenza D, Legrand YJ (1991) Thrombospondin: A component of microfibrils in various tissues. *J Histochem Cytochem* 39:1367-1375

Ayad S, Chambers CA, Shuttleworth CA, Grant ME (1985) Isolation from bovine elastic tissues of collagen type VI and characterization of its form in vivo. *Biochem J* 230:465-474

Ayer JP (1964) Elastic tissue. *Int Rev Connect Tiss Res* 2:33-100

Baccarani-Contri M, Vincenzi D, Quaglino D, Mori G, Pasquali-Ronchetti I (1989) Localization of human placental lysyl oxidase on human placenta, skin and aorta by immunoelectronmicroscopy. *Matrix* 9:428-436

Baltz ML, Caspi D, Evans DJ, Rowe IF, Hind CRK, Pepys MB (1986) Circulating serum amyloid P component is the precursor of amyloid P component in tissue amyloid deposits. *Clin Exp Immunol* 66:691-700

- Bendeck MP, Langille BL (1991) Rapid accumulation of elastin and collagen in the aortas of sheep in the immediate perinatal period. *Circ Res* 69:1165-1169
- Benninghoff A (1928) Über die Beziehungen zwischen elastischen Gerüst und glatter Muskulatur in der Arterienwand und ihre funktionelle Bedeutung. *Ztschr f Zellforsch u mikr Anat* 6:348-396
- Berry CL, Looker T, Germain J (1972a) The growth and development of the rat aorta. I. Morphological aspects. *J Anat* 113:1-16
- Berry CL, Looker T, Germain J (1972b) Nucleic acid and scleroprotein content of the developing human aorta. *J Pathol* 108:265-274
- Bierring F, Kobayasi T (1963) Electron microscopy of the normal rabbit aorta. *Acta Pathol Microbiol Scand* 57:154-168
- Bieth JG (1986) Elastases: Catalytic and biological properties. In: *Regulation of Matrix Accumulation*. Mecham RP (ed). Academic Press, New York. pp 217-320
- Birembaut P, Legrand YJ, Bariety J, Bretton R, Fauvel F, Belair MF, Pignaud G, Caen JP (1982) Histochemical and ultrastructural characterization of subendothelial glycoprotein microfibrils interacting with platelets. *J Histochem Cytochem* 30:75-80
- Blood CH, Sasse J, Brodt P, Zetter BR (1988) Identification of a tumor cell receptor for VGVAPG, an elastin-derived chemotactic peptide. *J Cell Biol* 107:1987-1993
- Blood CH, Zetter BR (1989) Membrane-bound protein kinase C modulates receptor affinity and chemotactic responsiveness of Lewis lung carcinoma sublines to an elastin-derived peptide. *J Biol Chem* 264:10614-10620



Breathnach SM, Melrose SM, Bhogal B, de Beer FC, Dyck RF, Tennent G, Black MM, Pepys MB (1981) Amyloid P component is located on elastic fibre microfibrils in normal human tissue. *Nature* 293:652-654

Breathnach SM, Pepys MB, Hintner <sup>††</sup> (1989) Tissue amyloid P component in normal human dermis is non-covalently associated with elastic fiber microfibrils. *J Invest Dermatol* 92:53-58

Bressan GM, Castellani I, Giro MG, Volpin D, Fornieri C, Pasquali-Ronchetti I (1983) Banded fibers in tropoelastin coacervates at physiological temperatures. *J Ultrastruct Res* 82:335-340

Bressan GM, Pasquali-Ronchetti I, Fornieri C, Mattioli F, Castellani I, Volpin D (1986) Relevance of aggregation properties of tropoelastin to the assembly and structure of elastic fibers. *J Ultrastruct Mol Struct Res* 94:209-216

Böck P (1978) Histochemical staining of lymphatic anchoring filaments. *Histochemistry* 58:343-345

Böck P (1983) Elastic fiber microfibrils: Filaments that anchor the epithelium of the epiglottis. *Arch Histol Jap* 46:307-314

Buck RC (1979) The longitudinal orientation of structures in the subendothelial space of the rat aorta. *Am J Anat* 156:1-14

Burton AC (1954) Relation of structure to function of the tissues of the wall of blood vessels. *Physiol Rev* 34:619-642

- Caldini EG, Caldini N, De-Pasquale V, Strocchi R, Guizzardi S, Ruggeri A, Montes GS (1990) Distribution of elastic system fibres in the rat tail tendon and its associated sheaths. *Acta Anat* 139:341-348
- Campbell FR (1987) An electron microscopic study of microfibrils of bone marrow. *Scan Microsc* 1:1711-1714
- Carmichael GG, Fullmer HM (1966) The fine structure of the oxytalan fiber. *J Cell Biol* 28:33-36
- Carton RW, Dainauskas J, Tews B, Hass GM (1960) Isolation and study of the elastic tissue network of the lung in three dimensions. *Am J Respir Diseases* 82:186-194
- Chavier C, Hartmann DJ, Couble ML, Herbage D (1988) Distribution and organization of the elastic system fibres in healthy human gingiva. Ultrastructural and immunohistochemical study. *Histochemistry* 89:47-52
- Chen LB, Murray A, Segal RA, Bushnell A, Walsh ML (1978) Studies on intercellular LETS glycoprotein matrices. *Cell* 14:377-391
- Clark JM, Glagov S (1979) Structural integration of the arterial wall. I. Relationships and attachments of medial smooth muscle cells in normally distended and hyperdistended aortas. *Lab Invest* 40:587-602
- Clark JM, Glagov S (1985) Transmural organization of the arterial media. The lamellar unit revisited. *Arteriosclerosis* 5:19-34
- Cleary EG, Fanning JC, Prosser I (1981) Possible roles of microfibrils in elastogenesis. *Connect Tiss Res* 8:161-166

- Cliff WJ (1967) The aortic tunica media in growing rats studied with the electron microscope. *Lab Invest* 17:599-615
- Cotta-Pereira G, Guerra Rodrigo F, Bittencourt-Sampaio S (1976) Oxytalan, elaunin, and elastic fibers in the human skin. *J Invest Dermatol* 66:143-148
- Cotta-Pereira G, Rodrigo FG, David-Ferreira JF (1977) The elastic system fibers. In: *Elastin and Elastic Tissue. Advances in Experimental Medicine and Biology*. Sandberg LB, Gray WR, Franzblau C (eds). Plenum Press, New York. vol 79, pp 19-30
- Cotta-Pereira G, Del-Caro LM, Montes GS (1984) Distribution of elastic system fibers in hyaline and fibrous cartilages of the rat. *Acta Anat* 119:80-85
- Cox BA, Starcher BC, Urry DW (1973) Coacervation of  $\alpha$ -elastin results in fiber formation. *Biochim Biophys Acta* 317:209-213
- Cox BA, Starcher BC, Urry DW (1974) Coacervation of tropoelastin results in fiber formation. *J Biol Chem* 249:997-998
- Cronlund AL, Kagan HM (1986) Comparison of lysyl oxidase of bovine aorta and lung. *Connect Tiss Res* 15:173-185
- Daga-Gordini D, Bressan GM, Castellani I, Volpin D (1987) Fine mapping of tropoelastin-derived components in the aorta of developing chick embryo. *Histochem J* 19:623-632
- Dahlbäck K, Löfberg H, Dahlbäck B (1986) Localization of vitronectin (S-protein of complement) in normal human skin. *Acta Derm Venereol (Stockh)* 66:461-467

- Dahlbäck K, Löfberg H, Dahlbäck B (1987) Immunohistochemical demonstration of vitronectin in association with elastin and amyloid deposits in human kidney. *Histochemistry* 87:511-515
- Dahlbäck K, Löfberg H, Alumets J, Dahlbäck B (1989) Immunohistochemical demonstration of age-related deposition of vitronectin (S-protein of complement) and terminal complement complex on dermal elastic fibers. *J Invest Dermatol* 92:727-733
- Dahlbäck K, Ljungquist A, Löfberg H, Dahlbäck B, Engvall E, Sakai LY (1990) Fibrillin immunoreactive fibers constitute a unique network in the human dermis: Immunohistochemical comparison of the distributions of fibrillin, vitronectin, amyloid P component, and orcein stainable structures in normal skin and elastosis. *J Invest Dermatol* 94:284-291
- Damiano V, Tsang A-L, Weinbaum G, Christner P, Rosenbloom J (1984) Secretion of elastin in the embryonic chick aorta as visualized by immunoelectron microscopy. *Coll Rel Res* 4:153-164
- Davidson JM, Leslie B, Wolt T, Crystal RG, Sandberg LB (1982) Characterisation of a signal peptide sequence in the cell-free translation product of sheep elastin mRNA. *Arch Biochem Biophys* 218:31-37
- Davidson JM, Giro MG (1986) Control of elastin synthesis: Molecular and cellular aspects. In: *Regulation of Matrix Accumulation*. Mecham RP (ed). Academic Press, New York. pp 177-216
- Davidson JM, Hill KE, Alford JL (1986) Developmental changes in collagen and elastin biosynthesis in the porcine aorta. *Dev Biol* 118:103-111

I  
de Beer FC, Baltz ML, Holford S, Feinstein A, Pepys MB (1981) Fibronectin and C4-binding protein are selectively bound by aggregated amyloid P component. *J Exp Med* 154:1134-1149

Dewey CF Jr (1979) Fluid mechanics of arterial flow. In: *Dynamics of Arterial Flow. Advances in Experimental Medicine and Biology*. Wolf S, Werthessen NT (eds). Plenum Press, New York. vol 115, pp 55-103

Dietz HC, Cutting GR, Pyeritz RE, Maslen CL, Sakai LY, Corson GM, Puffenberger EG, Hamosh A, Nanthakumar EJ, Curristin SM, Stetten G, Meyers DA, Francomano CA (1991) Marfan syndrome caused by a recurrent de novo missense mutation in the fibrillin gene. *Nature* 352:337-339

Dobrin PB (1978) Mechanical properties of arteries. *Physiol Rev* 58:397-460

Dubick MA, Rucker RB, Cross CE, Last JA (1981) Elastin metabolism in rodent lung. *Biochim Biophys Acta* 672:303-306

Ellis J (1987) Proteins as molecular chaperones. *Nature* 328:378-379

El-Magharaby MAHA, Gardner DL (1972) Development of connective tissue components of small arteries in the chick embryo. *J Pathol* 108:281-291

Eyre ER, Paz MA, Gallop PM (1984) Cross-linking in collagen and elastin. *Annu Rev Biochem* 53:717-748

Fahrenbach WH, Sandberg LB, Cleary EG (1966) Ultrastructural studies on early elastogenesis. *Anat Rec* 155:563-576

- Fanning JC, Cleary EG (1985) Identification of glycoproteins associated with elastin-associated microfibrils. *J Histochem Cytochem* 33:287-294
- Fanning JC, White JF, Polewski R, Cleary EG (1991) Immunoelectron microscopic localization of elastic tissue components in archival tissue samples. *J Microscopy* 162:355-367
- Fauvel F, Grant ME, Legrand YJ, Souchon H, Tobelem G, Jackson DS, Caen JP (1983) Interaction of blood platelets with an extract from bovine aorta: requirement for von Willebrand factor. *Proc Natl Acad Sci USA* 80:551-554
- Fauvel-Lafeve F, Picard P, Godeau G, Legrand YJ (1988) Characterization of an antibody directed against a 128 kDa glycoprotein involved in the thrombogenicity of the elastin-associated microfibrils. *Biochem J* 255:251-258
- Fischer GM (1971) Dynamics of collagen and elastin metabolism in rat aorta. *J Appl Physiol* 31:527-530
- Fischer GM, Swain ML (1978) *In vivo* effects of sex hormones on aortic elastin and collagen dynamics in castrated and intact male rats. *Endocrinology* 102:92-97
- Fleischmajer R, Timpl R (1984) Ultrastructural localization of fibronectin to different anatomic structures of human skin. *J Histochem Cytochem* 32:315-321
- Fleischmajer R, Contard P, Schwartz E, MacDonald ED II, Jacobs L II, Sakai LY (1991a) Elastin-associated microfibrils (10 nm) in a three-dimensional fibroblast culture. *J Invest Dermatol* 97:638-643

- Fleischmajer R, Perlsh JS, Faraggiana T (1991b) Rotary shadowing of collagen monomers, oligomers and fibrils during tendon fibrillogenesis. *J Histochem Cytochem* 39:51-58
- Fleischmajer R, Jacobs L, Schwartz E, Sakai LY (1991c) Extracellular microfibrils are increased in localized and systemic scleroderma skin. *Lab Invest* 64:791-798
- Fornieri C, Baccarani-Contri M, Quaglino D, Pasquali-Ronchetti I (1987) Lysyl oxidase activity and elastin/glycosaminoglycan interactions in growing chick and rat aortas. *J Cell Biol* 105:1463-1469
- Franc S, Garrone R, Bosch A, Franc J-M (1984) A routine method for contrasting elastin at the ultrastructural level. *J Histochem Cytochem* 32:251-258
- Franke R-P, Gräfe M, Schnittler H, Seiffge D, Mittermayer C (1984) Induction of human vascular endothelial stress fibres by fluid shear stress. *Nature* 307:648-649
- Frisch SM, Davidson JM, Werb Z (1985) Blockage of tropoelastin secretion by monensin represses tropoelastin synthesis at a pretranslational level in rat smooth muscle cells. *Mol Cell Biol* 5:253-258
- Fullmer HM, Lillie RD (1958) The oxytalan fiber: A previously undescribed connective tissue fiber. *J Histochem Cytochem* 6:425-430
- Gabbiani G, Gabbiani F, Lombardi D, Schwartz SM (1983) Organization of actin cytoskeleton in normal and regenerating arterial endothelial cells. *Proc Natl Acad Sci USA* 80:2361-2364

- Gadek JE, Fells GA, Zimmerman RL, Rennard SI, Crystal RG (1981) Antielastases of the human alveolar structures. Implications for the protease-antiprotease theory of emphysema. *J Clin Invest* 68:889-898
- Gawlik Z (1965) Morphological and morphochemical properties of the elastic system in the motor organ of man. *Folia Histochem Cytochem* 3:233-251
- Geiger B, Avnur Z, Rinnerthaler G, Hinssen H, Small VJ (1984) Microfilament-organizing centers in areas of cell contact: Cytoskeletal interactions during cell attachment and locomotion. *J Cell Biol* 99:83s-91s
- Gerli R, Ibba L, Fruschelli C (1990) A fibrillar elastic apparatus around human lymph capillaries. *Anat Embryol* 181:281-286
- Gerrity RG, Cliff WJ (1972) The aortic tunica intima in young and aging rats. *Exp Mol Pathol* 16:382-402
- Gerrity RG, Cliff WJ (1975) The aortic tunica media of the developing rat.  
I. Quantitative stereologic and biochemical analysis. *Lab Invest* 32:585-600
- Gerrity RG, Adams EP, Cliff WJ (1975) The aortic tunica media of the developing rat.  
II. Incorporation by medial cells of <sup>3</sup>H-proline into collagen and elastin: Autoradiographic and chemical studies. *Lab Invest* 32:601-609
- Gibson MA, Cleary EG (1982) A collagen-like glycoprotein from elastin-rich tissues. *Biochem Biophys Res Commun* 105:1288-1295
- Gibson MA, Cleary EG (1983) Distribution of CL glycoprotein in tissues: An immunohistochemical study. *Collagen Rel Res* 3:469-488

Gibson MA, Cleary EG (1985) CL glycoprotein is the tissue form of type VI collagen. J Biol Chem 260:11149-11159

Gibson MA, Hughes JL, Fanning JC, Cleary EG (1986) The major antigen of elastin-associated microfibrils is a 31-kDa glycoprotein. J Biol Chem 261:11429-11436

Gibson MA, Cleary EG (1987) The immunohistochemical localisation of microfibril-associated glycoprotein (MAGP) in elastic and non-elastic tissues. Immunol Cell Biol 65:343-356

Gibson MA, Kumaratilake JS, Cleary EG (1989) The protein components of the 12-nanometer microfibrils of elastic and nonelastic tissues. J Biol Chem 264:4590-4598

Gibson MA, Sandberg LB, Grosso LE, Cleary EG (1991) Complementary DNA cloning establishes microfibril-associated glycoprotein (MAGP) to be a discrete component of the elastin-associated microfibrils. J Biol Chem 266:7596-7601

Goldfischer S, Coltoff-Schiller B, Schwartz E, Blumenfeld OO (1983) Ultrastructure and staining properties of aortic microfibrils (oxytalan). J Histochem Cytochem 31:382-390

Goldfischer S, Coltoff-Schiller B, Goldfischer M (1985) Microfibrils, elastic anchoring components of the extracellular matrix, are associated with fibronectin in the zonule of Zinn and aorta. Tissue Cell 17:441-450

Gomori G (1950) Aldehyde fuchsin: A new stain for elastic tissue. Am J Clin Pathol 20:665-666

Gosline JM, Rosenbloom J (1984) Elastin. In: Extracellular Matrix Biochemistry. Piez KA, Reddi AH (eds). Elsevier Science Publishing, New York. pp 119-227

Gotte L, Giro MG, Volpin D, Horne RW (1974) The ultrastructural organization of elastin. *J Ultrastruct Res* 46:23-33

Gray WR, Sandberg LB, Foster JA (1973) Molecular model for elastin structure and function. *Nature* 246:461-466

Greenlee TK, Ross R, Hartman JL (1966) The fine structure of elastic fibers. *J Cell Biol* 30:59-71

Greenlee TK, Ross R (1967) The development of the rat flexor digital tendon. A fine structure study. *J Ultrastruct Res* 18:354-376

Hamazaki H (1987)  $Ca^{2+}$ -mediated association of human serum amyloid P component with heparan sulfate and dermatan sulfate. *J Biol Chem* 262:1456-1460

Haust MD (1965) Fine fibrils of extracellular space (microfibrils). Their structure and role in connective tissue organization. *Am J Pathol* 47:1113-1137

Herman IM, Brant AM, Warty VS, Bonaccorso J, Klein EC, Kormos RL, Borovetz HS (1987) Hemodynamics and the vascular endothelial cytoskeleton. *J Cell Biol* 105: 291-302

Hermo L, Lalli M, Clermont Y (1977) Arrangement of connective tissue components in the walls of seminiferous tubules of man and monkey. *Am J Anat* 148:433-446

Heuser JE (1981) Quick-freeze, deep etch preparations of samples for 3-D electron microscopy. *Trends Biochem Sci* 6:64-68

Hinek A, Wrenn DS, Mecham RP, Barondes SH (1988) The elastin receptor: A galactoside-binding protein. *Science* 239:1539-1541

Hinek A, Mecham RP (1990) Characterization and functional properties of the elastin receptor. In: *Elastin: Chemical and Biological Aspects*. Galatina Congedo Editore. pp 369-381

Hoeve CAJ, Flory PJ (1974) The elastic properties of elastin. *Biopolymers*. 13:677-686

Hornebeck W, Adnet JJ, Robert L (1978) Age dependent variation of elastin and elastase in aorta and human breast cancers. *Exp Geront* 13:293-298

Hornebeck W, Tixier JM, Robert L (1986) Inducible adhesion of mesenchymal cells to elastic fiber: Elastonection. *Proc Natl Acad Sci USA* 83:5517-5520

Hynes, R (1985) Molecular biology of fibronectin. *Annu Rev Cell Biol* 1:67-91

Inoue S (1991) Pentosome - a new connective tissue component - is a subunit of amyloid P. *Cell Tiss Res* 263:431-438

Inoue S, Leblond CP (1986) The microfibrils of connective tissue: I. Ultrastructure. *Am J Anat* 176:121-138

- Inoue S, Leblond CP, Grant DS, Rico P (1986a) The microfibrils of connective tissue: II. Immunohistochemical detection of amyloid P component. *Am J Anat* 176:139-152
- Inoue S, Skinner M, Leblond CP, Shirahama T, Cohen AS (1986b) Isolation of the amyloid P component from the Engelbreth-Holm-Swarm (EHS) tumor of the mouse. *Biochem Biophys Res Commun* 134:995-999
- Inoue S, Leblond CP, Rico P, Grant D (1989) Association of fibronectin with the microfibrils of connective tissue. *Am J Anat* 186:43-54
- Inoue S, Chan FL, Leblond CP (1991) Release of pentosomes results in the collapse of zonular microfibrils. *J Cell Biol* 115:296a
- Jacob M-P, Fülöp T Jr, Foris G, Robert L (1987) Effect of elastin peptides on ion fluxes in mononuclear cells, fibroblasts, and smooth muscle cells. *Proc Natl Acad Sci USA* 84:995-999
- Jaffe EA, Hoyer LW, Nachman RL (1973) Synthesis of anti-hemophilic factor antigen by cultured human endothelial cells. *J Clin Invest* 52:2737-2744
- Jaffe EA, Hoyer LW, Nachman RL (1974) Synthesis of von Willebrand factor by cultured human endothelial cells. *Proc Natl Acad Sci USA* 71:1906-1909
- Jaques A, Serafini-Fracassini A (1985) Morphogenesis of the elastic fiber: An immunoelectronmicroscopy investigation. *J Ultrastruct Res* 92:201-210
- Jaques A, Serafini-Fracassini A (1986) Immunolocalisation of a 35K structural glycoprotein to elastin-associated microfibrils. *J Ultrastruct Mol Struct Res* 95:218-227

- Kadar A, Bush V, Gardner DL (1971) The relationship between the fine structure of smooth muscle cells and elastogenesis in the chick embryo aorta. *J Pathol* 104: 253-259
- Kagan HM, Sullivan KA, Olsson TA III, Cronlund AL (1979) Purification and properties of four species of lysyl oxidase from bovine aorta. *Biochem J* 177:203-214
- Kagan HM, Vaccaro CA, Bronson RE, Tang S-S, Brody JS (1986) Ultrastructural immunolocalization of lysyl oxidase in vascular connective tissue. *J Cell Biol* 103:1121-1128
- Kagan HM, Trackman PC (1991) Properties and function of lysyl oxidase. *Am J Respir Cell Mol Biol* 5:206-210
- Kambe N, Hashimoto K (1987) Anti-elastofibril monoclonal antibody NKH-1: production and application. *J Invest Dermatol* 88:253-258
- Kao K-YT, Hilker DM, McGavack TH (1961) Connective tissue V. Comparison of synthesis and turnover of collagen and elastin in tissues of rat at several ages. *Proc Soc Exp Biol Med* 106:335-338
- Karr SR, Foster JA (1981) Primary structure of the signal peptide of tropoelastin b. *J Biol Chem* 256:5946-5949
- Karrer HE (1960) Electron microscope study of the developing chick embryo aorta. *J Ultrastruct Res* 4:420-454
- Karrer HE (1961) An electron microscope study of the aorta in young and in aging mice. *J Ultrastruct Res* 5:1-27

- Keech MK (1960) Electron microscope study of the lathyrotic rat aorta. *J Biophys Biochem Cytol* 7:539-545
- Keeley FW (1979) The synthesis of soluble and insoluble elastin in chicken aorta as a function of development and age. Effect of a high cholesterol diet. *Can J Biochem* 57:1273-1280
- Keeley FW, Jonhson DJ (1983) Measurement of the absolute synthesis of soluble and insoluble elastin by chick aortic tissue. *Can J Biochem Cell Biol* 61:1079-1084
- Keeley FW, Alatawi A (1991) Response of aortic elastin synthesis and accumulation to developing hypertension and the inhibitory effect of colchicine on this response. *Lab Invest* 64:499-507
- Keene DR, Sakai LY, Lunstrum GP, Morris NP, Burgeson RE (1987) Type VII collagen forms an extended network of anchoring fibrils. *J Cell Biol* 104:611-621
- Keene DR, Maddox BK, Kuo H-J, Sakai LY, Glanville RW (1991) Extraction of extendable beaded structures and their identification as fibrillin-containing extracellular matrix microfibrils. *J Histochem Cytochem* 39:441-449
- Kewley MA, Steven FS, Williams G (1977a) Preparation of a specific antiserum towards the microfibrillar protein of elastic tissue. *Immunology* 32:483-489
- Kewley MA, Steven FS, Williams G (1977b) Immunofluorescence studies with a specific antiserum to the microfibrillar protein of elastic fibres. Location in elastic and non-elastic connective tissues. *Immunology* 33:381-386

Khan AM, Walker F (1984) Age related detection of tissue amyloid P in the skin.  
J Pathol 143:183-186

Kim DW, Langille BL, Wong MKK, Gotlieb AI (1989a) Patterns of endothelial  
microfilament distribution in the rabbit aorta in situ. Circ Res 64:21-31

Kim DW, Gotlieb AI, Langille BL (1989b) In vivo modulation of endothelial F-actin  
microfilaments by experimental alterations in shear stress. Arteriosclerosis 9:439-445

Knight KR, Ayad S, Shuttleworth A, Grant ME (1984) A collagenous glycoprotein  
found in dissociative extracts of foetal bovine nuchal ligament. Evidence for a  
relationship with type VI collagen. Biochem J 220:395-403

Kobayashi R, Tashima Y, Masuda H, Shozawa T, Numata Y, Miyauchi K, Hayakawa  
T (1989) Isolation and characterization of a new 36-kDa microfibril-associated  
glycoprotein from porcine aorta. J Biol Chem 264:17437-17444

Kobayasi T (1968) Electron microscopy of the elastic fibers and the dermal membrane  
in normal human skin. Acta Derm Venereol (Stockh) 48:303-312

Kobayasi T (1977) Anchoring of basal lamina to elastic fibers by elastic fibrils. J Invest  
Dermatol 68:389-390

Kopriwa BM (1973) A reliable, standardized method for ultrastructural electron  
microscopic radioautography. Histochemie 37:1-17

Krauhs JM (1983) Microfibrils in the aorta. Connect Tiss Res 11:153-167

- Kuhn C III, Yu S-Y, Chraplyvy M, Linder HE, Senior RM (1976) The induction of emphysema with elastase. II. Changes in connective tissue. *Lab Invest* 34:372-380
- Kuivaniemi H, Savolainen E-R, Kivirikko KI (1984) Human placental lysyl oxidase. Purification, partial characterization, and preparation of two specific antisera to the enzyme. *J Biol Chem* 259:6996-7002
- Kumaratilake JS, Gibson MA, Fanning JC, Cleary EG (1989) The tissue distribution of microfibrils reacting with a monospecific antibody to MAGP, the major glycoprotein antigen of elastin-associated microfibrils. *Eur J Cell Biol* 50:117-127
- Lansing AI, Roberts E, Ramasarma GB, Rosenthal TB, Alex M (1951) Changes with age in amino acid composition of arterial elastin. *Proc Soc Exp Biol Med* 76:714-717
- Lazarides E, Weber K (1974) Actin antibody: the specific visualization of actin filaments in non-muscle cells. *Proc Natl Acad Sci USA* 71:2268-2272
- Leak LV, Burke JF (1966) Fine structure of the lymphatic capillary and the adjoining connective tissue area. *Am J Anat* 118:785-810
- Leak LV, Burke JF (1968) Ultrastructural studies on the lymphatic anchoring filaments. *J Cell Biol* 36:129-149
- Ledger PW, Tanzer ML (1984) Monensin - a perturbant of cellular physiology. *Trends Biochem Sci* 9:313-314
- Lee I, Yau MC, Rucker RB (1976) Arterial elastin synthesis in the young chick. *Biochim Biophys Acta* 442:432-436

Lee B, Godfrey M, Vitale E, Hori H, Mattei M-G, Sarfarazi M, Tsipouras P, Ramirez F, Hollister DW (1991) Linkage of Marfan syndrome and a phenotypically related disorder to two different fibrillin genes. *Nature* 352:330-334

Lefevre M, Rucker RB (1980) Aorta elastin turnover in normal and hypercholesterolemic Japanese quail. *Biochim Biophys Acta* 630:519-529

Lethias C, Chignier E, Garrone R, Hartmann DJ, Eloy R (1988) Elastogenesis in rat arterial grafts: elastin deposits on microfibrillar and non-microfibrillar structures. *Histochem J* 20:715-721

Lloyd CW, Smith CG, Woods A, Rees DA (1977) Mechanisms of cellular adhesion. II. The interplay between adhesion, the cytoskeleton, and morphology in substrate attached cells. *Exp Cell Res* 110:427-437

Looker T, Berry CL (1972) The growth and development of the rat aorta. II. Changes in nucleic acid and scleroprotein content. *J Anat* 113:17-34

Low FN (1961) Microfibrils, a small extracellular component of connective tissue. *Anat Rec* 139:250

Low FN (1962) Microfibrils: Fine filamentous components of the tissue space. *Anat Rec* 142:131-137

Maddox BK, Sakai LY, Keene DR, Glanville RW (1989) Connective tissue microfibrils. Isolation and characterization of three large pepsin-resistant domains of fibrillin. *J Biol Chem* 264:21381-21385

Marchi F, Leblond CP (1983) Collagen biogenesis and assembly into fibrils as shown by ultrastructural and <sup>3</sup>H-proline radioautographic studies on the fibroblasts of the rat foot pad. *Am J Anat* 168:167-197

Matoltsy AG, Gross J, Grignolo A (1951) A study of the fibrous components of the vitreous body of the electron microscope. *Proc Soc Exp Biol Med* 76:857-860

Mecham RP, Lange G, Madaras J, Starcher B (1981) Elastin synthesis by ligamentum nuchae fibroblasts: Effects of culture conditions and extracellular matrix on elastin production. *J Cell Biol* 90:332-338

Mecham RP, Whitehouse LA, Wrenn DS, Parks WC, Griffin GL, Senior RM, Crouch EC, Stenmark KR, Voelkel NF (1987) Smooth muscle-mediated connective tissue remodeling in pulmonary hypertension. *Science* 237:423-426

Mecham RP, Hinek A, Cleary EG, Kucich U, Lee SJ, Rosenbloom J (1988) Development of immunoreagents to ciliary zonules that react with protein components of elastic fiber microfibrils and with elastin-producing cells. *Biochem Biophys Res Commun* 151:822-826

Mecham RP, Hinek A, Entwistle R, Wrenn DS, Griffin GL, Senior RM (1989a) Elastin binds to a multifunctional 67-kilodalton peripheral membrane protein. *Biochemistry* 28:3716-3722

Mecham RP, Hinek A, Griffin GL, Senior RM, Liotta LA (1989b) The elastin receptor shows structural and functional similarities to the 67-kD tumor cell laminin receptor. *J Biol Chem* 264:16652-16657

- Mecham RP, Heuser JE (1990) Three-dimensional organization of extracellular matrix in elastic cartilage as viewed by quick freeze, deep etch electron microscopy. *Connect Tiss Res* 24:83-93
- Mecham RP, Heuser JE (1991) The elastic fiber. In: *Cell Biology of Extracellular Matrix*, 2<sup>nd</sup> edition. Hay ED (ed). Plenum Publishing Corp. (in press)
- Mecham RP, Whitehouse L, Hay M, Hinek A, Sheetz MP (1991a) Ligand affinity of the 67-kD elastin/laminin binding protein is modulated by the protein's lectin domain: Visualization of elastin/laminin-receptor complexes with gold-tagged ligands. *J Cell Biol* 113:187-194
- Mecham RP, Sienmark KR, Parks WC (1991b) Connective tissue production by vascular smooth muscle in development and disease. *Chest* 99:43S-47S
- Morocutti M, Raspanti M, Govoni P, Kadar A, Ruggeri A (1988) Ultrastructural aspects of freeze-fractured and etched elastin. *Connect Tiss Res* 18:55-64
- Mundel P, Elger M, Sakai T, Kriz W (1988) Microfibrils are a major component of the mesangial matrix in the glomerulus of the rat kidney. *Cell Tiss Res* 254:183-187
- Nakamura H (1988) Electron microscopic study of the prenatal development of the thoracic aorta in the rat. *Am J Anat* 181:406-418
- Nikai H, Obana I, Ijuhin N, Yamasaki A, Takata T, Elabardi E (1983) Ultrastructural cytochemical demonstration of elastin in the matrix of salivary gland tumours. *Acta Pathol Jpn* 33:1171-1178

- O'Shea KS, Dixit VM (1988) Unique distribution of the extracellular matrix component thrombospondin in the developing mouse embryo. *J Cell Biol* 107:2737-2748
- Palay SL (1963) Alveolate vesicles in purkinje cells of the rat's cerebellum. *J Cell Biol* 19:89A-90A
- Partridge SM (1967) Elastin structure and biosynthesis. In: *Symposium on Fibrous Proteins*. Crewther WG (ed). Plenum Press, New York. pp 246-256
- Partridge SM, Davis HF, Adair GS (1955) The chemistry of connective tissue. 2. Soluble proteins derived from partial hydrolysis of elastin. *Biochem J* 61:11-21
- Pasquali-Ronchetti IP, Fornieri C, Baccarani-Contri M, Volpin D (1979) The ultrastructure of elastin revealed by freeze-fracture electron microscopy. *Micron* 10:89-99
- Pasquali-Ronchetti I, Fornieri C (1984) The ultrastructural organization of the elastin fiber. In: *Ultrastructure of the Connective Tissue Matrix*. Ruggeri A, Motta PM (eds). Martinus Nijhoff Publishers, Boston. pp 126-139
- Paule WJ (1963) Electron microscopy of the newborn rat aorta. *J Ultrastruct Res* 8: 219-235
- Paz MA, Keith DA, Gallop PM (1982) Elastin isolation and cross-linking. *Methods Enzymol* 82:571-587
- Pease DC, Paule WJ (1960) Electron microscopy of elastic arteries; the thoracic aorta of the rat. *J Ultrastruct Res* 3:469-483



Peterson LH, Jensen RE, Parnell J (1960) Mechanical properties of arteries in vivo.  
Circ Res 8:622-639

Prosser IW, Gibson MA, Cleary EG (1984) Microfibrillar protein from elastic tissue:  
A critical evaluation. Aust J Exp Biol Med Sci 62:485-505

Prosser IW, Mecham RP (1988) Regulation of extracellular matrix accumulation: A  
short review of elastin biosynthesis. In: Self-Assembling Architecture. Varner JE (ed).  
Alan R Liss, Inc. pp 1-23

Prosser IW, Stenmark KR, Suthar M, Crouch EC, Mecham RP, Parks WC (1989)  
Regional heterogeneity of elastin and collagen gene expression in intralobar arteries  
in response to hypoxic pulmonary hypertension as demonstrated by in situ  
hybridization. Am J Pathol 135:1073-1088

Rasmussen BL, Bruenger E, Sandberg LB (1975) A new method for purification of  
mature elastin. Anal Biochem 64:255-259

Raviola G (1971) The fine structure of the ciliary zonule and ciliary epithelium with  
special regard to the organization and insertion of the zonular fibrils. Invest Ophthalmol  
10:851-869

Ren ZX, Brewton RG, Mayne R (1991) An analysis by rotary shadowing of the  
structure of the mammalian vitreous humor and zonular apparatus. J Struct Biol  
106:57-63

Reynolds ES (1963) The use of lead citrate at high pH as an electron opaque stain in  
electron microscopy. J Cell Biol 17:208-215



- Robert L (1977) Turnover and elastolysis in elastic tissue. In: Elastin and Elastic Tissue. Advances in Experimental Medicine and Biology. Sandberg LB, Gray WR, Franzblau C (eds). Plenum Press, New York. vol 79, pp 139-143
- Rodrigo FG, Cotta-Pereira G, David-Ferreira JF (1975) The fine structure of the elastic tendons in the human arrector pili muscle. Br J Dermatol 93:631-637
- Rosenbloom J (1982) Elastin: Biosynthesis, structure, degradation and role in disease processes. Connect Tiss Res 10:73-91
- Rosenbloom J (1987) Elastin: An overview. In: Structural and Contractile Proteins. Methods in Enzymology, Part D. Extracellular Matrix. Cunningham LW (ed). Orlando, Florida, Academic Press. vol 144, pp 172-196
- Rosenbloom J, Cywinski A (1976) Inhibition of proline hydroxylation does not inhibit secretion of tropoelastin by chick aorta cells. FEBS Lett 65:246-250
- Ross R (1971) The smooth muscle cell. II. Growth of smooth muscle in culture and formation of elastic fibers. J Cell Biol 50:172-186
- Ross R (1973) The elastic fiber. A review. J Histochem Cytochem 21:199-208
- Ross R (1981) Atherosclerosis: A problem of the biology of arterial wall cells and their interactions with blood components. Arteriosclerosis 1:293-311
- Ross R, Bornstein P (1969) The elastic fiber. I. The separation and partial characterization of its macromolecular components. J Cell Biol 40:366-381

Ross R, Klebanoff SJ (1971) The smooth muscle cell. I. In vivo synthesis of connective tissue proteins. J Cell Biol 50:159-171

Rostagno A, Frangione B, Pearlstein E, Garcia-Pardo A (1986) Fibronectin binds to amyloid P component. Localization of the binding site to the 31,000 dalton C-terminal domain. Biochem Biophys Res Commun 140:12-20

Rucker RB, Tinker D (1977) Structure and metabolism of arterial elastin. Int Rev Exp Pathol 17:1-47

Rucker RB, Dubick MA (1984) Elastin metabolism and chemistry: Potential roles in lung development and structure. Environ Health Perspect 55:179-191

Sakai LY, Keene DR, Engvall E (1986) Fibrillin, a new 350-kD glycoprotein, is a component of extracellular microfibrils. J Cell Biol 103:2499-2509

Sakai L.Y, Keene DR, Glanville RW, Bächinger HP (1991) Purification and partial characterization of fibrillin, a cysteine-rich structural component of connective tissue microfibrils. J Biol Chem 266:14763-14770

Sakariassen KS, Bolhuis PA, Sixma JJ (1979) Human blood platelet adhesion to artery subendothelium is mediated by factor VIII-Von Willebrand factor bound to the subendothelium. Nature 279:636-638

Sandberg LB, Weissman N, Smith DW (1969) The purification and partial characterization of a soluble elastin-like protein from copper-deficient porcine aorta. Biochemistry 8:2940-2945

Sandberg LB, Soskel NT, Leslie JG (1981) Elastin structure, biosynthesis, and relation to disease states. *New Eng J Med* 304:566-579

Saunders NA, Grant ME (1984) Elastin biosynthesis in chick-embryo arteries. Studies on the intracellular site of synthesis of tropoelastin. *Biochem J* 221:393-400

Saunders NA, Grant ME (1985) The secretion of tropoelastin by chick-embryo artery cells. *Biochem J* 230:217-225

Schwartz E, Goldfischer S, Coltoff-Schiller B, Blumenfeld OO (1985) Extracellular matrix microfibrils are composed of core proteins coated with fibronectin. *J Histochem Cytochem* 33: 268-274

Sear CHJ, Kewley MA, Jones CJP, Grant ME, Jackson DS (1978) The identification of glycoproteins associated with elastic-tissue microfibrils. *Biochem J* 170:715-718

Sear CHJ, Grant ME, Jackson DS (1981) The nature of the microfibrillar glycoproteins of elastic fibres. A biosynthetic study. *Biochem J* 194:587-598

Sengel A, Stoebner P (1970) Golgi origin of tubular inclusions in endothelial cells. *J Cell Biol* 44:223-226

Senior RM, Griffin GL, Mecham RP (1982) Chemotactic responses of fibroblasts to tropoelastin and elastin-derived peptides. *J Clin Invest* 70:614:618

Senior RM, Griffin GL, Mecham RP, Wrenn DS, Prasad KU, Urry DW (1984) Val-gly-val-ala-pro-gly, a repeating peptide in elastin, is chemotactic for fibroblasts and monocytes. *J Cell Biol* 99:870-874

- Senior RM, Hinek A, Griffin GL, Pipoly DJ, Crouch EC, Mecham RP (1989)  
Neutrophil show chemotaxis to type IV collagen and its 7S domain and contain a 67  
kD type IV collagen-binding protein with lectin properties. *Am J Respir Cell Mol Biol*  
1:479-487
- Serafini-Fracassini A (1984) Elastogenesis in embryonic and post-natal development. In:  
Ultrastructure of the Connective Tissue Matrix. Ruggeri A, Motta PM (eds). Martinus  
Nijhoff publishers, Boston. pp 140-150
- Serafini-Fracassini A, Field JM, Spina M, Stephens WGS, Delf B (1976) The  
macromolecular organization of the elastin fibril. *J Mol Biol* 100:73-84
- Serafini-Fracassini A, Ventrella G, Field MJ, Hinnie J, Onyezili NI, Griffiths R  
(1981) Characterization of a structural glycoprotein from bovine ligamentum nuchae  
exhibiting dual amine oxidase activity. *Biochemistry* 20:5424-5429
- Shapiro SD, Endicott SK, Province MA, Pierce JA, Campbell EJ (1991) Marked  
longevity of human lung parenchymal elastic fibers deduced from prevalence of  
D-aspartate and nuclear weapons-related radiocarbon. *J Clin Invest* 87:1828-1834
- Sheldon H, Robinson RA (1958) Studies on cartilage: Electron microscopic observations  
on normal rabbit ear cartilage. *J Biophys Biochem Cytol* 4:401-406
- Siegal RC, Fu JCC (1976) Collagen cross-linking. Purification and substrate specificity  
of lysyl oxidase. *J Biol Chem* 251:5779-5785
- Siegel RC, Chen KH, Greenspan JS, Aguiar JM (1978) Biochemical and  
immunochemical study of lysyl oxidase in experimental hepatic fibrosis in the rat. *Proc  
Natl Acad Sci USA* 75:2945-2949

- Singer II, Scott S, Kawka DW, Hassell JR (1987) Extracellular matrix fibers containing heparan sulfate proteoglycan coaligr. with focal contacts and microfilament bundles in stationary fibroblasts. *Exp Cell Res* 173:558-571
- Skinner M, Pepys MB, Cohen AS, Heller LM, Lian JB (1980) Studies on amyloid protein AP. In: *Amyloid and Amyloidosis*. Glenner GG, Pinho e Costa P, de Freitas F (eds). Excerpta Medica, Amsterdam. pp 384-391
- Slack HGB (1954) Metabolism of elastin in the adult rat. *Nature* 174:512-513
- Smith C, Seitner MM, Wang H-P (1951) Aging changes in the tunica media of the aorta. *Anat Rec* 109:13-39
- Smith DW, Weissman N, Carnes WH (1968) Cardiovascular studies on copper deficient swine. XII. Partial purification of a soluble protein resembling elastin. *Biochem Biophys Res Commun* 31:309-315
- Smith DW, Brown DM, Carnes WH (1972) Preparation and properties of salt-soluble elastin. *J Biol Chem* 247:2427-2432
- Stehbens WE (1966) The basal attachment of endothelial cells. *J Ultrastruct Res* 15: 389-399
- Stehbens WE, Meyer E (1965) Ultrastructure of endothelium of the frog heart. *J Anat* 99:127-134
- Streeten BW, Licari PA, Marucci AA, Dougherty RM (1981) Immunohistochemical comparison of ocular zonules and the microfibrils of elastic tissue. *Invest Ophthalmol* 21:130-135



Streeten BW, Licari PA (1983) The zonules and the elastic microfibrillar system in the ciliary body. *Invest Ophthalmol Vis Sci* 24:667-681

Streeten BW, Gibson SA (1988) Identification of extractable proteins from the bovine ocular zonule: major zonular antigens 32kD and 250kD. *Curr Eye Res* 7:139-146

Sutcliffe MC, Davidson JM (1990) Effect of static stretching on elastin production by porcine aortic smooth muscle cells. *Matrix* 10:148-153

Suzuki K, Mori I, Masawa N, Coneda G (1980) A case of basal cell adenoma showing elastic fiber (elastin-basement membrane complex) formation of the submandibular gland. *Acta Pathol Jpn* 30:275-283

Takagi M (1969) Electron microscopical and biochemical studies of the elastogenesis in embryonic chick aorta. I. Fine structure of developing embryonic chick aorta. *Kumamoto Med J* 22:1-14

Takagi K, Kawase O (1967) An electron microscopic study of elastogenesis in embryonic chick aorta. *J Electron Microsc (Tokyo)* 16:330-339

Thyberg J, Hinek A, Nilsson J, Friberg U (1979) Electron microscope and cytochemical studies of rat aorta. Intracellular vesicles containing elastin- and collagen-like material. *Histochem J* 11:1-17

Trackman PC, Pratt AM, Wolanski A, Tang S-S, Offner GD, Troxler RF, Kagan HM (1990) Cloning of rat aorta lysyl oxidase cDNA: Complete codons and predicted amino acid sequence. *Biochemistry* 29:4863-4870

- Ts'ao C-H, Glagov, S (1970) Basal endothelial attachment. Tenacity at cytoplasmic dense zones in the rabbit aorta. *Lab Invest* 23:510-516
- Tsuji T (1980) Elastic fibres on the dermal papilla. Scanning and transmission electron microscopic studies. *Br J Dermatol* 102:413-417
- Uitto J, Hoffman HP, Prockop DJ (1976) Synthesis of elastin and procollagen by cells from embryonic aorta. Differences in the role of hydroxyproline and the effects of proline analogs on the secretion of the two proteins. *Arch Biochem Biophys* 173:187-200
- Unna PG (1891) Notiz, betreffend die Taenzersche Orceinfärbung des elastischen Gewebes. *monatsh prakt Dermat* 12:394
- Urry DW, Long MM, Cox BA, Ohnishi T, Mitchell LW, Jacobs M (1974) The synthetic polypenta peptide of elastin coacervates and forms filamentous aggregates. *Biochem Biophys Acta* 371:597-602
- Vaccaro C, Brody JS (1978) Ultrastructure of developing alveoli. I. The role of the interstitial fibroblast. *Anat Rec* 192:467-480
- Varga Z, Kovács É, Paragh G, Jacob M-P, Robert L, Fülöp T Jr (1988) Effect of elastin peptides and N-formyl-methionyl-leucyl phenylalanine on cytosolic free calcium in polymorphonuclear leukocytes of healthy middle-aged and elderly subjects. *Clin Biochem* 21:127-130
- Vaughan L, Mendler M, Huber S, Bruckner P, Winterhalter KH, Irwin MH, Mayne R (1988) D-Periodic distribution of collagen type IX along cartilage fibrils. *J Cell Biol* 106:991-997

- Verhoeff FH (1908) Some new staining methods of wide applicability; including a rapid differential stain for elastic tissue. *J A M A* 50:876
- Volpin D, Pasquali-Ronchetti I (1977) The ultrastructure of high-temperature coacervates from elastin. *J Ultrastruct Res* 61:295-302
- von der Mark H, Aumailley M, Wick G, Fleischmajer R, Timpl R (1984) Immunocytochemistry, genuine size and tissue localization of collagen VI. *Eur J Biochem* 142:493-502
- Wagner RC (1976) The effect of tannic acid on electron images of capillary endothelial cell membranes. *J Ultrastruct Res* 57:132-139
- Wagner DD, Olmsted JB, Marder VJ (1982) Immunolocalization of von Willebrand protein in Weibel-Palade bodies of human endothelial cells. *J Cell Biol* 95:355-360
- Wakasaki H, Ooshima A (1990) Immunohistochemical localization of lysyl oxidase with monoclonal antibodies. *Lab Invest* 63:377-384
- Walford RL, Carter PK, Schneider RB (1964) Stability of aortic elastic tissue with age and pregnancy in the rat. *Arch Pathol* 78:43-45
- Warhol MJ, Sweet JM (1984) The ultrastructural localization of von Willebrand factor in endothelial cells. *Am J Pathol* 117:310-315
- Weber K, Groschel-Stewart U (1974) Antibody to myosin: the specific visualization of myosin-containing filaments in nonmuscle cells. *Proc Natl Acad Sci USA* 71:4561-4564

- Weibel ER, Palade GE (1964) New cytoplasmic components in arterial endothelia. *J Cell Biol* 23:101-112
- Weigert C (1898) Ueber eine methode zur Farbung elastischer Fasern. *Zentr pathol Anat u allgem Pathol* 9:289-292
- Weinstock M (1975) Elaboration of precursor collagen by osteoblasts as visualized by radioautography after  $^3\text{H}$ -proline administration. In: *Extracellular Matrix Influences on Gene Expression*. Slavkin HC, Greulich RC (eds). Academic Press, New York. pp 119-128
- Weinstock M, Leblond CP (1974) Synthesis, migration, and release of precursor collagen by odontoblasts as visualized by radioautography after [ $^3\text{H}$ ] proline administration. *J Cell Biol* 60:92-127
- Weis-Fogh T, Anderson SO (1970) New molecular model for the long-range elasticity of elastin. *Nature* 227:718-721
- White GE, Gimbrone MA, Fujiwara K (1983) Factors influencing the expression of stress fibers in vascular endothelial cells *in situ*. *J Cell Biol* 97:416-424
- White GE, Fujiwara K (1986) Expression and intracellular distribution of stress fibers in aortic endothelium. *J Cell Biol* 103:63-70
- White JF, Hughes JL, Kumaratilake JS, Fanning JC, Gibson MA, Krishnan R, Cleary EG (1988) Post-embedding methods for immunolocalization of elastin and related components in tissues. *J Histochem Cytochem* 36:1543-1551

- Wight TN, Raugi GJ, Mumby SM, Bornstein P (1985) Light microscopic immunolocation of thrombospondin in human tissues. *J Histochem Cytochem* 33: 295-302
- Wirtschafter ZT, Cleary EG, Jackson DS, Sandberg LB (1967) Histological changes during the development of the bovine nuchal ligament. *J Cell Biol* 33:481-488
- Wolinsky H, Glagov S (1964) Structural basis for the static mechanical properties of the aortic media. *Circ Res* 14:400-413
- Wolinsky H, Glagov S (1967) A lamellar unit of aortic medial structure and function in mammals. *Circ Res* 20:99-111
- Wolinsky H (1970) Response of the rat aortic media to hypertension. Morphological and chemical studies. *Circ Res* 26:507-522
- Wong AJ, Pollard TD, Herman IM (1983) Actin filament stress fibers in vascular endothelial cells in vivo. *Science* 219:867-869
- Wrenn DS, Parks WC, Whitehouse LA, Crouch EC, Kucich U, Rosenbloom J, Mecham RP (1987) Identification of multiple tropoelastins secreted by bovine cells. *J Biol Chem* 262:2244-2249
- Wrenn DS, Hinek A, Mecham RP (1988) Kinetics of receptor-mediated binding of tropoelastin to ligament fibroblasts. *J Biol Chem* 263:2280-2284
- Wright DW, Mayne R (1988) Vitreous humor of chicken contains two fibrillar systems: An analysis of their structure. *J Ultrastruct Mol Struct Res* 100:224-234

Yamada K, Akyama, Hasegawa T, Hasegawa E, Humphries M, Kennedy D, Nagata K, Urishihara H, Olden K, Chen W (1985) Recent advances in research on fibronectin and other cell attachment proteins. *J Cell Biochem* 28:79-97

Yohro T, Burnstock G (1973) Filament bundles and contractility of endothelial cell in coronary arteries. *Z Zellforsch* 138:85-95